Investigation of thiazyl radical – metalloporphyrin complexes

by

Laura Jane van Laeren

Dissertation presented in partial fulfilment of the requirements for the degree of

Doctor of Philosophy

at

Stellenbosch University

Supervisor: Prof. Delia A. Haynes

Co-supervisor: Dr Katherine A. de Villiers

Department of Chemistry and Polymer Science

Faculty of Science

March 2017

DECLARATION

By submitting this thesis electronically, I declare that the entirety of the work contained therein is my own, original work, that I am the authorship owner thereof (unless to the extent explicitly otherwise stated) and that I have not previously in its entirety or in part submitted it for obtaining any qualification.

Date: March 2017

Abstract

The aim of this project was to investigate the formation of novel dithiadiazolyl-metalloporphyrin complexes with the goal of forming complexes with interesting magnetic, conductive or redox behaviour. The crystal structure of one such dithiadiazolyl radical – metalloporphyrin complex, containing 4-(4′-pyridyl)-1,2,3,5-dithiadiazolyl and cobalt (II) tetraphenylporphyrin, was determined through the use of single crystal X-ray diffraction. The complex crystallizes as a coordination polymer, with each dithiadiazolyl radical bridging two cobalt porphyrins *via* a dithiadiazolyl sulfur atom and the pyridyl nitrogen. The sulfur-sulfur bond remains intact and is unusually long; it is proposed that this is as a result of delocalisation of the unpaired electron from the cobalt ion to the dithiadiazolyl radical, resulting in partial oxidation of the Co(II) centre with associated partial reduction of the dithiadiazolyl radical to a dithiadiazolide anion. This is only the third example of an isolated dithiadiazolyl anion. In solution, initial coordination occurs through the dithiadiazolyl sulfur atom. Following dissolution, the nitrogen-bound species predominates. Ligand-metalloporphyrin association was studied in solution through the use of ultraviolet-visible spectroscopy and a logβ value of 4.19 ± 0.05 in dichloromethane at 25 °C was determined. The interaction between a range of eight dithiadiazolyl radicals and three different cobalt porphyrins was subsequently studied spectroscopically. It was found that changing the substituents on the dithiadiazolyl radical has a limited effect on the strength of coordination, while changing the substituents on the porphyrin has a far greater effect. When electron-donating substituents were added, logβ values were higher than for the parent porphyrin while electron-withdrawing substituents resulted in lower logβ values with respect to any of the dithiadiazolyl ligands. Electrostatic potential maps were generated to provide further insight into the electron density across the eight dithiadiazolyl radicals and confirmed that the substituents had a negligible effect on the coordinating sulfur atoms, rationalising the spectrophotometric observations. Coordination of dithiadiazolyl radicals to cobalt, copper, iron and zinc porphyrins was reported, with negligible interaction with magnesium. Coordination to copper and iron was weaker than for cobalt, while coordination to zinc was stronger. The choice of metal affects the magnetic behaviour of the complexes. Coordination to a paramagnetic metal centre, such as cobalt, copper and iron, results in a diamagnetic complex, while coordination to the diamagnetic zinc leads to paramagnetic complexes. These zinc complexes associate at high concentration, leading to loss of paramagnetism. Finally, coordination of dithiadiazolyl radicals to haematin, an iron-containing biological metalloporphyrin, was investigated in order to illustrate a potential application of these dithiadiazolyl complexes to the understanding of haem chemistry and the treatment of malaria. The association of these ligands to haematin (logβ values of 3.07 ± 0.15 and 2.88 ± 0.07) in dichloromethane is weaker than for chloroquine (logβ value of 5.31 ± 0.04), an antimalarial drug known to interact with haematin.

This study provided valuable insight into the formation of dithiadiazolyl radical – metalloporphyrin complexes and lays important groundwork for future work in this field.

Opsomming

Die mikpunt van hierdie projek was die vorming van unieke ditiadiazolyl-metalloporfyrien komplekse, met die doelwit om komplekse met interessante magnetiese, geleidende of redoks-gedrag te skep. Die struktuur van een so `n ditiadiazolyl radikale-metalloporfyrien kompleks, met 4-(4'-piridyl) -1,2,3,5-ditiadiazolyl en kobalt (II) tetrafenielporphyrin, was bepaal deur die gebruik van enkelkristal X-straaldiffraksie. Dié kompleks kristalliseer as `n koördinasie-polimeer, met elke ditiadiazolyl wat twee kobalt porfiriene *via* `n dithiadiazolyl swael-atoom en die piridylstikstof atom oorbrug. Die swael-swael verbinding bly ongeskonde en is buitengewoon lank; dit word voorgestel dat hierdie as gevolg van delokalisasie van die ongepaarde elektron van die kobaltioon om die ditiadiazolyl radikale is, wat lei tot gedeeltelike oksidasie van die Co(II)-sentrum, wat gepaard gaan met die gedeeltelike reduksie van die ditiadiazolyl radikale tot `n ditiadiazolate anioon. Hierdié is slegs die derde voorbeeld van `n geïsoleerde ditiadiazolyl anioon. Ligand-metalloporfyrine assossiasie is in oplossing bestudeer deur middel van die gebruik van ultraviolet-sigbare spektroskopie, en `n logβ waarde van 4,19 ± 0,05 in dichloormetaan by 25 °C is vasgestel. Die interaksie tussen 'n verskeidenheid van agt ditiadiazolyl radikale en drie verskillende kobalt-porfiriene is daarna spektroskopies bestudeer. Daar is bevind dat die verandering van die substituente op die ditiadiazolylradikale `n beperkte invloed het op die sterkte van die koördinasie, terwyl die verandering van die substituente op die porfirien `n veel groter effek het. Wanneer elektron-skenkende substituente bygevoeg is, word logβ-waardes hoër as vir die oorspronklike porfirien, terwyl elektron-onttrekkende substituente lei tot laer logβ-waardes, met betrekking tot enige van die ditiadiazolyl ligande. Elektrostatiesepotensiaal-kaarte is opgestel om verdere insig in die elektrondigtheid van die agt dithiadiazolyl-radikale te verskaf. Dit het bevestig dat die substituente `n geringe uitwerking op die koördinering swael-atome het en dit het die spektrofotometriese waarnemings gerasionaliseer. Die koördinasie van ditiadiazolyl radikale tot kobalt, koper-, yster- en sink-porfiriene is aangemeld, met weglaatbare interaksie met magnesium. Die koördinasie aan koper en yster was swakker as dié tot kobalt, terwyl koördinasie tot sink sterker was. Die keuse van metaal affekteer die magnetiese gedrag van die komplekse. Koördinasie tot `n paramagnetiese metaalsentrum, soos kobalt, koper en yster, lei tot `n diamagnetiese kompleks, terwyl koördinasie met die diamagneties sink lei tot paramagnetiese komplekse. Hierdie sink-komplekse assosieer teen 'n hoë konsentrasie, en dit lei tot die verlies van paramagnetisme. Ten slotte, koördinasie van dithiadiazolyl-radikale aan haematin, `n biologiese metalloporfyrien wat yster bevat, is waargeneem. Die assosiasie van hierdie ligande aan haematin (logβ waardes van 3,07 ± 0,15 en 2,88 ± 0,07) in dichloormetaan is swakker as vir chlorokien (logβ waarde van 5,31 ± 0,04), `n bekende malariadwelm.

Hierdie studie het waardevolle insig bekendgemaak in die vorming van komplekse met dithiadiazolyl-radikale en metalloporfyrien en lê `n belangrik grondslag vir toekomstige werk in hierdie veld.

Acknowledgements

I would like to offer my sincere thanks to my supervisors, Prof Delia Haynes and Dr Katherine de Villiers, for their unbelievable support, wisdom, knowledge and mentorship – especially when times were tough and the finish-line seemed unreachable.

Special thanks to the people of the de Beers building. To the Supramolecular Group: there was never a dull moment in the student office or the lab, but together we learnt and laughed a lot! Thanks also to the technical staff for keeping everything running smoothly. I would also like to thank Dr Jaco Brand, for his assistance with NMR spectroscopy, and for helping run the first ^{59}Co NMR spectrum at Stellenbosch University!

To my friends, without whose unending support I would never have made it through: thank you for everything, from offering shoulders to cry on to providing wine when it was needed! I especially have to thank Helene Wahl, Varia Nikolayenko and Leigh Loots, for always being there. Thanks also to "The Company", my university family, for the last decade of friendship and mutual weirdness.

A special word of thanks to the scientific community on Twitter, especially the #RealTimeChem community and all the friends I've made, that have supported me, taught me, followed my journey and always let me know that I was not alone.

Most importantly, I have to thank my family. To my brother, Michael, my lifelong best friend, thank you for your support and for putting up with me! To my parents, Peter and Marian van Laeren, words cannot thank you enough for your infinite encouragement, motivation, support, love and guidance. Thank you for always giving me the opportunity to make my dreams come true. I love you.

Finally, I would like to thank Stellenbosch University for the opportunities provided, and to Sasol and the National Research Foundation for funding.

Publications

Part of this work

Delia A. Haynes, Laura J. van Laeren and Orde Q. Munro. "Structural, Spectroscopic, and DFT Studies of a Cobalt Porphyrin–Thiazyl Radical Coordination Polymer." *Manuscript in preparation.*

Conferences

1. **16th Biennual SACI Institute Inorganic Chemistry Conference**

Durban, South Africa, 30 June – 4 July 2013

Poster presentation: Investigation of thiazyl radical – metalloporphyrin complexes (#1)

2. **Pan African Conference and Summit, IYCR 2014 Africa**

University of the Free State, Bloemfontein, South Africa, 12 – 17 October 2014

Poster presentation: Investigation of thiazyl radical – metalloporphyrin complexes (#2)

3. **SACI Western Cape Young Chemists Symposium**

University of Cape Town, Cape Town, South Africa, 23 October 2014

Poster presentation: Investigation of thiazyl radical – metalloporphyrin complexes (#2)

4. **Indaba 8 – Serendipity vs Prediction**

Skukuza, Kruger National Park, South Africa, 16 – 21 August 2015

Poster presentation: Investigation of thiazyl radical – metalloporphyrin complexes (#3)

Atomic colour key

Atomic colours for crystal structures:

Carbon

Hydrogen

Sulfur

Nitrogen

Cobalt

Fluorine

Table of Contents

Attached CD contains relevant CIF files.

List of Figures

List of Abbreviations

ATR	Attenuated total reflection
CIF	Crystallographic information file
CSD	Cambridge Structural Database
DCM	Dichloromethane
DMSO	Dimethylsulfoxide
DTDA	Dithiadiazolyl
EPR	Electron Paramagnetic Resonance
FTIR	Fourier Transform Infrared
NMR	Nuclear Magnetic Resonance
PXRD	Powder X-ray Diffraction
SCD	Single Crystal X-ray Diffraction
SOMO	Singly Occupied Molecular Orbital
THF	Tetrahydrofuran
TPP	Tetraphenylporphyrin
UV-Vis	Ultraviolet-Visible
ΔH	Change in enthalpy
ΔS	Change in entropy

"It always seems impossible until it's done."

- Nelson Mandela

Chapter 1

General introduction

Dithiadiazolyl radicals are a fascinating class of heterocyclic organic radicals that show great potential for the development of organic magnetic materials. Molecule-based magnets are still being examined at a fundamental level and have not yet reached a practical application, however they may have potential technological applications in the future as a more tuneable alternative to traditional magnets.[1] Potential applications include their use in electronic and computing devices,[2] as conductive materials or as soluble magnets.[3] The use of dithiadiazolyl radicals as ligands, and the investigation of dithiadiazolyl metal complexes, builds upon the variety and complexity of materials that can be designed. However, this field is still relatively new and the prediction of the structures and properties of materials formed from dithiadiazolyl radicals is still problematic. It is therefore imperative that more work is done to better understand the reactivity of these organic radicals with regards to the formation of dithiadiazolyl-metal complexes, with the goal of forming new materials with useful magnetic, conductive or redox behaviour. The work described in this study investigated the formation of dithiadiazolyl-metalloporphyrin complexes.

1.1 Introduction to dithiadiazolyl radicals

Organic free radicals are widely known, particularly as a result of their significance in biological systems.[4] The first synthetic organic radical, the triphenylmethyl radical (Figure 1.1), was prepared in 1900 by Moses Gomberg and proved the existence of trivalent carbon.[5]

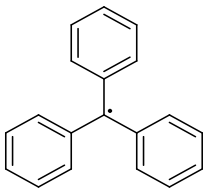

Figure 1.1: Structure of the triphenylmethyl radical

The field of radical chemistry has grown immensely since then, particularly in response to interest into the potential applications of organic radicals as a result of their unusual physical properties.[1] Several stable synthetic radicals have been shown to act as molecule-based magnets,[6] despite Heisenberg's claims in 1928 that long range magnetic ordering would only ever be found in a system with heavy (metallic) elements, never in a purely organic system.[7]

Interest in thiazyl radicals started with the discovery of polythiazyl (or polysulfur nitride, $(SN)_x$), which is a polymeric material first reported at the beginning of the 20th century that displays metallic characteristics and has a golden metallic luster.[8] Discovery of the metallic and super-conducting properties of the material led to increased interest in sulfur- and nitrogen-containing materials. Investigations into modifying the sulfur-nitrogen backbone of the polymer with functionalised carbon atoms resulted in unexpected carbon-sulfur-nitrogen heterocycles such as dithiatetrazocines (Figure 1.2).[9]

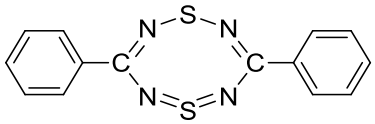

Figure 1.2: Structure of 3,7-diphenyl-l,5-dithia-2,4,6,8-tetrazocine (reproduced from reference 7)

Heterocyclic sulfur-nitrogen free radicals have been known for a long time. The first of these, $[S_3N_2^{+\bullet}]Cl^-$, was first prepared in 1880,[3] although the crystal structure was not determined until 1974.[10] Substitution of a sulfur (S^+) with an alkyl group (R–C) results in the isoelectronic $RCN_2S_2^{\bullet}$ heterocyclic system, known as dithiadiazolyls (Figure 1.3).[3]

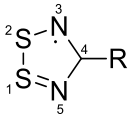

Figure 1.3: The 1,2,3,5-dithiadiazolyl radical

Thiazyl radicals have been investigated as potential building blocks for the design of molecular materials with interesting and desirable physical properties, such as conductivity and magnetism.[11,12] The development of new thiazyl radicals is a growing field of research. In particular, 1,2,3,5-dithiadiazolyls (Figure 1.3) have been investigated for their remarkable properties.[3] Dithiadiazolyl radicals, as well as their metal complexes, have been shown to display magnetic behaviour.[13,14] These properties are strongly dependent on the arrangement of the molecules in the solid state, as well as on

the intermolecular interactions present.[13] Consequently, attempts have been made to direct the crystal structures of these materials by modifying the properties of the R-group.[13]

1.1.1 The 1,2,3,5-dithiadiazolyl radical

Dithiadiazolyls can theoretically exist in four possible isomeric forms (Figure 1.4),[3] of which only **1** and **2** have been experimentally prepared. Molecular orbital calculations for the parent cations of the remaining two isomers, 3 and 4, have shown that while they can be formed, the potential loss of dinitrogen may significantly affect their stability.[3] 1,3,2,4-Dithiadizolyls will rearrange in solution and in the solid state (if heated) to form the thermodynamically more stable 1,2,3,5-dithiadiazolyl isomer.[15,16] The work in this thesis will focus on the 1,2,3,5-dithiadiazolyl radical, **1**, the first example of which was reported in 1980.[17]

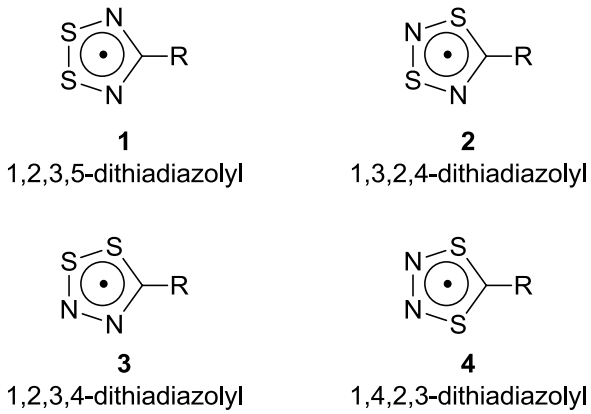

Figure 1.4: Possible isomers of dithiadiazolyl radicals (reproduced from reference 12)

Within the five-membered heterocyclic ring, the sulfur atoms provide two electrons each towards π bonding, while the carbon and nitrogen atoms each contribute one electron, leading to a neutral seven π-electron radical.[3] The singly-occupied molecular orbital (SOMO) is an anti-bonding orbital with $2a_2$ symmetry. The SOMO is nodal at the carbon atom and the unpaired electron resides over the sulfur and nitrogen atoms, as confirmed by Electron Paramagnetic Resonance Spectroscopy.[3,13] Consequently, the electronic properties of the dithiadiazolyl radical remain largely unaffected by changing the R-group.

Dithiadiazolyl radicals have a tendency to dimerise in the solid state. The interactions holding these dimers together are sometimes referred to as "pancake bonding", a term used to describe multi-centre two-electron bonding for π-stacked dimers.[18] The dimerization enthalpy is estimated at approximately 35 kJ/mol.[19] Dimerization involves π*-π* bonding interactions between SOMOs and results in spin-

pairing.[3,20,21,22] The spin-paired dimers display no conductive or magnetic properties, and thus a significant amount of research is focused on understanding and overcoming dimerization in the solid state. There are several dimer conformations, as shown in Figure 1.5. The energy differences between these conformations is relatively small (5 kJ/mol or less).[23]

Dithiadiazolyls with non-planar substituents are mostly likely to take up the twisted conformation (Figure 1.5 **a**).[3] This conformation minimizes steric repulsion. Examples of dithiadiazolyl dimers that take up this conformation include $(Me_2NCNSSN)_2$,[24] $(CF_3CNSSN)_2$,[23] $(MeCNSSN)_2$[25] and $(AdCNSSN)_2$ [26] (where Ad = adamantyl). The monomers associate with one S···S interaction (2.997 Å $\leq d_{SS} \leq$ 3.108 Å)[3] and several weaker S···N interactions. By far the most common dimer conformation is the *cis*-oid dimer (Figure 1.5 **b**), usually observed for dithiadiazolyls with planar substituents[3] such as the phenyl rings in $(PhCNSSN)_2$,[17] $(m\text{-}NCC_6H_4CNSSN)_2$[27] and $(p\text{-}NCC_6H_4CNSSN)_2$.[27] The dimer pair is held together in a *cis*-oid manner through two S···S interactions (3.10 Å $\leq d_{SS} \leq$ 3.13 Å).[3] The *trans*-oid (also called *trans*-antarafacial) dimer conformation is held together by two long S···S contacts, with no N···N interactions (Figure 1.5 **c**). This can be observed for the β-phase of $(m\text{-}NCC_6H_4CNSSN)_2$.[27] The *trans*-cofacial conformation (Figure 1.5 **d**) on the other hand, has very long S···S contacts and is primarily held together through four S···N contacts. An example of this dimer conformation is observed in the crystal structure of $(p\text{-}IC_6H_4CNSSN)_2$, which has S···S distances of 3.696 Å and S···N contacts in the range of 3.116 to 3.152 Å.[20] The most recently discovered dimer conformation is the orthogonal dimer (Figure 1.5 **e**), with S···S interactions between the two sulfur atoms of one dithiadiazolyl with one sulfur atom of a second dithiadiazolyl, and N···S interactions between the two nitrogen atoms of the first dithiadiazolyl with the second sulfur atom of the other dithiadiazolyl. The crystal structure of $(o\text{-}ClC_6H_4CNSSN)_2$ shows the presence of both *cis*-oid dimers and the novel orthogonal dimer.[22] Below 150K, this material is diamagnetic; however, above 150K an increase in paramagnetic character is observed.[22]

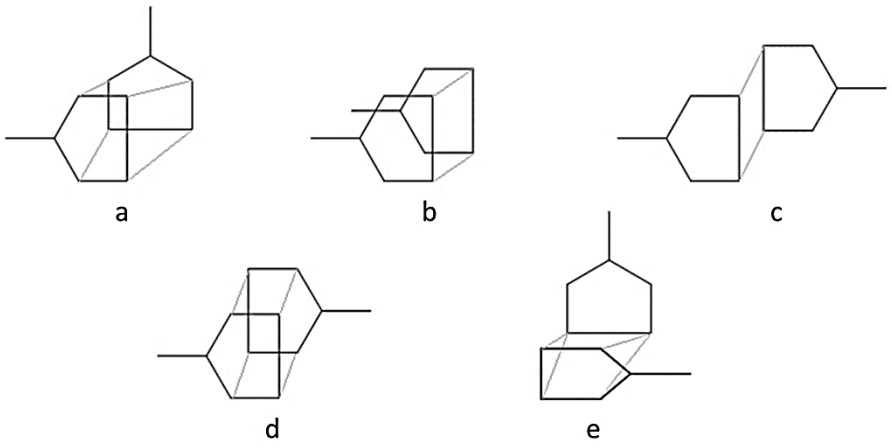

Figure 1.5: 1,2,3,5-Dithiadiazolyl dimer conformations: (a) twisted, (b) cis-oid, (c) trans-oid (trans-antarafacial), (d) trans-cofacial and (e) orthogonal (reproduced from reference 12)

1.1.2 Synthesis of 1,2,3,5-dithiadiazolyl radicals

Originally, dithiadiazolylium cations were synthesised from the reaction of organic nitriles with thiazyl chloride.[10] 1,2,3,5-Dithiadiazolyls are now most commonly prepared according to the general synthetic route outlined in Figure 1.6. Initially, a nitrile is reacted with lithium *bis*-(trimethylsilyl)amide to form a silylated amidinate. This intermediate is subsequently condensed with sulfur dichloride (SCl_2), yielding the dithiadiazolylium chloride salt as a brightly coloured powder. Finally, reduction can be achieved in the solid state using triphenylantimony (or, alternatively, Zn/Cu couple in tetrahydrofuran).[28] Purification by sublimation under reduced pressure yields intensely coloured crystals of the dithiadiazolyl radical in low to moderate yields.

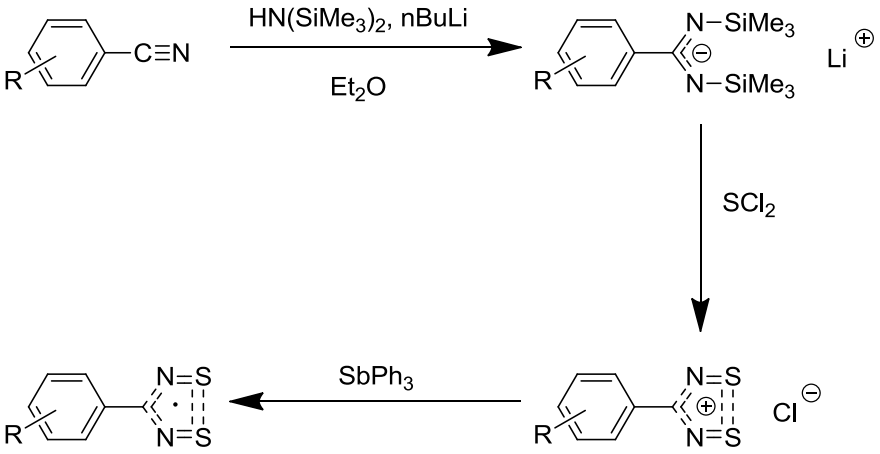

Figure 1.6: General synthetic scheme for dithiadiazolyl radicals.[3,28]

This approach has been applied to the preparation of aryl dithiadiazolyl radicals with a large variety of functional groups on the aryl ring, including CN, CH_3, CF_3, NO_2, SMe, OMe, F, Cl, Br and I.[20,21,29–31] The procedure is, however, limited to aprotic functionalities as in the presence of acidic protons, the $Li(N(SiMe_3)_2)$ has a tendency to behave as a base instead of as a nucleophile. Similarly, this procedure is unsuitable for substituents with protons α to the nitrile carbon, as these acidic protons again react with the basic $Li(N(SiMe_3))_2$.[32]

To circumvent this problem, the silylated amidine intermediate can be synthesised from an organolithium (prepared either by ortho-lithiation or lithium-halogen exchange) and bis(trimethylsilyl)carbodiimide.[33] This can then be followed by reacting with SCl_2 to form the dithiadiazolylium chloride salt, with subsequent reduction as previously described. An alternative is to directly condense an amidine with sulfur dichloride.[34]

1.1.3 Properties of 1,2,3,5-dithiadiazolyl radicals

1.1.3.1 Conductivity

For molecular materials to act as conductors, the material needs to have unpaired electrons that are mobile. Haddon proposed in 1975 that neutral, rather than charged, π-radicals could be used for the preparation of molecular conductors.[35] An idealized uniformly spaced stack of these radical molecules would result in a half filled energy band and consequently conductance.[13] These one-dimensional arrangements are however susceptible to Peierls distortion,[36] which produces a band gap. Peierls theorem - asserted by Rudolf Peierls in the 1930s - states that a one-dimensional equally spaced chain with one electron per ion is unstable, and as a result the chain will distort to lift degeneracy. This distortion can be overcome by maximising interstack interactions.

Dithiadiazolyl radicals may be considered suitable building blocks for conductive materials, provided the molecules form these uniformly spaced stacks (see Figure 1.7). Since the SOMO is nodal at the carbon atom, spin leakage onto the R-group is limited. Additionally, the R-group can be modified to tailor interstack and intrastack interactions to minimize Peierls distorsion.[3]

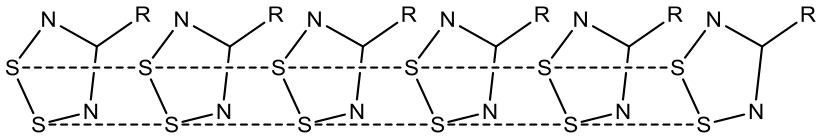

Figure 1.7: Idealized representation of π-stacking in 1,2,3,5-dithiadiazolyl radicals. Distortion of the equidistant spacing would lead to loss of magnetism or conductivity.

1.1.3.2 Magnetism

In order for a material to be considered magnetic, there must be evidence of long range magnetic ordering of electron spins. For a ferromagnetic material, all electron spins are aligned parallel to one another, such that the material displays a net magnetic moment. An antiferromagnetic material has spins aligned antiparallel, resulting in zero net magnetic moment.[37]

The magnetic behaviour of dithiadiazolyls is potentially interesting[12] but does present a challenge. Since most dithiadiazolyl radicals dimerize in the solid state (as discussed in section 1.1.1), they are diamagnetic materials.[3] Dimerization needs to be overcome in order to develop materials that possess bulk magnetic ordering. Additionally, long-range magnetic ordering requires there to be a network of short contacts between areas of unpaired spin density (i.e. the sulfur and nitrogen atoms of neighbouring dithiadiazolyl rings).

The first dithiadiazolyl radical that was shown to be monomeric in the solid state was *p*-NC-C_6F_4CNNSN•.[38] The α-phase of the dithiadiazolyl material has chains of the radical linked by

short contacts between the S – S bond of one dithiadiazolyl and the nitrile functional group of the next dithiadiazolyl. The chains run antiparallel to each other and are held together by S···S and S···N contacts. The α-phase of the material is paramagnetic, with short range anti-ferromagentic interactions, however there is no long range order. Subsequent studies revealed that a second phase could be formed.[39] This β-phase shows chains of dithiadiazolyls aligned co-parallel, with a network of S···N interactions linking the radicals (Figure 1.8). This material exhibits weak ferromagnetism (spontaneous magnetism with a net magnetic moment) at 36 K.[40]

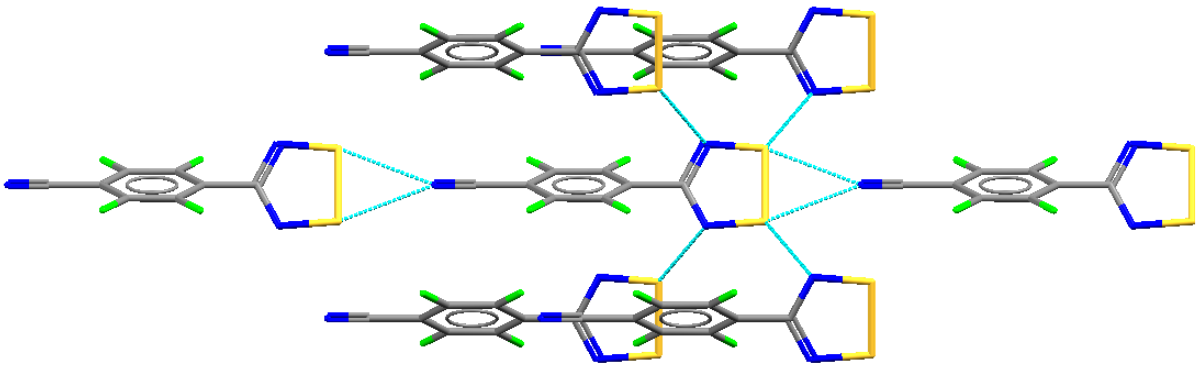

Figure 1.8: Crystal structure of p-*NC-C_6F_4CNSSN$^{\bullet}$ (β-phase) showing the co-parallel chains and the short S···N contacts (cyan lines) between radicals that form a magnetic exchange pathway*

Another *para*-substituted perfluorinated dithiadiazolyl, *p*-NO_2-C_6F_4CNNSN•, was the second example of a neutral organic radical to display ferromagnetism above 1 K.[41] The material packs in parallel chains with intermolecular S···N contacts, reminiscent of the packing for *p*-NC-C_6F_4CNNSN•.

It should be noted that some dithiadiazolyl radicals, for example 2′,5′-dichlorophenyl-1,2,3,5-dithiadiazolyl[22,42] and 2′-methylphenyl-1,2,3,5-dithiadiazolyl[43] dimerise in the solid state but show EPR evidence of having thermally accessible triplet states (S = 1, see Figure 1.9). These dimers have longer intermolecular distances with weaker dimerization bonding.

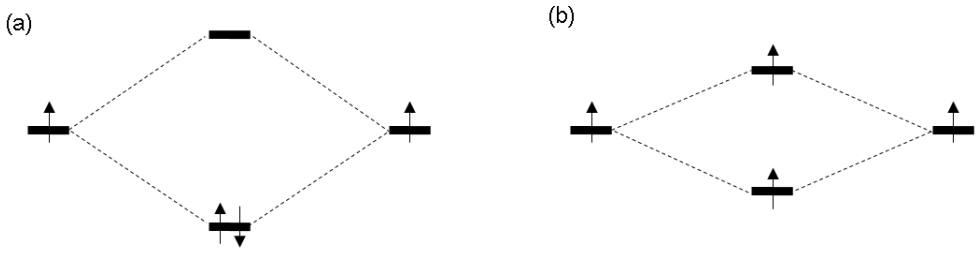

Figure 1.9: (a) Closed-shell singlet ground state for strongly interacting dimers and (b) thermally accessible triplet excited state for weakly interacting dimers (reproduced from reference 21).

1.1.3.3 Properties in Solution

1,2,3,5-Dithiadiazolyl radicals are predominantly dissociated in solution at room temperature, although a concentration-dependant monomer-dimer equilibrium exists, with dimerization occurring at high concentrations.[19] EPR spectroscopy can be used to study and characterise radical solutions.[3]

The typical EPR spectrum of a 1,2,3,5-dithiadiazolyl radical in solution is a pentet in a 1:2:3:2:1 ratio, with a g-value of approximately 2.01. The multiplicity of the signal is a result of coupling of the unpaired electron to the two chemically equivalent ^{14}N nuclei (with $I = 1$), according to the $2nI + 1$ rule.[3] Coupling to sulfur is theoretically possible, but is not usually observed as a result of the low natural abundance of ^{33}S.

1.1.4 Reactivity of 1,2,3,5-dithiadiazolyl radicals

Dithiadiazolyl radicals are thermally stable. They are air and moisture sensitive: nevertheless, they can be handled and manipulated with relative ease.[13] When 1,2,3,5-dithiadiazolyl radicals react with diatomic oxygen under forcing conditions, they form 1,5,2,4,6,8-dithiatetrazocines. The reaction with moisture, however, is much faster under ambient conditions.[80]

1,2,3,5-Dithiadiazolyl radicals are prepared by the reduction of their respective dithiadiazolylium salts. It therefore follows that they can be re-oxidized back to the salt.[3] For example, $(PhCNSSN)_2$ will react with halogens (I_2, Br_2, Cl_2) or with chloride sources ($SOCl_2$, $(NSCl)_3$) to form the analogous dithiadiazolylium halide salt.[44] The dithiadiazolyl $(PhCNSSN)_2$ can also be used as a radical trapping agent.[8] Oxidation can also be performed using high-oxidation-state Lewis acids (e.g. $SnCl_4$).[3]

In addition to undergoing one-electron oxidation to the dithiadiazolylium cation, electrochemical studies have shown that dithiadiazolyls can also undergo one-electron reduction to form a dithiadiazolyl anion, or dithiadiazolide.[29] However, isolation of these anions has been problematic as a result of poor stability and there are few examples in the literature. An unstable salt, [Na(18-C-6)][PhCNSSN] was prepared from reacting $(PhCNSSN)_2$ with sodium amalgam and 18-crown-6.[29] The salt could be isolated and was stable in the solid state but decomposed in solution, preventing recrystallization. Cyclic voltammetry showed that the formation of the dithiadiazolide anion from the neutral radical was a reversible process, provided there was no dithiadiazolyl cation to capture the anion. A dithiadiazolyl anion was prepared (with the utilisation of cyclic voltammetry to observe a reversible wave at $E_{1/2} = -0.95$ V) and encapsulated with cyanostar macrocycles that were shown to stabilise short-lived organic anions.[45] Both examples emphasise the instability of the anion, which decomposes rapidly even under inert atmospheres. Formal reduction of the dithiadiazolyl can occur during complexation to transition metals.

1.1.5 1,2,3,5-Dithiadiazolyl radical metal complexes

There is considerable interest in the use of organic radicals as ligands in metal complexes.[14] The use of "spin bearing" ligands can result in increasing the overall spin of a system. Additionally, radical ligands can potentially act a magnetic exchange pathway between paramagnetic metal centres. This means that radical ligands can form complexes that are useful in the development of materials such as molecule-based magnets (that is, magnetic materials based on discrete molecules rather than metallic materials).[46]

Organic radicals are often also capable of easily oxidising or reducing to a secondary "stable" oxidation state, reached by one-electron oxidation or reduction to produce a diamagnetic compound. This results in metal complexes with interesting physical properties directly related to the intramolecular redox ability. It has been shown that numerous metalloproteins contain radical ligands in their active sites,[47] and this has driven research into the use of organic radicals as ligands in metal complexes as models for studying bioinorganic processes.[14] Examples of non-thiazyl radical ligands include the phenoxyl radical and its derivatives, as well as the verdazyl and nitronitroxide neutral radicals.[13]

While a variety of thiazyl radicals have been synthesised and studied, the greatest number of coordination compounds is found for the 1,2,3,5-dithiadiazolyl radical.[14] This is predominantly due to the relative ease of synthesis and purification of a wide range of dithiadiazolyls.[14] The nature of the SOMO of the dithiadiazolyl radical presents an interesting feature to its coordination chemistry: the spin density is distributed over two types of heteroatom. Both the sulfur and nitrogen atoms have a significant positive spin density and can act as donor atoms.[14] Consequently, the coordination compounds of dithiadiazolyls can be divided into two categories: coordination through the sulfur atoms, and coordination through the nitrogen atoms.[14] A select few examples will be discussed.

1.1.5.1 Coordination through sulfur

The first coordination complex of a dithiadiazolyl involved sulfur-metal bonds. In general, this is observed when low valent metal ions are involved. In the simplest case, the dithiadiazolyl sulfur-sulfur bond can be considered analogous to a disulfide (RSSR) reacting to produce two thiolates (RS^-). The first complex was formed from $PhCNSSN^\bullet$ reacting with either $Fe_2(CO)_9$ or $Fe_3(CO)_{12}$.[48] The structure has a $(\mu^1\text{-}CO)_3Fe–Fe(\mu^1\text{-}CO)_3$ fragment coordinated to the two sulfur atoms of the radical in a μ^2 bridging fashion (Figure 1.10). The S–S bond distance, at 2.930(2) Å, is significantly longer than the ~2.1 Å observed for the dithiadiazolyl dimer[17], suggesting that the S–S bond breaks during the formation of the complex. Subsequent ^1H NMR and IR spectroscopic analysis, together with re-evaluation of the crystal structure data, revealed that there is a hydrogen atom bonded to one of the

nitrogen atoms and that the complex contained a closed shell imine, not a thiazyl radical.[49,50] The iron centre can be considered to be formally Fe(I), with the ligand being a dianion.

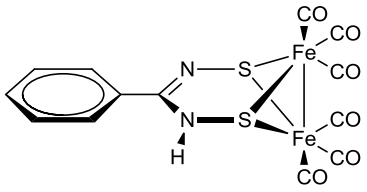

Figure 1.10: Iron(1) complex of 4-phenyl-1,2,3,5-dithiadiazolyl (reproduced from reference 13).

When PhCNSSN• is reacted with $[Ni(Cp)(CO)]_2$ (Cp = cyclopentadienyl), a complex similar to the iron analogue can be prepared (Figure 1.11).[51] The S–S distance of 2.905(2) Å again indicates that the sulfur-sulfur bond has broken, with the sulfur atoms being bridged by the CpNi-NiCp moiety. This complex, however, does not become protonated and retains the original paramagnetic nature of the radical, with EPR spectroscopic evidence and Hückel molecular orbital calculations indicating that the unpaired electron is primarily delocalised over the sulfur, carbon and nickel atoms. The original publication featured an unusually long Ni–Ni bond, with each metal atom having 19 electrons. Later analysis proposed an unusually short non-bonding distance between the nickel atoms, with each having 18 electrons.[52] Both these accounts view the dithiadiazolyl radical as a 6 electron donor. Considering the evidence that the unpaired electron is delocalised over the metal-containing part of the compound, the dithiadiazolyl should perhaps be regarded as a 5 electron donor with a formal charge of zero. This gives each nickel 17.5 electrons in the absence of a Ni–Ni bond, or 18.5 electrons in the presence of it. The ambiguity of the electron distribution and bonding in this complex hints towards the non-innocence[1] of the ligand.[14]

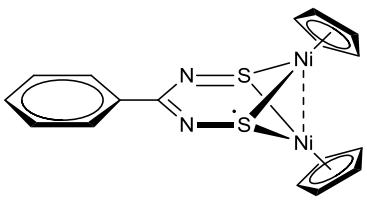

Figure 1.11: Nickel(II) complex of 4-phenyl-1,2,3,5-dithiadiazolyl (reproduced from reference 13).

Reacting PhCNSSN• with $Pt(PPh_3)_3$ results in the formation of a complex with different coordination geometry.[53] The two sulfur atoms are bridged with a platinum centre, which retains two triphenylphosphine ligands. The geometry around the platinum is pseudo-square planar, however the metalloheterocycle itself is not planar (Figure 1.12 (a)). EPR spectroscopy results show that the

[1] An innocent ligand is one for which the oxidation state is clear. A non-innocent, or suspect, ligand has an oxidation state that is unclear; these ligands are usually redox active.[79]

complex is paramagnetic, with coupling to the nitrogen, platinum and phosphorus nuclei observed. The dithiadiazolyl ligand can be considered as a radical dianion, as was seen for the Fe(I) and Ni(II) complexes. However, here the ligand acts as a $2e^-$ donor, unlike in the previous systems where the dithiadiazolyl acts as a $6e^-$ donor. The complex slowly decomposes in solution to form a diamagnetic triplatinum complex (Figure 1.12 (b)). Analogous tripalladium complexes can be synthesised from the reaction of RCNSSN$^\bullet$ (R = Ph, 3′-pyridyl or 4′-pyridyl) with $Pd(PPh_3)_4$.[54,55] For both the triplatinum and tripalladium complexes, the ligand acts as a $5e^-$ donor ligand that is formally $DTDA^{3-}$, with each M(II) metal centre adopting a $16e^-$ square planar coordination geometry. Through the use of chelate phosphines to slow down trimer formation, the monometallic palladium complex can be isolated.[81]

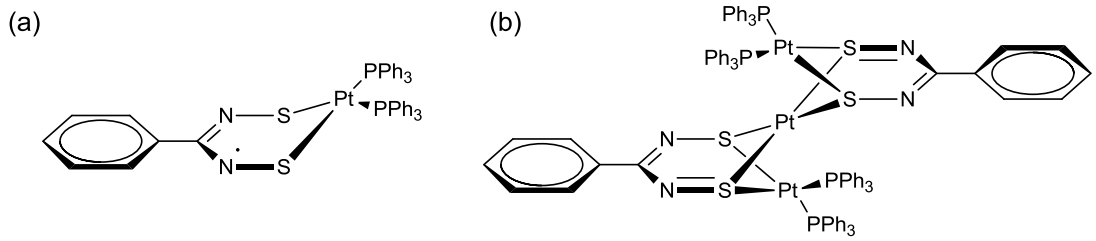

Figure 1.12: (a) Platinum(0) complex of 4-phenyl-1,2,3,5-dithiadiazolyl (b) The diamagnetic triplatinum complex formed upon decomposition of the monoplatinum complex (reproduced from reference 13).

The sulfur-coordinated complexes discussed thus far all involve cleavage of the S–S bond. In contrast, the chromium(I) complexes (Figure 1.13) of a range of R-PhCNSSN ligands have been shown to retain their S–S bonds (with bond distances between 2.114(1) and 2.146(3) Å).[56] All three complexes have a single chromium atom coordinated to both sulfur atoms. The chromium coordination sphere is completed with two carbonyl ligands and one cyclopentadienyl ligand. The crystal structures show the presence of the *exo* isomer for R = 4′-CH_3, and the *endo* isomer for R = 4′-Cl or R^1 = 3′-CN, R^2 = 5′-^{t}Bu. ^{1}H NMR spectra show that all three complexes have both isomers present in solution.[56]

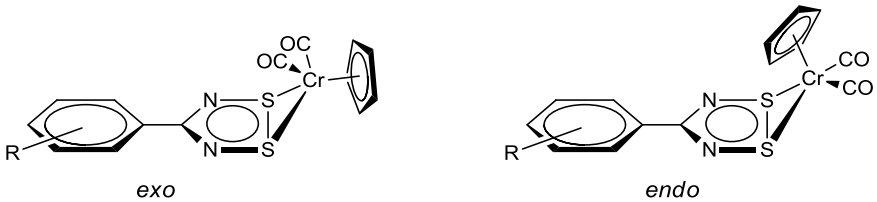

Figure 1.13: Chromium(I) complexes of 1,2,3,5-dithidiazolyls (R = 4′-CH_3, 4′-Cl or R^1 = 3′-CN, R^2 =5′-^{t}Bu) (reproduced from reference 13).

1.1.5.2 Coordination through Nitrogen

More recently, it has been shown that dithiadiazolyl radicals can form N-coordinated metal complexes. This is typically achieved by using divalent metal ions together with electron-withdrawing

ligands to ensure coordination to the relatively hard nitrogen atom instead of the softer sulfur atom. The lone pair of the nitrogen atom acts as a σ-donor and as a result, metal coordination occurs in the plane of the heterocycle (as opposed to the out-of-plane coordination for sulfur). The heterocycle remains intact, with no observed bond cleavage.[14] Unlike the complex differences in formal oxidation state of the dithiadiazolyl in the sulfur-bound ligand systems, these N-bound complexes remain neutral radicals.

Most examples in the literature involve the use of 4-(2′-pyridyl)-1,2,3,5-dithiadiazolyl, which can be considered a paramagnetic analogue of the commonly used 2,2′-bipyridyl ligand.[14] This ligand forms complexes with $M(hfac)_2$ fragments, as seen in Figure 1.14 (M = Co(II), Cu(II) or Mn(II), hfac = hexafluoroacetylacetonato ligand).[57,58] The complexes are typically paramagnetic, with the unpaired electron residing in a π* SOMO with a significant amount of spin density on the coordinating nitrogen atom. Relatively strong magnetic coupling is consequently observed between the dithiadiazolyl and the unpaired electrons of the metal. However, the Cu(II) and Mn(II) complexes form intermolecular dimers through S···S interactions.

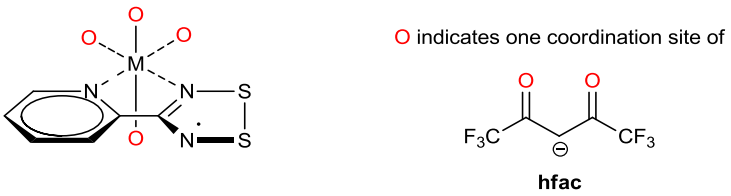

Figure 1.14: N-coordinated metal complexes of 4-(2'-pyridyl)-1,2,3,5-dithiadiazolyl (M = Co, Cu, Mn) and hfac (hexafluoroacetylacetonato ligand) (reproduced from reference 13).

Dithiadiazolyl ligands that coordinate to more than one metal centre have also been reported. The dimanganese (II) complex of 4-(2′-pyrimidine)-1,2,3,5-dithiadiazolyl has been prepared and shown to be paramagnetic (Figure 1.15).[59] Antiferromagnetic coupling between each metal ion and the paramagnetic ligand is observed and gives rise to a ground state spin of $S = 9/2$. Dimer formation is prevented by the steric bulk of the hfac ligands, and no close intermolecular thiazyl contacts are observed in the solid state.

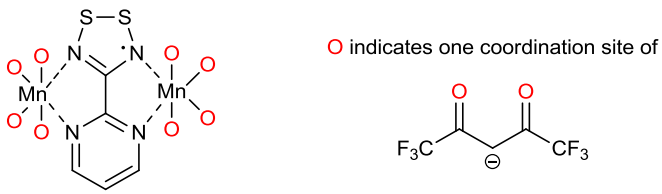

Figure 1.15: Manganese (II) complex of 4-(2'-pyrimidine)-1,2,3,5-dithiadiazolyl and hfac (reproduced from reference 13).

Chain-like coordination compounds can also be formed. Cyanofuryl dithiadiazolyl forms metal-ligand-metal-ligand coordination polymers with $M(hfac)_2$ fragments (M = Mn(II), Co(II) or Ni(II)).[60] This is the first example of a monodentate N-coordinated dithiadiazolyl ligand. There are two different coordination modes present in the polymeric species (Figure 1.16). One $M(hfac)_2$ unit has two axial dithiadiazolyl ligands, each coordinated through a single thiazyl nitrogen. The second $M(hfac)_2$ unit also has two axial dithiadiazolyl ligands, however these are coordinated through the nitrile nitrogen. The material is overall diamagnetic as the dithiadiazolyl radicals form dimers *via trans*-cofacial interactions between radicals in adjacent chains.

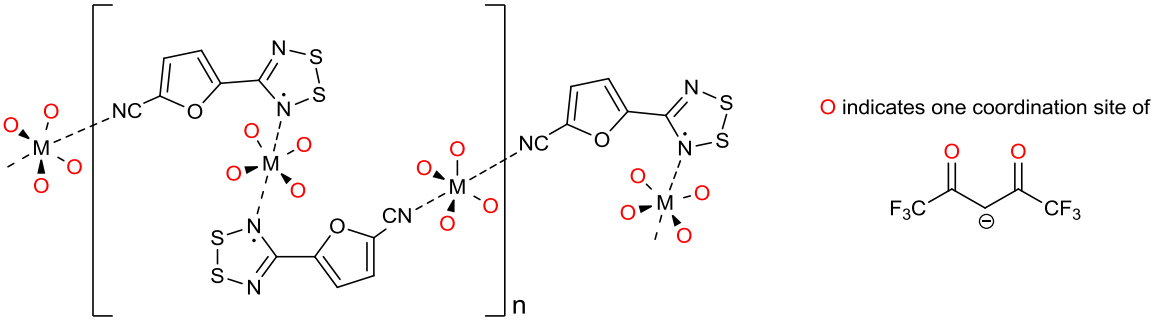

Figure 1.16: Coordination polymer of 4-(2'cyanofuryl)-1,2,3,5-dithiadiazolyl with $M(hfac)_2$ (M = Mn(II), Co(II) or Ni(II)) (reproduced from reference 13).

A nickel coordination complex , illustrated in Figure 1.17, has been shown to stack in a "staircase-like" arrangement.[61] This complex was the first example of a dithiadiazolyl metal complex that showed intermolecular ferromagnetic coupling, facilitated by ligand-ligand interactions.

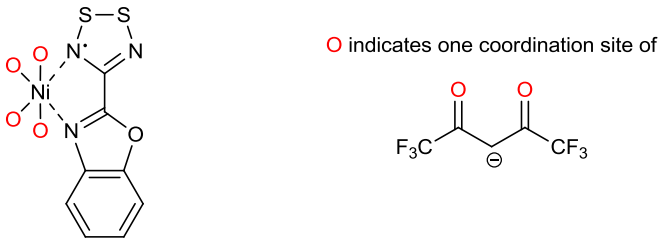

Figure 1.17: Coordination complex of $Ni(hfac)_2$ with 4-(benzoxazol-2 -yl)-1,2,3,5-dithiadiazolyl (reproduced from reference 60).

A benzoxazole dithiadiazolyl ligand has also been shown to coordinate to the rare-earth metal dysprosium (Figure 1.18).[62] A supramolecular species comprised of two of these Dy(II) complexes, held together as a twisted co-facial dimer, exhibits properties of a single-molecule magnet that can be fine-tuned through an external magnetic field.

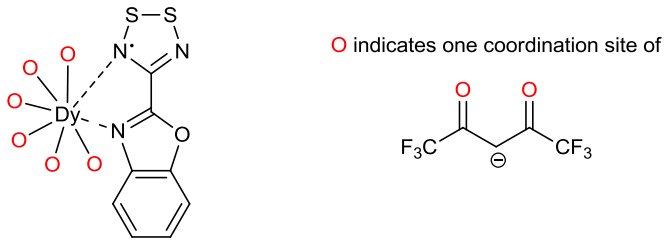

Figure 1.18: Coordination complex of Dy(hfac)$_3$ with 4-(benzoxazol-20 -yl)-1,2,3,5-dithiadiazolyl (reproduced from reference 61)

Another lanthanide-dithiadiazolyl complex, with ten-coordinate lanthanum (III) centres (Figure 1.19), uses the dimerization of the dithiadiazolyl radicals as a supramolecular synthon.[63] At 100 K, these complexes form chains through *trans*-cofacial dithiadiazolyl dimerization. At *ca* 160 K, half of these "pancake" bonds break. At higher temperatures, *ca.* 310 K, all the dimer "pancake bonding" is ruptured. With each breaking of the dithiadiazolyl dimers, the measured magnetic moment increases.

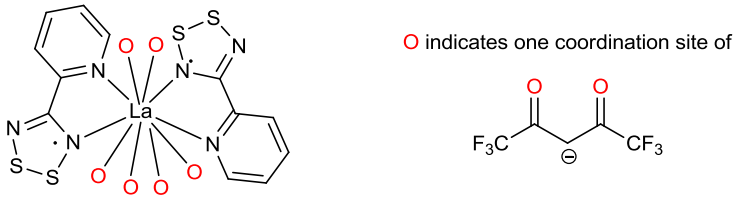

Figure 1.19: Complex of 4-(2′-pyridyl)-1,2,3,5-dithiadiazolyl and La(hfac)$_2$ (reproduced from reference 62).

Recently, introduction of a guest molecule has been used to interrupt dithiadiazolyl pancake bonding and isomerise the host.[64] A ten-coordinate cerium (III) complex can be prepared with two 5-bromo-4-(2′-pyridyl)-1,2,3,5-dithiadiazolyl ligands and three hfac ligands (Figure 1.20 (a)). This complex forms intermolecular twisted cofacial dimers, rendering the material diamagnetic. However, these dimers are slightly staggered and have longer distances than is typical for twisted cofacial dimers. When the material is exposed to triphenylantimony chloride ($SbPh_3Cl_2$), a 2:1 host-guest co-crystal is formed, with substantial rearrangement of the ligand sphere (Figure 1.20 (b)). The rearranged Ce(III) complexes again exhibit intermolecular pancake bonding, however, in this case the dimers have *cis*-cofacial geometry. Rearrangement thus requires breaking and reforming the dithiadiazolyl dimers.

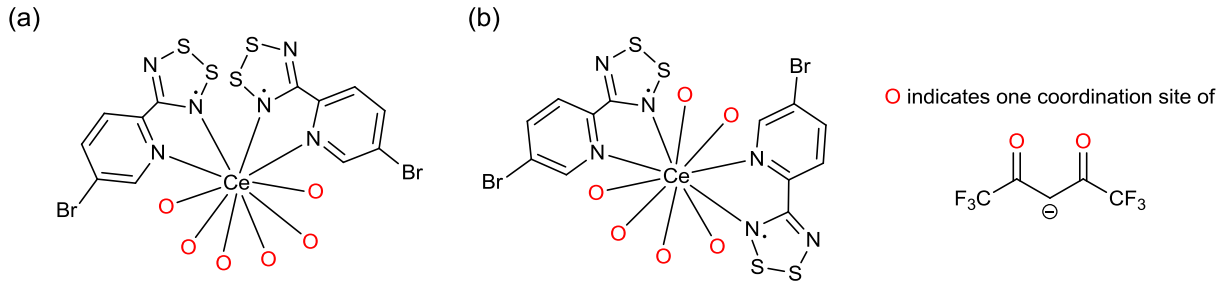

Figure 1.20: (a) Complex of 5-bromo-4-(2'-pyridyl)-1,2,3,5-dithiadiazolyl and Ce(hfac)$_3$ and (b) the isomerised complex after insertion of the $SbPh_3Cl_2$ guest (reproduced from reference 63).

1.2 Introduction to porphyrins

1.2.1 Structure and synthesis

The basic porphyrin scaffold is an aromatic core of four pyrrole units (numbered I, II, III and IV) joined with methine-carbon bridges (α, β, γ, δ). The structure of this scaffold is shown in Figure 1.21. If positions 5, 10, 15 and 20 contain hydrogen atoms, the molecule – the simplest porphyrin - is called porphin.[65,66]

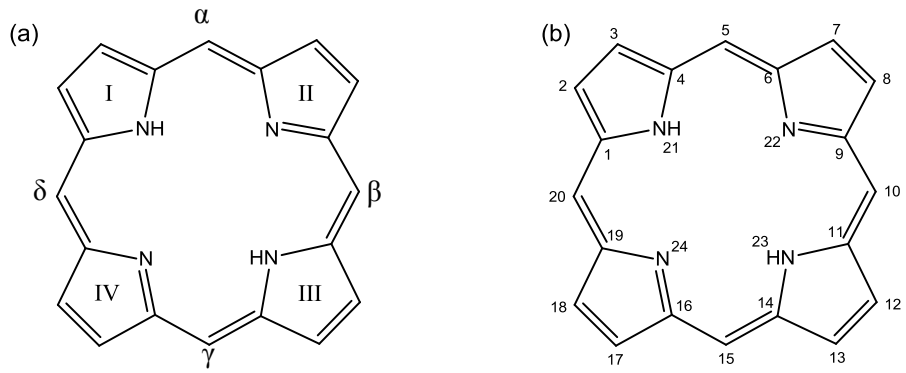

*Figure 1.21: Structure of the basic porphyrin scaffold with (a) ring numbering and bridging (*meso*) carbon notation and (b) atom numbering for the twenty-carbon porphyrin core*

If one of the pyrrole double bonds, between carbons 7 and 8, is reduced, the molecule is termed a chlorin.[67] If two of these bonds are reduced (between carbons 7 and 8, and between carbons 17 and 18), the molecule is termed a bacteriochlorin.[68] The inner two pyrrolic hydrogens are basic (as such, the parent porphyrin is sometimes referred to as the free-base porphyrin) and can be substituted with a variety of metals to form the porphyrin metal salts or metalloporphyrins, wherein the metal cation is chelated by the aromatic, doubly anionic porphyrin core.[65] The structures of a chlorin, bacteriochlorin and metalloporphyrin are shown in Figure 1.22.

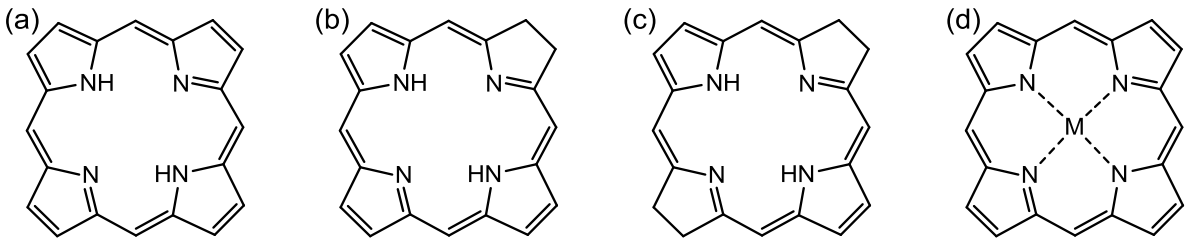

Figure 1.22: Core structures of (a) porphyrins, (b) chlorins, (c) bacteriochlorins and (d) metalloporphyrins

Early work on porphyrins focused on the study of biological porphyrins, such as haem, the molecule in blood responsible for binding and carrying oxygen (see Chapter 5 for more on haem), as well as biologically occurring chlorins such as chlorophyll. The structures of haem B, the most commonly occurring haem, and chlorophyll A, the most commonly occurring chlorophyll in terrestrial plants, are shown in Figure 1.23.

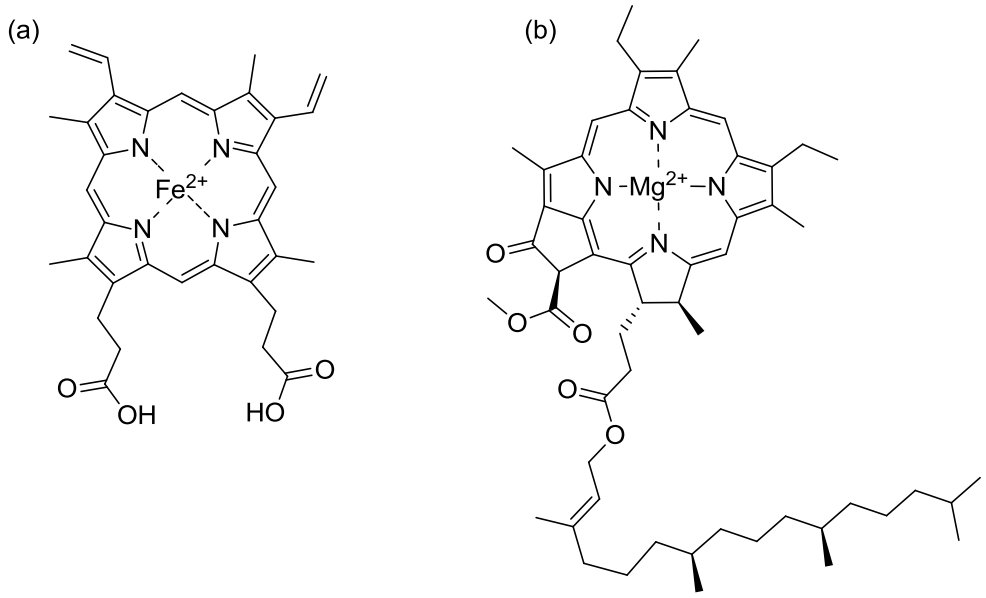

Figure 1.23: Structures of (a) haem B and (b) chlorophyll A

A synthetic porphyrin, α,β,γ,δ-tetramethylporphyrin, was first prepared in 1935 by Paul Rothemund from the condensation of pyrrole and acetaldehyde in methanol,[69] with the parent porphyrin, porphin, prepared from pyrrole and formaldehyde.[66,69] At the same time Hans Fischer, who had received the Nobel Prize in Chemistry in 1930 for his work on haemin and chlorophyll, reported the synthesis of porphin from pyrrole-α-aldehyde and formic acid.[70] Early synthetic routes to porphyrins were generally low yielding and produced by-products that required extensive purification procedures. In

1967, Adler and co-workers published an improved synthesis of *meso*-tetraphenylporphyrin (or 5,10,15,20-tetraphenylporphyrin) and other aromatic derivatives, based on the Rothemund synthesis. This procedure involved refluxing pyrrole and benzaldehyde in propionic acid, with atmospheric oxygen providing oxidation to the porphyrin (Figure 1.24).[71] Three years later, Adler published a procedure for the preparation of metalloporphyrins in high yield, namely refluxing the free-base porphyrin with a metal salt in *N*,*N*-dimethylformamide (Figure 1.24).[72] Both procedures are still widely used today.

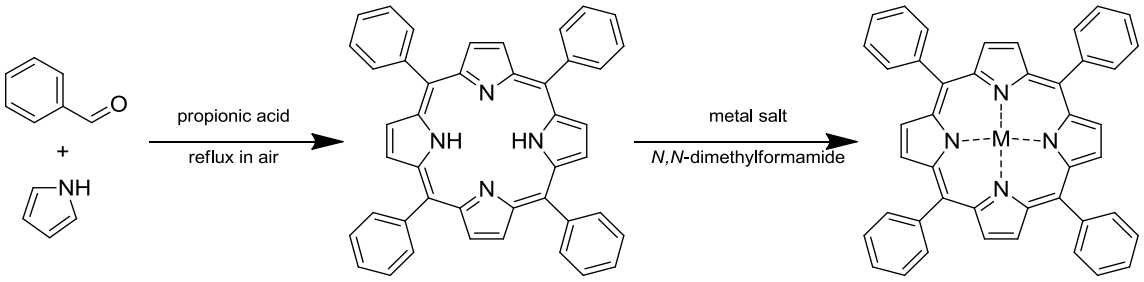

Figure 1.24: Synthetic scheme for the Adler synthesis of tetraphenylporphyrin and metalated tetraphenylporphyrin[71,72]

1.2.2 UV-Vis spectra of porphyrins

As a result of the high level of conjugation present in porphyrins, they are typically brightly coloured and absorb light in the ultraviolet-visible (UV-Vis) region. The UV-Vis spectrum of 5,10,15,20-tetraphenylporphyrin in dichloromethane is shown in Figure 1.25 as an example spectrum of a free-base porphyrin. Free base porphyrins display strong absorbance bands at around 400 nm (420 nm for tetraphenylporphyrin). This band is called the Soret band. There are also four weaker bands in the region between 500 nm and 660 nm, called the Q bands.[67]

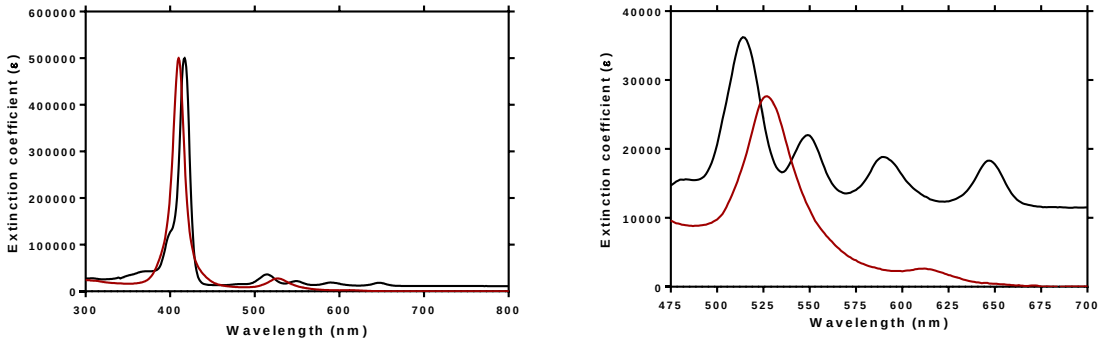

Figure 1.25: (left) UV-Vis spectrum between 300-800 nm and (right) close-up of 475-700 nm region for tetraphenylporphyrin (black) and cobalt (II) tetraphenyl porphyrin (red) (spectra from this work)

When the free base porphyrin is metalated, there is an associated spectroscopic change to both the Soret band and the Q bands. The Soret band shifts, with the direction and extent of the shift dependant on the metal. More noticeably, the four Q bands collapse into two bands as a result of the higher molecular symmetry, again with a shift in wavelength dependant on the metal.[67] The spectrum of cobalt (II) tetraphenylporphyrin is shown in Figure 1.25 as an example.

The UV-vis absorbance bands, both the near-UV Soret band and the visible Q bands, result from π-π* transitions.[67,73] The structure of the porphyrin core, without the peripheral groups, has D_{4h} symmetry.[67] The lowest unoccupied molecular orbitals for porphyrins are two degenerate e_g orbitals.[74] The highest occupied molecular orbital is an a_{2u} orbital, with the next highest being an a_{1u} orbital.[74] The Soret band results from an $a_{1u} \rightarrow e_g$ transition and the Q bands can be assigned to $a_{2u} \rightarrow e_g$ transitions. The energy and symmetry of these two excited states are similar and strong mixing occurs. Charge transfer from the ligand to the metal centre is possible for transition metals with open shells, this results in presence of Charge-Transfer (CT) bands. [74] Changing the substituents on the porphyrin or the nature of the metal influences these molecular orbitals and consequently results in the spectrum shifting and relative intensities of the bands changing.[67] Additionally, for metalloporphyrin-ligand complexes, metal-ligand and ligand-porphyrin interactions must be taken into consideration.[73] Stereoelectronic interactions between the porphyrin π electrons and an axial ligand bonded to the metal influence both the near-ultraviolet and visible transitions.[73] The near-ultraviolet Soret band shifts to longer wavelengths when the metalloporphyrin interacts with strong ligands, with the extent of the shift reliant on the nature of the ligand and the strength of binding to the metal.[73] The Q band region undergoes shifts that are less noticeable than for the Soret band; additionally, the peaks can shift in either direction.[73] By studying the spectroscopic changes upon addition of a ligand to a metalloporphyrin, information about the strength of the interaction between the ligand and the metal can be obtained.

1.2.3 Metalloporphyrins as supramolecular scaffolds

Supramolecular chemistry, or chemistry beyond the molecule, investigates the development of complex molecular systems that can self-assemble or self-organize through a variety of intermolecular interactions.[75] Large molecules like metalloporphyrins are invaluable precursors for supramolecular chemistry as their assemblies possess a variety of interesting architectures.[76] Linkage of metalloporphyrins through axial ligands or through weaker interaction such as π-π interactions and hydrogen bonding, can lead to dimers, one-dimensional chains, two-dimensional sheets or three-dimensional frameworks.[76] Additionally, porphyrins have interesting photo-, electro- and chemical properties that can translate to the materials they form.[76] As a result of their interesting chemical

properties, metalloporphyrins form an important part of biological systems as key elements in a supramolecular assembly. [76] Synthetic metalloporphyrin complexes have been used as model systems for natural complexes used in catalysis, oxygen carriers and photosynthesis.[77,78]

1.3 Aim and objectives of this project

Thiazyl radicals such as the dithiadiazolyl radicals have been shown to exhibit remarkable properties such as conductivity and magnetic behaviour: however, energetically-favoured dimerization of these molecules in the solid state leads to spin pairing and subsequent loss of the unique properties of the radical. As a result of this, research needs to be undertaken to attempt to control the arrangement of these radicals in the solid state. Based on the interesting behaviour of dithiadiazolyl radicals in the solid state, and with the knowledge of the variety of interesting supramolecular architectures that can be designed using porphyrin scaffolds, the initial aim of this project was to attempt to address the problem of controlling the solid-state arrangement of dithiadiazolyl radicals through the use of a metalloporphyrin to template the structural arrangement by means of coordination bonds. Once these materials had been obtained, investigation into their properties could be carried out. However, obtaining solid-state material of these dithiadiazolyl-metalloporphyrin complexes was problematic, so attention turned to investigating if there was an interaction in solution and how different variables affected the interaction, with the ultimate goal of investigating the potential for complexes with interesting magnetic properties.

The aim of this study was thus to investigate the interaction between dithiadiazolyl radicals and metalloporphyrins. To achieve this aim, the following objectives were set:

1. To obtain crystalline material of a coordination compound formed from 4-(4′-pyridyl)-1,2,3,5-dithiadiazolyl and cobalt (II) tetraphenylporphyrin, which had previously been prepared in our group, and to fully characterise this material.
2. To study the speciation of this coordination material in solution, through the use of NMR, EPR and UV-Vis spectroscopy.
3. To study the effect that different aryl substituents on the dithiadiazolyl radical have on the interaction between dithiadiazolyls and metalloporphyrins, through the use of UV-Vis spectroscopy.
4. To study the effect that different peripheral substituents on the metalloporphyrin have on the interaction between dithiadiazolyls and metalloporphyrins, through the use of UV-Vis spectroscopy.

5. To study the effect that different metal centres have on the interaction between dithiadiazolyls and metalloporphyrins, through the use of UV-Vis and EPR spectroscopy.
6. To investigate the interaction between dithiadiazolyl radicals and haematin, a porphyrin of biological origin, to explore any potential biological application.

1.4 References

(1) Miller, J. S. *Adv. Mater.* **1994**, *6* (4), 322.

(2) Rawson, J. M.; Alberola, A.; Whalley, A. *J. Mater. Chem.* **2006**, *16* (26), 2560–2575.

(3) Rawson, J. M.; Banister, A. J.; Lavender, I. *Adv. Heterocycl. Chem.* **1995**, *62*, 137.

(4) Fossey, J.; Lefort, D.; Sorba, J.; Trans. Lomas, J. *Free Radicals in Organic Chemistry*; John Wiley and Sons/Masson, 1995.

(5) Gomberg, M. *J. Am. Chem. Soc.* **1900**, *22* (11), 757–771.

(6) Veciana, J.; Editor. *π-Electron Magnetism: From Molecules to Magnetic Materials.*; Springer-Verlag, Berlin, 2001.

(7) Heisenberg, W. *Z. Phys.* **1928**, *49*, 619.

(8) Labes, M. M.; Love, P.; Nichols, L. F. *Chem. Rev.* **1979**, *79* (1), 1.

(9) Ernest, I.; Holick, W.; Rihs, G.; Schomburg, D.; Shoman, G.; Wenkert, D.; Woodward, R. B. *J. Am. Chem. Soc.* **1981**, *103*, 1540.

(10) Banister, A. J.; Clarke, H. G.; Rayment, I.; Shearer, H. M. M. *Inorg. Nucl. Chem. Lett.* **1974**, *10* (7), 647.

(11) Cordes, A. W.; Haddon, R. C.; Oakley, R. T. *Adv. Mater.* **1994**, *6*, 798.

(12) Rawson, J. M.; Palacio, F.; Veciana, J.; Editor. *Magnetic properties of thiazyl radicals, in: π-Electron Magnetism: From Molecules to Magnetic Materials*; Springer-Verlag, Berlin, 2001.

(13) Haynes, D. A. *CrystEngComm* **2011**, *13* (15), 4793.

(14) Preuss, K. E. *Dalton Trans.* **2007**, No. 23, 2357.

(15) Passmore, J.; Sun, X. *Inorg. Chem.* **1996**, *35*, 1313–1320.

(16) Aherne, C. M.; Banister, A. J.; Luke, A. W.; Rawson, J. M.; Whitehead, R. J. *J. Chem. Soc., Dalt. Trans.* **1992**, 1277.

(17) Vegas, A.; Pérez-Salazar, A.; Banister, A. J.; Hey, R. G. *J. Chem. Soc., Dalt. Trans.* **1980**,

1812.

(18) Preuss, K. E. *Polyhedron* **2014**, *79*, 1.

(19) Fairhurst, S. A.; Johnson, K. M.; Sutcliffe, L. H.; Preston, K. F.; Passmore, J.; Banister, A. J.; Hauptman, Z. V. *J. Chem. Soc., Dalt. Trans.* **1986**, 1465–1472.

(20) Bricklebank, N.; Hargreaves, S.; Spey, S. E. *Polyhedron* **2000**, *19*, 1163–1166.

(21) Barclay, T. M.; Cordes, A. W.; George, N. A.; Haddon, R. C.; Itkis, M. E.; Oakley, R. T. *Chem. Commun.* **1999**, *7*, 2269.

(22) Alberola, A.; Carter, E.; Constantinides, C. P.; Eisler, D. J.; Murphy, D. M.; Rawson, J. M. *Chem. Commun.* **2011**, *47* (9), 2532.

(23) Höfs, H. U.; Bats, J. W.; Gleiter, R.; Hartmann, G.; Mews, R.; Eckert-Maksic, M.; Oberhammer, H.; Sheldrick, G. M. *Chem. Ber.* **1985**, *118*, 3781.

(24) Cordes, A. W.; Goddard, J. D.; Oakley, R. T.; Westwood, N. P. C. *J. Am. Chem. Soc.* **1989**, *111*, 6147.

(25) Banister, A. J.; Hansford, M.; Hauptman, Z. V; Wait, S. T. *J. Chem. Soc., Dalt. Trans.* **1989**, 1705.

(26) Bridson, J. N.; Copp, S. B.; Schriver, M. J.; Shuguang, Z.; Zawarotko, M. *Can. J. Chem.* **1992**, *72*, 1143.

(27) Cordes, A. W.; Haddon, R. C.; Hicks, R. G.; Oakley, R. T.; Palstra, T. T. M. *Inorg. Chem.* **1992**, *31*, 1802.

(28) Robinson, S. W.; Haynes, D. A.; Rawson, J. M. *CrystEngComm* **2013**, *15* (47), 10205.

(29) Aherne, C. M.; Banister, A. J.; Gorrell, I. B.; Hansford, M. I.; Hauptman, Z. V; Luke, A. W.; Rawson, J. M. *J. Chem. Soc. Dalt. Trans.* **1993**, *6*, 968.

(30) Aherne, C. M.; Banister, A. J.; Hibbert, T. G.; Luke, A. W.; Rawson, J. M. *Polyhedron* **1997**, *16* (24), 4239.

(31) Boeré, R. T.; Moock, K. H.; Parvez, M. *Zeitschrift für Anorg. und Allg. Chemie* **1994**, *620* (9), 1589.

(32) Boeré, R. T.; Oakley, R. T.; Reed, R. W. *J. Organomet. Chem.* **1987**, *331*, 161.

(33) Edelmann, F. T. *Coord. Chem. Rev.* **1994**, *137*, 403.

(34) Haynes, D. A.; McInnes, E. J. L.; Passmore, J.; Rawson, J. M. *Phosphorus, Sulfur Silicon Relat. Elem.* **2004**, *179* (4), 869.

(35) Haddon, R. C. *Nature* **1975**, *256*, 394.

(36) Wright, J. D. *Molecular Crystals*; Cambridge University Press, 1995.

(37) Jiles, D. *Introduction to magnetism and magnetic materials*; Chapman and Hall: London, 1991.

(38) Banister, A. J.; Bricklebank, N.; Clegg, W.; Elsegood, M. R. J.; Gregory, C. I.; Lavender, I.; Rawson, J. M.; Tanner, B. K. *J. Chem. Soc. Chem. Commun.* **1995**, 679.

(39) Banister, A. J.; Bricklebank, N.; Lavender, I.; Rawson, J. M.; Gregory, C. I.; Tanner, B. K.; Clegg, W.; Elsegood, M. R. J.; Palacio, F. *Angew. Chemie, Int. Ed.* **1996**, *35* (21), 2533–2535.

(40) Palacio, F.; Antorrena, G.; Castro, M.; Burriel, R.; Rawson, J.; Smith, J. N. B.; Bricklebank, N.; Novoa, J.; Ritter, C. *Phys. Rev. Lett.* **1997**, *79* (12), 2336–2339.

(41) Alberola, A.; Less, R. J.; Pask, C. M.; Rawson, J. M.; Palacio, F.; Oliete, P.; Paulsen, C.; Yamaguchi, A.; Farley, R. D.; Murphy, D. M. *Angew. Chemie - Int. Ed.* **2003**, *42* (39), 4782–4785.

(42) Constantinides, C. P.; Eisler, D. J.; Alberola, A.; Carter, E.; Murphy, D. M.; Rawson, J. M. *CrystEngComm* **2014**, *16* (31), 7298–7312.

(43) Beldjoudi, Y.; Haynes, D. A.; Hayward, J. J.; Manning, W. J.; Pratt, D. R.; Rawson, J. M. *CrystEngComm* **2013**, *15* (6), 1107.

(44) Banister, A. J.; Smith, N. R. M.; Hey, R. G. *J. Chem. Soc. Perkin Trans. 1* **1983**, 1181.

(45) Benson, C. R.; Fatila, E. M.; Lee, S.; Marzo, M. G.; Pink, M.; Mills, M. B.; Preuss, K. E.; Flood, A. H. *J. Am. Chem. Soc.* **2016**, *138*, 15057.

(46) Caneschi, A.; Gatteschi, D.; Sessoli, R. *Acc. Chem. Res.* **1989**, *22*, 392.

(47) Stubbe, J.; van Der Donk, W. A. *Chem. Rev.* **1998**, *98*, 705.

(48) Banister, A. J.; Gorrell, I. B.; Clegg, W.; Jorgensen, K. A. *J. Chem. Soc., Dalt. Trans.* **1989**, 2229.

(49) Klaasen, V.; Preuess, K.; Moock, H.; Boeré, R. T. *Phosphorus, Sulfur Silicon Relat. Elem.* **1994**, *93*, 449.

(50) Boeré, R. T.; Moock, K. H.; Klaasen, V.; Weaver, J.; Lentz, D.; Michael-Shulz, H. *Can. J. Chem.* **1995**, *73*, 1444.

(51) Banister, A. J.; Gorrell, I. B.; Rawson, J. M.; Jorgensen, K. A. *J. Chem. Soc., Dalt. Trans.* **1991**, 1105.

(52) Banister, A. J.; May, I.; Rawson, J. M.; Smith, J. N. B. *J. Organomet. Chem.* **1998**, *550*, 241.

(53) Banister, A. J.; Gorrell, I. B.; Lawrence, S. E.; Lehmann, C. W.; May, I.; Tate, G.; Blake, A.

J.; Rawson, J. M. *J. Chem. Soc., Chem. Commun.* **1994**, 1779.

(54) Banister, A. J.; Gorrell, I. B.; Howard, J. A. K.; Lawrence, S. E.; Lehman, C. W.; May, I.; Rawson, J. M.; Tanner, B. K.; Gregory, C. I.; Blake, A. J.; Fricker, S. P. *J. Chem. Soc. Dalt. Trans. Inorg. Chem.* **1997**, No. 3, 377.

(55) Wong, W.-K.; Sun, C.; Wong, W.-Y.; Kwong, D. W. J.; Wong, W.-T. *Eur. J. Inorg. Chem.* **2000**, 1045.

(56) Lau, H. F.; Ng, V. W. L.; Koh, L. L.; Tan, G. K.; Goh, L. Y.; Roemmele, T. L.; Seagrave, S. D.; Boeré, R. T. *Angew. Chemie Int. Ed.* **2006**, *45* (27), 4498.

(57) Britten, J.; Hearns, N. G. R.; Preuss, K. E.; Richardson, J. F.; Bin-Salamon, S. *Inorg. Chem.* **2007**, *46* (10), 3934–3945.

(58) Hearns, N. G. R.; Preuss, K. E.; Richardson, J. F.; Bin-Salamon, S. *J. Am. Chem. Soc.* **2004**, *126* (32), 9942–9943.

(59) Jennings, M.; Preuss, K. E.; Wu, J. *Chem. Comm* **2006**, 341–343.

(60) Hearns, N. G. R.; Hesp, K. D.; Jennings, M.; Korcok, J. L.; Preuss, K. E.; Smithson, C. S. *Polyhedron* **2006**, *26*, 2047–2053.

(61) Fatila, E. M.; Clerac, R.; Jennings, M.; Preuss, K. E. *Chem. Commun. (Camb).* **2013**, *49* (82), 9431–9433.

(62) Fatila, E. M.; Rouzieres, M.; Jennings, M. C.; Lough, A. J.; Clerac, R.; Preuss, K. E. *J. Am. Chem. Soc.* **2013**, *135* (26), 9596.

(63) Fatila, E. M.; Mayo, R. A.; Rouzieres, M.; Jennings, M. C.; Dechambenoit, P.; Soldatov, D. V; Mathoniere, C.; Clerac, R.; Coulon, C.; Preuss, K. E. *Chem. Mater.* **2015**, *27* (11), 4023.

(64) Mills, M. B.; Hollingshead, A. G.; Maahs, A. C.; Soldatov, D. V.; Preuss, K. E. *CrystEngComm* **2015**, *17* (41), 7816.

(65) Hoard, J. L. *Science (80-.).* **1971**, *174* (4016), 1295.

(66) Rothemund, P. *J. Am. Chem. Soc.* **1936**, *58* (4), 625.

(67) Gouterman, M. *J. Mol. Spectrosc.* **1961**, *6* (1), 138.

(68) Inhoffen, H. H.; Jäger, P. *Tetrahedron Lett.* **1965**, *6* (38), 3387.

(69) Rothemund, P. *J. Am. Chem. Soc.* **1935**, *57* (10), 2010.

(70) Fischer, H.; Gleim, W. *Justus Liebigs Ann. Chem.* **1936**, *521* (1), 157.

(71) Adler, A. D.; Longo, F. R.; Finarelli, J. D.; Goldmacher, J.; Assour, J.; Korsakoff, L. *J. Org. Chem.* **1967**, *32* (2), 476.

(72) Adler, A. D.; Longo, F. R.; Kampas, F.; Kim, J. *J. Inorg. Nucl. Chem.* **1970**, *32* (7), 2443.

(73) Corwin, A. H.; Chivvis, A. B.; Poor, R. W.; Whitten, D. G.; Baker, E. W. *J. Am. Chem. Soc.* **1968**, *90* (24), 6577.

(74) Longuet-Higgens, H. C.; Rectore, C. W.; Platt, J. R. *J. Chem. Phys.* **1950**, *18*, 1174.

(75) Lehn, J.-M.; Ed. *Supramolecular Chemistry: Concept and Perspectives*; VCN: Weinheim, Germany, 1995.

(76) Beletskaya, I.; Tyurin, V. S.; Tsivadze, A. Y.; Guilard, R.; Stern, C. *Chem. Rev.* **2009**, *109*, 1659.

(77) Kadish, K. M.; Smith, K. M.; Guilard, R.; Eds. *Biochemistry and Binding: Activation of Small Molecules. The Porphyrin Handbook, Vol. 4*; Academic Press: San Diego, CA, 2000.

(78) Kadish, K. M.; Smith, K. M.; Guilard, R.; Eds. *Bioinorganic and Bioorganic Chemistry. The Porphyrin Handbook, Vol. 11*; Academic Press: San Diego, CA, 2003.

(79) Jørgensen, C. K. *Coord. Chem. Rev.* **1966**, *1* (1), 164.

(80) Moock, K. H.; Wong, K. M.; Boeré, R. T. *Dalton Trans.* **2011**, *40*, 11599.

(81) Banister, A. J.; Howard, J. A. K.; May, I.; Rawson, J. M. *Chem. Commun.* **1997**, 1763.

Chapter 2

A dithiadiazolyl radical - cobalt porphyrin coordination polymer

---

2.1 Introduction

Thiazyl radicals have been explored as building blocks for the design of molecular materials with desirable physical properties such as conductivity and magnetism.[1–3] Particularly, 1,2,3,5-dithiadiazolyl (DTDA) radicals,[3] together with their metal complexes,[4] have been investigated for their magnetic properties, which are strongly dependent on the arrangement of the molecules, as well as on intermolecular interactions, in the solid state.[5] Dithiadiazolyls tend to dimerise in the solid state, leading to loss of paramagnetism, and as a result attempts have been made to direct the crystal structures of these materials.[5] As dithiadiazolyl radicals have been shown to have interesting behaviour in the solid state, and with the knowledge of the interesting supramolecular architectures that can be designed with porphyrin scaffolds,[6] the aim of this study was to investigate the formation of dithiadiazolyl radical – metalloporphyrin complexes.

As discussed in Chapter 1, dithiadiazolyl radicals can coordinate to metals through several different binding modes.[4] Coordination through a nitrogen atom is the most common in recent literature, including monodentate coordination through one of the dithiadiazolyl nitrogen atoms[7] or bidentate coordination through one of the dithiadiazolyl nitrogen atoms and an adjacent *ortho*-pyridyl nitrogen atom.[8–10] An alternative coordination mode involves both dithiadiazolyl sulfur atoms coordinating to a metal ion, usually with simultaneous sulfur-sulfur bond breaking,[11–13] although a select few examples show retention of the sulfur-sulfur bond.[14] To date, no examples of dithiadiazolyl radicals coordinating to a metal centre through a single sulfur atom have been reported in the literature.

Preliminary work in our group studied the interaction of a *para*-pyridyl dithiadiazolyl radical ligand, which could potentially bridge metal centres, with the well-studied low-spin metalloporphyrin, cobalt (II) tetraphenylporphyrin. A coordination material had been obtained, the crystal structure had been determined and initial studies into its electron paramagnetic resonance behaviour had been performed. No further investigation into the coordination behaviour, redox behaviour or speciation in solution had been done at the time.

The initial aims of this research project were to reproducibly synthesise this material, to fully characterise it, to better understand the coordination behaviour and to study the speciation in solution through a variety of spectroscopic techniques.

2.2 Preparation of *p*-PyrDTDA – CoTPP

First, the two components of the coordination material had to be synthesised. The radical 4-(4′-pyridyl)-1,2,3,5-dithiadiazolyl (*p*-PyrDTDA, **R1**) was synthesised using a known literature procedure from 4-pyridinecarbonitrile (Figure 2.1).[3,15] Experimental details are given in section 2.9.1. The porphyrin 5,10,15,20-tetraphenylporphyrin (H_2TPP) was synthesised *via* the standard condensation of benzaldehyde with pyrrole (Figure 2.2),[16] and was reacted with cobalt (II) acetate to give the Co(II)TPP complex (CoTPP, **P1**).[17] Experimental details are given in section 2.9.2.

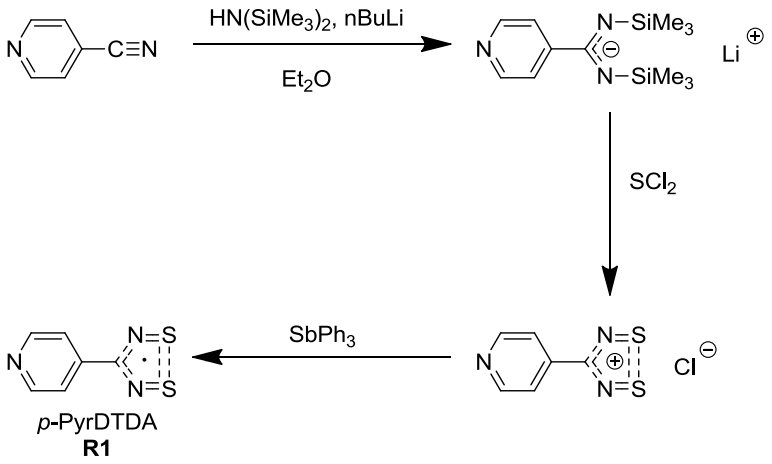

Figure 2.1: Synthesis of p-*PyrDTDA (**R1**)*

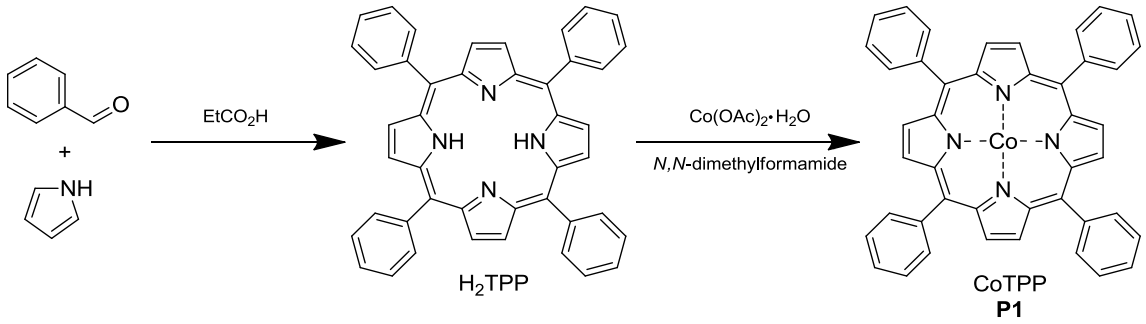

*Figure 2.2: Synthesis of H_2TPP and Co(II)TPP (**P1**)*

To prepare the coordination material, *p*-PyrDTDA was placed in a Schlenk tube under nitrogen with tetrahydrofuran (THF) and one equivalent of CoTPP. The solution was stirred and gently heated until all material dissolved. An equal volume of *n*-hexane was carefully layered above the dark maroon THF solution. After a week, crystals were visible on the sides of the Schlenk tube. The solution was filtered and the dark purple crystals of **R1•P1(THF)** were dried in air. These crystals are stable in air for over a year.

Preparation of pure bulk samples of **R1•P1(THF)** still remains challenging. Bulk samples are almost always contaminated with excess **P1**, even when two equivalents of **R1** are added to one equivalent of **P1**. Crystals of **R1•P1** form very thin plates that are difficult to analyse by X-ray diffraction. In an attempt at obtaining better quality crystals, as well as bulk samples with higher purity, other solvents, such as dichloromethane (DCM) and toluene, were attempted in place of THF but were unsuccessful in yielding diffraction-quality crystalline material that contained both dithiadiazolyl and metalloporphyrin. Alternative crystallization techniques including vapour diffusion, slow evaporation, sublimation and solvothermal conditions were attempted but failed where solvent layering succeeded. Liquid assisted grinding, using either THF or DCM, was also unsuccessful in transforming a physical mixture of dithiadiazolyl and metalloporphyrin into a coordination material, as determined by powder X-ray diffraction. An amorphous blue-green by-product sometimes forms together with **R1•P1(THF)**, however attempts to characterise this material by microanalysis, powder X-ray diffraction, nuclear magnetic resonance spectroscopy, ultraviolet-visible spectroscopy and electron paramagnetic resonance spectroscopy have thus far been unsuccessful. It appears that this material is a complex mixture of side products that cannot be separated.

2.3 Crystal structure of *p*-PyrDTDA – CoTPP

Preliminary work on *p*-PyrDTDA – CoTPP was done by our group, which included the crystal structure determination.[18] For the purposes of this study, crystals of *p*-PyrDTDA – CoTPP were synthesized and the crystal structure re-determined as it provided a good starting point for understanding the system, as well as establishing reproducibility. The material **R1•P1(THF)** crystallizes as a coordination polymer in the monoclinic space group Pn (Table 2.1). Full crystallographic details, as well as problems encountered during structure solution and refinement, are detailed in section 2.9.4 and Appendix A.

*Table 2.1: Table of parameters for **R1·P1(THF)***

Parameter	**Experimental value**
Complex identification	**R1·P1(THF)**
Empirical formula	$C_{58}H_{48}CoN_7O_2S_2$
Formula weight	998.02
Temperature	100(2) K
Wavelength	0.71073 Å
Crystal description	Thin red-purple plate
Crystal structure	monoclinic
Space group	*Pn*
a	12.8343(3) Å
b	24.280(6) Å
c	15.784(4) Å
α	90.00°
β	101.850(3)°
γ	90.00°
Volume	4813.63 $Å^3$
Z	4
Calculated density	1.377 $g.cm^{-3}$
F(000)	2080
Crystal size	0.53 mm × 0.19mm × 0.06mm
θ_{min}, θ_{max}	0.84 °, 27.90°
T_{min}, T_{max}	0.7778, 0.9689
Reflections collected / unique	52671 / 20710
R_{int}	0.0881
R1[I>2σ(I)]	0.0655

The asymmetric unit contains two metalloporphyrin-radical pairs, as well as four molecules of THF with incomplete occupancy. One such *p*-PyrDTDA – CoTPP unit is shown in Figure 2.3. Both

independent units display S_4 -ruffled porphyrin core conformations (that is, up-down-up-down displacement of the four porphyrin core methine carbon atoms), with mean absolute perpendicular displacements of the *meso*-carbon atoms, relative to the mean plane of the metalloporphyrin, of 0.44(4) and 0.40(3) Å for the two crystallographically independent units .[19] Additionally, the sulfur atoms coordinated to the cobalt centre are distorted out of the plane of their respective dithiadiazolyl rings. The two *p*-PyrDTDA – CoTPP pairs each represent the monomer unit of a crystallographically unique **R1•P1** coordination polymer, in which the dithiadiazolyl radical **R1** forms a bridge between two six-coordinate cobalt centres through both a Co–S bond and a Co–N_{pyr} bond (Figure 2.4). For the two crystallographically independent polymer chains, the Co–S distances are 2.2509(4) and 2.2597(4) Å, and the Co–N_{pyr} distances are 2.0996(3) and 2.0892(3) Å respectively.

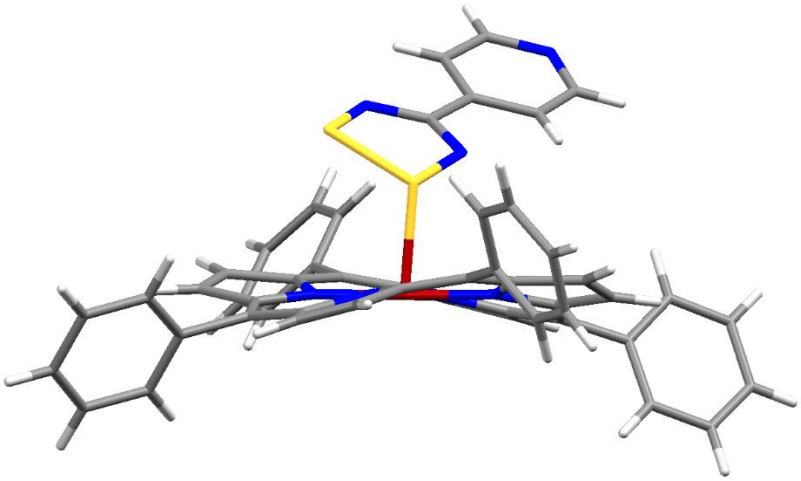

Figure 2.3: One of the p-*PyrDTDA - CoTPP monomers in the asymmetric unit of **R1•P1**, showing a coordination bond between one of the DTDA sulfur atoms and the cobalt centre. Ruffling of the porphyrin core can also be observed.*

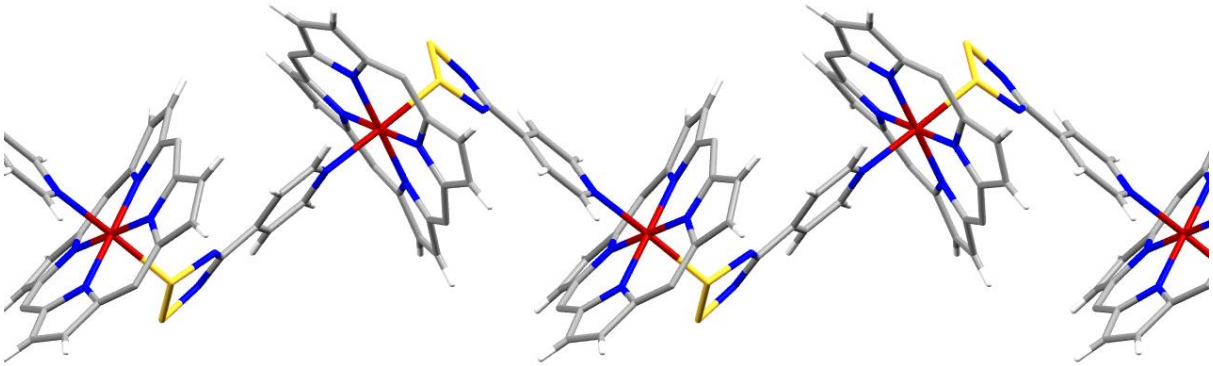

Figure 2.4: A coordination polymer chain formed from p-*PyrDTDA and CoTPP, as viewed down the b axis, showing coordination between the cobalt ion and the radical through both the heterocyclic sulfur and the pyridyl nitrogen. Phenyl groups on the porphyrin have been omitted for clarity.*

Coordination polymer chains are thus formed through the material; these run parallel to the c-axis and stack above each other along the a-axis (Figure 2.5). The two crystallographically independent chains alternate along the *b*-axis and run parallel to one another. The disordered THF molecules are located in channels that run along the *a*-axis, which can be modelled at approximately 80 % occupancy.

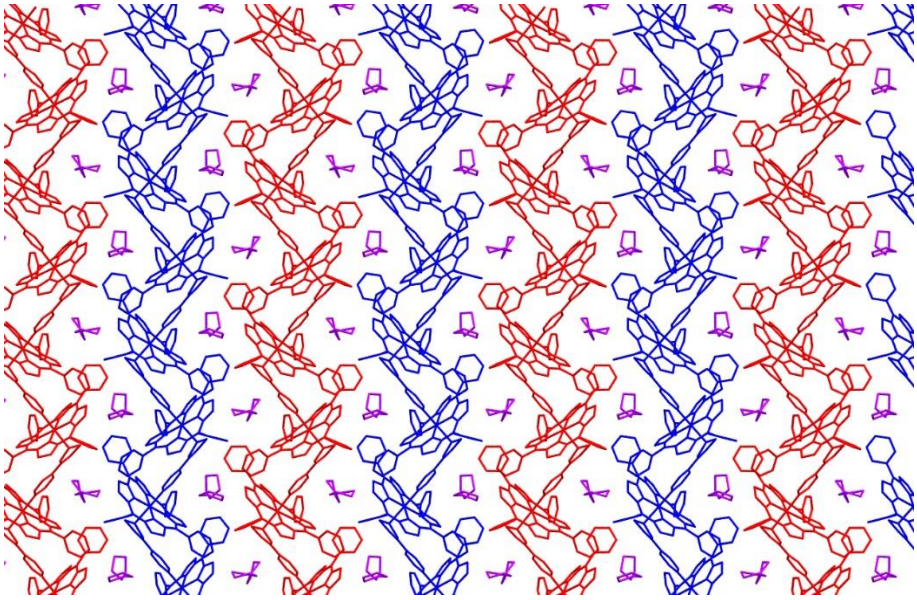

*Figure 2.5: Packing diagram of **R1•P1(THF)** as viewed down the* a*-axis. Hydrogen atoms have been omitted for clarity. There are two crystallographically independent coordination polymer chains, shown in red and blue. Disordered THF molecules are shown in purple.*

The S–S bond lengths in this structure were of particular interest, since it was necessary to determine if this bond remained intact upon coordination. The sum of the van der Waals radii for two sulfur atoms is 3.60 Å;[20] for an intact S–S bond, the interatomic distance must be significantly shorter than this. The S–S bond lengths for the two independent molecules in **R1•P1(THF)** are 2.120(2) and 2.122(2) Å respectively, which reinforces that the sulfur-sulfur bonds are indeed intact. Unfortunately, the S–S bond length in *p*-PyrDTDA (**R1**) alone is unknown as its crystal structure is currently not reported (the material sublimes as a crystalline powder, getting crystals has so far proved to be very difficult); however the average S–S bond length for 1,2,3,5-dithiadiazolyls reported in the Cambridge Structural Database[20] is 2.089(9) Å.[18] The longest S–S bond distance currently reported for a 1,2,3,5-dithiadiazolyl is 2.102 Å.[15] The bond lengths in **R1•P1(THF)**, with an average of 2.121 Å, are 0.02 Å longer than this, which is noteworthy.

A possible explanation for these unusually long sulfur–sulfur bonds is that there is delocalisation of electron density from the Co(II) ion to the dithiadiazolyl. Transfer of the unpaired electron from the cobalt $3dz^2$ orbital to the dithiadiazolyl π-SOMO would result in a lengthened S–S bond length, as the SOMO is antibonding with regards to this bond (see Chapter 1). The result of this electron transfer is the cobalt being oxidised to Co(III) while the dithiadiazolyl is reduced to the dithiadiazolide anion. It is most likely that this electron transfer is only partial, as the bond lengths are in-between that typical for Co(II) and Co(III), meaning that the coordination polymer is a resonance hybrid consisting of both Co(II) and Co(III) moieties in the solid state.

Having successfully synthesised the *p*-PyrDTDA – CoTPP coordination polymer, it was necessary to initiate investigation into the coordination behaviour occurring in solution, as this had not been studied previously. Firstly, electron paramagnetic resonance spectroscopy was utilized to study the formation and dissolution of the coordination polymer, to establish if the species involved were paramagnetic or diamagnetic. Secondly, nuclear magnetic resonance spectroscopy was used to investigate the solution speciation of the system. Finally, ultraviolet-visible spectroscopy was employed to study the initial association of the dithiadiazolyl **R1** to the porphyrin **P1** in solution. However, it was first necessary to ensure that the bulk sample of **R1•P1**(**THF**) synthesised was indeed a coordination material and not a physical mixture of the radical and porphyrin. Powder X-ray diffraction of the sample was inconclusive owing to the partially amorphous nature of the sample (see section 2.9.5 for PXRD patterns). Infrared spectroscopy was consequently used to establish if the bulk sample contained the coordination material.

2.4 Infrared Spectroscopy

Fourier transfer infrared spectroscopy (FT-IR) of a bulk sample of the coordination material compared to *p*-PyrDTDA reveals some subtle differences in the fingerprint region (Figure 2.6). Bands for the dithiadiazolyl[22] shift to lower frequencies for the coordination material. This is consistent with coordination to a metal centre and with metal-to-ligand backbonding reducing bond orders. For example, the asymmetric stretch for the dithiadiazolyl N-S shifts from 816 cm^{-1} to 795 cm^{-1}, the pyridyl C-N-C in-plane bend shifts from 640 cm^{-1} to 582 cm^{-1} and the in-plane dithiadiazolyl N-C-N bend shifts from 777 cm^{-1} to 752 cm^{-1}.[22] The shift of these peaks is consistent with the sample containing the dithiadiazolyl coordinated to CoTPP. The tailing evident between 3000 and 2200 cm^{-1} for the spectrum belonging to the coordination material could be an absorption band arising from low energy charge-transfer.

Having confirmed that the bulk sample did indeed contain coordination material of **R1•P1**(**THF**), electron paramagnetic resonance spectroscopy was used to study the material.

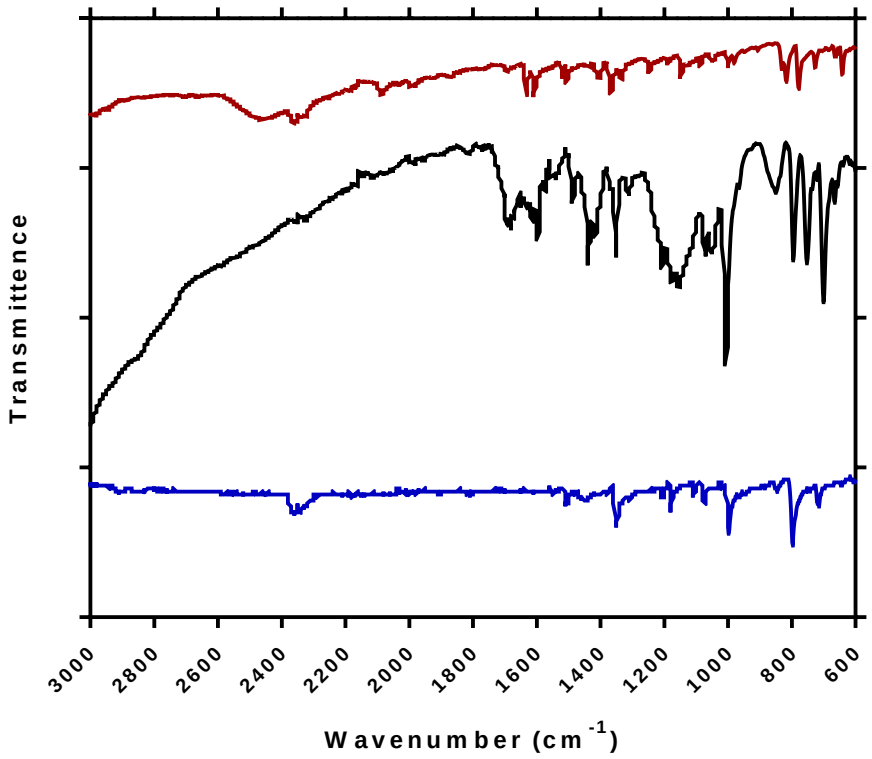

Figure 2.6: Infrared spectra for p-*PyrDTDA (in red), the coordination polymer* ***R1•P1*** *(in black) and CoTPP (in blue)*

2.5 Electron Paramagnetic Resonance Spectroscopy

As discussed in Chapter 1, dithiadiazolyl radicals display a characteristic Electron Paramagnetic Resonance (EPR) signal. The typical EPR spectrum of a 1,2,3,5-dithiadiazolyl radical in solution is a pentet in a 1:2:3:2:1 ratio, with a g-value of approximately 2.01. The EPR experiments in this study were run under ambient conditions.

However, coordination polymer **R1•P1(THF)** is EPR silent both as a solid and in dichloromethane solution (as shown by previous work in our group).[18] It was therefore of interest whether this effect is present when the two components interact in solution. A 5 mM solution of *p*-PyrDTDA in 9:1 dichloromethane:dimethylsulfoxide was made up. An aliquot of this solution was placed in an oven-dried sample tube and the EPR spectrum collected. As quickly as possible, 0.25 molar equivalents of CoTPP (2 mM stock solution in DCM) were added, the tube inverted to mix and the spectrum recollected. This was repeated until 1 full equivalent of CoTPP had been added. The resulting spectra are shown in Figure 2.7 (for simplicity, only the first and last additions of CoTPP are shown).

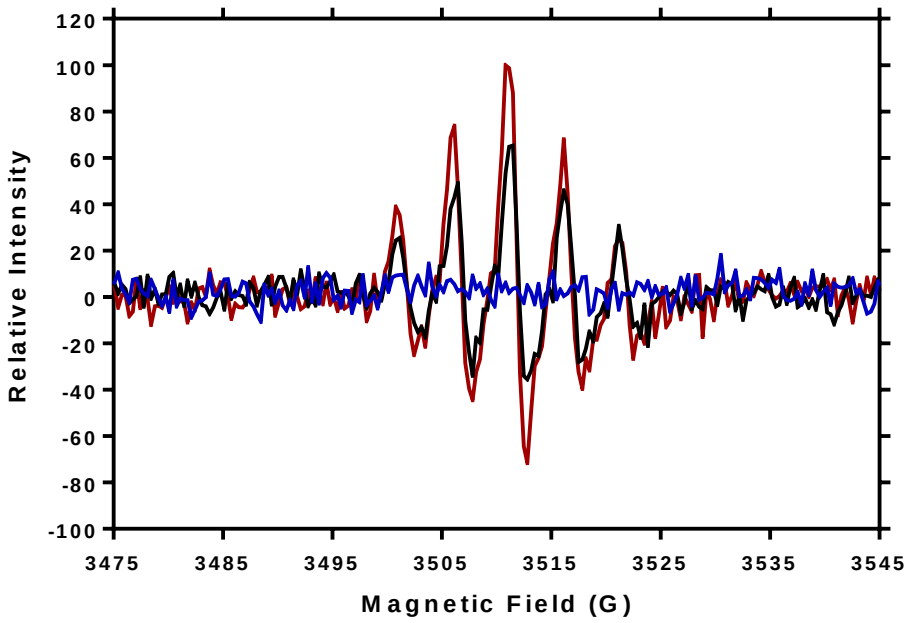

Figure 2.7: Room temperature EPR spectra for p-*PyrDTDA in DCM (shown in red), after the addition of 0.25 equivalents of CoTPP (shown in black) and after the addition of one mole equivalent of CoTPP (shown in blue). Microwave frequency = 9.878 GHz; g = 2.009; a_N = 5.0 G.*

As predicted, *p*-PyrDTDA displays a pentet signal with g = 2.009 and a_N = 5.0 G (literature: g = 2.007 and a_N = 5.0 G).[15] On addition of a small amount of CoTPP, the signal persists, however it is observed at a lower intensity. After addition of a full molar equivalent of CoTPP, the signal disappears altogether and only the baseline noise is observed.

This quenching of the EPR signal is to be expected if there is antiferromagnetic coupling between the unpaired electron of *p*-PyrDTDA and the unpaired electron in the $3dz^2$ orbital of the Co(II) ion upon coordination in solution. This observation is consistent with an S-bound species **S-R1•P1** unit being formed in solution. If an N-bound species formed in solution, this Co(II) species would be unlikely to have spin pairing between the metal ion and the radical and so would maintain the characteristic EPR signal.

When the coordination polymer dissolved, the species formed in solution is also EPR silent. From the crystal structure, there appears to be partial intermolecular electron transfer from the Co(II) ion to the coordinated dithiadiazolyl, resulting in reduction of the neutral dithiadiazolyl to the corresponding dithiadiazolide anion and oxidation of the metal centre to Co(III). Upon dissolution, this results in either **S- R1•P1** or the formation of the Co(III) N-bound species **N-R1•P1**, which is also EPR silent owing to the spin-paired nature of the dithiadiazolide anion. To confirm the solution speciation, nuclear magnetic resonance spectroscopy was employed.

2.6 Nuclear magnetic resonance spectroscopy

When the coordination polymer breaks up into its monomer units upon dissolution, there are three possibilities: the dithiadiazolyl N-bound (**N-R1•P1**) or S-bound (**S-R1•P1**), or with the dithiadiazolyl and the porphyrin unbound. While five-coordinate Co(II) porphyrins coordinated with N-heterocyclic ligands (e.g. pyridines) are relatively uncommon, there are examples in the literature that have been characterised.[23] To investigate which species dominates, nuclear magnetic resonance (NMR) spectroscopy was employed to study the solution speciation.

A sample of coordination polymer **R1•P1(THF)** was dissolved in deuterated dimethylsulfoxide (DMSO-d_6). The ^{1}H NMR spectrum of this is shown in Figure 2.8.

In order to establish which species was present, the protons of the pyridine ring were the most useful. When uncoordinated, the resonances for these protons can be found at 7.75 and 8.85 ppm, which is typical of aromatic protons. A similar result would be seen for **S-R1•P1**, as the pyridine ring would be directed away from the cobalt centre and the porphyrin ring, and would therefore be minimally affected. However, should coordination occur through the pyridyl nitrogen, the situation would be markedly different. The highly conjugated porphyrin core generates a significant ring current. Protons

directly above or below the porphyrin would subsequently experience a significant amount of anisotropic shielding as a result of this ring current and shift substantially upfield.

After careful study of the ^{1}H NMR spectrum of dissolved **R1•P1(THF)**, the resonance at 0.59 ppm was assigned to the pyridine α-protons, with that at 5.43 being assigned to the β-protons. In Figure 2.8 these appear as broad singlets owing to the concentrated nature of the sample. From the chemical shift of these particular resonances, it is inferred that the N-bound species **N-R1•P1** is present in solution when **R1•P1(THF)** is dissolved.

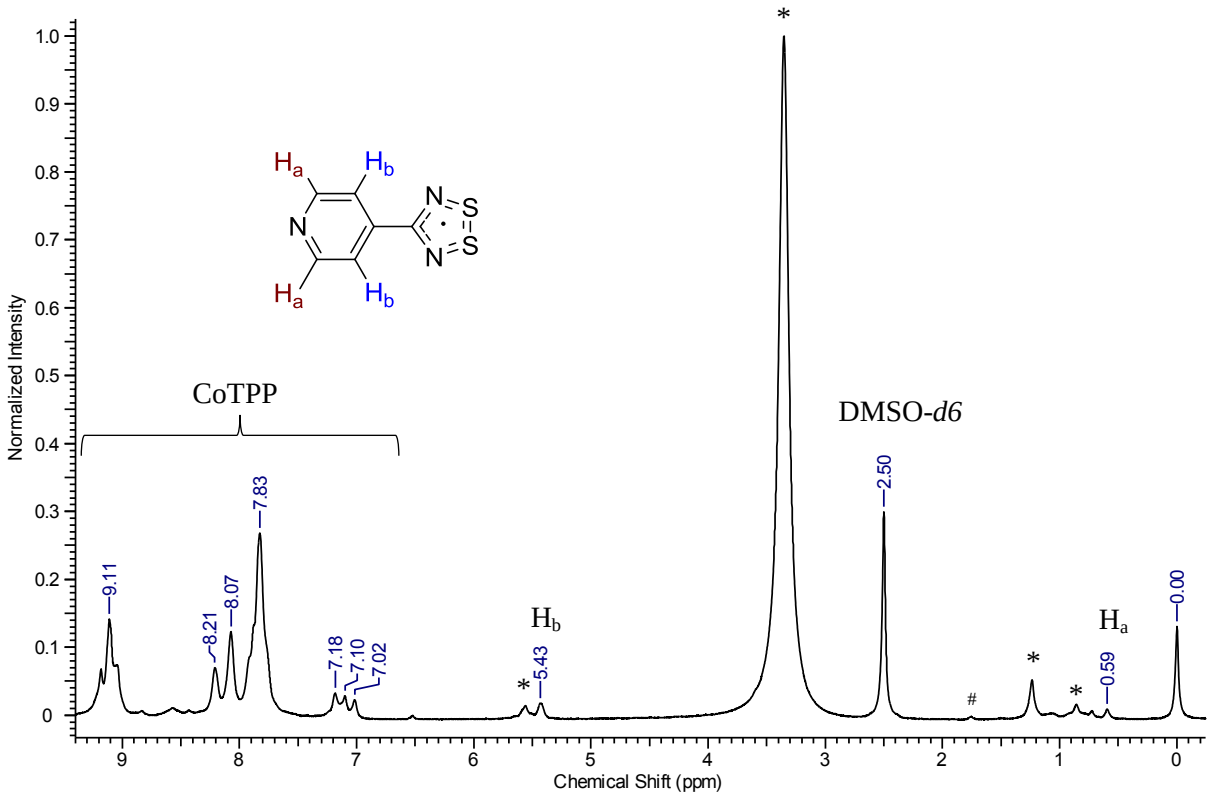

*Figure 2.8: ^{1}H NMR (600 MHz) spectrum of **R1•P1(THF)** coordination polymer dissolved in DMSO-d_6 (wet). The structure of **R1** is shown to demonstrate the positions of the alpha- (H_a) and beta- (H_b) pyridyl protons. Peaks labelled * are solvent impurities, # is residual THF.*

It was then considered which species is formed when *p*-PyrDTDA and CoTPP react directly in solution. Equimolar amounts of the two components were dissolved in DMSO-d_6, mixed well and the ^{1}H NMR spectrum was obtained (Figure 2.9). In this case, the pyridyl protons are not seen upfield and instead appear in the typical aromatic region. This suggests that the two components initially through the dithiadiazolyl ring, forming **S-R1•P1** prior to formation of oligomers and the crystallization of the coordination polymer, which is consistent with what is observed in the EPR experiments.

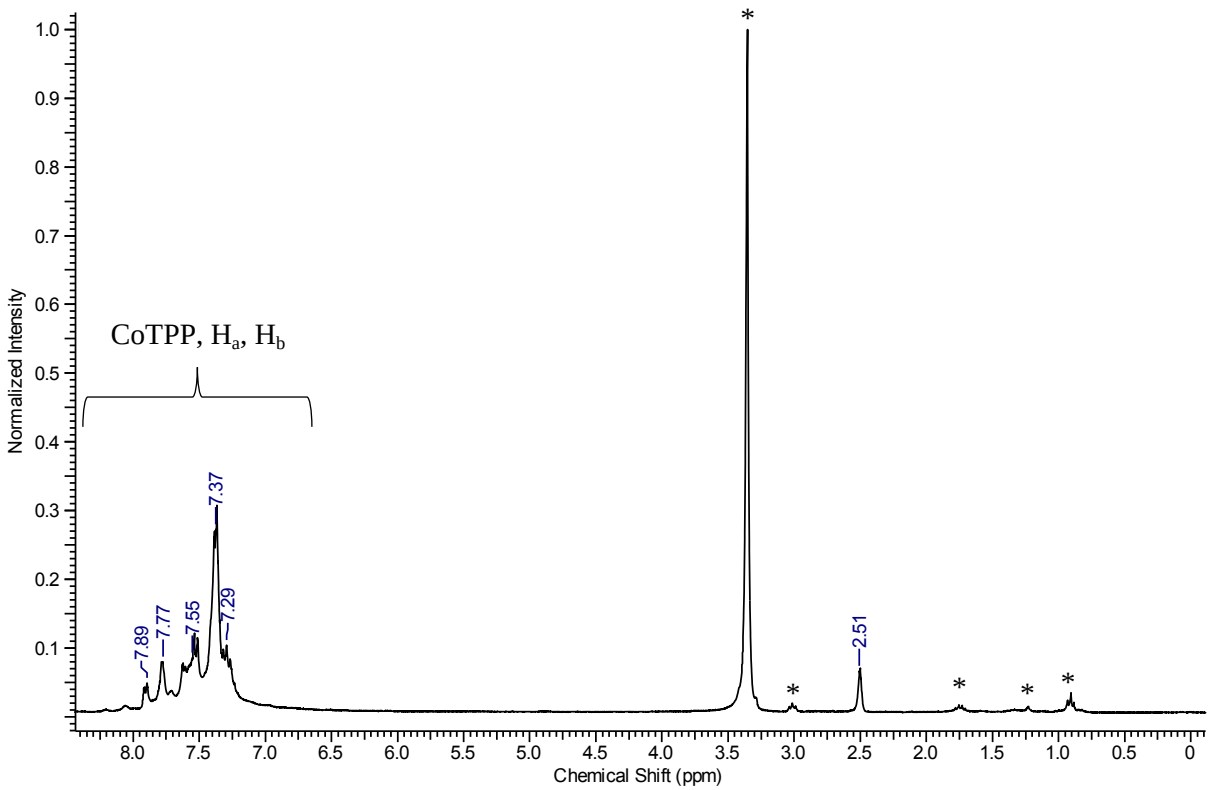

Figure 2.9: [1]H NMR (300 MHz) spectrum of p-*PyrDTDA and CoTPP mixed in DMSO-d_6 (wet). The signals for the pyridyl protons are found in the typical aromatic region, overlapping with the porphyrin aromatic protons, instead of being shifted upfield by porphyrin shielding. Peaks labelled * are solvent impurities..*

A wide ^{1}H NMR spectroscopic scan of the dissolved coordination polymer revealed a singlet at -5.07 ppm.[18] This upfield signal raised suspicions that DMSO might be axially coordinated to the cobalt centre in addition to the dithiadiazolyl ligand, forming a mixed ligand six-coordinate species. However, six-coordinate cobalt(II) porphyrins are known to be thermodynamically unfavoured.[23] In contrast, six-coordinate cobalt(III) porphyrins have been reported.[24] This, together with the bond length data from the crystal structure analysis, led us to investigate the oxidation state of the cobalt ion in the dissolved coordination polymer.

^{59}Cobalt has a nucleus with spin = 7/2 and 100 % natural abundance, and has the widest chemical shift range of all NMR active nuclei. While cobalt (II) is paramagnetic and NMR silent, low-spin cobalt (III) is diamagnetic and can be easily observed with NMR spectroscopy. With the knowledge that ^{59}Co NMR can be used to characterise six-coordinate Co(III) porphyrins,[25] a ^{59}Co NMR spectrum of the dissolved coordination polymer sample was obtained (Figure 2.10).

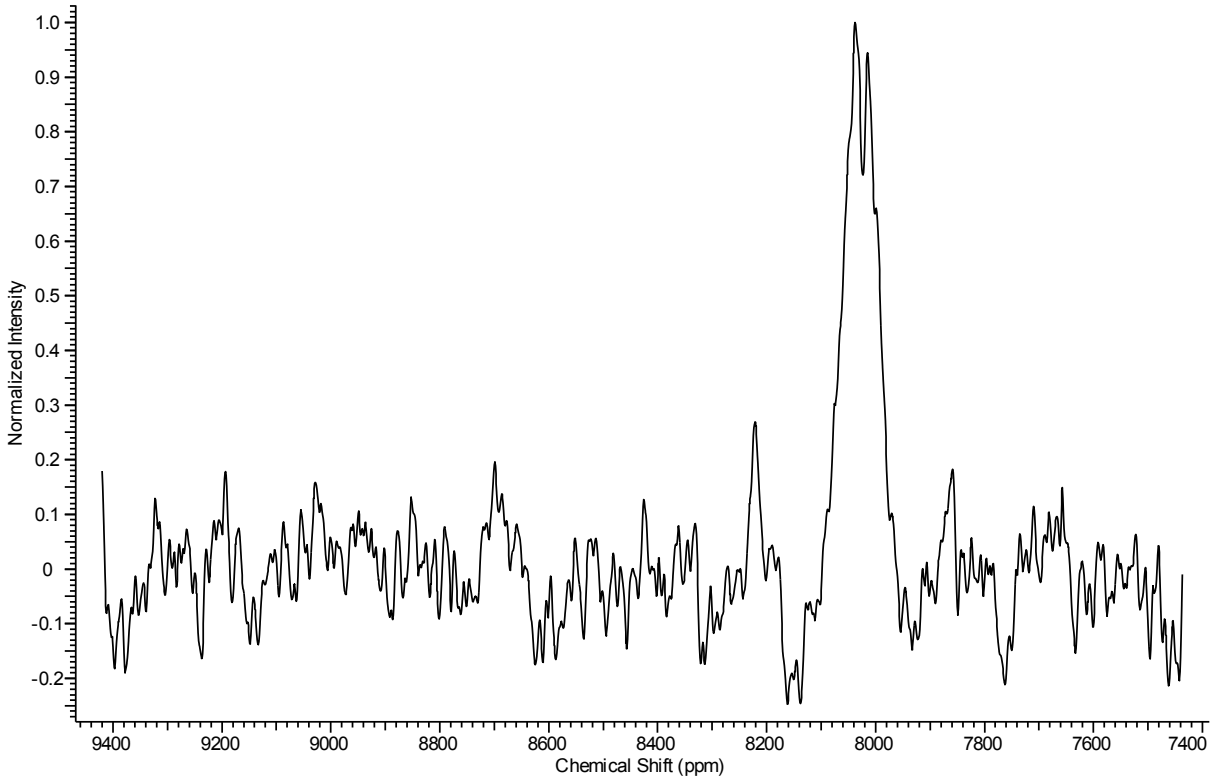

*Figure 2.10: ^{59}Co NMR (142 MHz) spectrum of **R1•P1(THF)** coordination polymer dissolved in DMSO-d_6*

The presence of the peak in Figure 2.10 thus definitively proves that the sample contains Co(III) nuclei. The chemical shift of approximately 8040 ppm is consistent with that of other six-coordinate Co(III) porphyrins with nitrogen-bound ligands.[25] An exact chemical shift is not reported as this signal is not referenced, due to the insolubility of the reference compound in DMSO. There were no additional peaks in the region between 0 and 3000 ppm, indicating that there is no Co(I) in the sample (which would occur if electron transfer happened from the dithiadiazolyl to the metal, reducing the cobalt and oxidising the ligand to the dithiadiazolylium cation).

From the combined ^{1}H and ^{59}Co data, it seems that the mostly likely species in solution when coordination polymer **R1•P1(THF)** is dissolved is **N-R1•P1**. It is worth noting that this solution is EPR-silent. To form this diamagnetic species, there must be electron transfer from the Co(II) ion to the dithiadiazolyl, oxidising the Co(II) to Co(III) and reducing the dithiadiazolyl radical to a dithiadiazolylium anion. This five-coordinate Co(III) species is capable of coordinating the DMSO solvent, resulting in the six-coordinate species **N-R1•P1(DMSO)** (Figure 2.11). This six-coordinate species contains a dithiadiazolide anion. This anion is likely stabilised within a pocket formed from the phenyl substituents of the CoTPP, which are twisted out of the plane of the porphyrin ring.

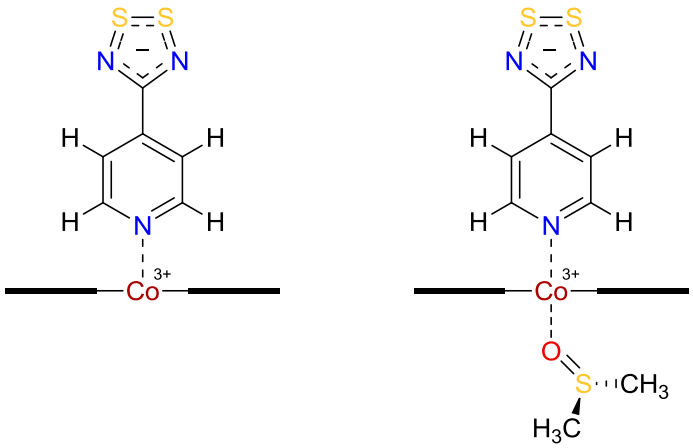

*Figure 2.11: Proposed structures of **N-R1•P1** and **N-R1•P1(DMSO)**, viewed along the plane of the porphyrin core. The porphyrin structure around the Co(III) centre is represented in bold for visual simplicity.*

In contrast to the N-bound unit formed when the coordination polymer dissolves, it is proposed that when **R1** and **P1** react in solution, the initial species formed is the S-bound unit **S-R1•P1** (Figure 2.12).

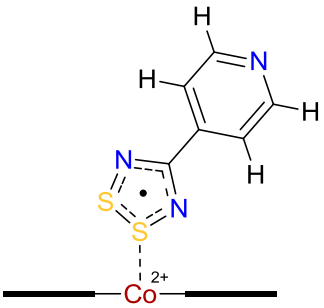

*Figure 2.12: Proposed structure of **S-R1•P1**, viewed along the plane of the porphyrin core. The porphyrin structure around the Co(II) centre is represented in bold for visual simplicity.*

To further investigate the formation of the S-bound species **S-R1•P1** in solution, UV-vis spectroscopy was employed.

2.7 Ultraviolet-visible spectrophotometry

As discussed in Chapter 1, porphyrins have very distinctive ultraviolet-visible (UV-Vis) spectra, and the technique is thus ideally suited to studying porphyrins and their chemistry.

For a free base porphyrin, the UV-Vis spectrum contains an extremely strong absorption band around 400 nm, known as the Soret band, and four bands of weak to moderate absorption in the 400 – 600 nm

region, known as the Q-bands.[26] With the metal salt of a porphyrin, such as CoTPP, the Soret band still dominates the spectrum, although it is shifted relative to the free base porphyrin, and only two Q bands are observed as a result of the higher symmmetry.[26] Changing the electronic structure of a porphyrin, for example by the addition of an axial ligand, has a marked effect on the absorption spectrum, both in terms of the bands shifting and in the bands changing in intensity.

When coordination polymer **R1•P1(THF)** is dissolved in DMSO, such that the predominant species in solution is the nitrogen-bound **N-R1•P1(DMSO)**, the spectrum shown in Figure 2.13 is observed. The spectrum is dominated by the Soret band at 434 nm, with two Q bands at 550 and 590 nm.

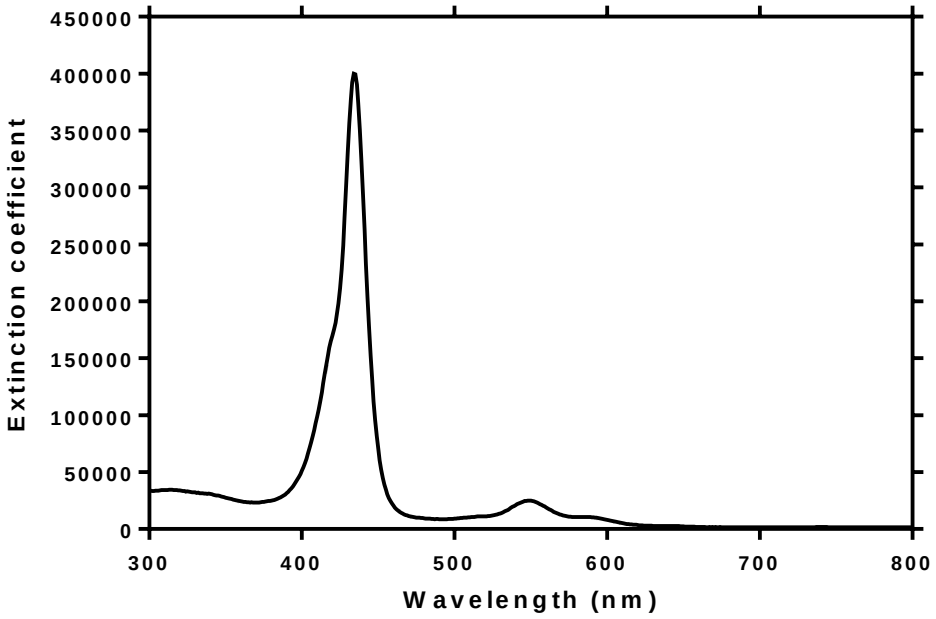

*Figure 2.13: UV-Vis spectrum of **R1•P1(THF)** in dimethylsulfoxide at 25 °C.*

To study the association between CoTPP and *p*-PyrDTDA in solution, the following spectrophotometric titration experiment was carried out. A *p*-PyrDTDA stock solution was made up in 9:1 dichloromethane:dimethylsulfoxide. A working solution of CoTPP in dichloromethane (DCM) was made up and the UV-Vis spectrum at 25 °C was determined against a reference solution of DCM. Aliquots of the *p*-PyrDTDA stock solution were added to both the working solution and the reference solution, and the UV-Vis spectrum measured after each addition. The result of this spectrophotometric titration is shown in Figure 2.14.

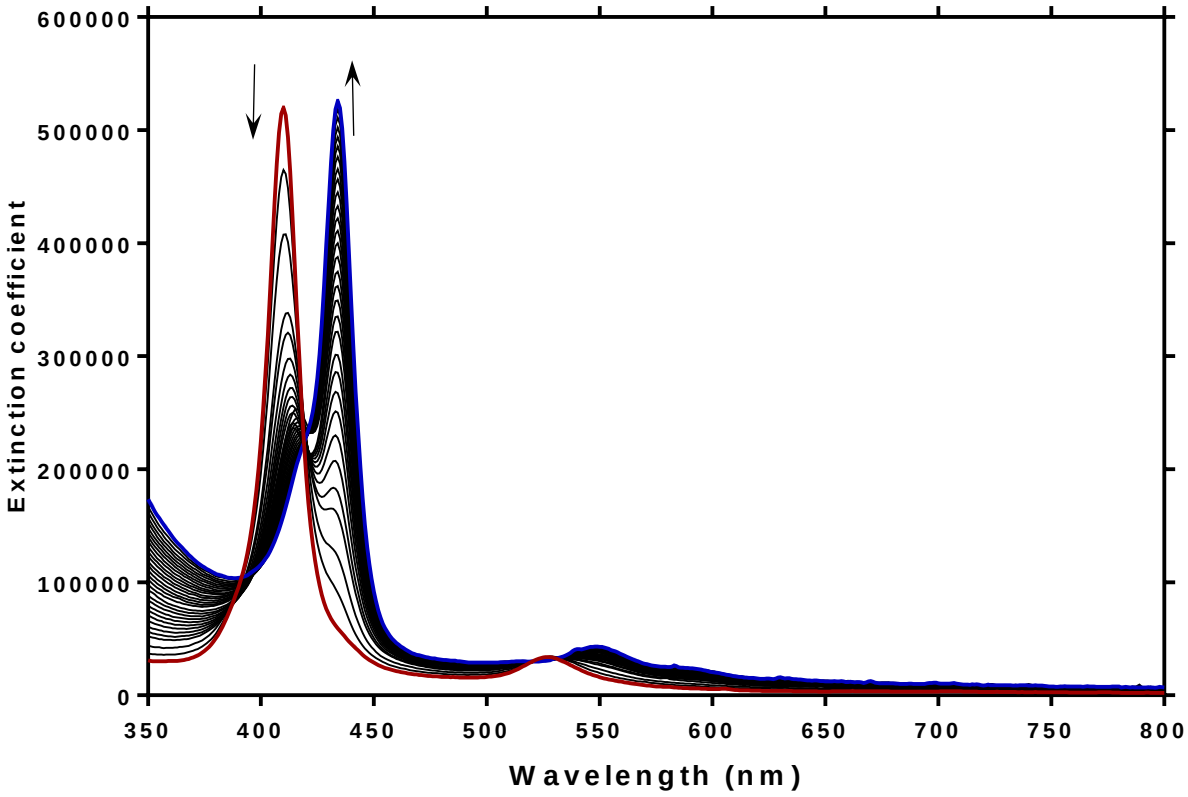

Figure 2.14: UV-Vis spectrophotometric titration for CoTPP in DCM (2 μM) with increasing p-*PyrDTDA concentration. The original CoTPP spectrum is shown in red, the final titration spectrum ([*p-*PyrDTDA] = 0.67 mM) is shown in blue. Titration spectra have been corrected for dilution. Arrows indicate direction of spectroscopic change.*

In the original spectrum for CoTPP in DCM (shown in Figure 2.14 in red), λ_{max} is at 410 nm - this is the Soret band. Addition of *p*-PyrDTDA results in this peak slowly reducing in intensity, while a new peak develops at 434 nm. At the end of the titration the λ_{max} is at 434 nm. There are Q bands at 550 and 590 nm. While a direct comparison with that of **N- R1•P1(DMSO)** is not possible as a result of solvent effects,[*] from NMR and EPR spectroscopic data it is proposed that this spectrum represents the **S- R1•P1** species.

Considering that most of the changes to the spectrum were observed in the region of the Soret band, further investigations focused on this portion of the spectrum. Having a smaller wavelength window to sweep meant that experimental timeframes decreased significantly, which meant that the inevitable degradation of the radical stock solution over time could be minimised. Error in the experiment, particularly for the latter half of the additions, was likewise also minimised.

[*] The use of different solvents was unfortunately unavoidable. The solid material **R1•P1(THF)** did not dissolve fully in DCM, so NMR spectroscopy had to be performed in DMSO. However, for EPR spectroscopy, tuning the sample cavity was very difficult when using DMSO as a result of the high dielectric constant, so DCM with a small percentage of DMSO had to be used instead. DCM was used for the UV-Vis for the best comparison between the UV-Vis and EPR spectroscopy results, as well as to avoid coordination of the DMSO.

For further spectrophotometric titration studies, the spectrum between 375 and 450 nm was collected and titrations were repeated in triplicate. The results of one such spectrophotometric titration are shown in Figure 2.15.

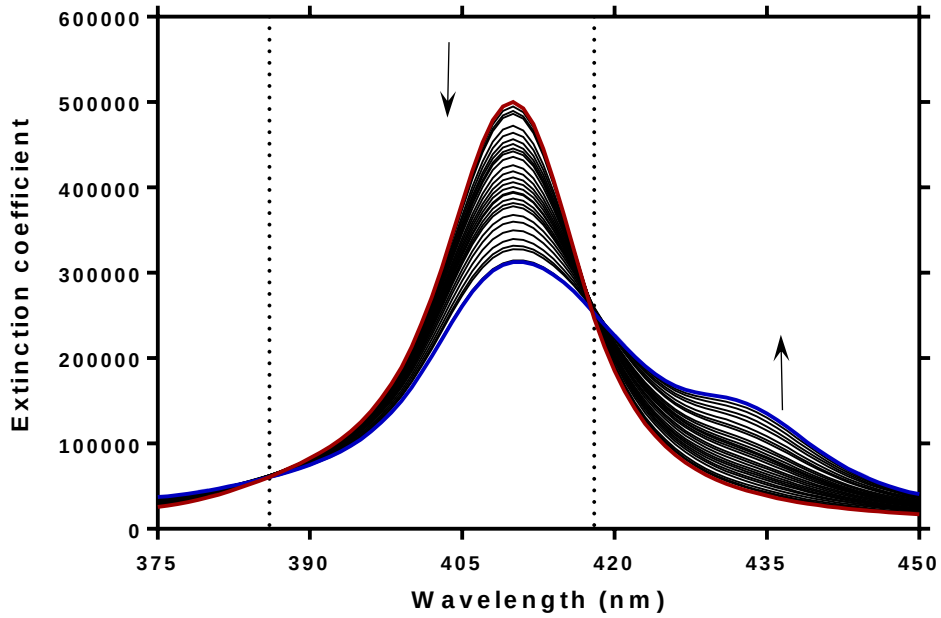

Figure 2.15: UV-Vis spectrophotometric titration for CoTPP in DCM (2 μM) at 25 °C with gradually increasing p-*PyrDTDA concentration. The original CoTPP spectrum is shown in red, the final titration spectrum ([*p-*PyrDTDA] = 0.46 mM) is shown in blue. Isosbestic points indicated with dotted gridlines. Arrows indicate direction of spectroscopic change. Titration spectra have been corrected for dilution.*

Data were corrected for dilution and analysed using HypSpec.[27] The same pattern is seen as in Figure 2.14, with the Soret peak at 410 nm gradually decreasing in intensity, and a new peak beginning to evolve in the 434 nm region. Isosbestic points are observed at 386 and 418 nm.[†]

Changes in the UV-Vis spectrum can be attributed to the formation of **R1•P1**. HypSpec was used to determine the association constant for the five-coordinate dithiadiazolyl – metalloporphyrin complex, as shown in equation 2.1. Several models were attempted, however the best fit was a 1:1 *p*-PyrDTDA – CoTPP model (see Appendix B). To reduce variable parameters and aid fitting, the spectrum of CoTPP was constrained to a known spectrum instead of being freely refined. The predicted spectrum of the product complex and the value of the equilibrium constant β were allowed to freely refine.

[†] During a chemical reaction, if the absorbance does not change at a specific wavelength at any point in the reaction, this wavelength is referred to as an isosbestic point. The presence of isosbestic points indicates that the stoichiometry of the reaction remains the same during the chemical process occurring, and also that no additional secondary reactions take place.

$$R1 + P1 \overset{\beta}{\rightleftharpoons} R1 \bullet P1 \qquad (2.1)$$

Using the spectrophotometric titration data, it was determined that for CoTPP and p-PyrDTDA in DCM at 25 °C the association constant,[‡] logβ, was 4.19 ± 0.05. From EPR (Figure 2.7) and 1H NMR data (Figure 2.9), it is proposed that this reaction forms the five-coordinate sulfur-bound species S-R1•P1. As an illustration of the fit of the model, the predicted absorbance data for the model were plotted against the observed data (Figure 2.16).

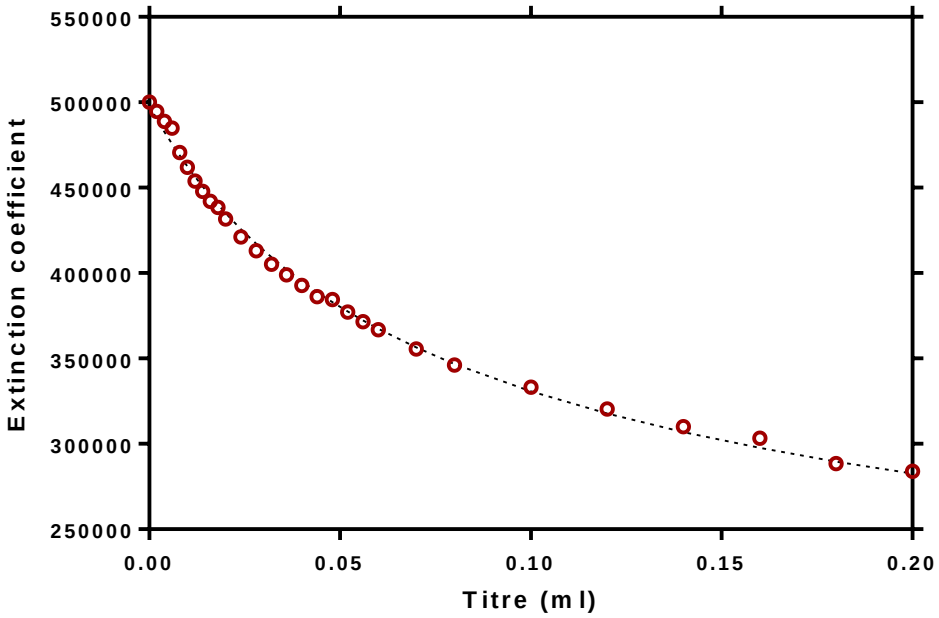

Figure 2.16: Experimental (red circles) and predicted (black dotted line) UV-Vis absorption at 410 nm for p-*PyrDTDA – CoTPP spectrophotometric titration using a 1:1 ligand-to-metal model, showing a good agreement between the model and the experimental data.*R^2 *= 0.9971, P<00.00001..*

From the spectrophotometric changes, the spectrum for **R1•P1** could be calculated and the speciation plot (Figure 2.17) was determined, showing that at the end of the spectrophotometric titration, 26.3 % of the CoTPP remained as free CoTPP, while 73.7 % had been converted to the five-coordinate *p*-PyrDTDA – CoTPP complex. Note that this speciation plot is concentration dependent and thus is calculated for the exact concentration range used in the titration. Adding more dithiadiazolyl ligand results in a higher percentage of **R1•P1** complex with less free CoTPP (see Figure 2.14).

[‡] Synonyms used in the literature include binding constant or formation constant. Additionally, some sources use logβ and others use the general term logK. In this study, the terms "association constant" and "logβ" will be used throughout.

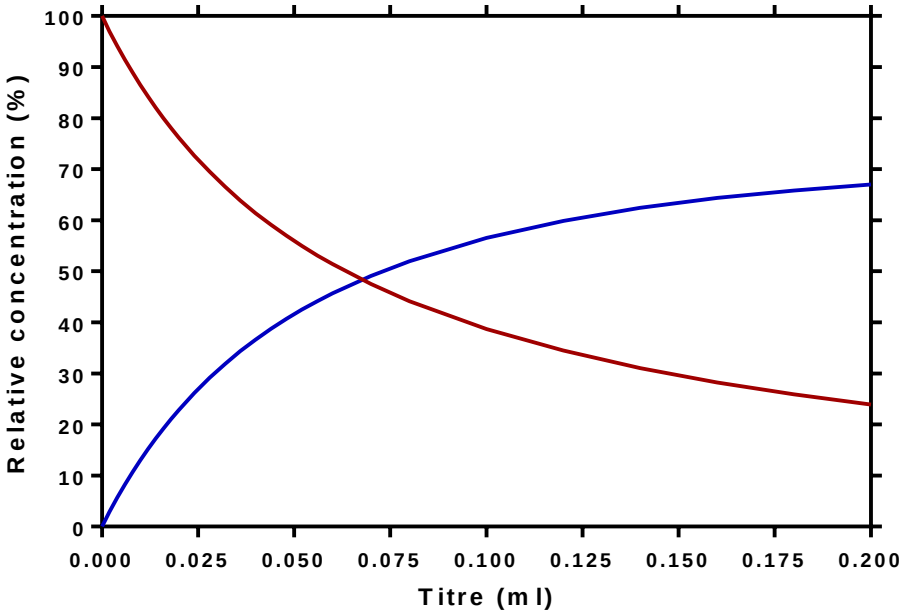

Figure 2.17: The predicted speciation plot following titration of CoTPP with p-*PyrDTDA, showing the decrease in free CoTPP (red) and the increase of* ***R1•P1*** *(blue)*

The observations described above led to understanding how to study the reaction by means of spectrophotometric titrations and how to use this data to determine the equilibrium constant, or association constant, for the reaction. In order to obtain a better understanding of the system as a whole, the thermodynamics of the reaction was investigated.

Under standard conditions, the van 't Hoff equation (equation 2.2) can be used to describe a reversible reaction.

$$\ln K_{eq} = -\frac{\Delta H}{RT} + \frac{\Delta S}{R} \qquad (2.2)$$

For the reaction between **R1** and **P1**, the equilibrium constant K_{eq}, which is the same as the association constant β, had been determined at 25 °C (298.15 K). To obtain the necessary thermodynamic data, spectrophotometric titrations were repeated at 20 °C (293.15 K), 30 °C (303.15 K), 35 °C (308.15 K) and 40 °C (313.15 K) in a similar manner as those carried out at 25 °C.[§] The spectra for these titrations are shown in Figure 2.18. The equilibrium constant, log Keq, was determined for each temperature (Table 2.2) in the same manner as for the 25 °C experiment, with a 1:1 ligand-to-metal model being the best fit at each temperature.

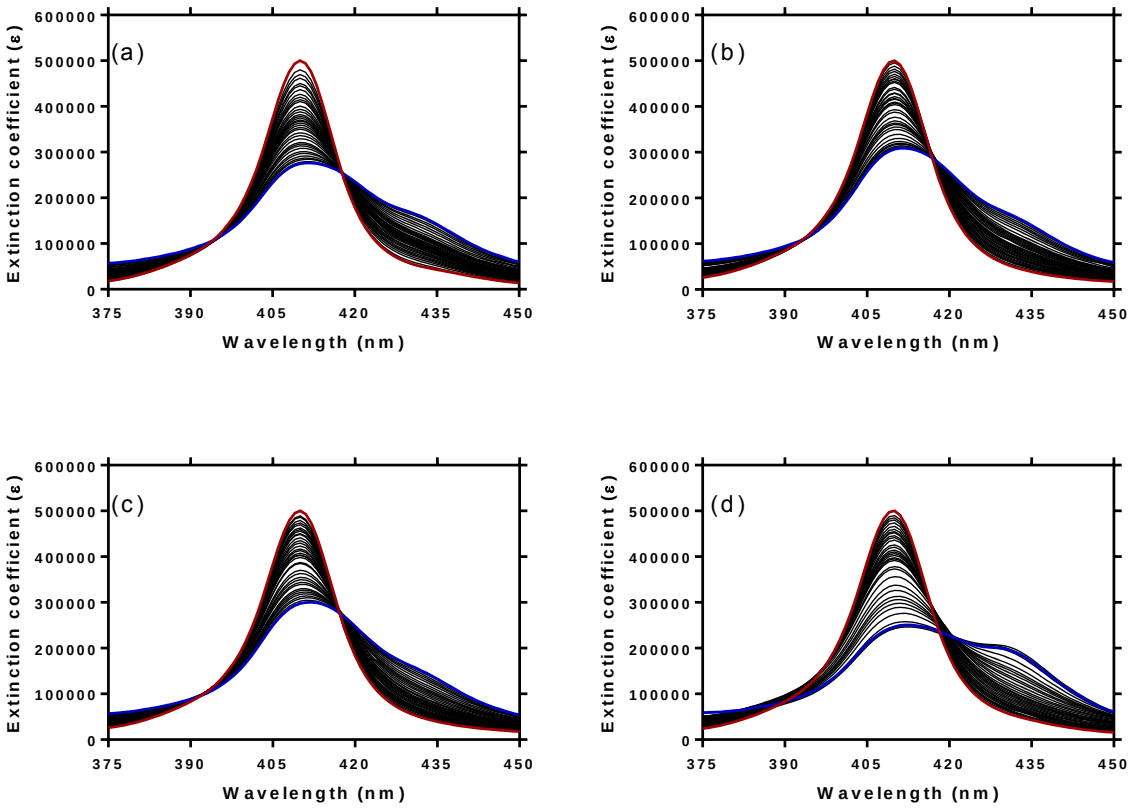

Figure 2.18: UV-Vis spectrophotometric titration for CoTPP in DCM (2 μM) with gradually increasing p-*PyrDTDA concentration at (a) 20 °C, (b) 30 °C, (c) 35 °C and (d) 40 °C. The original CoTPP spectrum is shown in red, the final titration spectrum is shown in blue. Titration spectra have been corrected for dilution.*

To better illustrate the subtle differences in the spectrophotometric titrations, the change in absorbance at 410 nm was plotted for all five temperatures (Figure 2.19).

[§] The lower limit of this temperature range was determined by the instrumental capabilities available, and the upper limit by the boiling point of the solvent. Error could be minimised by the use of a larger temperature range, if this were possible.

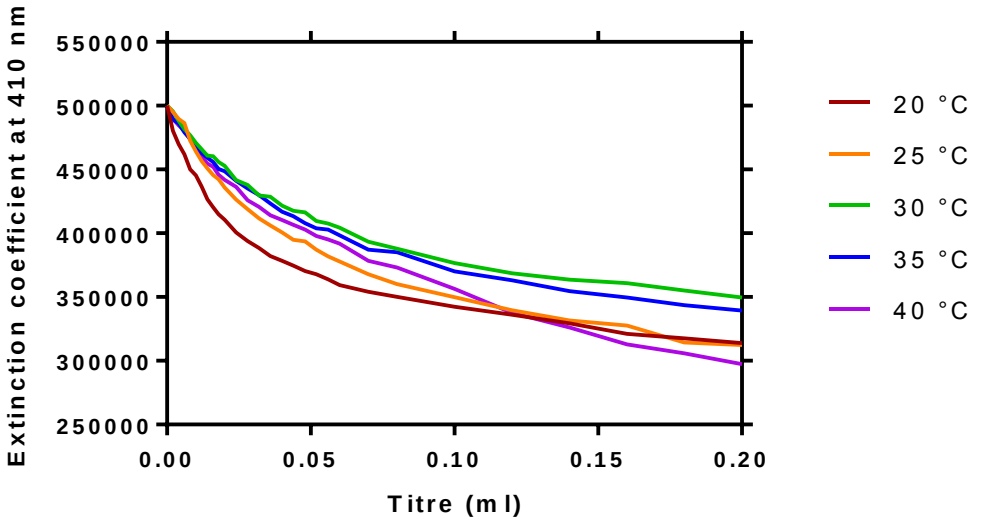

Figure 2.19: UV-Vis absorbance at 410 nm for CoTPP with gradually increasing p-PyrDTDA concentration at 20, 25, 30, 35 and 40 °C.

Absorbance at 410 nm has a greater decrease at a lower **R1** concentration for 20 °C than for the other temperatures. There is less of a decrease as the temperature increases. The slope for the initial decrease becomes less steep at the higher temperatures as well. This indicates that the reaction occurs more readily at lower temperature.

*Table 2.2: Equilibrium constants for the association of **R1** with **P1** in dichloromethane as a function of temperature*

T (°C / K)	log K_{eq}
20 / 293.15	4.32 ± 0.04
25 / 298.15	4.19 ± 0.05
30 / 303.15	4.15 ± 0.04
35 / 308 .15	4.07 ± 0.04
40 / 313.15	3.96 ± 0.05

For each of these temperatures, the natural logarithm of the equilibrium constant was determined (see section 2.9.6.1 and Table 2.4). These values were then plotted as a function of 1/T to form a van 't Hoff plot (Figure 2.20).

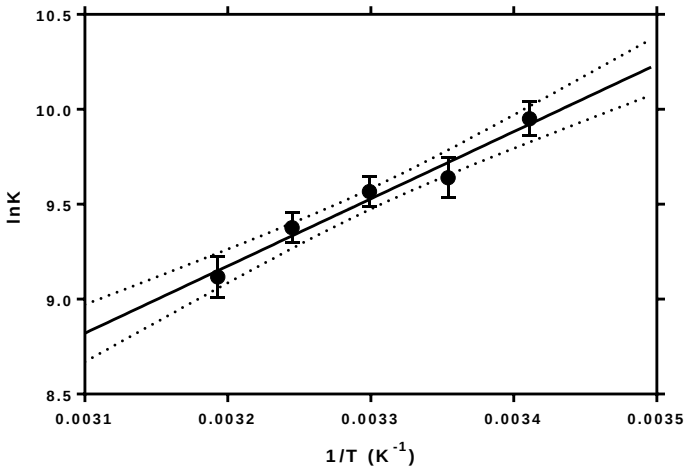

Figure 2.20: The van 't Hoff plot for the reaction of p-*PyrDTDA with CoTPP between 293.15 and 313.15 K. Experimental data points are shown as black circles with error bars. The linear regression line (R^2 = 0.9012, P < 0.0001) is shown in solid black, with the 95 % confidence interval shown as dotted lines.*

From the van 't Hoff plot shown in Figure 2.20, it is possible to determine the enthalpy, ΔH from the slope of the linear regression line that fits the experimental data as shown in equation 2.3. In a similar manner the entropy, ΔS (equation 2.4), can be determined from the y-intercept of the linear regression line.

$$\text{Slope} = -\frac{\Delta H}{R} = 3540 \pm 325.1 \qquad (2.3)$$

$$\Delta H = -29.43 \pm 2.70 \text{ KJ.mol}^{-1}$$

$$\text{y Intercept} = \frac{\Delta S}{R} = -2.154 \pm 1.073 \qquad (2.4)$$

$$\Delta S = -17.90 \pm 8.92 \text{ J.mol}^{-1}$$

Thus, for the formation of **R1•P1** from **R1** and **P1** in DCM, the enthalpy, ΔH, was determined to be −29.42 ± 2.70 KJ.mol^{-1} and the entropy, ΔS, was determined to be −17.90 ± 8.92 J.mol^{-1}. The negative ΔH value indicates that the process will occur spontaneously over the temperature range investigated and is exothermic. The ΔS value is negative, as is predicted for an associative process. No data for a similar system, either studying a dithiadiazolyl metal complex or studying a heterocyclic sulfur ligand coordinating to a cobalt porphyrin, was found to enable comparison.

2.8 Summary and Conclusion

The first known dithiadiazolyl radical – metalloporphyrin complex was synthesised and characterised. This complex is prepared from 4-(4′-pyridyl)-1,2,3,5-dithiadiazolyl (**R1**) and cobalt (II) tetraphenylporphyrin (**P1**). The compound crystallizes as a coordination polymer **R1•P1(THF)**, with each dithiadiazolyl bridging two cobalt porphyrins.

The dithiadiazolyl coordinates to one cobalt porphyrin with a single cobalt–sulfur bond, and to the next cobalt porphyrin through the pyridyl nitrogen. This structure is of particular interest as it reveals a previously unknown coordination mode for dithiadiazolyls, namely the single metal–sulfur bond, with the sulfur–sulfur bond still intact.

The structure shows an unusually long sulfur-sulfur bond length, at 2.121 Å compared to an average dithiadiazolyl S – S bond length of 2.089 Å. It is proposed that this is a result of partial electron transfer from the cobalt ion to the dithiadiazolyl, weakening the bond order and lengthening the sulfur – sulfur bond. The result is a coordination polymer that exists as a resonance hybrid with both Co(II)-dithiadiazolyl and Co(III)-dithiadiazolide units.

Upon dissolution, the coordination polymer **R1•P1(THF)** breaks up into dithiadiazolyl – metalloporphyrin **R1•P1** monomer units. ^{1}H and ^{59}Co NMR data suggest that this species is the cobalt (III) species **N-R1•P1**, where the dithiadiazolyl **R1** is coordinated to the metal centre of **P1** through the pyridyl nitrogen. Transfer of an electron from the cobalt to the dithiadiazolyl means that the cobalt (II) centre is oxidised to a cobalt (III) ion, with simultaneous reduction of the dithiadiazolyl radical to the corresponding dithiadiazolide anion. This species no longer has unpaired electrons and hence is EPR silent. In DMSO, which is known to be a coordinating solvent, the six-coordinate **N-R1•P1(DMSO)** complex forms. The change in solution speciation is presumably as a result of the redox change occurring.

When radical **R1** and metalloporphyrin **P1** react in solution however, they do not form the species **N-R1•P1**. Instead, initial coordination to the cobalt (II) ion occurs through a dithiadiazolyl sulfur atom forming **S-R1•P1**. The formation of this species was studied through UV-Vis spectrophotometric titrations. The association constant, logβ, for this reaction was determined to be 4.19 ± 0.05 at 25 °C. A thermodynamic study was subsequently undertaken, studying the association of **R1** to **P1** between 20 °C and 40 °C. The enthalpy, ΔH, for this reaction was determined to be −29.43 ± 2.70 KJ.mol^{-1}, indicating the reaction is exothermic. The entropy, ΔS, was determined to be −17.90 ± 8.92 J.mol^{-1}. From the thermodynamic data, it appears that the reaction occurs more readily at lower temperature, which should be kept in mind for future experiments.

The formation of **S-R1•P1** was also studied through EPR spectroscopy. This species is EPR silent, indicating that it is diamagnetic as a result of spin pairing between the dithiadiazolyl radical unpaired electron and the d^7 cobalt (II) centre. Once **S-R1•P1** is formed, oligomerisation can occur to form the coordination polymer **R1•P1(THF)**. A schematic summary of the processes involved is shown in Figure 2.21.

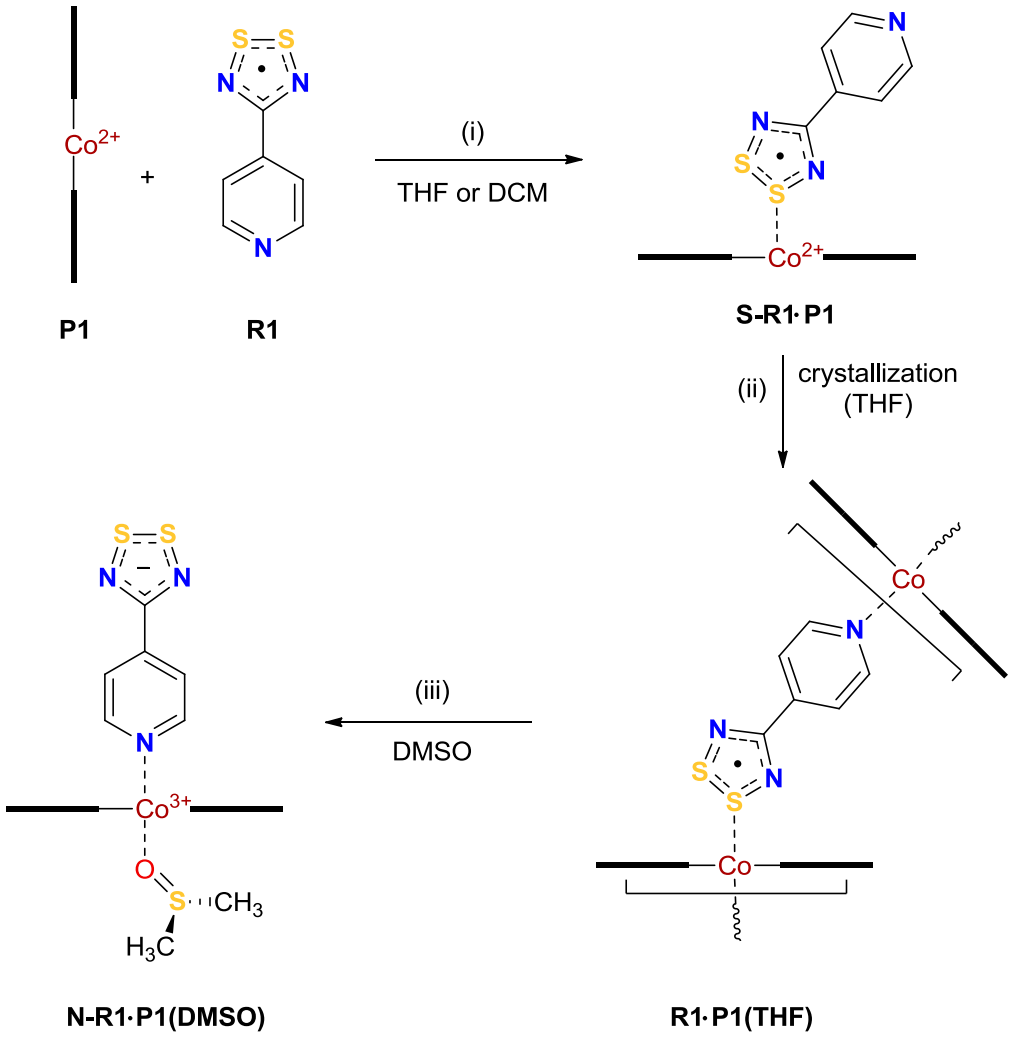

*Figure 2.21: Summary scheme showing (i) Reaction of p-PyrDTDA (**R1**) and CoTPP (**P1**) in solution to form **S-R1•P1**. (ii) Oligomerisation and crystallization of the **R1•P1** coordination polymer (with THF present in the crystal structure). Monomer unit indicated with parentheses. (iii) Dissolution of the coordination polymer to form **N-R1•P1**. Porphyrin plane represented graphically with bold lines for simplicity. THF = tetrahydrofuran. DCM = dichloromethane. DMSO = dimethylsulfoxide.*

In conclusion, this dithiadiazolyl radical – metalloporphyrin complex shows novel and interesting coordination behaviour in both solid and solution state. A new coordination mode for dithiadiazolyl radicals has been shown, offering an opportunity to develop of a new class of dithiadiazolyl radical metal complexes. The dithiadiazolyl – cobalt bond is labile and affords a different species upon

dissolution to that formed upon coordination (Figure 2.21). The complex undergoes intermolecular redox chemistry that shows promise for the development of materials with interesting redox chemistry.

2.9 Experimental details

General information on instruments and experimental procedures can be found in Appendix A.

2.9.1 Synthesis of 4-(4′-pyridyl)-1,2,3,5-dithiadiazolyl (*p*-PyrDTDA, **R1**)

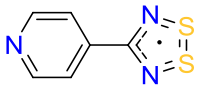

p-PyrDTDA
R1

Dry diethyl ether (30 mL) was placed in a nitrogen-filled Schlenk flask and cooled to -78 °C. Hexamethyldisilylazane (2.0 mL, 9.6 mmol) and *n*-butyl lithium (7.2 mL, 1.6M, 11.52 mmol) were added. The cooling bath was removed and the solution was stirred for 45 minutes until warmed to room temperature and the solution was clear. 4-Pyridinecarbonitrile (1.002 g, 9.62 mmol) was added to the solution, which was left to stir overnight. The ochre-coloured solution was subsequently cooled to 0 °C. Sulfur dichloride (1.2 mL, 19.2 mmol) was added slowly with vigorous stirring. After complete addition, the solution was allowed to warm to room temperature and stirred for a further 1 hour. Stirring was then stopped and the yellow-orange precipitate allowed to settle. Excess solvent was removed by cannula filtration. The remaining precipitate was washed with dry diethyl ether (3 x 10 mL), then dried under vacuum. The dry dithiadiazolylium chloride salt (1.502 g, 6.92 mmol) was transferred to a clean, dry Schlenk flask under nitrogen. Triphenylantimony (1.222 g, 3.46 mmol) was added to the flask and the contents were gently mixed. The mixture was heated to 70 °C for approximately 3 hours, when a complete colour change from yellow-orange to purple was observed. The flask was fitted with a water-cooled cold finger, placed under vacuum and sealed. Heating was increased to 140 °C and the product *p*-PyrDTDA **R1** was isolated by sublimation onto the water-cooled cold finger as dark blocks (0.252 g, 1.385 mmol, 14 % yield). (+)-ESI-MS: m/z 182.9915. EPR (9.878 GHz, CH_2Cl_2): 3515 G (pentet, a_n = 5.0 G), g = 2.008.

2.9.2 Synthesis of 5,10,15,20-tetraphenylporphyrin (H_2TPP) and cobalt (II) 5,10,15,20-tetraphenylporphyrin (CoTPP, **P1**)

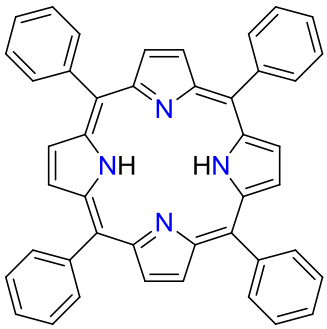

H_2TPP

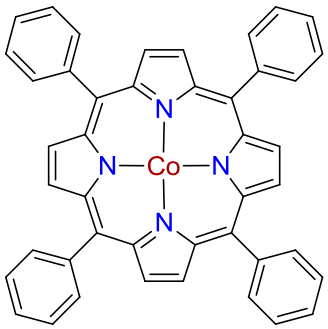

CoTPP
P1

Freshly distilled pyrrole (5.0 mL, 72 mmol) and benzaldehyde (7.3 mL, 72 mmol) were added to propionic acid (300 mL) in a 500 mL round bottomed flask. Boiling stones were added and the solution was brought to reflux in air for 1 hour. Heating was ceased and the flask was allowed to cool to room temperature before cooling in the refrigerator for 1 hour. The solution was filtered and the precipitate was washed with hot distilled water (3 x 30 mL) to yield 5,10,15,20-tetraphenylporphyrin as a fine purple microcrystalline material (2.173 g, 3.43 mmol, 20 % yield). ^{1}H NMR (300 MHz, $CDCl_3$): δ ppm -2.75 (s, 2H, N-H), 7.73-7.82 (m, 12H, *para*- and *meta*- $C_{Ar}H$), 8.22-8.26 (m, 8H, *ortho*- $C_{Ar}H$), 8.86 (s, 8H, pyrrole-H). UV-Vis (CH_2Cl_2): 420 nm, 516 nm, 525 nm, 595 nm, 650 nm.

Tetraphenylporphyrin (400 mg, 0.65 mmol) and cobalt (II) acetate tetrahydrate (0.169 g, 0.68 mmol) were added to degassed dimethylformamide (50 mL) in a 100 mL round bottomed flask under nitrogen. The solution was heated and reflux was maintained for 45 minutes. Thereafter, heating was ceased and the flask was allowed to cool to room temperature before cooling in the refrigerator for 1 hour. The solution was filtered and the precipitate was washed with distilled water (2 x 20 mL) to yield cobalt (II) tetraphenylporphyrin **P1** as fine purple crystals (433 mg, 0.64 mmol, 98 % yield). ^{1}H NMR (300 MHz, $CDCl_3$): δ ppm 9.74 (br s, 4H, *para*- $C_{Ar}H$), 9.95 (br s, 8H, *meta*- $C_{Ar}H$), 13.14 (br s, 8H, *ortho*- $C_{Ar}H$), 15.93 (br s, 8H, pyrrole-H). UV-Vis (CH_2Cl_2): 410 nm, 529 nm.

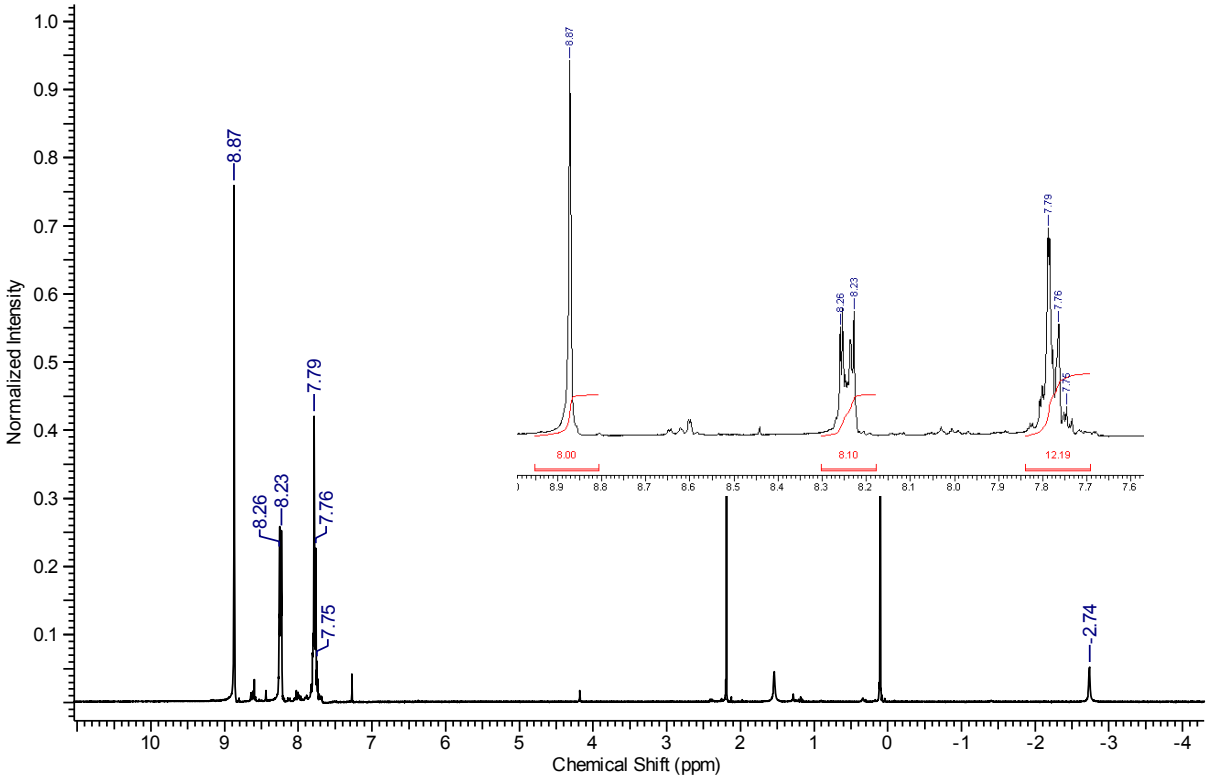

Figure 2.22: ^{1}H NMR (300 MHz) spectrum of H_2TPP in $CDCl_3$, with insert of aromatic region.

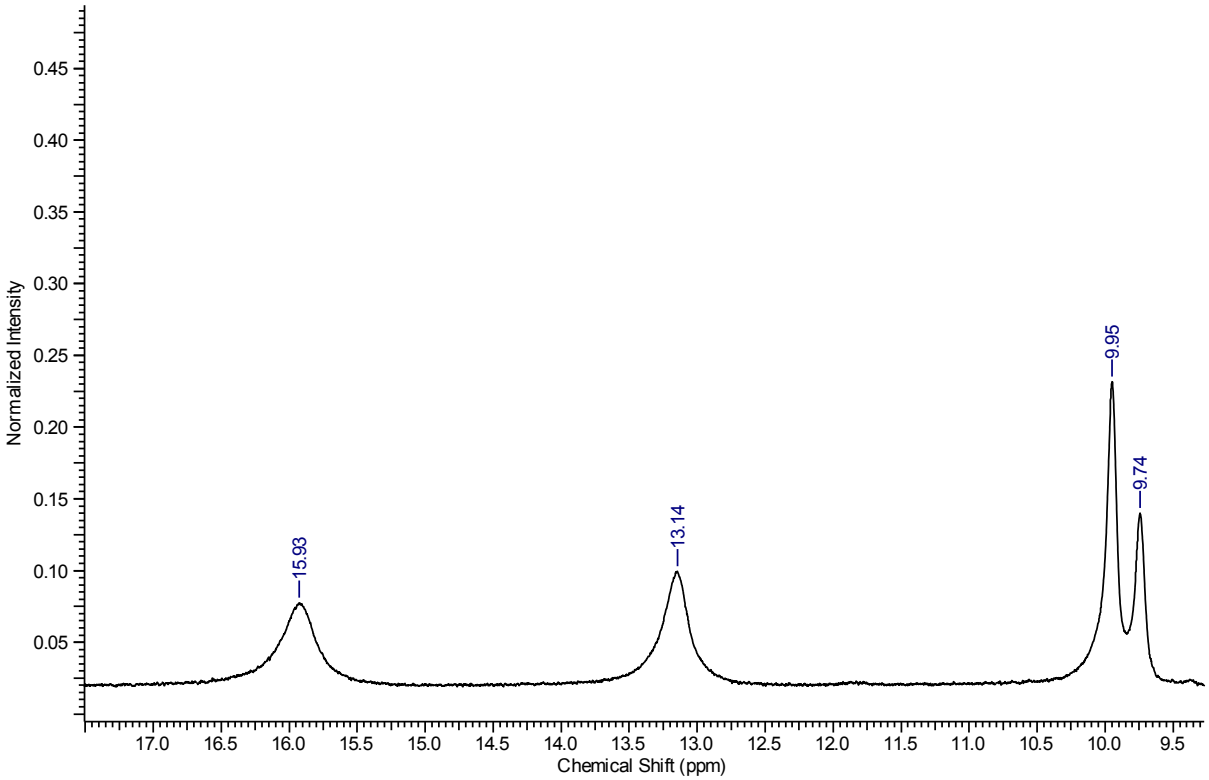

Figure 2.23: ^{1}H NMR (300 MHz) spectrum of CoTPP in $CDCl_3$. The presence of Co(II) results in a significant downfield shift relative to H_2TPP, as well as signal broadening.

2.9.3 Preparation of *p*-PyrDTDA – CoTPP coordination material (**R1•P1(THF)**)

A 2 cm wide Schlenk tube was evacuated and filled with nitrogen using standard Schlenk techniques. To this was added *p*-PyrDTDA (14 mg, 0.077 mmol), CoTPP (50 mg, 0.075 mmol) and dry THF (10 mL). The solution was magnetically stirred and gently heated until all the material dissolved. The stirrer bar was removed and dry *n*-hexane (10 mL) was carefully layered above the dark maroon THF solution. The flask was sealed and allowed to stand at room temperature. After one week, thin purple plate-like crystals could be seen on the sides of the Schlenk and a dark purple precipitate formed at the bottom of the Schlenk.

2.9.4 Single crystal X-Ray Diffraction

Experimental details of the crystal structure determination can be found in Appendix A.

The initial crystal structure determination of **R1•P1(THF)** solved in the space group *Pn*, with two **R1•P1** units in the asymmetric unit giving rise to two crystallographically independent coordination polymer chains. During this research project, an additional structure determination of **R1•P1(THF)** could only be modelled in the space group *Cc*, with only one unit in the asymmetric unit as a result of an additional symmetry element (a glide plane). When the **R1•P1** units of the two structures are overlayed it is clear that they are the same. The *Pn* structure was modelled with a lower R-factor than the *Cc* structure (6.53 % vs 8.74 %), which is why the data reported is for the *Pn* structure. Both CIF files are included in the attached CD.

2.9.5 Powder X-Ray Diffraction

Powder X-ray diffraction was used to analyse the bulk sample of **R1•P1(THF)**. The PXRD profile reveals the bulk sample is largely amorphous, and contains some free CoTPP (which was confirmed by UV-Vis spectroscopy).[**]

[**] The sample could not be recrystallized to remove unreacted CoTPP owing to poor solubility in a large variety of organic solvents. Upon dissolution in dimethylsulfoxide, the sample remained in solution.

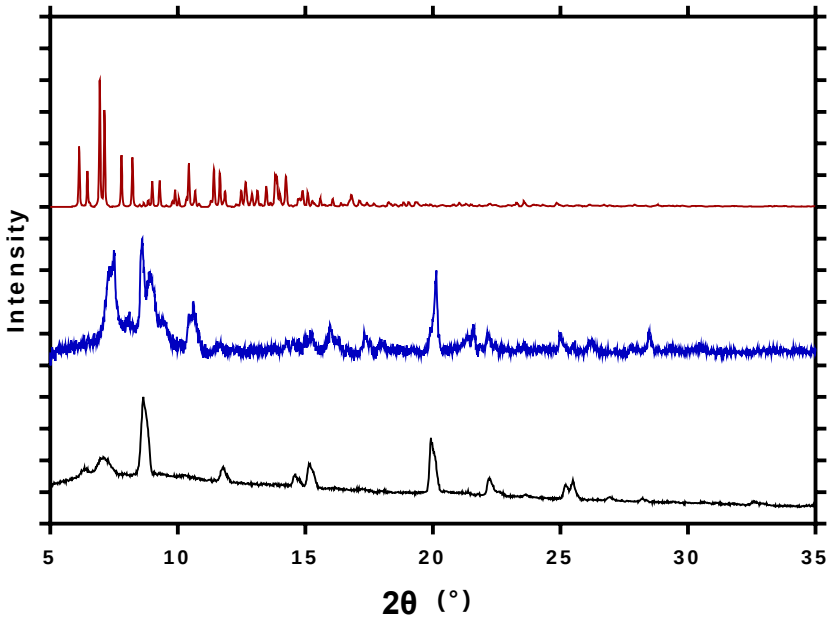

*Figure 2.24: Simulated PXRD pattern for **R1•P1(THF)** (top, red), experimental pattern for the bulk sample of **R1•P1(THF)** (middle, blue) and experimental pattern for **P1** (bottom, black)*

2.9.6 Spectrophotometric titrations

All glassware, except microsyringes, were dried in an oven overnight. All solvents were dried over 4 Å molecular sieves. Microsyringes were flushed three times with clean, dry solvent and three times with the solution of interest before being used.

A fresh 2 mM stock solution of *p*-PyrDTDA was made up in a 5 mL volumetric flask prior to each experiment using a 9:1 dichloromethane:dimethylsulfoxide solvent system. The flask was flushed with nitrogen for 1 minute before being sealed with a septum and paraffin laboratory film. A 1 mM stock solution of CoTPP was made up in a screw-cap glass using dichloromethane.

A 2μM working solution of CoTPP was made up in a quartz cuvette with 1996 μL dichloromethane (measured by micropipette) and 4 μL of the CoTPP stock solution (measured by glass Hamilton microsyringe). A 2000 μL portion of dichloromethane was placed in the reference cuvette (measured by micropipette).

Both cuvettes, with their lids, were placed in the UV-vis spectrophotometer and allowed to equilibrate to 25 °C before the spectrum was collected between 375 and 450 nm.

Aliquots of the *p*-PyrDTDA stock solution were added to both the working solution cuvette and the reference solution cuvette using a glass Hamilton microsyringe. The solutions were stirred with a wire

microsyringe plunger[††] and the lids replaced. The spectrum was collected after each addition. This was continued until a total of 600 µL of the dithiadiazolyl solution was added by means of 10 x 2 µL, 10 x 4 µL, 2 x 10 µL, 6 x 20 µL and 8 x 50 µL aliquots of stock solution to both sample and reference. The spectrophotometric titrations were performed in triplicate.

For the visual representation of the spectra, data were normalised and a dilution correction was performed for each data set as follows:

$$\mathrm{Abs_{corr}} = \frac{\mathrm{Abs_{sample}} \times \mathrm{V_{sample}}}{\mathrm{V_{orig}}}$$

Where $\mathrm{Abs_{corr}}$ is the absorbance corrected for dilution

$\mathrm{Abs_{obs}}$ is the observed absorbance for the sample

$\mathrm{V_{sample}}$ is the total volume of the sample

and $\mathrm{V_{orig}}$ is the volume of the original working solution (i.e. 2000 µL)

For example, the corrected absorbance readings for a sample that contains a total of 20 µL ligand solution added would be calculated using:

$$\mathrm{Abs_{corr}} = \frac{\mathrm{Abs_{sample}} \times 2020\ \mu\mathrm{L}}{2000\ \mu\mathrm{L}}$$

Association constants (logβ values) were calculated in HypSpec using a 2-reagent model with a 1:1 molar ratio. The raw spectroscopic data (that is, without dilution correction) was used as the HypSpec software takes the titration volumes into consideration. No additional coordination of DMSO could be modelled. The average logβ of each three identical spectrophotometric titrations was reported.

2.9.6.1 Thermodynamic study and van 't Hoff plot

Spectrophotometric titrations of CoTPP and *p*-PyrDTDA in DCM were performed at 20 °C[‡‡], 25 °C, 30 °C, 35 °C and 40 °C, following the same procedure as that listed above for the 25 °C experiments. For each temperature point, the titrations were performed in triplicate and the association constant for

[††] Metal stirrers are standard lab procedure as haem is known to adsorb onto glass and plastic surfaces. Plungers from broken glass syringes are reused for this purpose.

[‡‡] For the 20 °C titrations, only data corresponding to a total of 400 µL of dithiadiazolyl stock was used to determine the association constant, as aggregation and precipitation was observed at higher dithiadiazolyl concentrations.

each titration was determined. These values are listed in Table 2.3. The data for the van ‘t Hoff plot is shown in Table 2.4.

Table 2.3: All log values for CoTPP and p-*PyrDTDA*

Temperature	**1**	**2**	**3**	**Average**
20 °C	4.36	4.32	4.28	4.32 ± 0.04
25 °C	4.19	4.14	4.23	4.19 ± 0.05
30 °C	4.15	4.12	4.19	4.15 ± 0.04
35 °C	4.04	4.11	4.07	4.07 ± 0.04
40 °C	3.91	3.97	4.00	3.96 ± 0.05

Table 2.4: Data for van 't Hoff plot

T (K)	**1/T**	**log K_{eq}**	**K_{eq}**	**lnK_{eq}**
293.15	0.003411	4.32 ± 0.04	20952 ± 1928	9.95 ± 0.09
298.15	0.003354	4.19 ± 0.05	15425 ± 1590	9.64 ± 0.10
303.15	0.003299	4.15 ± 0.04	14265 ± 1159	9.56 ± 0.08
308.15	0.003245	4.07 ± 0.04	11865 ± 964	9.38 ± 0.08
313.15	0.003193	3.96 ± 0.05	9154 ± 949	9.12 ± 0.11

2.10 References

(1) Cordes, A. W.; Haddon, R. C.; Oakley, R. T. *Adv. Mater*. **1994**, *6*, 798.

(2) Rawson, J. M.; Palacio, F.; Veciana, J.; Editor. *Magnetic properties of thiazyl radicals, in: π-Electron Magnetism: From Molecules to Magnetic Materials*; Springer-Verlag, Berlin, 2001.

(3) Rawson, J. M.; Banister, A. J.; Lavender, I. *Adv. Heterocycl. Chem.* **1995**, *62*, 137.

(4) Preuss, K. E. *Dalton Trans.* **2007**, *23*, 2357.

(5) Haynes, D. A. *CrystEngComm* **2011**, *13* (15), 4793.

(6) Beletskaya, I.; Tyurin, V. S.; Tsivadze, A. Y.; Guilard, R.; Stern, C. *Chem. Rev.2* **2009**, *109*, 1659.

(7) Hearns, N. G. R.; Hesp, K. D.; Jennings, M.; Korcok, J. L.; Preuss, K. E.; Smithson, C. S. *Polyhedron* **2006**, *26*, 2047.

(8) Britten, J.; Hearns, N. G. R.; Preuss, K. E.; Richardson, J. F.; Bin-Salamon, S. *Inorg. Chem.* **2007**, *46* (10), 3934.

(9) Jennings, M.; Preuss, K. E.; Wu, J. *Chem. Comm* **2006**, 341.

(10) Hearns, N. G. R.; Preuss, K. E.; Richardson, J. F.; Bin-Salamon, S. *J. Am. Chem. Soc.* **2004**, *126* (32), 9942.

(11) Antorrena, G.; Brownridge, S.; Cameron, T. S.; Palacio, F.; Parsons, S.; Passmore, J.; Thompson, L. K.; Zarlaida, F. *Can. J. Chem.* **2002**, *80*, 1568.

(12) Banister, A. J.; Gorrell, I. B.; Rawson, J. M.; Jorgensen, K. A. *J. Chem. Soc., Dalt. Trans.* **1991**, 1105.

(13) Banister, A. J.; Gorrell, I. B.; Lawrence, S. E.; Lehmann, C. W.; May, I.; Tate, G.; Blake, A. J.; Rawson, J. M. *J. Chem. Soc. Chem. Commun.* **1994**, No. 15, 1779.

(14) Lau, H. F.; Ng, V. W. L.; Koh, L. L.; Tan, G. K.; Goh, L. Y.; Roemmele, T. L.; Seagrave, S. D.; Boeré, R. T. *Angew. Chemie Int. Ed.* **2006**, *45* (27), 4498.

(15) Robinson, S. W.; Haynes, D. A.; Rawson, J. M. *CrystEngComm* **2013**, *15* (47), 10205.

(16) Adler, A. D.; Longo, F. R.; Finarelli, J. D.; Goldmacher, J.; Assour, J.; Korsakoff, L. *J. Org. Chem.* **1967**, *32* (2), 476.

(17) Adler, A. D.; Longo, F. R.; Kampas, F.; Kim, J. *J. Inorg. Nucl. Chem.* **1970**, *32* (7), 2443.

(18) Haynes, D. A.; van Laeren, L. J.; Munro, O. Q. Manuscript in preparation.

(19) Kadish, K. M.; Smith, K. M.; Guilard, R.; Eds. *Inorganic, Organometallic and Coordination Chemistry. The Porphyrin Handbook, Vol. 3*; Academic Press: San Diego, CA, 2000.

(20) Batsanov, S. S. *Inorg. Mater.* **2001**, *37* (9), 871.

(21) Allen, F. H. *Acta Crystallogr.* **2002**, *B58*, 380.

(22) Cordes, A. W.; Bryan, C. D.; Davis, W. M.; de Laat, R. H.; Glarum, S. H.; Goddard, J. D.; Haddon, R. C.; Hicks, R. G.; Kennepohl, D. K.; Oakley, R. T.; Scott, R. S.; Westwood, N. P. C. *J. Am. Chem. Soc.* **1993**, *115*, 7232.

(23) Terazono, Y.; Patrick, B. O.; Dolphin, D. H. *Inorg. Chim. Acta* **2003**, *346*, 265.

(24) Summers, J. S.; Petersen, J. L.; Stolzenberg, A. M. *J. Am. Chem. Soc.* **1994**, *116* (16), 7189.

(25) Bang, H.; Edwards, J. O.; Kim, J.; Lawler, R. G.; Reynolds, K.; Ryan, W. J.; Sweigart, D. a. *J. Am. Chem. Soc.* **1992**, *114* (8), 2843.

(26) Gouterman, M. *J. Mol. Spectrosc.* **1961**, *6*(1), 138.

(27) Hyp Spec, Protonic Software, Leeds, England.

Chapter 3

Investigating the interaction between dithiadiazolyl radicals and cobalt porphyrins using UV-Vis spectroscopy

---

3.1 Introduction

In Chapter 2, the synthesis of the dithiadiazolyl radical – metalloporphyrin complex **R1•P1** from 4-(4′-pyridyl)-1,2,3,5-dithiadiazolyl (**R1**) and cobalt (II) tetraphenylporphyrin (**P1**) (Figure 3.1) was discussed.

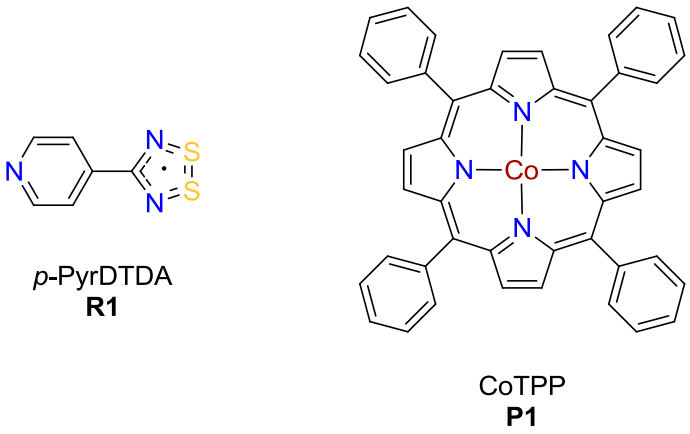

*Figure 3.1: Structures of **R1** and **P1***

When the two components are combined in solution, a five-coordinate cobalt complex, **S-R1•P1** is formed, with the dithiadiazolyl radical coordinating to the cobalt ion through a sulfur atom. The sulfur – metal bond displayed in this structure is a novel coordination mode for dithiadiazolyls. In the solid state, these units form coordination polymers and crystallize as **R1•P1(THF)**. In addition to the sulfur-cobalt bond, the dithiadiazolyl radical also coordinates to the cobalt ion through the pyridyl nitrogen, forming bridges between six-coordinate metalloporphyrin units. Electron transfer from the cobalt ion to the dithiadiazolyl occurs, such that the cobalt (II) is oxidised to cobalt (III) and the dithiadiazolyl is reduced to the dithiadiazolyl anion. It appears that this electron transfer is only partial and that the coordination polymer represents a resonance hybrid between the Co(II)-dithiadiazolyl and Co(III)-dithiadiazolide species. Upon dissolution, the coordination polymer dissociates into five-

coordinate dithiadiazolyl-metalloporphyrin monomer units that differ from the initial complex formed. ^{1}H and ^{59}Co NMR spectroscopy confirmed that this complex is a cobalt (III) species with a dithiadiazolide anion axial ligand, coordinated through the pyridyl nitrogen.

After studying the coordination of *p*-PyrDTDA to cobalt (II) tetraphenylporphyrin in detail, the focus of the study shifted to other systems, with the consideration that similar coordination materials could potentially be made using different combinations of dithiadiazolyls and metalloporphyrins.

While the possibilities that could be investigated were extensive, for this study it was decided to limit the investigation to a set array of dithiadiazolyl radicals. Following the success with the pyridyl dithiadiazolyl radical ligand (**R1**), the phenyl analogue was investigated as it could only coordinate through the dithiadiazolyl ring. If coordination of the phenyl dithiadiazolyl to CoTPP did occur, it was expected to give a similar result to that found for **R1**. Additionally, without the pyridyl substituent, radical-metalloporphyrin units would be unable to oligomerise and form coordination polymers as seen for **R1•P1**, the result of which would be interesting to observe in the solid state. On the other hand, to investigate the effect of the position of the pyridyl nitrogen on the formation of both discrete complexes as well as oligomerisation, *meta*-pyridyl dithiadiazolyl was chosen. Moreover, the effect that electron-withdrawing groups, such as fluorine substituents, or electron-donating groups, such as methyl substituents, would have was of interest to investigate how changing the electrostatics of the aryl substituent would change the overall electrostatics of the dithiadiazolyl molecule and consequently affect the relative strength of coordination. It is worth noting that the electronic effect of aryl substituents on the dithiadiazolyl ring has been established to be small, as a result of the nodal SOMO. For example, electrochemical and EPR studies reveal little change to the radical with functional group.[3]

With these criteria set, a series of dithiadiazolyl radicals that had been successfully synthesised in the literature was examined, taking into consideration the relative cost and availability of the starting materials necessary to synthesise the desired radicals. Ultimately, eight dithiadiazolyl radicals, **R1** through **R8**, that fit the criteria were decided upon (Figure 3.2).

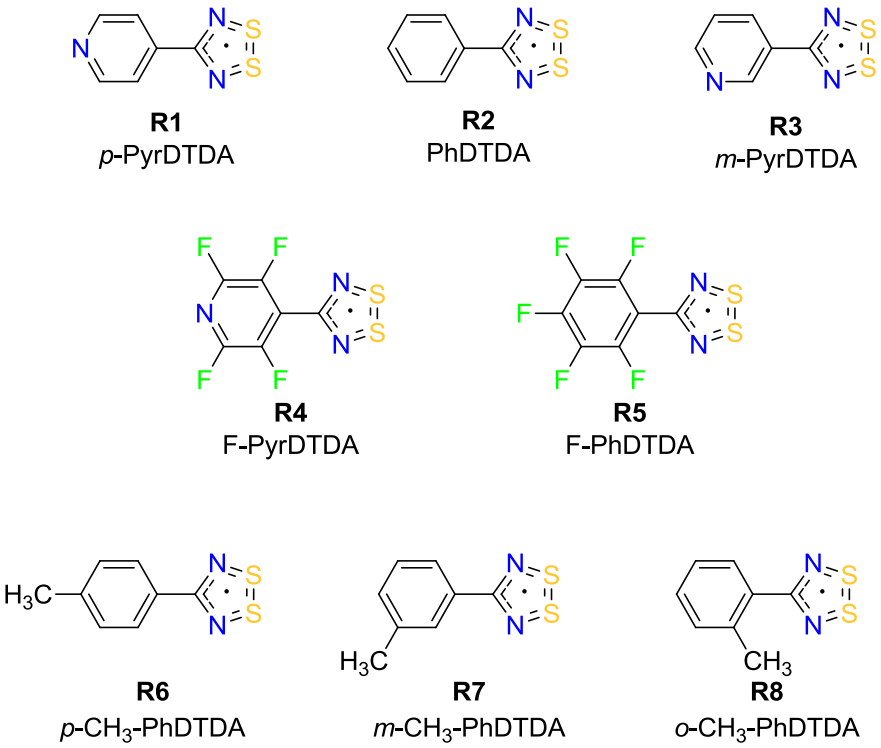

*Figure 3.2: Structures of dithiadiazolyl radicals **R1** to **R8***

Following the success with **R1** and CoTPP (**P1**) the study started with these radicals and CoTPP. Initial experimental work focussed on attempting to synthesise solid coordination materials through a range of crystallization techniques, hoping to isolate materials with similar unusual coordination and/or redox behaviour. However, after numerous attempts, it became apparent that obtaining solid-state material was non-trivial, as the isolation of any solid material of coordination compounds beyond **R1•P1(THF)** was unsuccessful. The focus of the study consequently turned to studying these systems in solution. Ultraviolet-Visible (UV-Vis) spectroscopy had proved to be an invaluable tool for studying the association of **R1** to **P1**, and so it was decided to use this analytical technique to determine if similar association could be observed for the remaining seven dithiadiazolyl radicals and **P1**. Attempts to isolate these complexes are ongoing.

In addition to changing the functionality of the dithiadiazolyl radical, the effect that changing the nature of the porphyrin had on the association of a dithiadiazolyl ligand, if any, was studied. Following from the criteria for choosing the dithiadiazolyl ligands, two additional cobalt porphyrins (Figure 3.3) were selected. One porphyrin with electron-withdrawing fluorine substituents, namely cobalt (II) tetrakis(pentafluorophenyl)porphyrin (CoTFP, **P2**) was chosen, as well as one with electron-donating methyl substituents, namely cobalt (II) tetratolylporphyrin (CoTTP, **P3**). It was hypothesised that dithiadiazolyl ligand association to CoTFP would be stronger than for CoTPP, as

there was literature precedent for electron-withdrawing substituents on a porphyrin resulting in stronger axial ligand binding.[1] These electron-withdrawing substituents reduce the electron density on the metal ion, resulting it in being a stronger Lewis acid. On the other hand, it was thought that dithiadiazolyl radical association to CoTTP would be weaker than for CoTPP, as a result of the electron-donating methyl substituents.

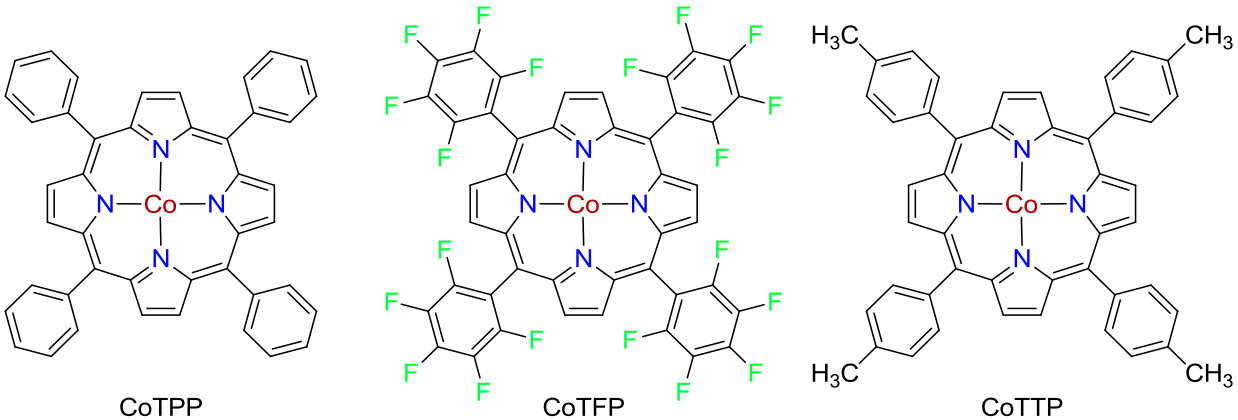

*Figure 3.3: Structures of porphyrins **P1** to **P3***

Dithiadiazolyl radicals **R1** to **R8** were prepared using a known literature one-pot procedure from their respective nitriles (see Chapter 2).[2] The free-base porphyrins $TPPH_2$, $TFPH_2$ and $TTPH_2$ were synthesised from their respective benzaldehydes and underwent condensation with freshly-distilled pyrrole as described by Adler and coworkers,[3] and were subsequently metalated with $Co(OAc)_2{\cdot}4H_2O$ to give porphyrins **P1**, **P2** and **P3** respectively[4] (see Chapter 2).

3.2 Investigating dithiadiazolyl radicals as axial ligands with cobalt (II)tetraphenylporphyrin

3.2.1 Spectrophotometric titrations

In Chapter 2 it was shown that UV-Vis spectroscopy is a useful technique to study the coordination of *p*-PyrDTDA (**R1**) to CoTPP (**P1**) in solution. A spectrophotometric titration was performed and the resulting spectral data was used to determine the association constant, logβ, for the reaction shown in equation 3.1.

$$R1 + P1 \overset{\beta}{\rightleftharpoons} R1 \bullet P1 \qquad (3.1)$$

The Soret band for CoTPP in DCM is found at 410 nm. Addition of **R1** induces a hypochromic shift, while a new peak develops at 434 nm. This change is also visible as the colour of the working solution changes from red for the CoTPP solution to a yellow-orange after addition of the *p*-PyrDTDA (Figure 3.4). Clean isosbestic points are seen at 386 and 418 nm. The spectra for this spectrophotometric titration can be seen in Figure 3.5(a).

Figure 3.4: The red CoTPP solution (left) and the visible shift in colour to yellow-orange after titration with p-*PyrDTDA (right)*

Based on the success of UV-Vis spectroscopy with regards to studying the **R1•P1** system, it was decided to use this technique to investigate whether similar radical – porphyrin association could be observed for other dithiadiazolyl radicals. If radical-porphyrin association is occuring, a profile similar to that for **R1•P1** will be observed, with the Soret band at 410 nm diminishing in intensity

while absorbance at a different wavelength increasing; however, if there is no association, the porphyrin spectrum will remain unchanged.

A series of spectrophotometric titrations were performed with CoTPP and dithiadiazolyl radicals **R2** through **R8**. For each titration, a 2 μM solution of CoTPP in DCM was prepared and the spectrum was recorded between 375 and 450 nm. Aliquots of a 2 mM stock solution of the relevant dithiadiazolyl radical were added to the solution (and the reference cuvette) and the spectrum recorded following each addition. For each dithiadiazolyl radical, the titration was repeated in triplicate. The resulting spectra for these spectrophotometric titrations are shown in Figure 3.5.

PhDTDA (**R2**), the phenyl analogue of *p*-PyrDTDA, was the second radical investigated. Unlike the pyridyl radical, this dithiadiazolyl can only coordinate through the atoms of the heterocyclic ring. This means that any association observed must be occurring between the cobalt ion and the dithiadiazolyl ring, in a similar manner to the S-bound geometry observed for **R1**. A similar pattern is seen in this titration as for that of **R1**. The Soret band of CoTPP at 410 nm slowly decreases in intensity as the concentration of **R2** increases. A shoulder starts to appear in the region of 430 to 440 nm and an isosbestic point can be seen at 420 nm. This indicates that radical-porphyrin association is occurring to form the complex **R2•P1**. (Figure 3.5(b))

The next dithiadiazolyl tested, **R3**, was selected in order to investigate if the position of the pyridyl nitrogen relative to the dithiadiazolyl ring has an effect on the association constant (Figure 3.5(c)). The titration for the *meta*-pyridyl dithiadiazolyl shows a similar profile to that of **R1**. The Soret band at 410 nm steadily decreases and a new peak evolves at 430 nm. There is an isosbestic point at 418 nm for the majority of the titration; however the isosbestic point is not shared for the last few additions of ligand.

The following ligands to be investigated were the perfluorinated pyridyl (**R4,** Figure 3.5(d)) and perfluorinated phenyl (**R5,** Figure 3.5(e)) dithiadiazolyl radicals, to determine the effect of electron-withdrawing groups on the dithiadiazolyl towards coordination. Both spectra show the peak at 410 nm steadily decreasing, while a peak at 433 nm starts to appear. The spectra do not have distinct isosbestic points throughout the titrations. This is possibly a result of the electron-withdrawing fluorine substituents slowing the reaction rate, meaning that the system was not sufficiently equilibrated at the times the spectra were collected.

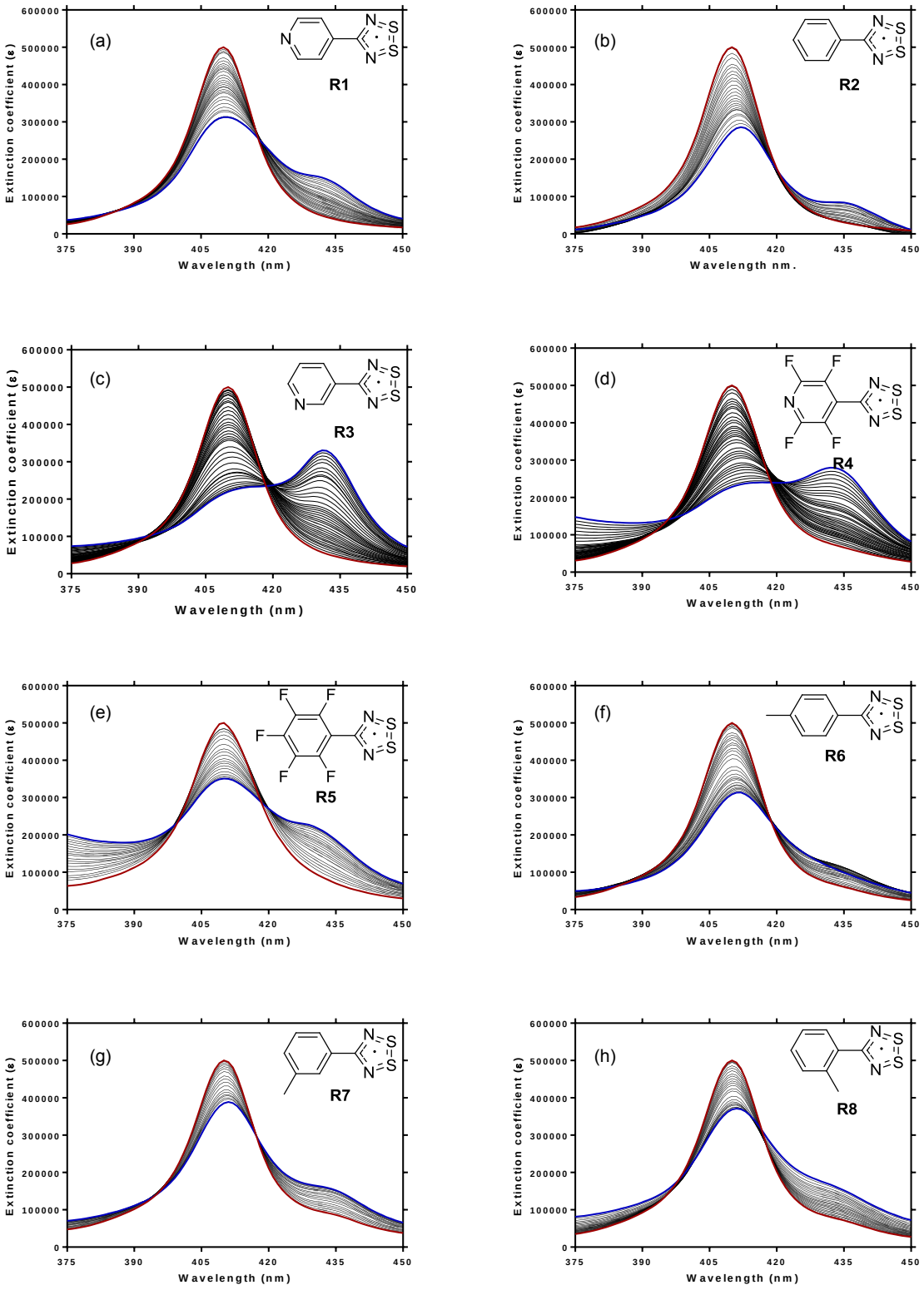

*Figure 3.5: UV-Vis spectrophotometric titrations for CoTPP (**P1**) in DCM at 25 °C with increasing dithiadiazolyl ligand concentration, forming **R1•P1** (a), **R2•P1** (b), **R3•P1** (c), **R4•P1** (d), **R5•P1** (e), **R6•P1** (f), **R7•P1** (g) and **R8•P1** (h). The original CoTPP spectrum is shown in red. The final addition of ligand is shown in blue with intermediate additions shown in black. Titration spectra have been corrected for dilution.*

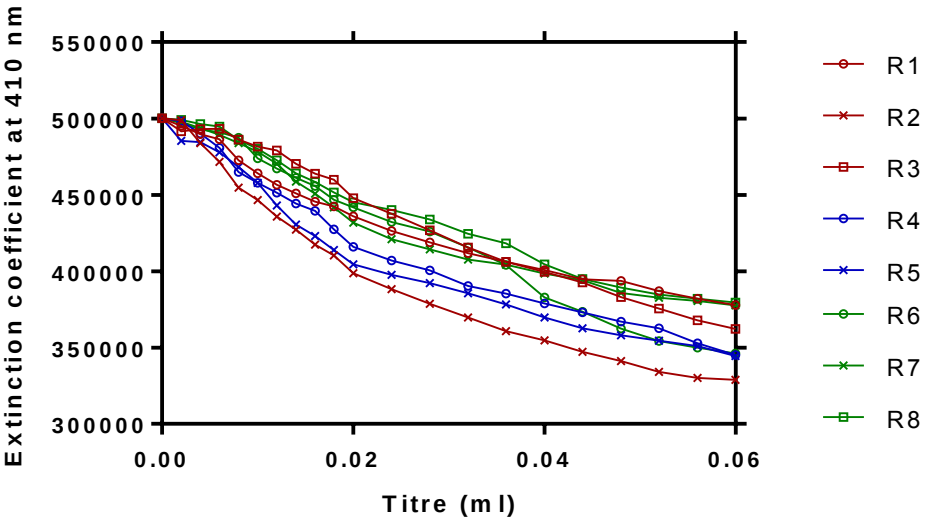

Figure 3.6: UV-Vis absorbance at 410 nm for CoTPP with increasing dithiadiazolyl ligand concentration for ligands R1 – R8.

The final three dithiadiazolyl radicals investigated were phenyl dithiadiazolyls with methyl substituents in the *para*-, *meta*- and *ortho*-positions. All three sets of spectrophotometric titrations display similar spectroscopic changes, as seen in Figure 3.5(f) (*p*-CH_3-PhDTDA), Figure 3.5(g) (*m*-CH_3-PhDTDA) and Figure 3.5(h) (*o*-CH_3-PhDTDA). The Soret band slowly decreases in intensity, and absorbance in the region 420 to 450 nm increases with clean isosbestic points (419 nm for **R6**, 394 nm and 418 nm for **R7** and 416 nm for **R8**).

Figure 3.6 shows the change in absorbance at 410 nm for the addition of all eight ligands to CoTPP. It is apparent that there is little difference between the ligands, with no clear trend that emerges relating the change in absorbance to the type of ligand.

3.2.2 Association constants

The spectroscopic data from the spectrophotometric titrations were analysed and a binding model was fitted using HypSpec.[5] All eight of the dithiadiazolyl radicals investigated showed 1:1 coordination to CoTPP, as shown in reaction equation 5, forming the five-coordinate Co(II) species **R*n*•P1** (where R*n* represents any radical **R1** to **R8**).[1] The logarithm of the equilibrium constant, β, for the reaction is referred to as the association constant in this study. The association constant, logβ, was determined for each spectrophotometric titration using HypSpec.[5]

[1] In addition to the 1:1 metal-to-ligand binding model, a 2:1 metal-to-ligand binding model and a 1:2 metal-to-ligand binding model was also fitted. However, the 1:1 model gave the best fit. See Appendix B for an example of these models fitted to the binding of **R1** to **P1**.

$$Rn + P1 \overset{\beta}{\rightleftharpoons} Rn \bullet P1 \qquad (3.2)$$

A summary of the association constants for radicals **R1** to **R8** coordinating to CoTPP is given in Table 3.1, showing the average logβ value from the triplicate titrations. A higher logβ value indicates a stronger association between the metalloporphyrin and the axial dithiadiazolyl ligand.

Table 3.1: Association constants for dithiadiazolyl radicals coordinating to Co(II) tetraphenylporphyrin (DCM, 25 °C)

	Dithiadiazolyl Ligand	Average logβ with CoTPP (P1)
R1	*p*-PyrDTDA	4.19 ± 0.05
R2	PhDTDA	4.27 ± 0.04
R3	*m*-PyrDTDA	3.92 ± 0.06
R4	F-PyrDTDA	4.12 ± 0.02
R5	F-PhDTDA	3.66 ± 0.04
R6	*p*-CH_3-PhDTDA	4.49 ± 0.02
R7	*m*-CH_3-PhDTDA	3.85 ± 0.03
R8	*o*-CH_3-PhDTDA	4.37 ± 0.03

As previously discussed in Chapter 2, the coordination of *p*-PyrDTDA to CoTPP has a logβ value of 4.19 ± 0.05. This is substantially different compared to the logβ for heterocyclic nitrogen-based ligands, such as pyridine binding to CoTPP (logβ: 2.90 in DCM)[6] or 4-cyanopyridine binding to CoTPP (logβ: 2.60 in DCM).[7] No association constants for the coordination of similar heterocyclic sulfur-based ligands to CoTPP could be found. Based on the NMR, EPR and UV-Vis spectroscopy data presented in Chapter 2, it is proposed that the dithiadiazolyl is coordinating through the heterocyclic sulfur instead of the pyridyl nitrogen.

For PhDTDA, an association constant of 4.27 ± 0.04 was determined. This is within 3 standard deviations of that of **R1**, meaning the values can be considered to be the same. As **R2** can only coordinate to CoTPP through the dithiadiazolyl heterocyclic ring, the similarity between the coordination of these two radicals to CoTPP supports the hypothesis that association in solution is occurring between the cobalt ion and a sulfur atom of the dithiadiazolyl heterocyclic ring.

For pyridyl dithiadiazolyl radicals, the position of the pyridyl nitrogen atom relative to the dithiadiazolyl ring does seem to have an influence on the coordination of the ligand to the cobalt ion, as *m*-PyrDTDA has an association constant of 3.92 ± 0.06, lower than that of the *para*-pyridyl isomer.

The perfluorinated pyridyl dithiadiazolyl **R4** has a logβ value of 4.12 ± 0.02, comparable to 4.19 ± 0.05 for **R1**. This was surprising as the original hypothesis was that the presence of the fluorine substituents would significantly lower the association constant. The perfluorinated pyridyl dithiadiazolyl **R5** has an association constant of 3.66 ± 0.04, which is appreciably lower than the logβ value of 4.27 ± 0.04 for **R2**. The greater difference for the perfluorinated phenyl radical compared to the perfluorinated pyridyl radical may be a result of this radical having the additional fluorine atom in the *para* position adding further to the electron-withdrawing effect, which is supported by the different Hammett parameters of the two fluorinated substituents.[8]

As predicted, the presence of weakly electron-donating methyl groups had the opposite effect than the electron-withdrawing fluorine substituents did. This effect is particularly evident when the methyl group is in the *para* or *ortho* position relative to the dithiadiazolyl ring, as the theoretical electron-donating effect to the *ipso* dithiadiazolyl ring is largest in these positions. The *para*-substituted isomer, **R6**, has a logβ value of 4.49 ± 0.02, which is the strongest of the radical ligands investigated. The *m*-CH_3-PhDTDA ligand, **R7**, has an association constant of 3.85 ± 0.03, lower than that of the unsubstituted phenyl ligand **R2**. Finally, the *ortho*-substituted radical **R8** has an association constant of 4.37 ± 0.03. This is less than that of **R6**, and is not significantly higher than that of **R1**, possibly as a result of the increased steric bulk in the *ortho* position having an effect on the approach of the radical ligand to the porphyrin.

It is clear that the system is remarkably tolerant of substituents on the dithiadiazolyl radical. While small changes in the strength of cobalt-radical association were observed, all eight ligands could be observed interacting with CoTPP with approximately the same strength. After it had been successfully shown that a range of dithiadiazolyl radicals with different functionalities formed coordination compounds with CoTPP, the next step was to investigate if similar compounds could be formed with other cobalt porphyrins, as well as how altering the electron density distribution across the porphyrin system affected coordination of the ligand to the metal.

The second porphyrin investigated, tetrakis(pentafluorophenyl)porphyrin, probed the influence that electron-withdrawing fluorine atoms on the periphery of the porphyrin has on the system.

3.3 Investigating dithiadiazolyl radicals as axial ligands with cobalt (II) tetrakis(pentafluorophenyl)porphyrin

3.3.1 Spectrophotometric titrations

The same series of experiments was carried out for Co(II) tetrakis(pentafluorophenyl)porphyrin (CoTFP) as for CoTPP. Spectrophotometric titrations were carried out with the porphyrin and each of the dithiadiazolyl radicals **R1** to **R8**, under the same conditions as for the original porphyrin, and the association constant, logβ, was determined for each radical-porphyrin pair. A series of spectrophotometric titrations were performed with CoTFP and dithiadiazolyl radicals **R1** through **R8**. For each titration, a 2 μM solution of CoTFP in DCM was prepared and the spectrum was recorded between 375 and 450 nm. Aliquots of a 2 mM stock solution of the relevant dithiadiazolyl radical were added to the solution (and the reference cuvette) and the spectrum recorded following each addition. For each dithiadiazolyl radical, the titration was repeated in triplicate. The resulting spectra for these spectrophotometric titrations are shown in Figure 3.7.

The Soret band for CoTFP in DCM has a λ_{max} wavelength of 404 nm. Titration with *p*-PyrDTDA (**R1**) results in this peak reducing in intensity, as well as a red-shift to 406 nm (Figure 3.7(a)). Two isosbestic points can be seen at 395 nm and 409 nm. A 1:1 binding model was fitted to the spectroscopic data, confirming that the coordination complex **R1•P2** was formed in solution. For the addition of the phenyl dithiadiazolyl **R2** to CoTFP (Figure 3.7(b)), the result is similar that of **R1**.The peak at 404 nm shifts slightly and broadens with increasing ligand concentration. There is an isosbestic point at 413 nm.

For the addition of *m*-PyrDTDA, **R3**, to CoTFP, the Soret band at 404 nm steadily decreases and absorbance in the region 420 to 450 nm increases (Figure 3.7(c)). There is an isosbestic point at 416 nm. For both the perfluorinated radicals, the changes to the spectrum after titration are less extensive than observed for previous radical-metalloporphyrin combinations.

Looking at the spectrum for the titration of CoTTP with F-PyrDTDA (**R4,** (Figure 3.7(d))), the Soret band can be observed decreasing in intensity and shifting from 404 nm to 408 nm, with an isosbestic point at 385 nm. However, unlike the previous examples, there is little change to the spectrum in the region between 410 and 450 nm. Addition of the perfluorinated phenyl radical **R5** to CoTFP shows the smallest change to the spectrum, with a decrease in absorbance at 404 nm after the first addition of ligand, followed by small increases in absorbance at 405 nm (Figure 3.7(e)). There is an isosbestic point at 408 nm and absorbance at 375 nm increases with increasing ligand concentration.

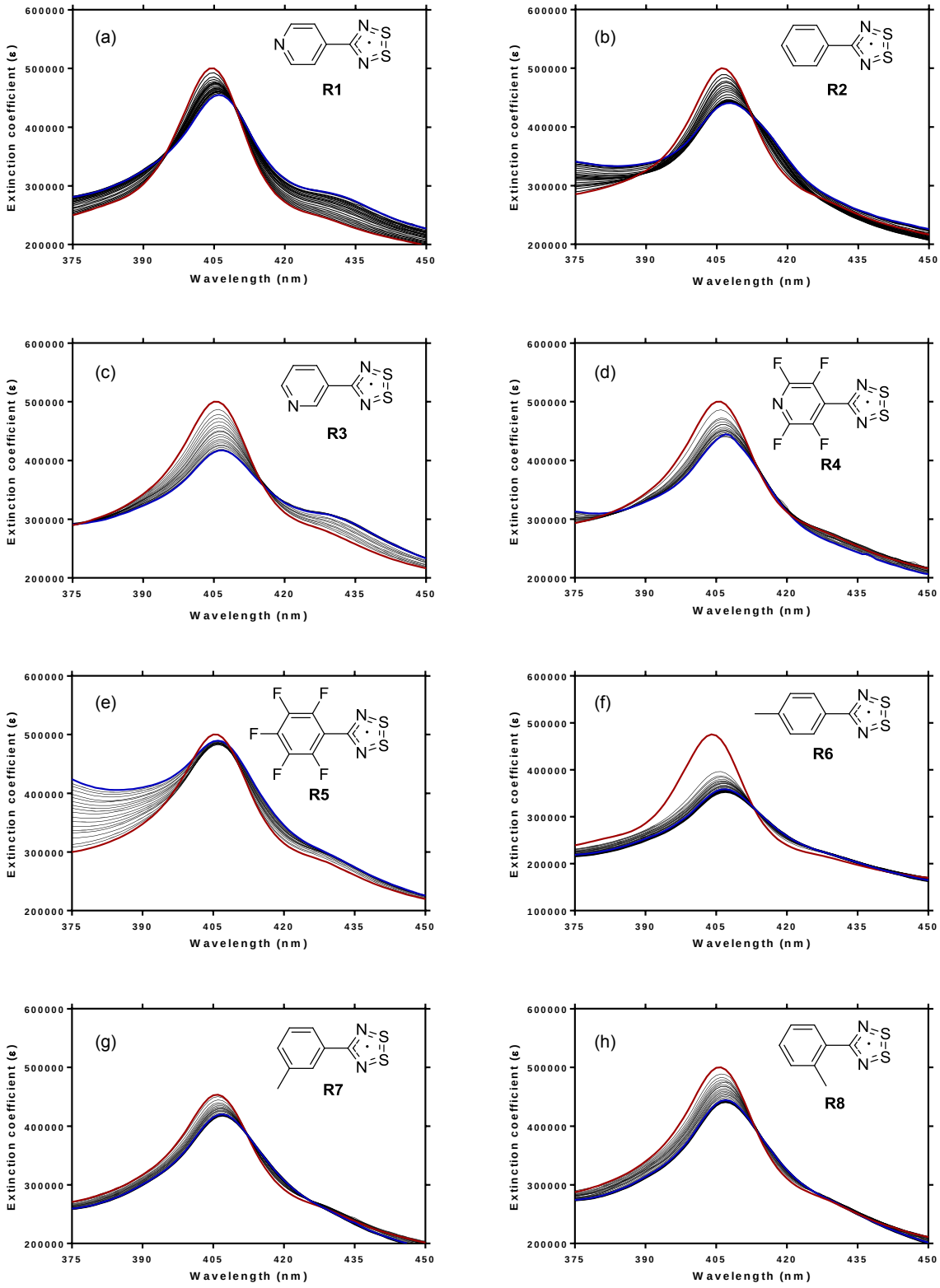

*Figure 3.7: UV-Vis spectrophotometric titrations for CoTFP (**P2**) in DCM at 25 °C with increasing dithiadiazolyl ligand concentration, forming **R1•P2** (a), **R2•P2** (b), **R3•P2** (c), **R4•P2** (d), **R5•P2** (e), **R6•P2** (f), **R7•P2** (g) and **R8•P2** (h). The original CoTFP spectrum is shown in red. The final addition of ligand is shown in blue with intermediate additions shown in black. Titration spectra have been corrected for dilution.*

The reaction of CoTFP with *p*-CH_3-PhDTDA shows a profound change to the spectrum on initial addition of the ligand solution (Figure 3.7(f)). The Soret band at 404 nm decreases in intensity sharply with a corresponding shift to 407 nm. An isosbestic point occurs at 414 nm. Addition of *m*-CH_3-PhDTDA to CoTFP results in the peak at 404 nm steadily decreasing in intensity with a gradual shift to 408 nm (Figure 3.7(g)). An isosbestic point occurs at 412 nm. The *ortho*-substituted isomer, **R8**, appears to react with CoTFP in a manner similar to the *para*-substituted isomer. The Soret band at 404 nm decreases in intensity sharply, with a shift to 407 nm, immediately on addition of ligand. An isosbestic point occurs at 413 nm (Figure 3.7(h)).

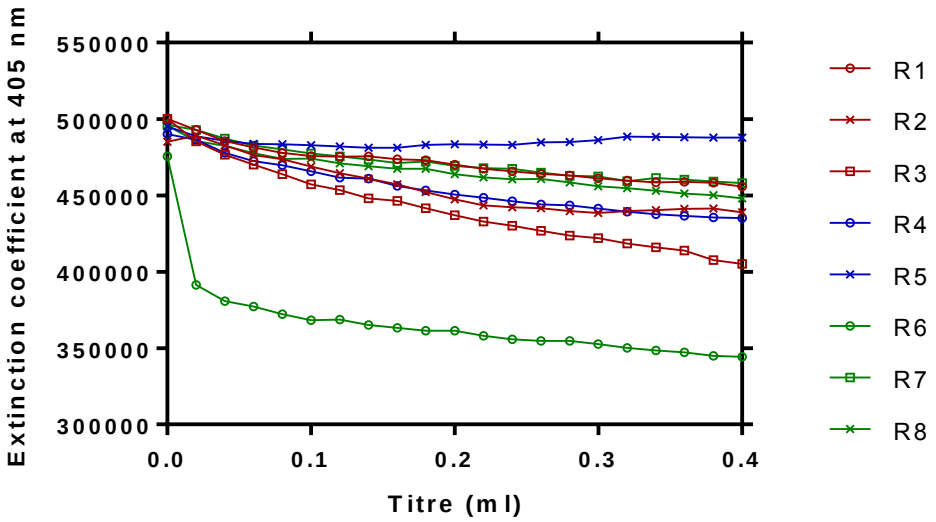

Figure 3.8: UV-Vis absorbance at 405 nm for CoTFP with increasing dithiadiazolyl ligand concentration for ligands R1 – R8.

Figure 3.8 shows the change in absorbance at 405 nm for different ligands. For R6 there is a clear difference, with the absorbance decreasing more rapidly at low ligand concentration than for the remaining ligands. For R5, there is very little change in absorbance. The remaining ligands are similar to one another.

3.3.2 Association constants

The spectroscopic data from the spectrophotometric titrations were analysed and a binding model was fitted using HypSpec.[5] All of the dithiadiazolyl radicals investigated showed 1:1 coordination to CoTFP, as shown in reaction equation 3.3, forming the five-coordinate Co(II) species **R*n*•P2** (where R*n* represents any radical **R1** to **R8**). The association constant, logβ, was determined for each spectrophotometric titration.

$$Rn + P2 \overset{\beta}{\rightleftharpoons} Rn \bullet P2 \qquad (3.3)$$

The summary of the association constants for radicals **R1** to **R8** coordinating to CoTFP is given in Table 3.2, showing the average logβ value from the triplicate titrations.

Table 3.2: Association constants for dithiadiazolyl radicals coordinating to Co(II) tetrakis(pentafluorophenyl)-porphyrin (DCM, 25 °C)

	Dithiadiazolyl Ligand	Average logβ with CoTFP (P2)
R1	*p*-PyrDTDA	4.52 ± 0.04
R2	PhDTDA	4.56 ± 0.02
R3	*m*-PyrDTDA	4.39 ± 0.02
R4	F-PyrDTDA	3.59 ± 0.14
R5	F-PhDTDA	2.92 ± 0.10
R6	*p*-CH_3-PhDTDA	4.71 ± 0.07
R7	*m*-CH_3-PhDTDA	4.46 ± 0.08
R8	*o*-CH_3-PhDTDA	4.60 ± 0.06

Based on literature precedent, it was predicted that the inclusion of the electron-withdrawing fluorine atoms on the porphyrin periphery would increase the strength of cobalt-dithiadiazolyl binding. With the exception of the two fluorinated dithiadiazolyl ligands, higher logβ values were observed for the dithiadiazolyls coordinating to cobalt (II) tetrakis(pentafluorophenyl)porphyrin than for the original cobalt (II) tetraphenylporphyrin.

R1, *p*-PyrDTDA was found to have an association constant of 4.52 ± 0.04 with CoTFP, a marked increase from the value of 4.19 ± 0.05 with CoTPP. As with CoTPP, PhDTDA (**R2**) with CoTFP has a statistically equivalent association constant to **R1**, with a value of 4.56 ± 0.02 (within 3 standard deviations), and *m*-PyrDTDA (**R3**) has a lower logβ than **R1**, with a value of 4.39 ± 0.02.

The perfluorinated radicals coordinate far more weakly than their protonated analogues. F-PyrDTDA (**R4**) has an association constant of 3.59 ± 0.14, and F-PhDTDA (**R5**) has a logβ of only 2.89 ± 0.10, the weakest association constant of all radical – cobalt porphyrin systems investigated. Based on the results seen with CoTPP, it was expected that the perfluorinated radicals would have lower logβ values in comparison to the non-fluorinated analogues. However, these values are unusually low, as these two radicals are the only ones showing weaker association to CoTFP that to CoTPP, indicating

there are other variables that have not yet been identified. It is possible that this is a result of electrostatics and fluorine – fluorine repulsion.

Like the non-methylated **R2**, the three methylated phenyl radicals react with CoTFP more strongly than with CoTPP. The largest association constant was found for the *p*-CH_3-PhDTDA ligand, **R6**, with a logβ value of 4.71 ± 0.07. The *meta*-methylated phenyl radical **R7** had an association constant of 4.46 ± 0.08, comparable to the parent **R2** dithiadiazolyl. The final dithiadiazolyl, *o*-CH_3-PhDTDA (**R8**) had a logβ value of 4.60 ± 0.06, again comparable to **R2**.

It is evident that the presence of fluorine substituents on the periphery of the metalloporphyrin has a noticeable effect on the coordination of the dithiadiazolyl axial ligand. Indeed, changing the substituents on the porphyrin has a greater influence on the strength of ligand association than changing the substituents on the dithiadiazolyl. In general, dithiadiazolyl radicals coordinating to this cobalt porphyrin have higher association constants when compared to the original protonated cobalt tetraphenyl porphyrin (with the notable exception of the perfluorinated dithiadiazolyl radicals). This is consistent with the original hypothesis and with literature precedent that addition of electron-withdrawing substituents on the periphery of a porphyrin increases the logβ with respect to the same axial ligand, as this reduces the electron density on the metal centre and makes the metal centre more Lewis acidic (i.e. a better electron acceptor).[1,6] As seen with CoTPP, changing the nature of the substituents on the dithiadiazolyl resulted in relatively minor changes to the strength of association, with *p*-CH_3-PhDTDA having the strongest association to CoTFP and F-PhDTDA having the weakest association to CoTFP.

The third and final porphyrin used in this study explored the effect that electron-donating methyl substituents would have on the reactivity of the porphyrin with dithiadiazolyl ligands. It was anticipated that this would reverse the effect seen with CoTFP, resulting in lower association constants than for CoTFP and CoTPP.

3.4 Investigating dithiadiazolyl radicals as axial ligands with cobalt (II) tetratolylporphyrin

3.4.1 Spectrophotometric titrations

Initial investigations with a methylated porphyrin involved the use of tetramesitylporphyrin (H_2TMP). However, the solubility of CoTMP in DCM was too low for solution studies to be easily carried out. The *para*-methylphenyl porphyrin, tetratolylporphyrin (H_2TTP) was subsequently chosen as a suitable alternative. The same series of experiments was carried out for Co(II) tetratolylporphyrin (CoTTP) as for CoTPP. A series of spectrophotometric titrations were performed with CoTTP and dithiadiazolyl radicals **R1** through **R8**. For each titration, a 2 μM solution of CoTTP in DCM was prepared and the spectrum was recorded between 375 and 450 nm. Aliquots of a 2 mM stock solution of the relevant dithiadiazolyl radical were added to the solution (and the reference cuvette) and the spectrum recorded following each addition. For each dithiadiazolyl radical, the titration was repeated in triplicate. The resulting spectra for these spectrophotometric titrations are shown in Figure 3.9.

The Soret band for CoTTP in DCM has a λ_{max} wavelength of 414 nm. Titration with *p*-PyrDTDA results in this peak reducing in intensity, as well as a red-shift to 418 nm. A new peak starts to appear at 436 nm and isosbestic points can be seen at 388 and 423 nm. A 1:1 binding model was fitted to the spectroscopic data, confirming that the coordination complex **R1•P3** was formed in solution. The spectra for titration with PhDTDA show a less dramatic change than for **R1**, but have similar characteristics. The initial addition of ligand solution results in a large decrease in Soret band intensity with a corresponding red shift. Further additions of ligand show small incremental changes to the same effect, with an isosbestic point at 422 nm.

For *m*-PyrDTDA, the structural isomer of **R1**, evidence of coordination to the metalloporphyrin can again be observed. The Soret band does not shift from 414 nm, however it does decrease in intensity with increasing ligand concentration. Absorbance increases to either side of the Soret band, with a new peak appearing at 434 nm towards the end of the titration. Isosbestic points are seen at 400 nm and 418 nm.

For both the perfluorinated radicals, each addition of radical ligand results in small incremental changes to the spectrum observed. For the addition of **R4** (F-PyrDTDA), the Soret band decreases in intensity and shifts from 414 nm to 418 nm, a new peak develops at 436 nm and an isosbestic point occurs at 427 nm.

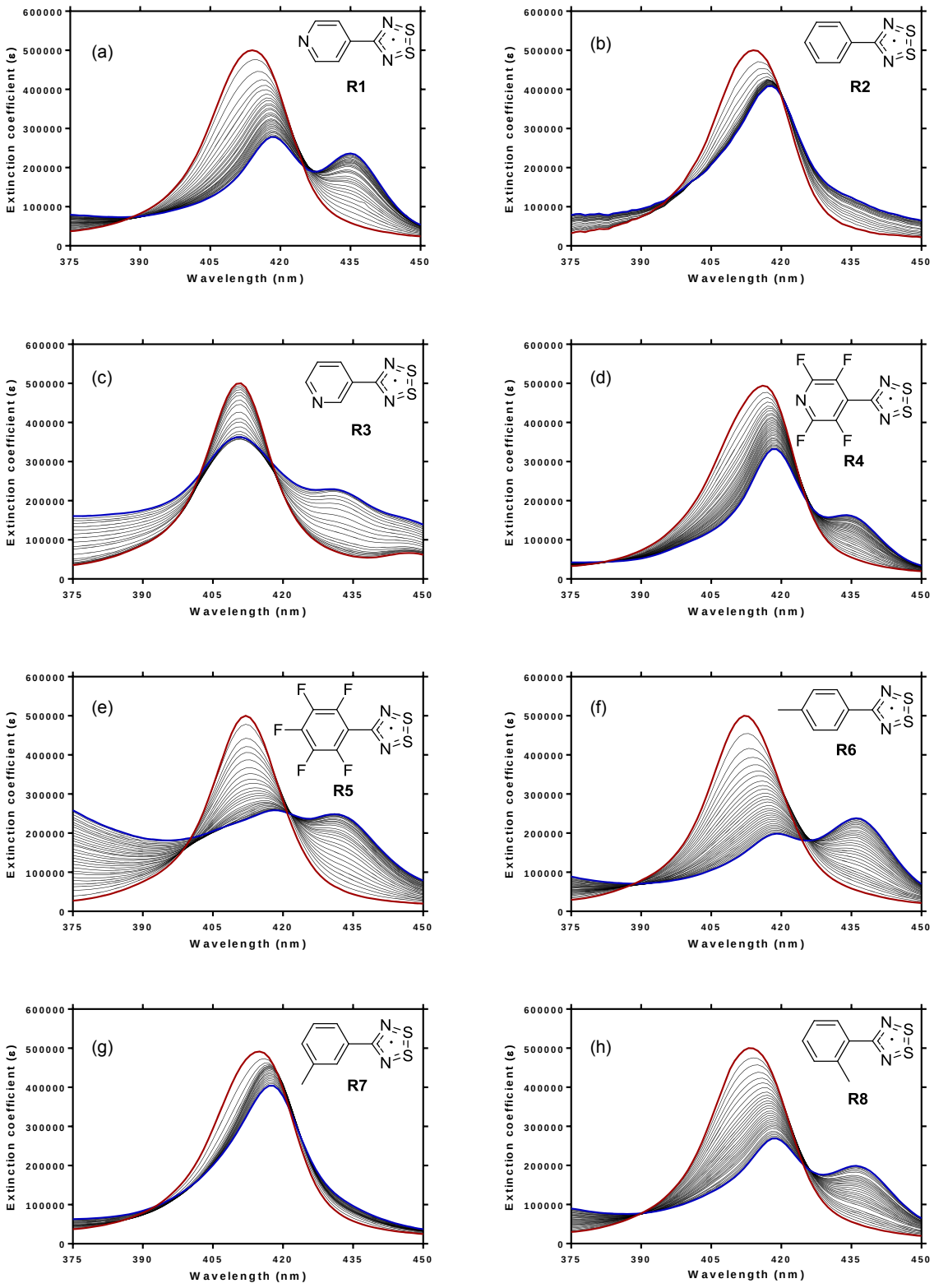

*Figure 3.9: UV-Vis spectrophotometric titrations for CoTTP (**P3**) in DCM at 25 °C with increasing dithiadiazolyl ligand concentration, forming **R1•P3** (a), **R2•P3** (b), **R3•P3** (c), **R4•P3** (d), **R5•P3** (e), **R6•P3** (f), **R7•P3** (g) and **R8•P3** (h). The original CoTTP spectrum is shown in red. The final addition of ligand is shown in blue with intermediate additions shown in black. Titration spectra have been corrected for dilution.*

For the titration of CoTTP with F-PhDTDA, the absorbance at 414 nm decreases and the local maximum shifts to 418 nm. Absorbance at 432 nm steadily increases, with an isosbestic point at 421 nm.

When looking at the spectra for the reaction of CoTTP with *p*-CH_3-PhDTDA the now-familiar pattern continues, with the Soret band at 414 nm decreasing in intensity with a corresponding shift to 418 nm. The absorbance at 436 nm increases to become a global maximum and an isosbestic point is seen at 388 nm. Addition of *m*-CH_3-PhDTDA to CoTTP results in a more subtle change to the spectrum, visually similar to that seen for PhDTDA. On initial addition of the radical to the cobalt porphyrin, the largest change is observed, with subsequent additions having increasingly smaller effects. The λ_{max} shifts from 414 nm to 418 nm, with absorbance decreasing with increasing ligand concentration. There is a small increase in absorbance in the region of 430 to 440 nm with an isosbestic point at 425 nm. The final ligand, *o*-CH_3-PhDTDA, shows titration spectra visually similar to those for *p*-CH_3-PhDTDA (as seen with CoTPP and CoTFP). The Soret band decreases steadily in intensity with a corresponding shift to 419 nm, while absorbance at 436 nm simultaneously increases. There are isosbestic points at 388 and 424 nm.

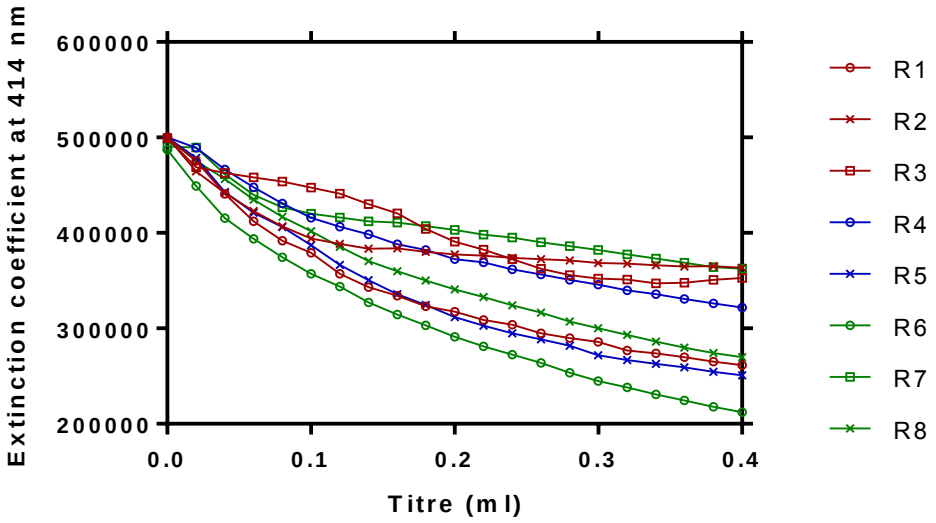

Figure 3.10: UV-Vis absorbance at 414 nm for CoTTP with increasing dithiadiazolyl ligand concentration for ligands R1 – R8.

Figure 3.10 shows the change in absorbance at 414 nm for the eight ligands. Unlike for CoTFP, there is no dramatically different profile for any of the eight ligands and there is no clear trend visible.

3.4.2 Association constants

The spectroscopic data from the spectrophotometric titrations were analysed and a binding model was fitted using HypSpec once again.[5] All of the dithiadiazolyl radicals investigated showed 1:1 coordination to CoTTP, as seen in reaction equation 3.4, forming the five-coordinate Co(II) species **R*n*•P3** (where R*n* represents any radical **R1** to **R8**). The association constant, logβ, was determined for each spectrophotometric titration.

$$\mathrm{R}n \; + \; \mathrm{P3} \overset{\beta}{\rightleftharpoons} \mathrm{R}n \bullet \mathrm{P3} \qquad (3.4)$$

A summary of the association constants for radicals **R1** to **R8** coordinating to CoTTP is given in Table 3.3, showing the average logβ value from the triplicate titrations.

Table 3.3: Association constants for dithiadiazolyl radicals coordinating to Co(II) tetratolylporphyrin (DCM, 25 °C)

	Dithiadiazolyl ligand	Average logβ with CoTTP (P3)
R1	*p*-PyrDTDA	3.57 ± 0.02
R2	PhDTDA	3.67 ± 0.05
R3	*m*-PyrDTDA	3.61 ± 0.04
R4	F-PyrDTDA	3.44 ± 0.05
R5	F-PhDTDA	3.55 ± 0.01
R6	*p*-CH_3-PhDTDA	4.03 ± 0.04
R7	*m*-CH_3-PhDTDA	3.37 ± 0.06
R8	*o*-CH_3-PhDTDA	3.72 ± 0.02

It is immediately apparent that there is a general lowering of logβ for all eight ligands relative to those found for CoTPP and CoTFP. As anticipated, while association constants were raised relative to CoTPP when CoTFP (with electron-withdrawing fluorine substituents) was investigated, the reverse was seen for CoTTP (with electron-donating methyl substituents). This is presumably a result of the tetratolylporphyrin increasing the electron density on the cobalt ion, reducing the Lewis acidity of the metal.

Amongst the range of dithiadiazolyl radicals investigated, similar trends emerge for the reaction with CoTTP as seen for CoTPP and CoTFP. For the coordination to CoTTP in DCM at 25 °C, the initial baseline dithiadiazolyl **R1** has an association constant of 3.57 ± 0.02. The phenyl analogue **R2** has an association constant of 3.67 ± 0.05. *m*-PyrDTDA (**R3**) has an association constant of 3.61 ± 0.04. These three dithiadiazolyl ligands have logβ values that are all within 3 standard deviations of each other and can be considered the same.

As seen with CoTPP and CoTFP, the perfluorinated radicals bind more weakly than their protonated analogues, although the effect is far less marked with CoTTP than with CoTPP and CoTFP. F-PyrDTDA (**R4**) has an association constant of 3.44 ± 0.05, while F-PhDTDA (**R5**) has a logβ of 3.55 ± 0.01. The average of the logβ values are lower than for the non-fluorinated analogues, however overall they are within the margin of error.

The methylated phenyl radicals also react with CoTTP in a similar manner as for CoTPP and CoTFP. The *para*-substituted analogue **R6** has the strongest affinity for CoTTP of the radicals investigated, with a logβ value of 4.03 ± 0.04, appreciably higher than that of **R2**. The *meta*-substituted isomer **R7** has an association constant of 3.37 ± 0.06, equivalent to that of the non-methylated **R2**. Finally, the *ortho*-substituted isomer **R8** has an association constant of 3.72 ± 0.02, again comparable to that of **R2**.

3.5 Summary and Conclusions

A total of 24 dithiadiazolyl radical-cobalt porphyrin complexes were formed *in situ* and studied in solution. One of these was previously known, but had not been studied in solution in detail, and 23 are new. Spectrophotometric titrations were performed to study the formation of these complexes. A blank titration (adding only the solvent system with no ligand) resulting in no spectroscopic change, confirming that the changes observed are as a result of ligand-metalloporphyrin interaction. In contrast, each radical-metalloporphyrin system investigated showed significant spectroscopic change that could be attributed to ligand-to-porphyrin association, with each titration spectrum being characteristic of the complex being formed. Unfortunately, no additional complexes (beyond **R1•P1(THF)**) could be isolated as solid materials.

Association constants (logβ) for the formation of these complexes in dichloromethane solution were determined. A full summary of these association constants is shown in Table 3.4.

.

*Table 3.4: Association constants for ligands **R1** to **R8** coordinating to porphyrins **P1**, **P2** and **P3***

Dithiadiazolyl ligand		Average logβ values		
		with CoTPP (P1)	with CoTFP (P2)	with CoTTP (P3)
R1	*p*-PyrDTDA	4.19 ± 0.05	4.52 ± 0.04	3.57 ± 0.02
R2	PhDTDA	4.27 ± 0.04	4.56 ± 0.02	3.67 ± 0.05
R3	*m*-PyrDTDA	3.92 ± 0.06	4.39 ± 0.02	3.61 ± 0.04
R4	F-PyrDTDA	4.12 ± 0.02	3.59 ± 0.14	3.44 ± 0.05
R5	F-PhDTDA	3.66 ± 0.04	2.92 ± 0.10	3.55 ± 0.01
R6	*p*-CH_3-PhDTDA	4.49 ± 0.02	4.71 ± 0.07	4.03 ± 0.04
R7	*m*-CH_3-PhDTDA	3.85 ± 0.03	4.46 ± 0.08	3.37 ± 0.06
R8	*o*-CH_3-PhDTDA	4.37 ± 0.03	4.60 ± 0.06	3.72 ± 0.02

All eight dithiadiazolyl radicals tested showed 1:1 coordination to all three cobalt porphyrins in dichloromethane. The association constants determined for the set of ligands with each porphyrin generally remained within an order of magnitude of each other. The choice of porphyrin used affects the strength of the cobalt-radical interaction, however, all three cobalt porphyrins formed coordination complexes with the dithiadiazolyl radicals, regardless of their different structures and electron distributions. Adding electron-withdrawing fluorine groups to the tetraphenylporphyrin periphery, in the case of CoTFP (**P2**), generally increased the cobalt-radical association constant and adding electron-donating methyl groups, as in the case of CoTTP (**P3**), decreased the logβ for all eight

ligands. Changing the electron density distribution of the porphyrin has a marked change to the electron density on the cobalt centre, which influences the strength of coordination to an axial ligand.

Certain trends were observable between the radical ligands with all three porphyrins. The parent pyridyl- and phenyl-dithiadiazolyls **R1** and **R2** displayed similar logβ values, confirming that coordination was most likely occurring through the dithiadiazolyl sulfur atom. In all cases, **R2** had a logβ value equivalent to that of **R1**, indicating that it was most likely that the two molecules are associating to the cobalt porphyrins in the same manner (that is, coordination to the cobalt through a dithiadiazolyl sulfur atom). Changing the position of the pyridyl nitrogen from the *para* position, relative to the dithiadiazolyl ring, to the *meta* position lowered the logβ value with all three cobalt porphyrins. This difference may be accounted for by the different values of the Hammett substituent constants for the 4-pyridyl and 3-pyridyl substituents, with the 4-pyridyl substituent being a better Lewis base.[8]

For the dithiadiazolyl radicals with electron-withdrawing fluorine atoms, **R4** and **R5**, the association constants were generally lower than for the parent dithiadiazolyl radicals, **R1** and **R2**. The decrease in association constant is more pronounced for F-PhDTDA (**R5**), possibly owing to the additional fluorine atom in the *para* position that is not present for F-PyrDTDA adding to the electron-withdrawing effect.

In the case of a dithiadiazolyl radical with electron-donating methyl substituents, if the methyl group is in the *para*-position (**R6**), such that the *ipso* dithiadiazolyl ring would experience the electron-donating effect, the association constant was found to be higher than for the non-methylated phenyl dithiadiazolyl **R2**. This resulted in *p*-CH_3-PhDTDA (**R6**) displaying the highest logβ value found for all three cobalt porphyrins. If the methyl group was *meta* to the dithiadiazolyl ring (**R7**), the association constant was the same (within the margin of error) as for **R2**, as was also the case for the *ortho* isomer **R8**.

In order to rationalise and interpret the differences in the strength of ligand association between the different dithiadiazolyl radicals, molecular electrostatic potential maps of the eight ligands were calculated. This technique has previously been utilized to interpret the packing arrangement of dithiadiazolyls.[9,10] It was hypothesised that the presence of the different substituents on the dithiadiazolyl radicals would influence the electron density around the sulfur atoms, which in turn would influence the association constant. Electrostatic potential maps are shown in Figure 3.11. Numerical values for the minimum and maximum electrostatic potentials for the two sulfur atoms, as well as the partial charge, can be found in the experimental section.

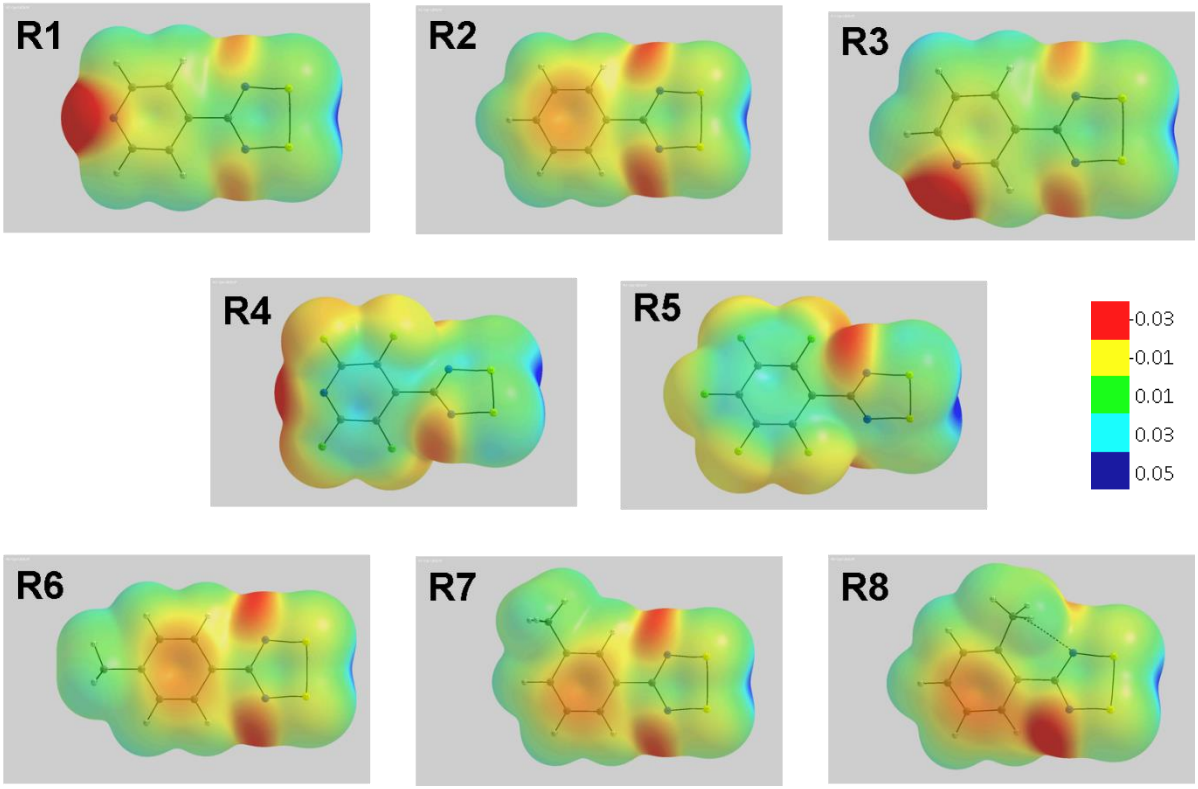

*Figure 3.11: Molecular electrostatic potential maps for dithiadiazolyl radicals **R1** to **R8**, calculated with a 0.0001 cubic Bohr isosurface. Red indicates an area of negative electrostatic potential (min = −0.03) while blue indicates an area of positive electrostatic potential (max = 0.05).*

Somewhat surprisingly, there is no clear trend observed in the electrostatic potential or partial charge of the dithiadiazolyl sulfur atoms that correlates with the association constants. This could indicate that the substituents on the dithiadiazolyl radical have a smaller influence on the electrostatic potential around the sulfur atoms than originally predicted. This in turn supports the results seen that changing the substituents on the dithiadiazolyl radicals results in relatively minor changes in the strength of association. It is known that the SOMO that the unpaired electron resides in is nodal at the carbon, so is unaffected by the substituents on the R-group. This result builds on this, showing that there is little electronic interaction between the R-group and the overall electrostatics of the heterocyclic ring. Steric interactions may play an important role in the association between the radical and the metalloporphyrin. Further DFT calculations should be performed in the future to establish the extend to which steric factors influence coordination.

It appears that the rationalization of the behaviour of association of dithiadiazolyl radicals to these cobalt porphyrins is not trivial. It is possible that in addition to the direct coordination to the metal ion through the heterocyclic dithiadiazolyl sulfur atom, electrostatic interactions between the

dithiadiazolyl radical and the porphyrin molecule itself, such as π-stacking, must occur in order to bring the two molecules together. Furthermore, the association constants for the fluorinated radicals **R4** and **R5** with the fluorinated porphyrin **P2** were unusually low; this is possibly as a result of electrostatic repulsion between fluorine atoms on the porphyrin and fluorine atoms on the dithiadiazolyls. Based on the differences observed with *p*-CH_3-PhDTDA (**P6**) and *o*-CH_3-PhDTDA (**P8**) and all three cobalt porphyrins, for example, it also appears probable that steric factors play a role in ligand-to-metal association.

It is clear that the system is tolerant of changes to the structure and functionality of both the dithiadiazolyl radical and the metalloporphyrin. With this knowledge, for future work ligands and/or porphyrins with functional groups that make up supramolecular synthons may be chosen, increasing the possibility of intermolecular interactions between the radical-metalloporphyrin coordination compounds. Coordination is likely to be strongest if the substituents on the metalloporphyrin are electron-withdrawing and the substituents on the dithiadiazolyl are electron-donating. It is worth noting that unlike the parent dithiadiazolyl radicals, the coordination compounds are relatively stable in solution once formed. UV-Vis spectra of solutions after titration remain unchanged after the sample has spent 30 minutes in air, unlike the dithiadiazolyl stock solutions, which decompose rapidly in air. Additionally, the one solid complex that has been isolated, **R1•P1(THF)**, remains stable in air for over a year.

In conclusion, the formation of 23 new dithiadiazolyl radical-cobalt porphyrin complexes was studied in solution by means of UV-Vis spectrophotometry. The association constant for each ligand-porphyrin complexation was determined. Attempts to isolate these complexes as solids were unsuccessful. Having investigated a range of dithiadiazolyl radicals with cobalt porphyrins of differing functionalities, the next logical step was to see if dithiadiazolyl radical-metalloporphyrin complexes could be obtained using metal ions other than cobalt. This work is described in Chapter 4.

3.6 Experimental details

The synthesis of dithiadiazolyl radical **R1** was discussed in Chapter 2. Dithiadiazolyl radicals **R2** to **R8** were synthesised with an analogous procedure.[2,11] The structures of these radicals are shown in Figure 3.12, together with their shorthand names. The full names for these radicals are:

R1: 4-(4′-pyridyl)-1,2,3,5-dithiadiazolyl

R2: 4-phenyl-1,2,3,5,-dithiadiazolyl

R3: 4-(3′-pyridyl)-1,2,3,5-dithiadiazolyl

R4: 4-(4′-perfluoropyridyl)-1,2,3,5-dithiadiazolyl

R5: 4-perfluorophenyl-1,2,3,5-dithiadiazolyl

R6: 4-(4′-methylphenyl)-1,2,3,4-dithiadiazolyl

R7: 4-(3′-methylphenyl)-1,2,3,4-dithiadiazolyl

R8: 4-(2′-methylphenyl)-1,2,3,4-dithiadiazolyl

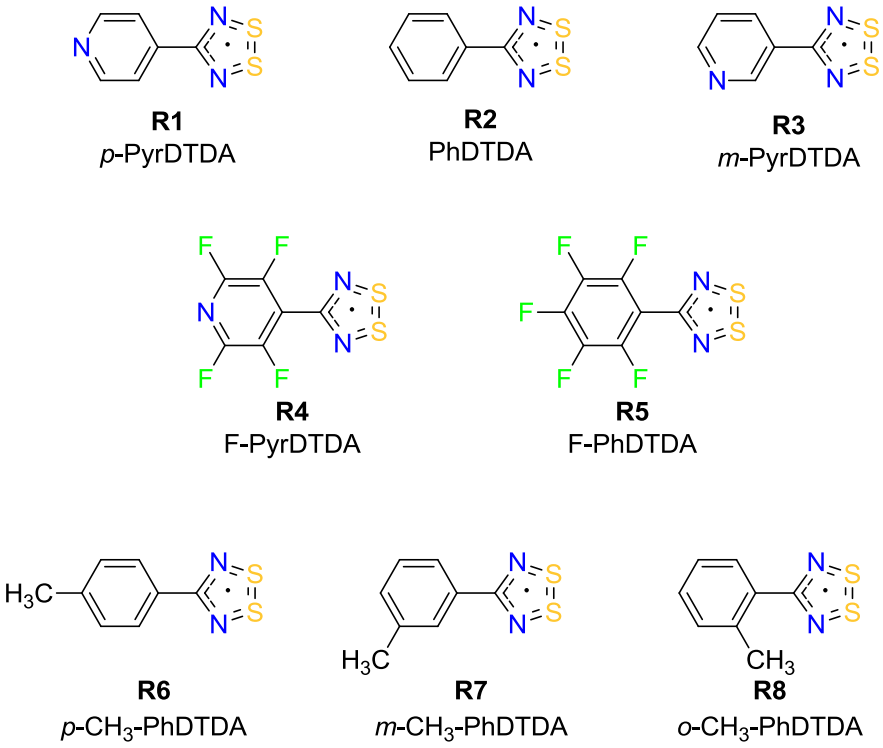

*Figure 3.12: Structures of dithiadiazolyl radicals **R1** to **R8***

3.6.1 Synthesis of dithiadiazolyl radicals **R1** – **R8**

Dry diethyl ether (30 mL) was placed in a nitrogen-filled Schlenk flask and cooled to -78 °C. Hexamethyldisilylazane (2.0 mL, 9.6 mmol) and *n*-butyl lithium (7.2 mL, 1.6M, 11.52 mmol) were added. The cooling bath was removed and the solution was stirred for 45 minutes until warmed to room temperature and the solution was clear. The corresponding nitrile (9.6 mmol) was added to the solution, which was left to stir overnight. The brightly coloured solution was subsequently cooled to 0 °C. Sulfur dichloride (1.2 mL, 19.2 mmol) was added slowly with vigorous stirring. After complete addition, the solution was allowed to warm to room temperature and stirred for a further 1 hour. Stirring was then stopped and the precipitate allowed to settle. Excess solvent was removed by cannula filtration. The remaining precipitate was washed with dry diethyl ether (3 x 10 mL), then dried under vacuum. A weighed portion of the dry dithiadiazolylium chloride salt was transferred to a clean, dry Schlenk flask under nitrogen. Triphenylantimony (0.5 eq, relative to dithiadiazolyl salt) was added to the flask and the contents were gently mixed. The mixture was heated to 70 °C for approximately 3 hours or until a complete colour change from yellow-orange to purple was observed. The flask was fitted with a water-cooled cold finger, placed under vacuum and sealed. The base of the flask was heated and the product dithiadiazolyl was isolated by sublimation onto the water-cooled cold finger. EPR spectroscopy was used to confirm reduction from the salt to the radical was successful. Samples were stored in oven-dried Schlenk flasks under a nitrogen atmosphere and handled using standard Schlenk techniques. Yields were calculated based on the starting nitrile and are in a range consistent with those reported in literature.[2,10]

R1 (*p*-PyrDTDA): Sublimation temperature 140 °C. Product isolated as dark blocks (0.252 g, 1.385 mmol, 14 % yield). EPR (9.878 GHz, CH_2Cl_2): pentet, a_N = 5.005 G, g = 2.0078.

R2 (PhDTDA): Sublimation temperature 100 °C. Product isolated as black needles (0.221 g, 1.219 mmol, 13 % yield). EPR (9.845 GHz, CH_2Cl_2): pentet, a_N = 5.009 G, g = 2.0012.

R3 (*m*-PyrDTDA): Product was received as a purple solid from a former student in the lab, S. V. Potts. EPR (9.837 GHz, CH_2Cl_2): pentet, a_N = 5.002 G, g = 2.0081.

R4 (F-PyrDTDA): Sublimation temperature 140 °C. Product isolated as dark blue-black blocks (0.342 g, 1.345 mmol, 14 % yield). EPR (9.845 GHz, CH_2Cl_2): pentet, a_N = 5.105 G, g = 2.0097.

R5 (F-PhDTDA): Sublimation temperature 50 °C. Product isolated as red oily solid (0.043 g, 0.159 mmol, 1.6 % yield). EPR (9.846 GHz, CH_2Cl_2): pentet, a_N = 5.205 G, g = 2.0099.

R6 (*p*-CH_3-PhDTDA): Sublimation temperature 120 °C. Product isolated as dark purple blocks (0.234 g, 1.98 mmol, 12 % yield). EPR (9.839 GHz, CH_2Cl_2): pentet, a_N = 5.105 G, g = 2.0085.

R7 (*m*-CH_3-PhDTDA): Sublimation temperature 90 °C. Product isolated as black blocks (0.212 g, 1.086 mmol, 11 % yield). EPR (9.880 GHz, CH_2Cl_2): pentet, a_N = 5.103 G, g = 2.0169.

R8 (*o*-CH_3-PhDTDA): Sublimation temperature 130 °C. Product isolated as dark purple blocks (0.087 g, 0.446 mmol, 4.6 % yield). EPR (9.877 GHz, CH_2Cl_2): pentet, a_N = 4.998 G, *g* = 2.0077.

3.6.2 Synthesis of H_2TPP and CoTPP (**P1**)

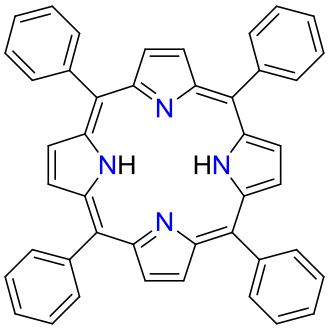

H_2TPP

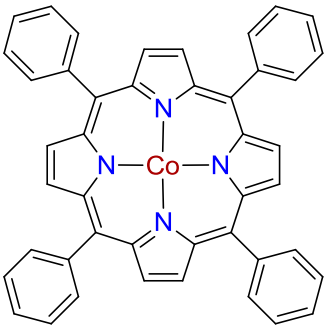

CoTPP
P1

The synthesis of tetraphenylporphyrin and cobalt (II) tetraphenylporphyrin is described in Chapter 2.

3.6.3 Synthesis of 5,10,15,20-tetrakis(pentafluorophenyl)porphyrin (H_2TFP)[3,12] and cobalt (II) 5,10,15,20-tetrakis(pentafluorophenyl)-porphyrin (CoTFP, **P2**)[4]

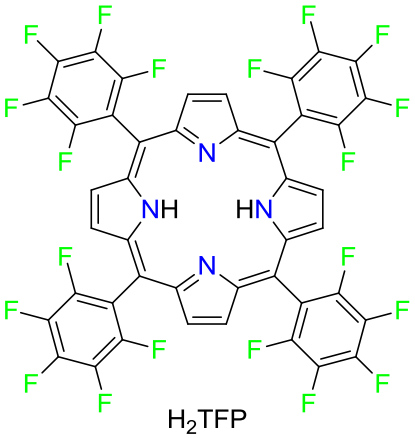

H_2TFP

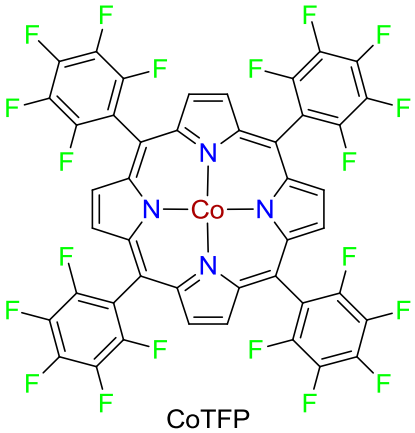

CoTFP
P2

Freshly distilled pyrrole (1.8 mL, 25.5 mmol) and pentafluorobenzaldehyde (5.0 g, 25.5 mmol) were added to propionic acid (100 mL) in a 250 mL round bottomed flask. Boiling stones were added and the solution was brought to reflux in air for 1 hour. Heating was ceased and the flask was allowed to

cool to room temperature before cooling in a fridge overnight. Thereafter, the solution was filtered and the precipitate was washed with hot water (4 x 20 mL) and methanol (4 x 20 ml) to yield 5,10,15,20-tetrakis(pentafluorophenyl)porphyrin as a fine black-purple crystalline material (2.112 g, 2.05 mmol, 32 % yield). ^{1}H NMR (300 MHz, $CDCl_3$): δ ppm -2.91 (br s, 2H, N-H), 8.12 (s, 8H, pyrrole-H). UV-Vis (CH_2Cl_2): 412 nm, 504 nm, 581 nm, 678 nm, 722 nm.

Tetrakis(pentafluorophenyl)porphyrin (1.025g, 1.052 mmol) and cobalt (II) acetate tetrahydrate (0.260 g, 1.044 mmol) were added to degassed dimethylformamide (50 mL) in a 100 mL round bottomed flask under nitrogen. The solution was heated and reflux was maintained for 45 minutes. An additional portion of cobalt (II) acetate tetrahydrate (0.260 g, 1.044 mmol) was added and reflux was maintained for a further 30 minutes. Thereafter, heating was ceased and the flask was allowed to cool to room temperature before cooling in a fridge overnight. Cold distilled water (50 ml) was added. The solution was filtered and the precipitate was washed with distilled water (3 x 10 mL) to yield cobalt (II) tetrakis(pentafluorophenyl)porphyrin **P2** as a fine black-purple powder (901 mg, 0.875 mmol, 83 % yield). UV-Vis (CH_2Cl_2): 404 nm, 522 nm.

3.6.4 Synthesis of 5,10,15,20-tetratolylporphyrin (H_2TTP)[3,13] and cobalt (II) 5,10,15,20-tetratolylporphyrin (CoTTP, **P3**)[4]

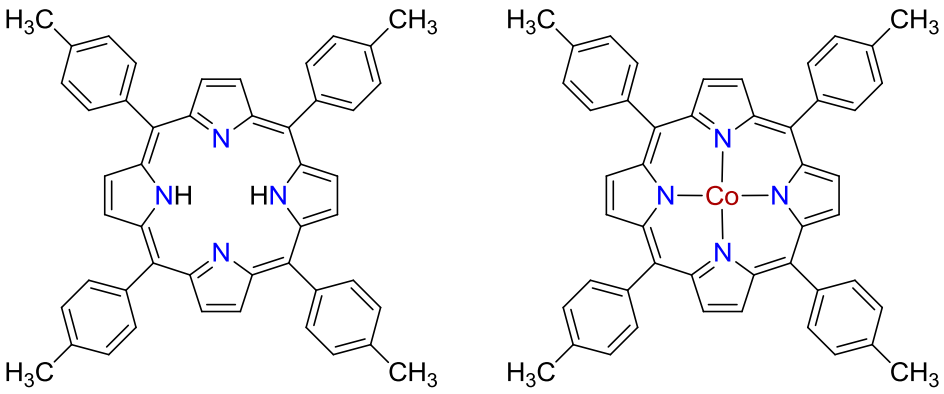

Freshly distilled pyrrole (2.0 mL, 28.8 mmol) and 4-methylbenzaldehyde (3.4 mL, 28.8 mmol) were added to propionic acid (120 mL) in a 250 mL round bottomed flask. Boiling stones were added and the solution was brought to reflux in air for 1 hour. Heating was ceased and the flask was allowed to cool to room temperature. The solution was left to stand at room temperature for 24 hours. Thereafter, the solution was filtered and the precipitate was washed with methanol (2 x 10 mL) and *n*-hexane (2 x

10 mL) to yield 5,10,15,20-tetratolylporphyrin as a lustrous purple crystalline material (1.546 g, 2.31 mmol, 32 % yield). ^{1}H NMR (300 MHz, $CDCl_3$): δ ppm -2.76 (s, 2H, N-H), 2.72 (2, 12H, Ar-CH_3), 7.55 (d, *J* = 7.68 Hz, 8H, $C_{Ar}H$), 8.09 (d, *J* = 7.68 Hz, 8H, $C_{Ar}H$), 8.86 (s, 8H, pyrrole-H). UV-Vis (CH_2Cl_2): 419 nm, 517 nm, 553 nm, 594 nm, 649 nm.

Tetratolylporphyrin (400 mg, 0.596 mmol) and cobalt (II) acetate tetrahydrate (0.148 g, 0.594 mmol) were added to degassed dimethylformamide (50 mL) in a 100 mL round bottomed flask under nitrogen. The solution was heated and reflux was maintained for 45 minutes. Thereafter, heating was ceased and the flask was allowed to cool to room temperature. The solution was left to stand at room temperature for 24 hours. The solution was filtered and the precipitate was washed with distilled water (2 x 20 mL) to yield cobalt (II) tetratolylporphyrin **P3** as fine purple crystals (352 mg, 0.484 mmol, 81 % yield). ^{1}H NMR (300 MHz, $CDCl_3$): δ ppm 4.17 (s, 12H, Ar-CH_3), 9.77 (br s, 8H, $C_{Ar}H$), 13.09 (br s, 8H, $C_{Ar}H$), 15.95 (br s, 8H, pyrrole-H). UV-Vis (CH_2Cl_2): 412 nm, 527 nm, 573 nm.

3.6.5 Crystallization experiments

The procedure below was performed with **P1** (with **R2** to **R8**), **P2** (with **R1** to **R8**) and with **P3** (with **R1** to **R8**).

A narrow Schlenk tube was evacuated and filled with nitrogen using standard Schlenk techniques. To this was added dithiadiazolyl radical (13 – 15 mg), cobalt porphyrin (50 mg) and dry THF (10 mL). The solution was magnetically stirred and gently heated until as much of the material as possible dissolved. An aliquot of this mixture was transferred to a glass tube. Dry *n*-hexane (6 mL) was carefully layered above the dark maroon THF solution. The tube was sealed and allowed to stand at room temperature. After one month, no diffraction quality crystals or powder was obtained. Reduction of solvent volume did not result in pure solid samples of coordination material. Crystals broke up into a powder or decomposed when removed from the mother liquor. PXRD showed any stable solid products to be predominantly the starting porphyrin (premature precipitation of the metalloporphyrin was a common problem when studying the **R1·P1(THF)** complex as well)). It appears that concentration is very important to form these complexes, considering that both the radical and the porphyrin have a monomer-dimer equilibrium in solution. At the higher concentrations required for precipitation, radical-radical and porphyrin-porphyrin interactions appear to be favoured above radical-porphyrin interactions. Something to be attempted in the future is setting up a large scale experiment at the concentration range used for the UV-Vis experiments (~2 μM porphyrin) in order to form the complex, followed by reduction of the solvent volume to precipitate out the complex. A mechanochemical approach was attempted in order to circumvent the solubility problem and was

unsuccessful, although there is still room for optimisation of this process. An additional problem limiting the number of crystallizations that could be set up at once was that the dithiadiazolyl radicals are air-sensitive, and so the crystallisations must be set up in Schlenk flasks under nitrogen, and a limited number of these Schlenk flasks were available at once. Attempts were made to set up crystallisations in conventional glass vials but samples degraded before precipitation or crystallization was achieved.

3.6.6 UV-Vis spectrophotometric titrations

All glassware, except microsyringes, was dried in an oven overnight. All solvents were dried over 3 Å molecular sieves. Microsyringes were flushed three times with clean, dry solvent and three times with the solution of interest before being used.

A fresh 2 mM stock solution of the dithiadiazolyl radical was made up in a 5 mL volumetric flask prior to each experiment using a 9:1 dichloromethane:dimethylsulfoxide solvent system. The flask was flushed with nitrogen for 1 minute before being sealed with a septum and paraffin laboratory film. A 1 mM stock solution of the cobalt porphyrin was made up in a screw-cap glass vial using dichloromethane.

A 2μM working solution of the cobalt porphyrin was prepared directly in a quartz cuvette (1 cm path length) with 1996 μL dichloromethane (measured by micropipette) and 4 μL of the relevant cobalt porphyrin stock solution (measured by glass Hamilton microsyringe). A 2000 μL portion of dichloromethane was placed in the reference cuvette (measured by micropipette).

Both cuvettes, with their lids, were placed in the UV-Vis spectrophotometer and allowed to equilibrate to 25 °C before the initial spectrum was collected between 375 and 450 nm.

Aliquots of the dithiadiazolyl stock solution were added to both the working solution cuvette and the reference solution cuvette using a glass Hamilton microsyringe. The solutions were stirred with a wire microsyringe plunger and the lids replaced. The spectrum was collected after each addition. This was continued until a total of 600 μL of the dithiadiazolyl solution was added.

Spectrophotometric titrations of CoTPP were performed by the addition of 10 × 2 μL, 10 × 4 μL, 2 × 10 μL, 6 × 20 μL and 8 × 50 μL aliquots of ligand stock solution (total volume 600 μL) to both sample and reference. Spectrophotometric titrations of CoTFP and CoTTP were performed by the addition of 30 × 20 μL aliquots of ligand stock solution (total volume 600 μL) to both sample and reference. The spectrophotometric titration was performed in triplicate for each radical – porphyrin pair.

To confirm that the DMSO in the dithiadiazolyl stock solution was not coordinating to CoTPP under the conditions of the spectrophotometric titrations, two additional experiments were carried out: firstly, titrating CoTPP with 9:1 DCM:DMSO without the presence of dithiadiazolyl and secondly, titrating CoTPP with PhDTDA in pure DCM (PhDTDA has vastly improved solubility in DCM compared to other dithiadiazolyls, such as *p*-PyrDTDA). No changes to the spectrum of CoTPP beyond the effect of dilution were observed when no dithiadiazolyl was present. Conversely, titrating with PhDTDA in pure DCM gave the same result as in 9:1 DCM:DMSO (with a logβ value of 4.27).

For the visual representation of the spectra, the data were normalised and a dilution correction was performed for each data set as follows:

$$\mathrm{Abs_{corr}} = \frac{\mathrm{Abs_{sample}} \times \mathrm{V_{sample}}}{\mathrm{V_{orig}}}$$

Where $\mathrm{Abs_{corr}}$ is the absorbance corrected for dilution

$\mathrm{Abs_{obs}}$ is the observed absorbance for the sample

$\mathrm{V_{sample}}$ is the total volume of the sample

and $\mathrm{V_{orig}}$ is the volume of the original working solution (i.e. 2000 µL)

For example, the corrected absorbance readings for a sample that contains a total of 20 µL ligand solution added would be calculated using:

$$\mathrm{Abs_{corr}} = \frac{\mathrm{Abs_{sample}} \times 2020\ \mu\mathrm{L}}{2000\ \mu\mathrm{L}}$$

Association constants (logβ values) were calculated in HypSpec using a 2-reagent model with a 1:1 molar ratio. The raw spectral data (that is, without dilution correction) was used as the HypSpec software takes the titration volumes into consideration. No additional coordination of DMSO could be modelled. The average logβ of the three repeat spectrophotometric titrations was reported. All logβ values are given in Table 3.5 (for **P1**), Table 3.6 (for **P2**) and Table 3.7 (for **P3**).

*Table 3.5: All log values for CoTPP and dithiadiazolyls **R1 - R8***

Dithiadiazolyl ligand		logβ values with CoTPP (P1)			
		1	**2**	**3**	**Average**
R1	*p*-PyrDTDA	4.19	4.14	4.23	4.19 ± 0.05
R2	PhDTDA	4.23	4.28	4.31	4.27 ± 0.04
R3	*m*-PyrDTDA	3.92	3.97	3.85	3.92 ± 0.06
R4	F-PyrDTDA	4.13	4.10	4.14	4.12 ± 0.02
R5	F-PhDTDA	3.62	3.63	3.70	3.66 ± 0.04
R6	*p*-CH_3-PhDTDA	4.48	4.49	4.51	4.49 ± 0.02
R7	*m*-CH_3-PhDTDA	3.84	3.89	3.83	3.85 ± 0.03
R8	*o*-CH_3-PhDTDA	4.40	4.35	4.37	4.37 ± 0.03

*Table 3.6: All log values for CoTFP and dithiadiazolyls **R1 - R8***

Dithiadiazolyl ligand		logβ values with CoTFP (P2)			
		1	**2**	**3**	**Average**
R1	*p*-PyrDTDA	4.49	4.51	4.56	4.52 ± 0.04
R2	PhDTDA	4.56	4.54	4.57	4.56 ± 0.02
R3	*m*-PyrDTDA	4.38	4.41	4.37	4.39 ± 0.02
R4	F-PyrDTDA	3.74	3.56	3.46	3.59 ± 0.14
R5	F-PhDTDA	2.81	2.94	3.01	2.92 ± 0.10
R6	*p*-CH_3-PhDTDA	4.64	4.78	4.72	4.71 ± 0.07
R7	*m*-CH_3-PhDTDA	4.43	4.41	4.55	4.46 ± 0.08
R8	*o*-CH_3-PhDTDA	4.55	4.58	4.67	4.60 ± 0.06

*Table 3.7: All log values for CoTTP and dithiadiazolyls **R1 - R8***

Dithiadiazolyl ligand		logβ values with CoTTP (P3)			
		1	**2**	**3**	**Average**
R1	*p*-PyrDTDA	3.59	3.55	3.58	3.57 ± 0.02
R2	PhDTDA	3.62	3.67	3.71	3.67 ± 0.05
R3	*m*-PyrDTDA	3.65	3.61	3.58	3.61 ± 0.04
R4	F-PyrDTDA	3.39	3.48	3.44	3.44 ± 0.05
R5	F-PhDTDA	3.54	3.54	3.56	3.55 ± 0.01
R6	*p*-CH_3-PhDTDA	3.98	4.06	4.05	4.03 ± 0.04
R7	*m*-CH_3-PhDTDA	3.37	3.43	3.32	3.37 ± 0.06
R8	*o*-CH_3-PhDTDA	3.70	3.73	3.72	3.72 ± 0.02

3.6.7 Electrostatic Potentials

Computational work was performed by Mr A.B. Dippernaar at Stellenbosch University. Geometry optimisation was performed at the UB3LYP/6-311++G(d,p) level of theory with a multiplicity of 2 (one unpaired electron). This was performed on Gaussian 09, Revision B.01.[14] Where possible, existing structural data in the Cambridge Structural Database[15] was used as the starting point (reference codes: PHTHAZ[16] (**R2**), QUNQOG[17] (**R5**), LELPOJ[18] (**R6**), LELPUP[18] (**R7**) and LELQAW[18] (**R8**)). Frequencies were also calculated. Subsequently, wavefunction files (*.wfx) were generated, from which electron density calculations were performed on AIMALL (v.15.05.18).[19,20] Electrostatic potentials and partial charges for the two dithiadiazolyl sulfur atoms (S1 and S2) for dithiadiazolyl radicals R1 to R8 are given in Table 3.8.

*Table 3.8: Maximum electrostatic potential (ESP Max), minimum electrostatic potential (ESP Min) and partial charge (q) for the sulfur atoms of dithiadiazolyl radicals **R1** to **R8**. (Units: e/bohr^3)*

Dithiadiazolyl	Atom	ESP Max	ESP Min	q
R 1	S1	0.0563861	-0.000498	0.595911
	S2	0.0563507	-0.000452	0.596312
R 2	S1	0.0487125	-0.008131	0.585240
	S2	0.0486842	-0.008126	0.585713
R 3	S1	0.0535553	-0.003885	0.596352
	S2	0.0535608	-0.002586	0.587386
R 4	S1	0.0643777	0.004037	0.591655
	S2	0.0644337	0.004454	0.591565
R 5	S1	0.0596069	-0.000794	0.584127
	S2	0.0596013	-0.000816	0.584603
R 6	S1	0.0468448	-0.009816	0.581844
	S2	0.0468645	-0.009941	0.582711
R 7	S1	0.0474120	-0.009302	0.581530
	S2	0.0473831	-0.009256	0.585057
R 8	S1	0.0478181	-0.008466	0.570946
	S2	0.0476654	-0.009506	0.584260

3.7 References

(1) Terazono, Y.; Patrick, B. O.; Dolphin, D. H. *Inorg. Chim. Acta* **2003**, *346*, 265.

(2) Robinson, S. W.; Haynes, D. A.; Rawson, J. M. *CrystEngComm* **2013**, *15* (47), 10205.

(3) Adler, A. D.; Longo, F. R.; Finarelli, J. D.; Goldmacher, J.; Assour, J.; Korsakoff, L. *J. Org. Chem.* **1967**, *32* (2), 476.

(4) Adler, A. D.; Longo, F. R.; Kampas, F.; Kim, J. *J. Inorg. Nucl. Chem.* **1970**, *32* (7), 2443.

(5) Hyp Spec, Protonic Software, Leeds, England.

(6) Kadish, K. M.; Bottomley, L. A.; Beroiz, D. *Inorg. Chem.* **1978**, *17* (5), 1124.

(7) Yamamoto, K. *Inorg. Chim. Acta* **1986**, *113* (2), 181.

(8) Hansch, C.; Leo, A.; Taft, R. W. *Chem. Rev.* **1991**, *91*, 165.

(9) Bond, A. D.; Haynes, D. A.; Pask, C. M.; Rawson, J. M. *J. Chem. Soc. Dalt. Trans.* **2002**, No. 12, 2522–2531.

(10) Clarke, C. S.; Haynes, D. A.; Smith, J. N. B.; Batsanov, A. S.; Howard, J. A. K.; Pascu, S. I.; Rawson, J. M. *CrystEngComm* **2010**, *12* (1), 172–185.

(11) Rawson, J. M.; Banister, A. J.; Lavender, I. *Adv. Heterocycl. Chem.* **1995**, *62*, 137–247.

(12) Han, Y.; Fang, H.; Jing, H.; Sun, H.; Lei, H.; Lai, W.; Cao, R. *Angew. Chemie Int. Ed.* **2016**, *55* (18), 5457.

(13) Wang, S.; Forsyth, C.; Langford, S. J. *CrystEngComm* **2015**, *17* (16), 3060.

(14) Frisch, M. J.; Trucks, G. W.; Schlegel, H. B.; Scuseria, G. E.; Robb, M. A.; Cheeseman, J. R.; Scalmani, G.; Barone, V.; Mennucci, B.; Petersson, G. A.; Nakatsuji, H.; Caricato, M.; Li, X.; Hratchian, H. P.; Izmaylov, A. F.; Bloino, J.; Zheng, G.; Sonnenberg, J. L.; Hada, M.; Ehara, M.; Toyota, K.; Fukuda, R.; Hasegawa, J.; Ishida, M.; Nakajima, T.; Honda, Y.; Kitao, O.; Nakai, H.; Vreven, T.; Montgomery, J. A., J.; Peralta, J. E.; Ogliaro, F.; Bearpark, M.; Heyd, J. J.; Brothers, E.; Kudin, K. N.; Staroverov, V. N.; Kobayashi, R.; Normand, J.; Raghavachari, K.; Rendell, A.; Burant, J. C.; Iyengar, S. S.; Tomasi, J.; Cossi, M.; Rega, N.; Millam, M. J.; Klene, M.; Knox, J. E.; Cross, J. B.; Bakken, V.; Adamo, C.; Jaramillo, J.; Gomperts, R.; Stratmann, R. E.; Yazyev, O.; Austin, A. J.; Cammi, R.; Pomelli, C.; Ochterski, J. W.; Martin, R. L.; Morokuma, K.; Zakrzewski, V. G.; Voth, G. A.; Salvador, P.; Dannenberg, J. J.; Dapprich, S.; Daniels, A. D.; Farkas, Ö.; Foresman, J. B.; Ortiz, J. V.; Cioslowski, J.; Fox, D. J. Gaussian, Inc., Wallingford CT, 2009.

(15) Allen, F. H. *Acta Crystallogr.* **2002**, *B58*, 380.

(16) Vegas, A.; Pérez-Salazar, A.; Banister, A. J.; Hey, R. G. *J. Chem. Soc., Dalt. Trans.* **1980**, 1812.

(17) Allen, C.; Haynes, D. A.; Pask, C. M.; Rawson, J. M. *CrystEngComm* **2009**, *11* (10), 2048–2050.

(18) Beldjoudi, Y.; Haynes, D. A.; Hayward, J. J.; Manning, W. J.; Pratt, D. R.; Rawson, J. M. *CrystEngComm* **2013**, *15* (6), 1107.

(19) Bader, R. F. W. *Acc. Chem. Res.* **1985**, *18* (1), 9.

(20) Keith, T. A. AIMAll, TK Gristmaill Software, 2012.

Chapter 4

Investigating the interaction between dithiadiazolyl radicals and metalated tetraphenylporphyrins using UV-Vis and EPR spectroscopy

---

4.1 Introduction

In Chapter 3, the UV-Vis spectroscopic study of the coordination of eight dithiadiazolyl radicals to three cobalt porphyrins was described. All eight of the radical ligands investigated showed association to the cobalt centre of the porphyrins. The choice of porphyrin scaffold had the greatest influence on the association constant for this reaction. The presence of electron-withdrawing fluorine substituents on the porphyrin periphery resulted in a stronger ligand association, while electron-donating methyl substituents reversed this effect.

The choice of dithiadiazolyl radical had a lesser influence on the association constant. Dithiadiazolyl radicals with electron-donating substituents generally had stronger ligand association constants than those with electron-withdrawing substituents when reacting with the same cobalt porphyrin. However, it was evident that complex formation was influenced by a variety of factors beyond the electrostatic potentials of the coordinating sulfur atoms.

Following the success with forming a range of dithiadiazolyl-metalloporphyrin complexes in solution with cobalt as the metal centre, the next step was to investigate if similar complexes could be formed with different metals and, if successful, how the choice of metal ion would influence the coordination behaviour.

Four additional metallo-tetraphenylporphyrins were synthesised for this study (Figure 4.1), the choice of which was dictated by the metal salts readily available and the relative ease of synthesis.[1] In addition to the d^7 cobalt (II) tetraphenylporphyrin, the paramagnetic d^9 copper (II) tetraphenylporphyrin and the diamagnetic d^{10} zinc (II) tetraphenylporphyrin were chosen. A non-transition metal, magnesium, was also chosen as a simple analogue for the biological chlorin, chlorophyll. Finally, the trivalent iron (III) tetraphenylporphyrin chloride was chosen as a simple analogue for the biological porphyrin, haematin (ferriporphyrin IX, see Chapter 5). The interaction

between the metalloporphyrin and the dithiadiazolyl radical in solution was studied through the use of ultraviolet-visible (UV-Vis) spectroscopy and electron paramagnetic resonance (EPR) spectroscopy.

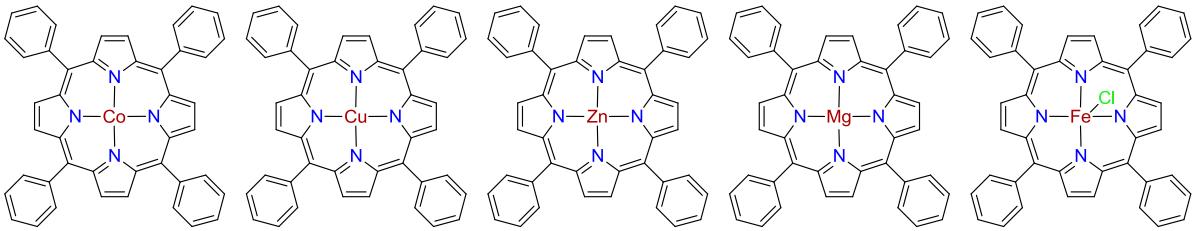

Figure 4.1: Structures of the five metalated tetraphenylporphyrins used in this study.

The metalloporphyrins were all prepared from the free base tetraphenylporphyrin by refluxing in DMF with the relevant metal salt, as described by Adler *et al*.[1] UV-Vis spectroscopy and ^{1}H NMR spectroscopy were used to confirm that there was no more free base porphyrin present in the bulk material.

Two of the previously studied dithiadiazolyl radicals were used: *p*-PyrDTDA (**R1**) and PhDTDA (**R2**) (Figure 4.2).

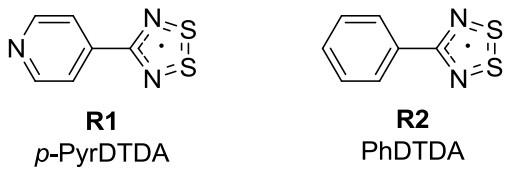

Figure 4.2: Structures of the two dithiadiazolyl radicals used in this study

4.2 UV-Vis Spectroscopy

4.2.1 Dithiadiazolyl radicals with cobalt(II) tetraphenylporphyrin

In Chapter 2 and Chapter 3, the use of UV-Vis spectroscopy to study the coordination of *p*-PyrDTDA (**R1**) and PhDTDA (**R2**) to CoTPP (**P1**) in solution was described. A spectrophotometric titration was performed and the resulting spectroscopic data could be used to determine the association constant,

logβ. To facilitate comparison across the different metalated tetraphenylporphyrins, the spectra resulting from the spectrophotometric titration for CoTPP with either *p*-PyrDTDA or PhDTDA, in dichloromethane (DCM), as described previously, are shown again in Figure 4.3.

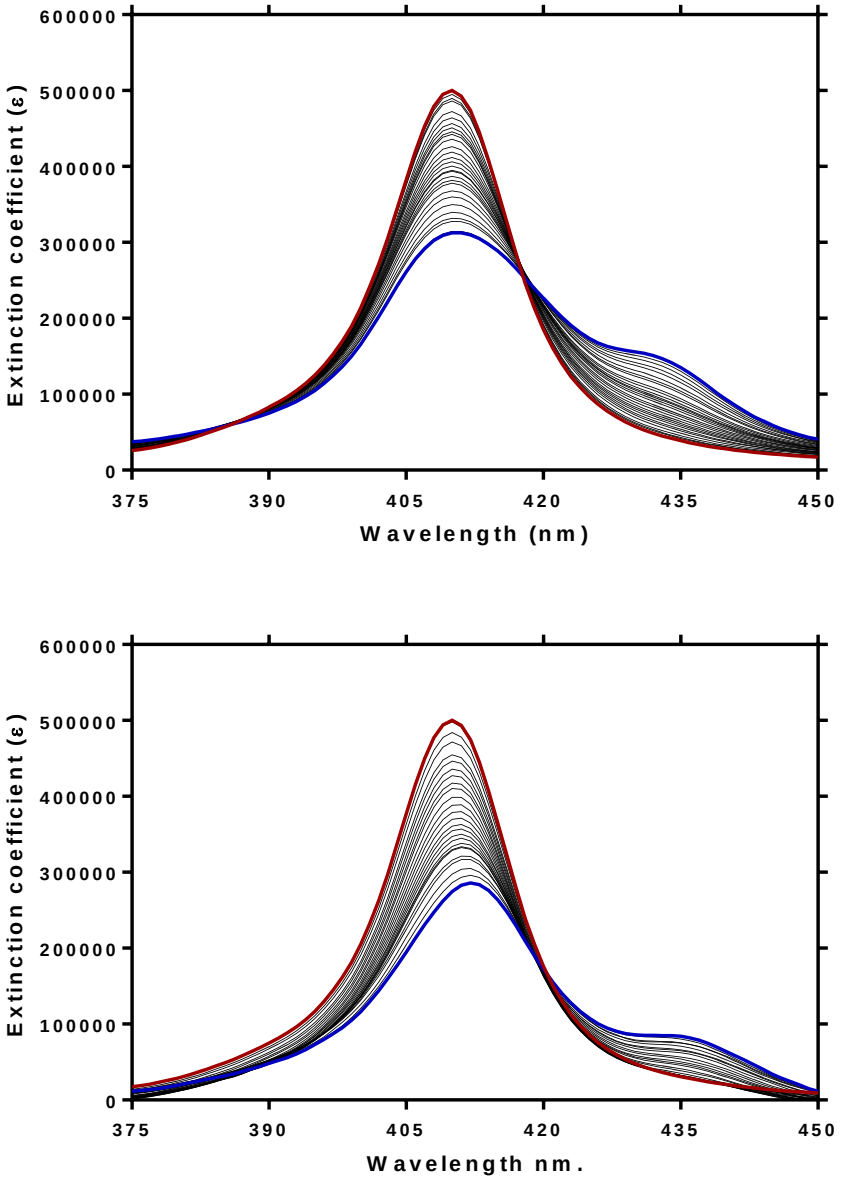

*Figure 4.3: UV-Vis spectrophotometric titration for CoTPP (**P1**) in DCM with increasing* p*-PyrDTDA (**R1**, top) and PhDTDA (**R2**, bottom) concentration, at 25 °C, forming **R1•P1** and **R2•P1** respectively. The original CoTPP spectrum is shown in red. The final addition of dithiadiazolyl is shown in blue with intermediate additions shown in black. Titration spectra have been corrected for dilution. The **R1•P1** spectrum has the two isosbestic points (385 nm and 418 nm) indicated with dotted lines for clarity.*

^{1}H NMR spectroscopy data suggest that *p*-PyrDTDA is coordinating to CoTPP in solution through the dithiadiazolyl sulfur atom, not the pyridyl nitrogen (see Chapter 2). The similarity of the

spectroscopic data for **R1** and **R2** confirms this, as this suggests that both dithiadiazolyl radicals are coordinating to the metal in a similar fashion.

Spectrophotometric titrations were performed in triplicate for CoTPP and for all the following metalloporphyrins. The association constant, logβ, was calculated for each titration and the average of these results was determined.

For the coordination of *p*-PyrDTDA to CoTPP, the reaction has a logβ value of 4.19 ± 0.05. This is substantially different compared to the logβ for nitrogen-based ligands, such as pyridine binding to CoTPP (logβ: 2.90 in DCM)[2] or 4-cyanopyridine binding to CoTPP (logβ: 2.60 in DCM).[3] For PhDTDA, an association constant of 4.27 ± 0.04 was determined, comparable to that of *p*-PyrDTDA (within 3 standard deviations).

4.2.2 Dithiadiazolyl radicals with copper(II) tetraphenylporphyrin

To determine if dithiadiazolyl radical – metalloporphyrin complexes could be formed using CuTPP, UV-Vis spectrophotometric titrations were performed in an analogous manner to those done with CoTPP. The spectra resulting from the spectrophotometric titration for CuTPP with either *p*-PyrDTDA or PhDTDA, in dichloromethane (DCM), are shown in Figure 4.4. The Soret band for CuTPP in DCM is found at 414 nm. Addition of *p*-PyrDTDA results in this peak slowly reducing in intensity with an associated shift to 415 nm. An isosbestic point occurs at 399 nm. When PhDTDA is added to CuTPP, the band at 414 nm slowly decreases in absorbance intensity and shifts to 415 nm, with an isosbestic point at 407 nm. The spectroscopic changes are more subtle when compared to the same ligand concentration added to CoTPP, but nevertheless indicate that ligand – porphyrin association is occurring. The association constant, logβ, was calculated for each titration and the average of these results was determined. The results are shown in Table 4.1.

.

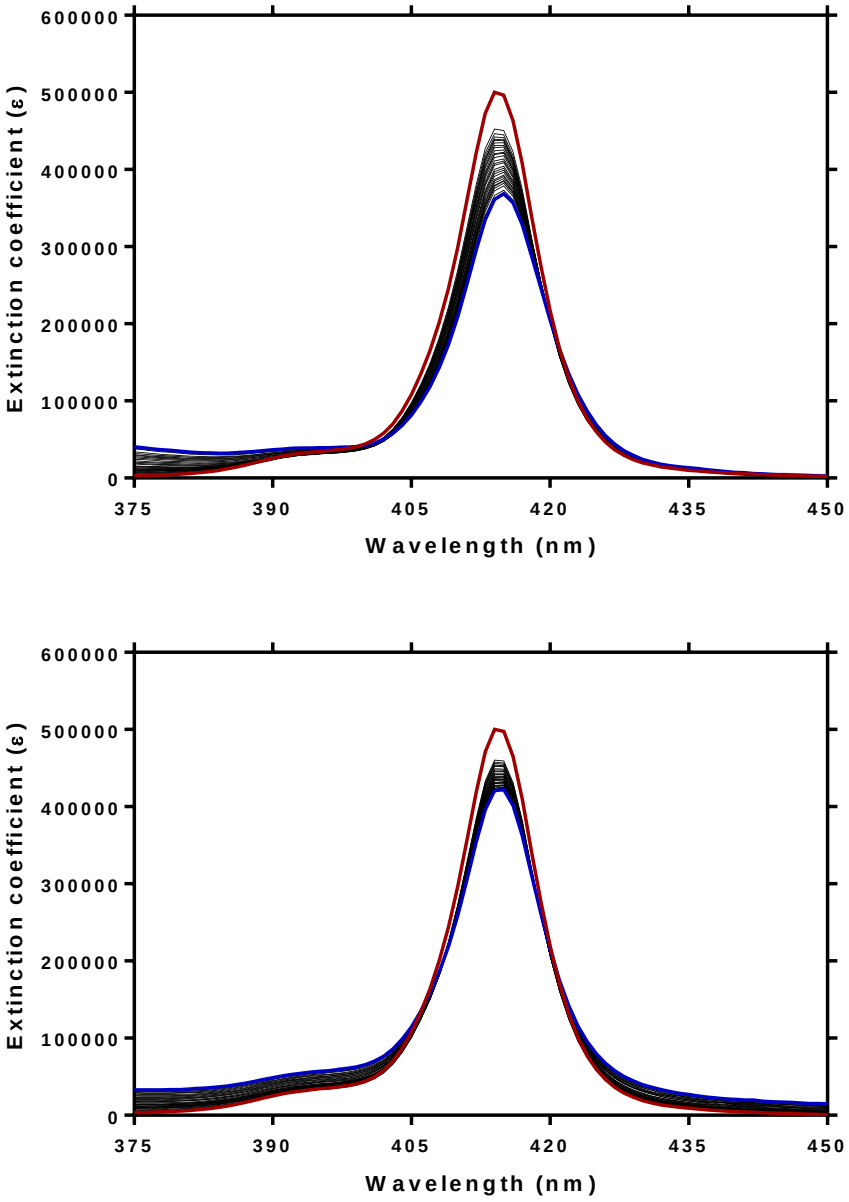

*Figure 4.4: UV-Vis spectrophotometric titration for CuTPP (**P4**) in DCM with increasing* p*-PyrDTDA (**R1**, top) and PhDTDA (**R2**, bottom) concentration, at 25 °C, forming **R1•P4** and **R2•P4** respectively. The original CuTPP spectrum is shown in red. The final addition of dithiadiazolyl is shown in blue with intermediate additions shown in black. Titration spectra have been corrected for dilution.*

Table 4.1: Association constants for dithiadiazolyl radicals coordinating to Cu(II) tetraphenylporphyrin (DCM, 25 °C)

	Dithiadiazolyl Ligand	Average logβ with CuTPP
R1	*p*-PyrDTDA	3.51 ± 0.14
R2	PhDTDA	2.94 ± 0.08

Both *p*-PyrDTDA and PhDTDA showed evidence of one-to-one ligand coordination to CuTPP. For the coordination of *p*-PyrDTDA to CuTPP, the reaction has a logβ value of 3.51 ± 0.14. For PhDTDA, an association constant of 2.94 ± 0.08 was determined, marginally smaller than that of *p*-PyrDTDA. These values are an order of magnitude lower than those for CoTPP.

4.2.3 Dithiadiazolyl radicals with zinc(II) tetraphenylporphyrin

UV-Vis spectrophotometric titrations were performed in an analogous manner for ZnTPP to those carried out with CoTPP and CuTPP. The spectra resulting from the spectrophotometric titration for ZnTPP with either *p*-PyrDTDA or PhDTDA, in dichloromethane (DCM), are shown in Figure 4.5. However, when using the exact same procedure as for CoTPP and CuTPP, it was found that a dramatic spectroscopic change occurred following the first ligand addition with negligible change thereafter. It was therefore necessary to change the quantities of ligand stock solution added during the spectrophotometric titration (see Experimental section for details).

The Soret band for ZnTPP in DCM is found at 418 nm. Addition of *p*-PyrDTDA results in this peak dramatically reducing in intensity, while a new peak evolves at 425 nm with an isosbestic point at 422 nm. Similarly, as PhDTDA is added to ZnTPP, the Soret band at 418 nm quickly diminishes and a new band develops at 425 nm, with an isosbestic point at 422 nm. These changes to the UV-Vis spectra observed are more intense when compared to the ligands being added to CoTPP and CuTPP, and the fact that significantly lower ligand concentration is required indicates that the ligand – porphyrin association is far stronger. The dramatic red-shift of the Soret bands observed in these spectrophotometric titrations are not uncommon when ZnTPP is axially ligated, and can be considered the result of charge transfer from the donor ligand to the porphyrin through the metal centre following coordination.[4] The extent of this shift is determined by the nature of the ligand donor atoms, with N- and O-donor ligands inducing smaller shifts than more polarizable S- or P-donor ligands.[4] This is interesting, as the opposite is seen after coordination to cobalt, where electron transfer from the cobalt to the dithiadiazolyl occurs. The association constant, logβ, was calculated for each titration and the average of these results was determined (Table 4.2).

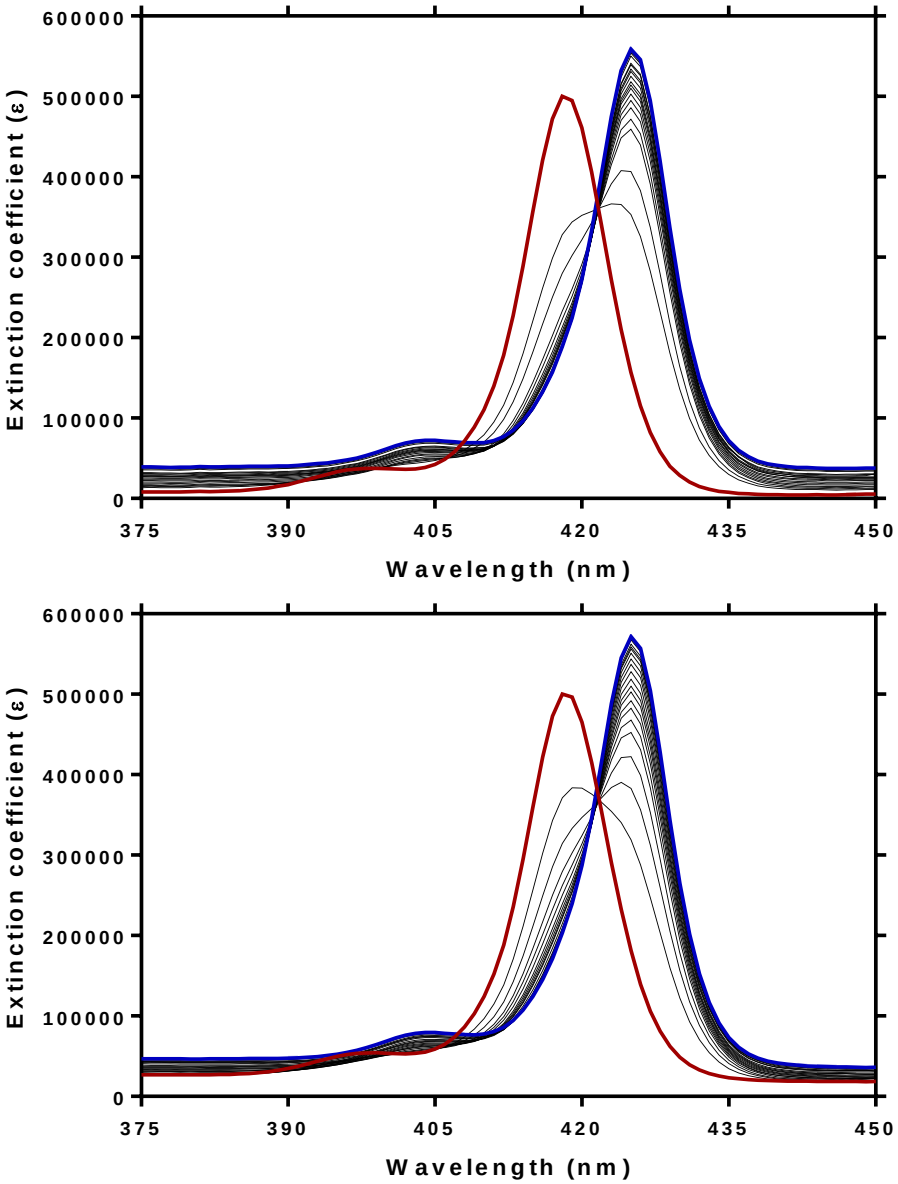

*Figure 4.5: UV-Vis spectrophotometric titration for ZnTPP (**P5**) in DCM with increasing* p-*PyrDTDA (**R1**, top) and PhDTDA (**R2**, bottom) concentration, at 25 °C, forming **R1•P5** and **R2•P5** respectively. The original ZnTPP spectrum is shown in red. The final addition of dithiadiazolyl is shown in blue with intermediate additions shown in black. Titration spectra have been corrected for dilution. (See section 4.5.3 for deviations from standard experimental procedure)*

Table 4.2: Association constants for dithiadiazolyl radicals coordinating to Zn(II) tetraphenylporphyrin (DCM, 25 °C)

	Dithiadiazolyl Ligand	Average logβ with ZnTPP
R1	*p*-PyrDTDA	6.21 ± 0.06
R2	PhDTDA	5.91 ± 0.06

For the coordination of *p*-PyrDTDA to ZnTPP, the reaction has a logβ value of 6.21 ± 0.06, two orders of magnitude greater than that determined for coordination to CoTPP. This is also significantly higher than the logβ for nitrogen-based ligands binding to ZnTPP; for example pyridine binding to ZnTPP has a logβ of 3.84 ± 0.02 in DCM[4] and 4-picoline binds to ZnTPP in DCM with a logβ of 4.10 ± 0.06.[5,6] For **R2**, an association constant of 5.91 ± 0.06 was determined, comparable to that of **R1**.

4.2.4 Dithiadiazolyl radicals with magnesium(II) tetraphenylporphyrin

The spectra resulting from the spectrophotometric titration for MgTPP with either *p*-PyrDTDA or PhDTDA, in dichloromethane (DCM), are shown in Figure 4.6. These were performed in an analogous manner to those done with CoTPP. The Soret band for MgTPP in DCM is found at 424 nm. Addition of *p*-PyrDTDA resulted in very little change to the spectrum. The band at 424 nm reduced in intensity to a small extent, with an isosbestic point at 413 nm. However, addition of PhDTDA to MgTPP resulted in no change to the UV-Vis spectrum, beyond the absorption increasing uniformly across all wavelengths, possibly as a result of porphyrin aggregation. The association constant, logβ, was calculated for each titration (where possible) and the average of these results was determined. The results are shown in Table 4.3.

Table 4.3: Association constants for dithiadiazolyl radicals coordinating to Mg (II) tetraphenylporphyrin (DCM, 25 °C)

Dithiadiazolyl Ligand		Average logβ with MgTPP
R1	*p*-PyrDTDA	1.51 ± 0.16
R2	PhDTDA	n/a

For *p*-PyrDTDA a one-to-one ligand coordination to MgTPP was modelled. The reaction has a logβ value of 1.51 ± 0.16, several orders of magnitude lower than the systems studied previously. For PhDTDA, no coordination could be successfully modelled and an association constant could not be determined.

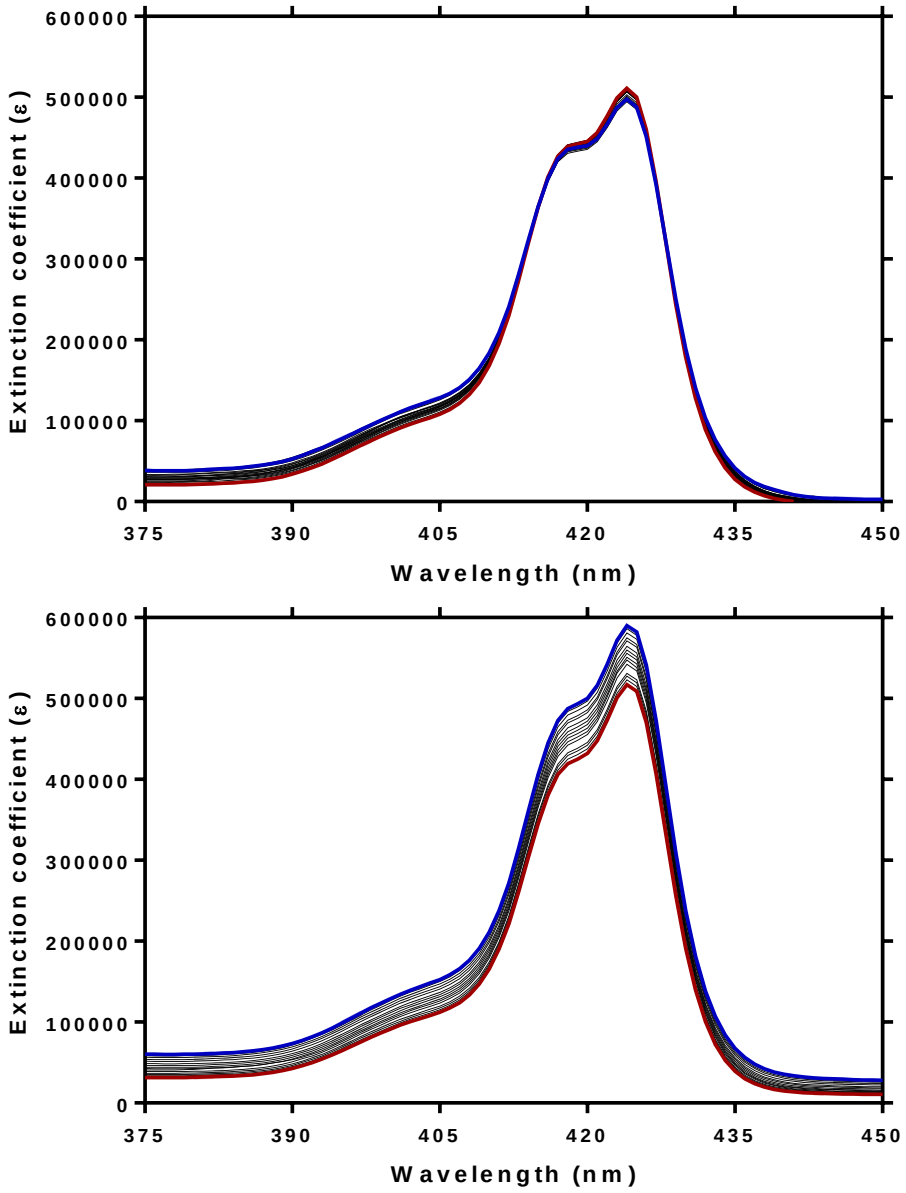

*Figure 4.6: UV-Vis spectrophotometric titration for MgTPP (**P6**) in DCM with increasing* p-*PyrDTDA (**R1**, top) and PhDTDA (**R2**, bottom) concentration, at 25 °C. Complex **R1•P6** is not formed in appreciable quantities and complex **R2•P6** is not formed. The original MgTPP spectrum is shown in red. The final addition of dithiadiazolyl is shown in blue with intermediate additions shown in black. Titration spectra have been corrected for dilution.*

4.2.5 Dithiadiazolyl radicals with iron(III) tetraphenylporphyrin

The same spectrophotometric titrations were to investigate if dithiadiazolyl radicals could be observed interacting with iron(III) tetraphenylporphyrin. The spectra resulting from the spectrophotometric titration of FeTPPCl with either *p*-PyrDTDA or PhDTDA, in dichloromethane (DCM), are shown in Figure 4.7. The Soret band for FeTPPCl in DCM is found at 417 nm. Addition of *p*-PyrDTDA results in this peak steadily reducing in intensity with no associated shift. An isosbestic point occurs at 402 nm. Similarly, when PhDTDA is added to FeTPPCl, the band at 417 nm slowly reduces in intensity, with an isosbestic point at 412 nm. The spectroscopic changes are more subtle when compared to the same ligand concentration added to CoTPP, more closely resembling those observed with CuTPP. The association constant, logβ, was calculated for each titration and the average of these results was determined. The results are shown in Table 4.4.

Table 4.4: Association constants for dithiadiazolyl radicals coordinating to Fe(III) tetraphenylporphyrin chloride (DCM, 25 °C)

	Dithiadiazolyl Ligand	Average logβ with FeTPPCl
R1	*p*-PyrDTDA	3.73 ± 0.09
R2	PhDTDA	2.39 ± 0.12

Both *p*-PyrDTDA and PhDTDA showed evidence of one-to-one ligand coordination to FeTPPCl. For the coordination of *p*-PyrDTDA to FeTPPCl, the reaction has a logβ value of 3.73 ± 0.09. In the case of PhDTDA, an association constant of 2.39 ± 0.12 was determined, lower than that of *p*-PyrDTDA. These values are an order of magnitude lower than those for CoTPP and comparable to those determined with CuTPP.

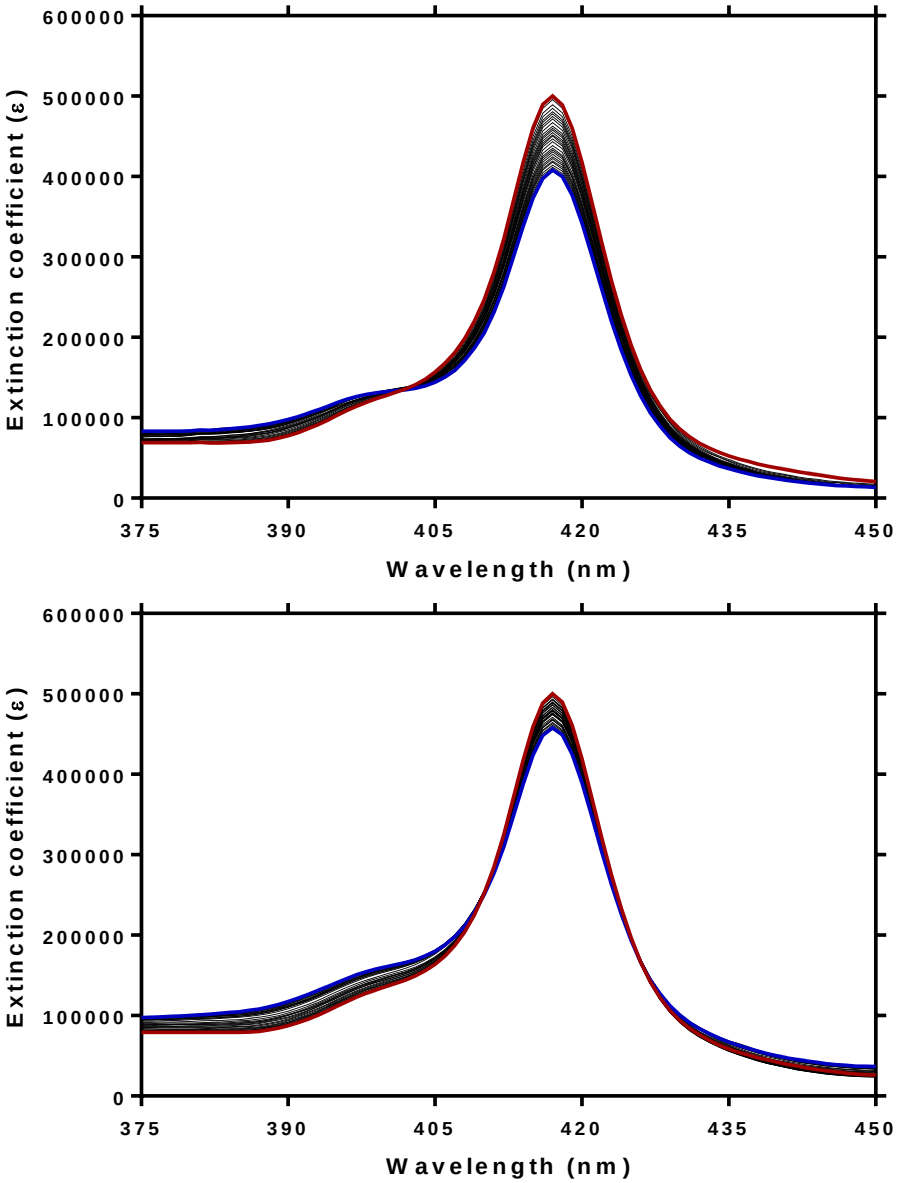

*Figure 4.7: UV-Vis spectrophotometric titration for FeTPPCl (**P7**) in DCM with increasing* p-*PyrDTDA (**R1**, top) and PhDTDA (**R2**, bottom) concentration, at 25 °C, forming **R1•P7** and **R2•P7** respectively. The original FeTPPCl spectrum is shown in red. The final addition of dithiadiazolyl is shown in blue with intermediate additions shown in black. Titration spectra have been corrected for dilution.*

4.3 EPR Spectroscopy

4.3.1 Dithiadiazolyl radicals with cobalt(II) tetraphenylporphyrin

Preliminary investigations of the interaction between **R1** and **P1** using electron paramagnetic resonance (EPR) spectroscopy showed spin coupling between the radical and the cobalt ion unpaired electron upon addition of **P1** to a solution of **R1**. These initial experiments were expanded into a series of EPR titrations. As the EPR experimental setup did not allow for the acquisition of spectra in an inert atmosphere, and with the knowledge that dithiadiazolyl radical solutions are relatively unstable in air, it was first necessary to determine to what extent the dithiadiazolyl radical EPR signal would decay during a titration experiment, as well as account for dilution of the sample. A blank experimental run, adding only aliquots of solvent, was consequently performed to establish how dilution and exposure to air would influence the dithiadiazolyl solution within the timeframe of a typical titration experiment. The signal intensity for *p*-PyrDTDA decayed to 45 % of the original intensity, while that of PhDTDA decayed to 40 % of the original intensity. To suggest any spin-pairing interaction between the metal and the dithiadiazolyl, the signal intensity would consequently have to decrease significantly further than this. It was necessary to perform all the EPR titrations at higher concentrations than for the UV titrations as a result in the different sensitivities of the two techniques.

For the initial spectrum of the dithiadiazolyl, 0.5 mL of a 2mM stock solution (in 95:5 DCM:DMSO) was transferred to a dry EPR tube and the spectrum collected. Thereafter, 50 µL aliquots of a 2mM stock solution of CoTPP (in DCM) were added, with the spectrum recollected after each addition until no further substantial spectroscopic changes were observed.

The EPR titration spectra for *p*-PyrDTDA and PhDTDA in dichloromethane with increasing CoTPP concentration are shown in Figure 4.8. The signal-to-noise ratio for *p*-PyrDTDA is worse than that of PhDTDA owing to the poor solubility of *p*-PyrDTDA in DCM, nevertheless, both titrations were performed in DCM to allow better comparison to the reaction conditions present in the UV-Vis spectrophotometric titrations (albeit at different concentration ranges).

Addition of CoTPP to *p*-PyrDTDA reduced the signal intensity to below 23 % of the original intensity. Addition of CoTPP to PhDTDA reduced the signal intensity to below 2 % of the original intensity. For both dithiadiazolyl radicals, this reduced the peak to within the range of noise, such that any further reduction in signal intensity could not be experimentally observed. As this diminishment of the distinctive dithiadiazolyl radical EPR signal was observably greater than that of the blank, this is evidence of spin interaction between the dithiadiazolyl unpaired electron and the cobalt ion unpaired electron.

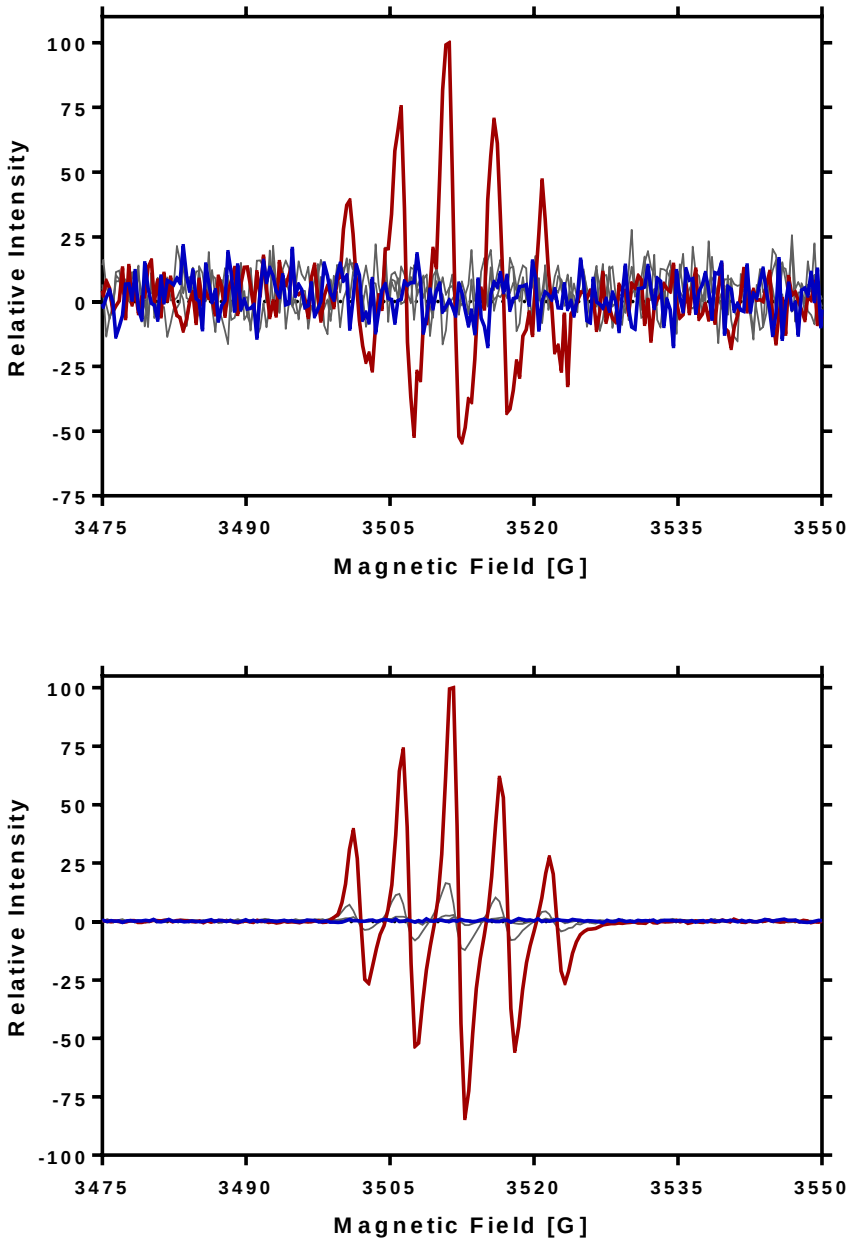

Figure 4.8: EPR titration spectra for p-*PyrDTDA (**R1**, top) and PhDTDA (**R2**, bottom) in DCM with increasing CoTPP (**P1**) concentration, at ambient temperature, forming **R1•P1** and **R2•P1** respectively. The original dithiadiazolyl spectrum is shown in red. The final addition of CoTPP is shown in blue with intermediate additions shown in grey.*

4.3.2 Dithiadiazolyl radicals with copper(II) tetraphenylporphyrin

The EPR titration spectra for *p*-PyrDTDA and PhDTDA in dichloromethane with increasing CuTPP concentration are shown in Figure 4.9.

As seen for CoTPP, addition of CuTPP to *p*-PyrDTDA reduced the signal intensity to below 27 % of the original intensity. Addition of CuTPP to PhDTDA reduced the signal intensity to below 3 % of the original intensity. Such reduction of the dithiadiazolyl EPR signal is most likely the result of spin pairing between the dithiadiazolyl radical and the copper ion. However, unlike for CoTPP, for both dithiadiazolyl radicals, this reduction in peak intensity did not completely diminish the signal within the range of noise. Even after addition of excess CuTPP, a weak signal could still be identified amongst the noisy baseline.

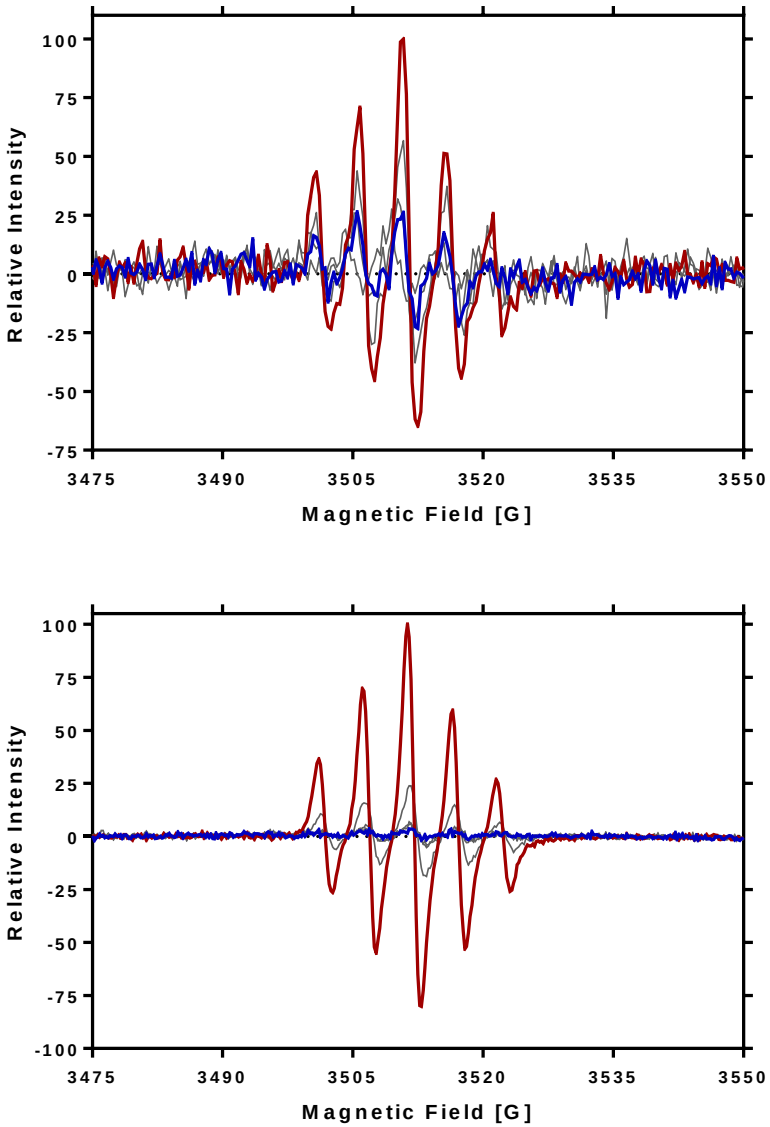

Figure 4.9: EPR titration spectra for p-*PyrDTDA (**R1**, top) and PhDTDA (**R2**, bottom) in DCM with increasing CuTPP (**P4**) concentration, at ambient temperature, forming **R1•P4** and **R2•P4** respectively. The original dithiadiazolyl spectrum is shown in red. The final addition of CuTPP is shown in blue with intermediate additions shown in grey.*

Figure 4.10 shows the EPR spectra for *p*-PyrDTDA and PhDTDA after addition of excess CuTPP, plotted on a different scale.* The remaining signal appears to represent both a residual dithiadiazolyl signal and a signal for the excess paramagnetic CuTPP. The spectrum for CuTPP in the absence of dithiadiazolyl is shown in Figure 4.11 for comparison.

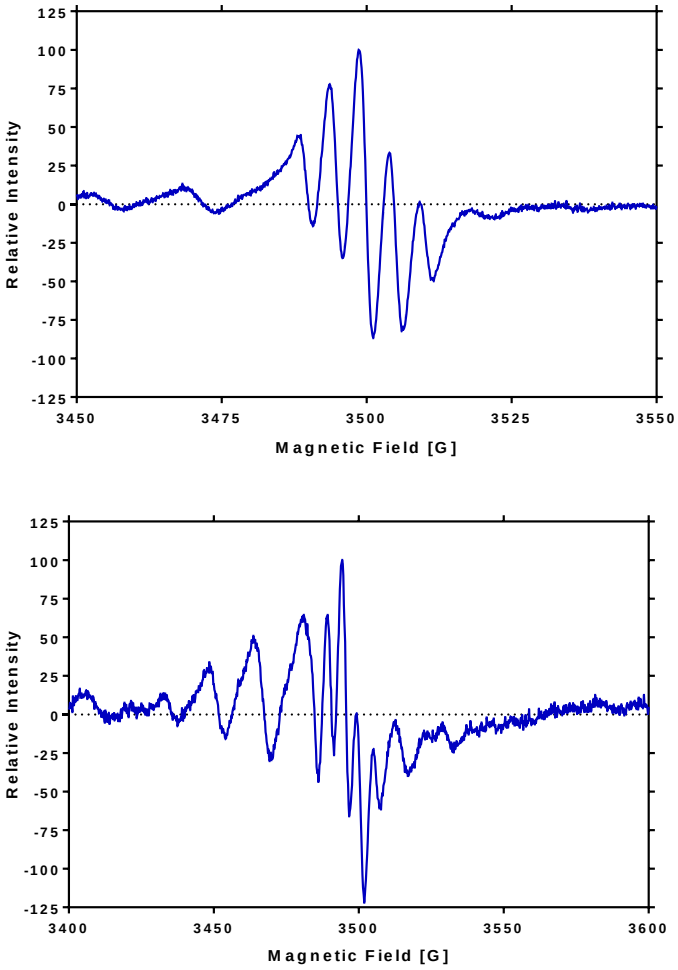

Figure 4.10: EPR spectra for the addition of excess CuTPP to p-*PyrDTDA (top, in DMSO) and PhDTDA (bottom, in DCM), showing a residual dithiadiazolyl radical signal together with the signal of the excess CuTPP.*

* The spectrum for CuTPP with *p*-PyrDTDA was run in DMSO in order to improve the signal-to-noise ratio.

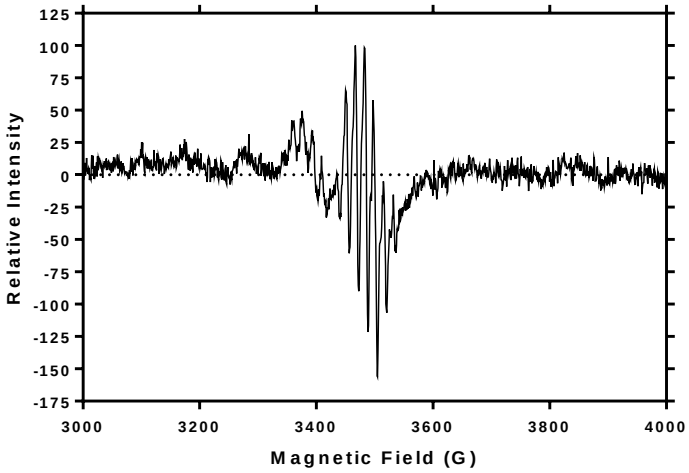

*Figure 4.11: EPR spectrum for CuTPP (**P4**) in DCM*

4.3.3 Dithiadiazolyl radicals with zinc(II) tetraphenylporphyrin

The EPR titration spectra for *p*-PyrDTDA and PhDTDA in dichloromethane with increasing ZnTPP concentration are shown in Figure 4.12.

As seen for CoTPP, addition of ZnTPP to *p*-PyrDTDA reduced the signal intensity to below 24 % of the original intensity. Addition of ZnTPP to PhDTDA reduced the signal intensity to below 4 % of the original intensity. For *p*-PyrDTDA, it is difficult to determine any residual dithiadiazolyl radical signal, however this may be as a result of the signal-to-noise ratio. If the experiment is repeated using dimethylsulfoxide as solvent, this remaining dithiadiazolyl signal can be observed as a result of the improved signal-to-noise ratio. For PhDTDA, the reduction in peak intensity did not completely diminish the signal within the range of noise. Even after addition of excess ZnTPP, a weak signal could still be identified, indicating that there is at least some dithiadiazolyl ligand with radical character. As the d^{10} zinc centre is diamagnetic, this decrease in the dithiadiazolyl radical signal cannot be the result of ligand-metal spin pairing and must be a result of spin pairing between complexes. As the EPR titrations were performed at a higher concentration range than the UV experiments, it is possible that complex association could be occurring. There is a slight shift in g-factor upon addition of the porphyrin, while a_N remains constant.

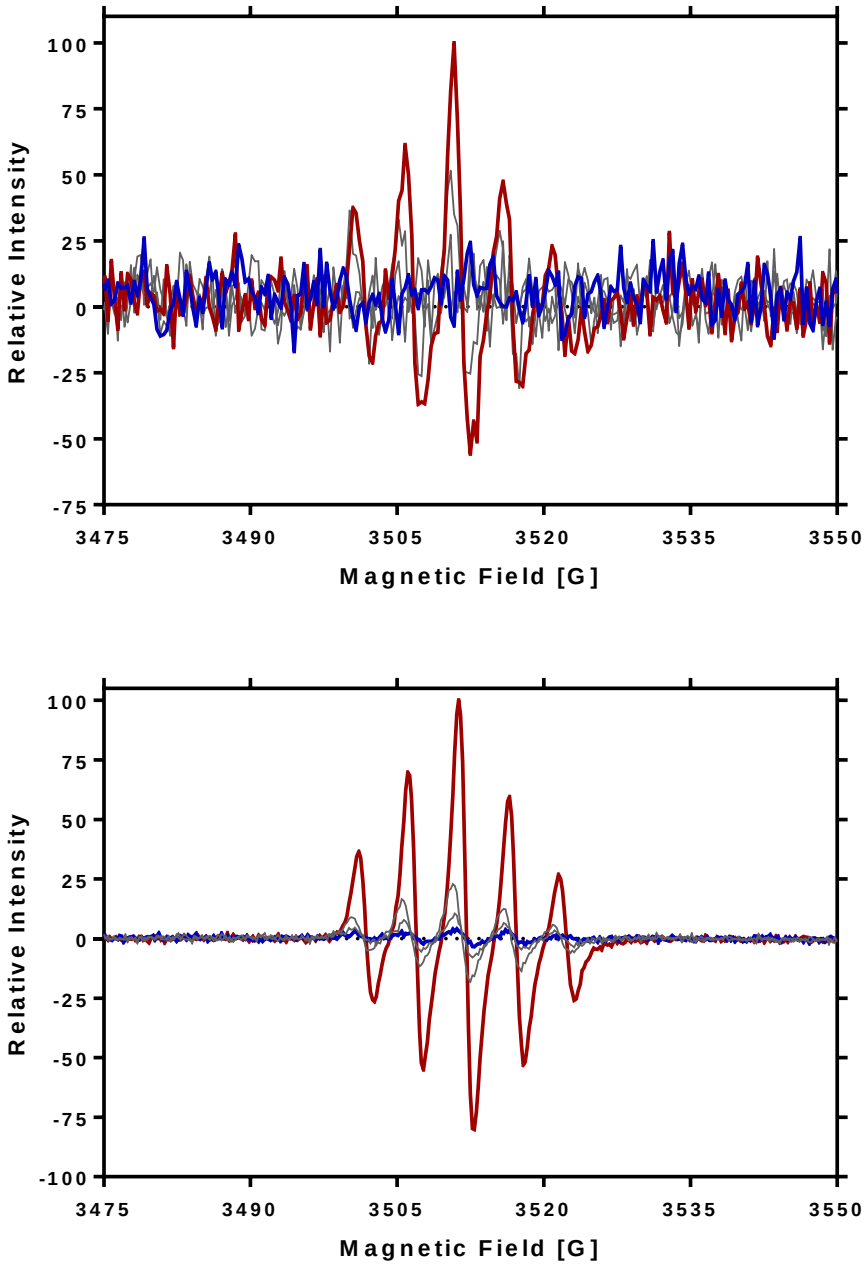

Figure 4.12: EPR titration spectra for p-*PyrDTDA (**R1**, top) and PhDTDA (**R2**, bottom) in DCM with increasing ZnTPP (**P5**) concentration, at ambient temperature, forming **R1•P5** and **R2•P5** respectively. The original dithiadiazolyl spectrum is shown in red. The final addition of CoTPP is shown in blue with intermediate additions shown in grey.*

To establish if concentration-dependant complex association, and resultant spin pairing, was responsible for the quenching of the EPR signal, a dilution study was carried out and a Beer's law plot for **R2•P5** was determined. A solution of ZnTPP and PhDTDA was prepared to form **R2•P5** at a high concentration, as near the end of the EPR titration (0.250 mM), and the UV-Vis spectrum between 300 and 800 nm was collected. The solution was diluted to half of the original concentration with dichloromethane and the spectrum was recollected. This was performed a total of 12 times, until the

concentration was lower than for the UV-Vis titrations. The absorbance at 558 nm (a peak unique to **R2•P5**) was plotted as a function of the concentration of **R2•P5** (Figure 4.13). Concentrations were based on the amount of ZnTPP present in the sample. Selected spectra are shown in Figure 4.14 and Figure 4.15. Analysis of the spectra confirmed that at all concentrations the spectrum collected was that of **R2•P5**, not ZnTPP, as at all concentrations, the spectrum of the solution match that found for the formation of **R2•P5** in the UV-Vis titrations and not that of ZnTPP. Figure 4.14 shows the UV-Vis spectrum for the dilution study at a range of concentrations compared to the UV-Vis spectrum of ZnTPP. Notice that for **R2•P5**, absorption maxima are seen at 425, 585 and 599 nm, while for ZnTPP the absorbance bands are at 418, 549 and 587 nm.

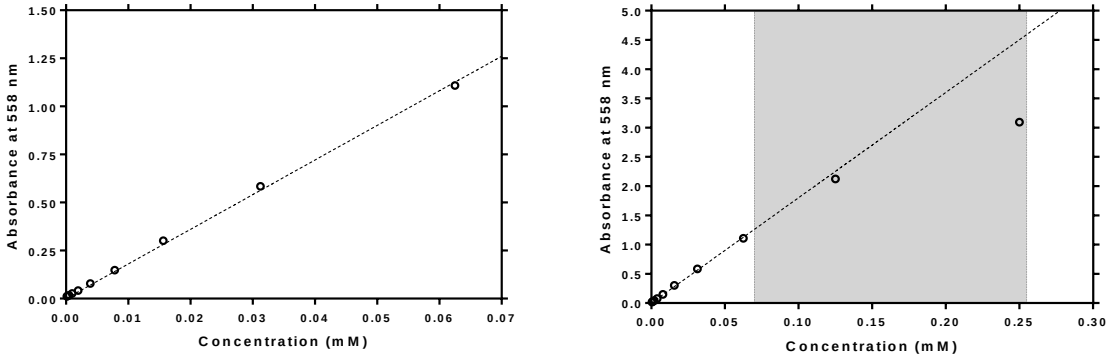

*Figure 4.13: Beer's law plot for **R2•P5**, showing deviation at high concentration (left: 0.0 mM to 0.07 mM; right: 0.0 mM to 0.30 mM). Experimental data points shown as open black circles, linear regression shown as a dotted black line (R^2 = 0.993, $P < 0.0001$). Concentration range of ZnTPP for the EPR titrations shown in grey (0.070 mM to 0.255 mM).*

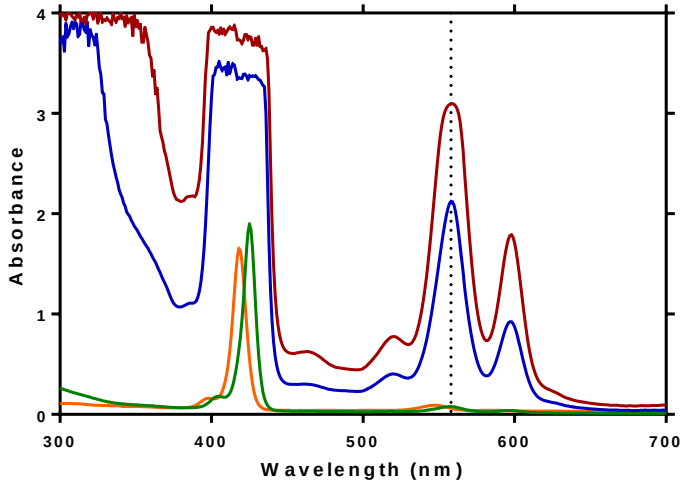

*Figure 4.14: UV-Vis spectra for **R2•P5** at 0.250 mM (red), 0.125 mM (blue) and 0.00391 mM (green), as well as ZnTPP (**P5**) at 0.00368 mM (orange). The wavelength used for the Beer's law plot, 558 nm, is indicated with a dotted gridline. At high concentrations, absorbance between 300 and 450 nm was outside the limit of detection.*

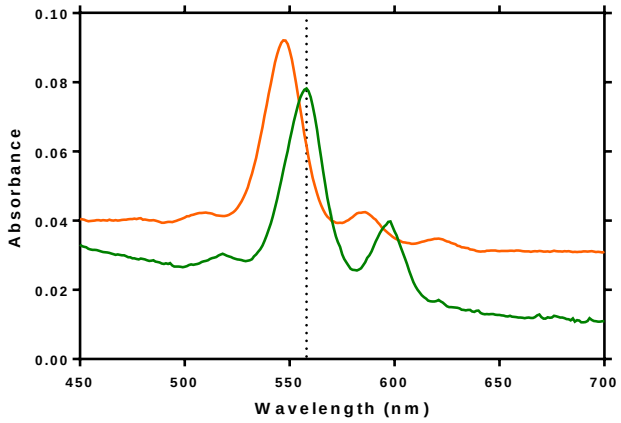

*Figure 4.15: A comparison of the UV-Vis spectra of **R2•P5** (3.91 µM, green) and **P5** (3.68 µM, orange) between 450 and 700 nm. The wavelength used for the Beer's law plot, 558 nm, is indicated with a dotted gridline.*

From Figure 4.13 it is apparent that at the concentration range used in the EPR titration there is deviation from linearity. This suggests that **R2•P5** units are associating with each other at high concentration, most likely resulting in the formation of dithiadiazolyl dimers (see Chapter 1 for more detail on dithiadiazolyl dimerization and pancake bonding). Pancake bonding between dithiadiazolyl ligands has previously been observed in a lanthanide dithiadiazolyl complex.[7] Spin-pairing between the paramagnetic units explains why the dithiadiazolyl EPR signal diminishes in intensity as the EPR titration progresses. Based on the results seen in the EPR titration, the same dimerization appears to be occurring with **R1•P5**. A schematic representation of this proposed association is shown in Figure 4.16.

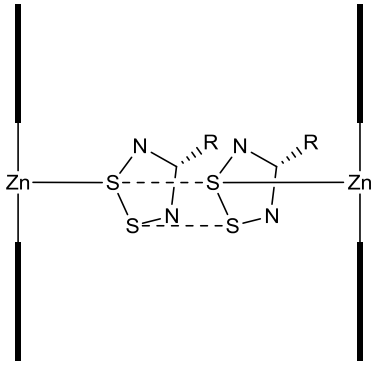

Figure 4.16: Schematic representation of ZnTPP-dithiadiazolyl complexes associating through pancake bonding between the dithiadiazolyl ligands. Porphyrin plane represented graphically with bold lines for simplicity.

The dithiadiazolyl dimer has been drawn in the *cis*-oid conformation, however this dimerization could occur in any dimerization mode (see Section 1.1.1). It is most likely that the sterics associated with the ZnTPP molecules would dictate the dimerization mode, as the twisted phenyl rings typically disfavour an eclipsed association of porphyrin units.[8]

4.3.4 Dithiadiazolyl radicals with magnesium(II) tetraphenylporphyrin

The EPR titration spectra for *p*-PyrDTDA and PhDTDA in dichloromethane with increasing MgTPP concentration are shown in Figure 4.17.

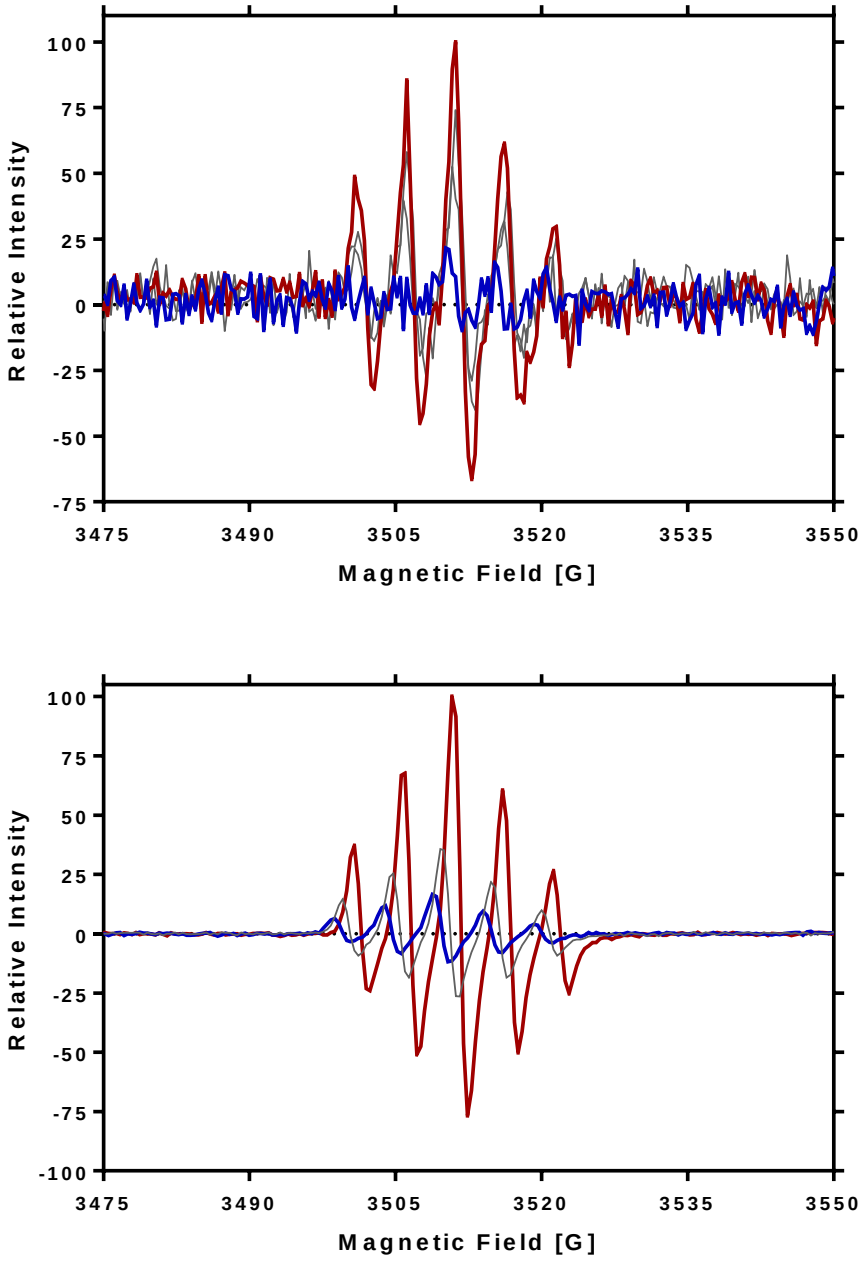

Figure 4.17: EPR titration spectra for p-*PyrDTDA (**R1**, top) and PhDTDA (**R2**, bottom) in DCM with increasing MgTPP (**P6**) concentration, at ambient temperature. The complexes **R1•P6** and **R2•P6** are not formed in appreciable quantities. The original dithiadiazolyl spectrum is shown in red. The final addition of CoTPP is shown in blue with intermediate additions shown in grey.*

Addition of MgTPP to *p*-PyrDTDA reduced the signal intensity to approximately 39 % of the original intensity, while addition of MgTPP to PhDTDA reduced the signal intensity to 37 % of the original intensity. This is not appreciably more than the blank titration (45 % and 40 % respectively). As Mg^{2+} is a closed-shell ion, no signal reduction as a result spin pairing is expected.

4.3.5 Dithiadiazolyl radicals with iron(III) tetraphenylporphyin

The EPR titration spectra for *p*-PyrDTDA and PhDTDA in dichloromethane with increasing FeTPPCl concentration are shown in Figure 4.18.

Addition of FeTPPCl to a solution of *p*-PyrDTDA reduced the signal intensity to only 10 % of the original intensity, and addition of FeTPPCl to PhDTDA reduced the signal intensity to 2 % of the original intensity. Addition of the porphyrin resulted in complete quenching of the dithiadiazolyl EPR signal for both radicals, with no identifiable signal remaining. As for CoTPP, this reduction of the dithiadiazolyl EPR signal is most likely the result from spin pairing between the dithiadiazolyl radical and the iron cation, indicating that coordination must be occurring in solution.

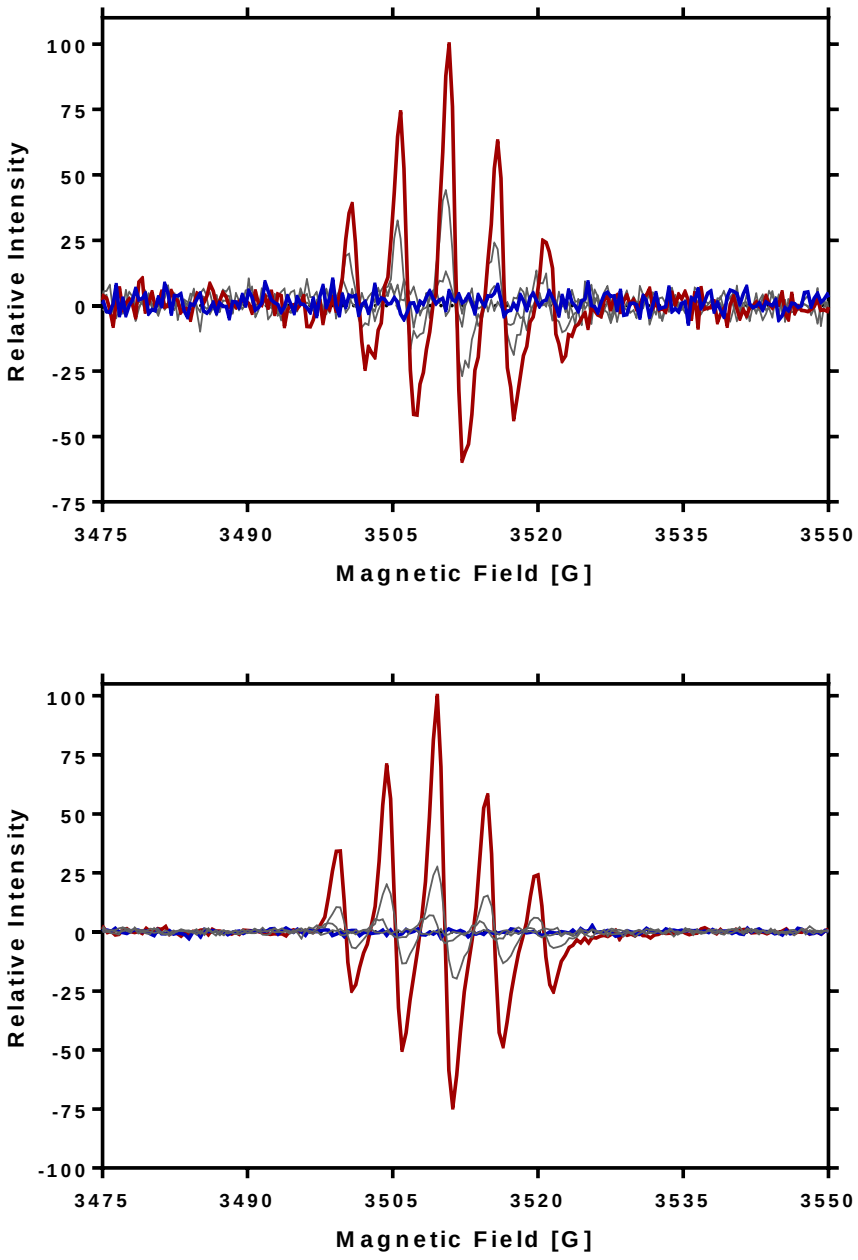

Figure 4.18: EPR titration spectra for p*-PyrDTDA (**R1**, top) and PhDTDA (**R2**, bottom) in DCM with increasing FeTPPCl (**P7**) concentration, at ambient temperature, forming **R1•P7** and **R2•P7** respectively. The original dithiadiazolyl spectrum is shown in red. The final addition of CoTPP is shown in blue with intermediate additions shown in grey.*

4.4 Summary and Conclusions

The interaction between two dithiadiazolyl radicals and five metalated tetraphenylporphyrins was studied in solution through the use of UV-Vis and EPR spectroscopy.

UV-Vis spectrophotometric titrations were carried out to assess if the relevant dithiadiazolyl radical – metalloporphyrin complexes would form in solution. Where possible, the association constant for this coordination reaction was determined. A summary of the association constants found for *p*-PyrDTDA (**R1**) and PhDTDA (**R2**) with CoTPP (**P1**), CuTPP (**P4**), ZnTPP (**P5**), MgTPP (**P6**) and FeTPPCl (**P7**) is shown in Table 4.5.

*Table 4.5: Association constants for **R1** and **R2** coordinating to **P1**, **P4**, **P5**, **P6** and **P7**, as relative ratios to β for **R1•P1***

	Dithiadiazolyl Ligand	with CoTPP (P1)	with CuTPP (P4)	with ZnTPP (P5)	with MgTPP (P6)	with FeTPPCl (P7)
R1	*p*-PyrDTDA	1.000 ± 0.103	0.218 ± 0.067	106.6 ± 14.8	0.002 ± 0.001	0.356 ± 0.074
R2	PhDTDA	1.220 ± 0.112	0.058 ± 0.011	52.63 ± 7.22	n/a[†]	0.016 ± 0.004

Both ligands **R1** and **R2** showed coordination to CuTPP, ZnTPP and FeTPPCl, as previously seen with CoTPP. **R1** showed weak coordination to MgTPP, while **R2** did not coordinate to MgTPP at all.

For the coordination of **R1** to CuTPP, the reaction has a logβ value of 3.51 ± 0.14. For **R2**, an association constant of 2.94 ± 0.08 was determined, somewhat weaker than that of **R1**. The association constants for both **R1** and **R2** with CuTPP are an order of magnitude lower than those determined with CoTPP.

Both dithiadiazolyl radicals coordinated to FeTPPCl to form iron complexes. For the coordination of **R1** to FeTPPCl, the reaction has a logβ value of 3.73 ± 0.09. For **R2**, an association constant of 2.39 ± 0.12 was determined. These values are an order of magnitude lower than those for CoTPP and comparable to those determined with CuTPP.

Conversely, coordination of both dithiadiazolyl radicals to ZnTPP occurred at an appreciably lower ligand concentration than for the other metals, to the extent that the titration volumes had to be changed in order to accurately determine the logβ values. The coordination of **R1** to ZnTPP has an association constant of 6.21 ± 0.06, two orders of magnitude higher than that determined for coordination to the original CoTPP (a 100-fold increase). For **R2**, a logβ of 5.91 ± 0.06 was determined, comparable to that of **R1** with ZnTPP.

[†] As an association constant could not be determined for **R2·P6**, no ratio is given.

For **R1,** a one-to-one ligand coordination to MgTPP was modelled with an association constant of 1.51 ± 0.16, several orders of magnitude lower than for the other metals investigated. For **R2**, coordination could not modelled.

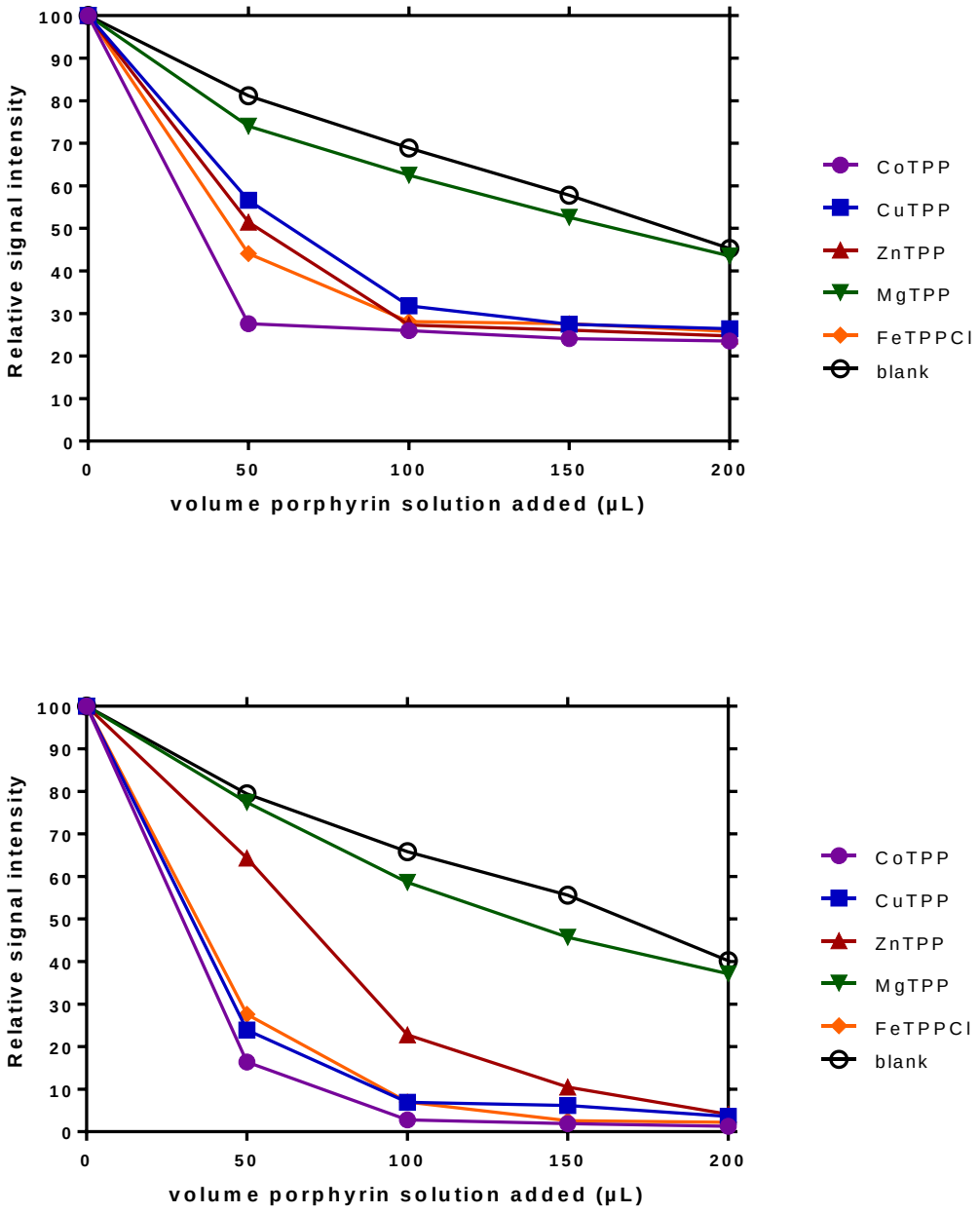

Figure 4.19: Relative intensity of the p*-PyrDTDA (**R1**, top) and PhDTDA (**R2**, bottom) EPR signal with increasing amounts of metalloporphyrin solution*

The characteristic 1:2:3:2:1 pentet EPR signal of the dithiadiazolyl radicals were studied to evaluate the electronic behaviour of the system in solution when metalloporphyrin is added. A graphical representation of the results of the EPR titrations is shown in

Figure 4.19. The addition of CoTPP to both **R1** and **R2** in solution results in the signal for the dithiadiazolyl radical rapidly being quenched, as a result of the radical spin-pairing with the cobalt centre. This quenching of the radical signal is also seen with the addition of FeTPPCl to **R1** or **R2**, indicating that these complexes also have ligand – metal spin pairing. When CuTPP is added to a solution of either dithiadiazolyl, the EPR signal of the radical decreases as a result of spin-pairing; however, complete quenching of the EPR spectrum is not observed. Instead, a residual low-intensity dithiadiazolyl radical EPR signal is observed together with the EPR signal for the paramagnetic CuTPP. Future work should attempt to understand the different components observed in solution through simulation and deconvolution of the EPR signal.

The addition of ZnTPP to both **R1** and **R2** results in the EPR signal decreasing in intensity to a greater extent than for the blank experiment, but not as extensively as for cobalt, copper or iron. The residual dithiadiazolyl EPR signal indicates that a portion of the ligands remain as radicals when coordinated to ZnTPP. However, the reduction of the signal's intensity cannot result from radical – metal spin-pairing, as Zn^{2+} is a d^{10} centre. Instead, radical-porphyrin units probably associate through dithiadiazolyl pancake bonding. The resultant dimers are diamagnetic and consequently their formation results in quenching of the dithiadiazolyl EPR signal. Association of the **R2•P5** complex at high concentration was confirmed though UV-Vis spectroscopy. The differences in the signal decay for **R2•P5** and **R1•P5** may be a result of the difference in complex dimerization for the two different dithiadiazolyls. Finally, for the addition of MgTPP to either **R1** or **R2**, the reduction in dithiadiazolyl EPR signal intensity is not appreciably greater than for that of the blank. It is likely that is a result of the relatively weak interaction between the soft sulfur-donor ligand and the small, hard magnesium cation.

In conclusion, dithiadiazolyl radical – metalloporphyrin complexes have been shown to form with four metals. The choice of metal has an effect on the electronic nature of the ligand, as evidenced by the EPR spectra of the complexes formed *in situ*. The complexes formed with Co^{2+}, Cu^{2+} and Fe^{3+} are diamagnetic as a result of spin pairing between the paramagnetic metal and the paramagnetic ligand. The complexes formed with diamagnetic Zn^{2+} are paramagnetic; however, these paramagnetic complexes associate at high concentration to form diamagnetic dimeric complexes. There is no clear trend to explain the relative strength of ligand association to the different metals.

Following successful association to iron (III) tetraphenylporphyrin chloride, it remained to be seen if dithiadiazolyl association to the biological porphyrin iron (III) protoporphyrin IX, or haematin, could be observed. A preliminary study of this, demonstrating the potential biological application of these complexes, follows in Chapter 5.

4.5 Experimental details

4.5.1 Synthesis of dithiadiazolyl radicals **R1** and **R2**

The synthesis of 4-(4′-pyridyl)-1,2,3,5-dithiadiazolyl (**R1**) and 4-phenyl-1,2,3,5-dithiadiazolyl (**R2**) was previously described in Chapter 2 and Chapter 3 respectively.

4.5.2 Synthesis of metalloporphyrins **P1**, **P4**, **P5**, **P6** and **P7**

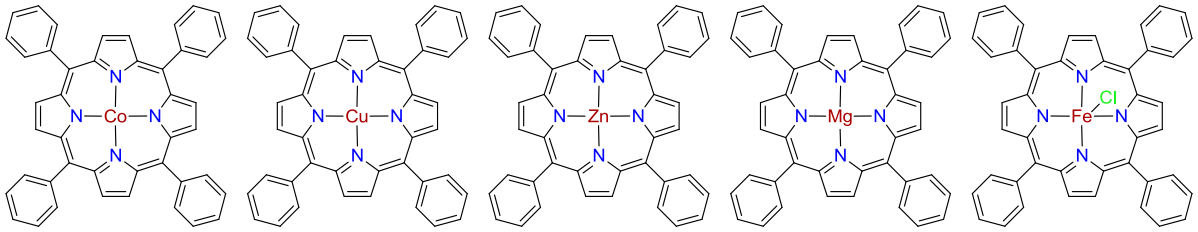

*Cobalt (II) tetraphenylporphyrin (**P1**)*

The synthesis of free-base tetraphenylporphyrin (H_2TPP) and cobalt (II) tetraphenylporphyrin (**P1**) was previously described in Chapter 2.

Porphyrins **P4** to **P7** were synthesised from tetraphenylporphyrin in an analogous fashion to that of CoTPP using the method described by Adler and coworkers.[1]

*Copper (II) tetraphenylporphyrin (**P4**)*

Tetraphenylporphyrin (500 mg, 0.81 mmol) and copper (II) acetate monohydrate (0.162 g, 0.81 mmol) were added to degassed dimethylformamide (50 mL) in a 100 mL round bottomed flask under nitrogen. The solution was heated and reflux was maintained for 45 minutes until the UV-Vis spectrum of an aliquot of the reaction solution confirmed complete metalation. Thereafter, heating was ceased and the flask was allowed to cool to room temperature before cooling in the refrigerator for 1 hour. The solution was filtered and the precipitate was washed with cold distilled water to yield copper (II) tetraphenylporphyrin **P4** as fine purple crystals (0.545 g, 0.81 mmol, 99 %). UV-Vis (CH_2Cl_2): 414 nm, 540 nm.

*Zinc (II) tetraphenylporphyrin (**P5**)*

Tetraphenylporphyrin (500 mg, 0.81 mmol) and zinc (II) acetate dihydrate (0.356 g, 1.63 mmol) were added to degassed dimethylformamide (50 mL) in a 100 mL round bottomed flask under nitrogen.

The solution was heated and reflux was maintained for 2.5 hours until the UV-Vis spectrum of an aliquot of the reaction solution confirmed complete metalation. Thereafter, heating was ceased and the flask was allowed to cool to room temperature before cooling in the refrigerator overnight. The solution was filtered and the precipitate was washed with cold distilled water to yield zinc (II) tetraphenylporphyrin **P5** as a bright purple solid (0.540 g, 0.81 mmol, 98 %). UV-Vis (CH_2Cl_2): 418 nm, 549 nm.

*Magnesium (II) tetraphenylporphyrin (**P6**)*

Tetraphenylporphyrin (500 mg, 0.81 mmol) and magnesium chloride (0.774 g, 8.13 mmol) were added to degassed dimethylformamide (50 mL) in a 100 mL round bottomed flask under nitrogen. The solution was heated and reflux was maintained for 3 hours until the UV-Vis spectrum of an aliquot of the reaction solution confirmed complete metalation. Thereafter, heating was ceased and the flask was allowed to cool to room temperature before cooling in the refrigerator overnight. The solution was filtered and the precipitate was washed with distilled water to yield magnesium (II) tetraphenylporphyrin **P6** as a bright purple solid (0.503 g, 0.76 mmol, 93 %). UV-Vis (CH_2Cl_2): 424 nm, 523 nm.

*Iron (III) tetraphenylporphyrin chloride (**P7**)*

Tetraphenylporphyrin (500 mg, 0.81 mmol) and iron (III) chloride (0.264 g, 1.63 mmol) were added to degassed dimethylformamide (50 mL) in a 100 mL round bottomed flask under nitrogen. The solution was heated and reflux was maintained for 1.5 hours until the UV-Vis spectrum of an aliquot of the reaction solution confirmed complete metalation. Thereafter, heating was ceased and the flask was allowed to cool to room temperature before cooling in the refrigerator for 1 hour. The solution was filtered and the precipitate was washed with distilled water to yield iron (III) tetraphenylporphyrin chloride **P7** as a dark purple powder (0.554 g, 0.79 mmol, 97 %). UV-Vis (CH_2Cl_2): 417 nm, 510 nm.

4.5.3 UV-Vis spectrophotometric titrations

All glassware, except microsyringes, was dried in a 120 °C oven overnight. All solvents were dried over 3 Å molecular sieves. Microsyringes were flushed three times with clean, dry solvent and three times with the solution of interest before being used.

A fresh 2 mM stock solution of the dithiadiazolyl radical was made up in a 5 mL volumetric flask prior to each experiment using a 9:1 dichloromethane : dimethylsulfoxide solvent system. The flask was flushed with nitrogen for 1 minute before being sealed with a septum and paraffin laboratory film. A 1 mM stock solution of the cobalt porphyrin was made up in a screw-cap glass using dichloromethane.

A 2μM working solution of the cobalt porphyrin was made up in a quartz cuvette with 1996 μL dichloromethane (measured by micropipette) and 4 μL of the cobalt porphyrin stock solution (measured by glass Hamilton microsyringe). A 2000 μL portion of dichloromethane was placed in the reference cuvette (measured by micropipette).

Both cuvettes, with their lids, were placed in the UV-vis spectrophotometer and allowed to equilibrate to 25 °C before the spectrum was collected between 375 and 450 nm.

Aliquots of the dithiadiazolyl stock solution were added to both the working solution cuvette and the reference solution cuvette using a glass Hamilton microsyringe. The solutions were stirred with a wire microsyringe plunger and the lids replaced. The spectrum was collected after each addition. This was continued until a total of 600 μL of the dithiadiazolyl solution was added.

Spectrophotometric titrations of CoTPP were performed by the addition of 10 x 2 μL, 10 x 4 μL, 2 x 10 μL, 6 x 20 μL and 8 x 50 μL aliquots of ligand stock solution (total volume 600 μL) to both sample and reference.

Spectrophotometric titrations of CuTPP, MgTPP and FeTPPCl were performed by the addition of 30 x 20 μL aliquots of ligand stock solution (total volume 600 μL) to both sample and reference.

Spectrophotometric titrations of ZnTPP were performed by the addition of 10 x 1 μL and 10 x 2 μL aliquots of ligand stock solution (total volume 30 μL) to both sample and reference. Initial titrations used 30 x 20 μL aliquots but showed complete change after the first addition with no further spectroscopic changes with subsequent additions.

The spectrophotometric titration was performed in triplicate for each radical – porphyrin pair. Association constants (logβ values) were calculated in HypSpec using a 2-reagent model with a 1:1 molar ratio. The raw spectroscopic data (that is, without dilution correction) were used as the HypSpec software takes the titration volumes into consideration. No additional coordination of

DMSO could be modelled. The average logβ of each three identical spectrophotometric titrations was reported. All logβ values are given in Table 4.6 (for **P1**), Table 4.7 (for **P4**), Table 4.8 (for **P5**), Table 4.9 (for **P6**) and Table 4.10 (for **P7**). No logβ values could be determined for **R2** with **P6**.

*Table 4.6: All log values for CoTPP (**P1**) and dithiadiazolyls **R1** and **R2***

Dithiadiazolyl ligand		**logβ values with CoTPP (P1)**			
		1	**2**	**3**	**Average**
R1	*p*-PyrDTDA	4.19	4.14	4.23	4.19 ± 0.05
R2	PhDTDA	4.23	4.28	4.31	4.27 ± 0.04

*Table 4.7: All log values for CuTPP (**P4**) and dithiadiazolyls **R1** and **R2***

Dithiadiazolyl ligand		**logβ values with CuTPP (P4)**			
		1	**2**	**3**	**Average**
R1	*p*-PyrDTDA	3.51	3.65	3.38	3.51 ± 0.14
R2	PhDTDA	2.85	3.01	2.97	2.94 ± 0.08

*Table 4.8: All log values for ZnTPP (**P5**) and dithiadiazolyls **R1** and **R2***

Dithiadiazolyl ligand		**logβ values with ZnTPP (P5)**			
		1	**2**	**3**	**Average**
R1	*p*-PyrDTDA	6.28	6.19	6.17	6.21 ± 0.06
R2	PhDTDA	5.92	5.96	5.84	5.91 ± 0.06

*Table 4.9: All log values for MgTPP (**P6**) and dithiadiazolyl **R1***

Dithiadiazolyl ligand		**logβ values with MgTPP (P6)**			
		1	**2**	**3**	**Average**
R1	*p*-PyrDTDA	1.35	1.66	1.52	1.51 ± 0.16

*Table 4.10: All log values for FeTPPCl (**P7**) and dithiadiazolyls **R1** and **R2***

Dithiadiazolyl ligand		logβ values with FeTPPCl (P7)			
		1	**2**	**3**	**Average**
R1	*p*-PyrDTDA	3.66	3.83	3.71	3.73 ± 0.09
R2	PhDTDA	2.50	2.26	2.42	2.39 ± 0.12

4.5.4 Beer's Law experiment

A Beer's law study was performed on **R2•P5** to confirm complex association at higher concentrations.

A fresh 4 mM stock solution of the dithiadiazolyl radical was made up in a 5 mL volumetric flask using a 9:1 dichloromethane : dimethylsulfoxide solvent system. The flask was flushed with nitrogen for 1 minute before being sealed with a septum and paraffin laboratory film. A 1.47 mM stock solution of the ZnTPP was made up in a screw-cap glass using dichloromethane.

A 0.250 mM solution of **R2•P5** was made up in a quartz cuvette with 1.5 ml dithiadiazolyl stock solution, 0.34 ml ZnTPP stock solution and 0.16 ml DCM (all measured by micropipette, ZnTPP limiting reagent with excess PhDTDA[‡]). A 2000 µL portion of dichloromethane was placed in the reference cuvette (measured by micropipette). Both cuvettes, with their lids, were placed in the UV-vis spectrophotometer and allowed to equilibrate to 25 °C before the spectrum was collected between 300 and 700 nm. A 1000 µL portion of the working solution was removed and 1000 µL of dichloromethane was added. The 0.125 mM solution was stirred and the spectrum recollected. This was repeated to collect the spectra at 62.5 µM, 31.3 µM, 15.6 µM, 7.81 µM, 3.91 µM, 1.95 µM, 0.977 µM, 0.488 µM, 0.244 µM and 0.122 µM. The absorption of the intense Soret band could not be determined at high concentration so absorbance at 558 nm was monitored instead.

4.5.5 EPR titrations

Data collection: Experimental parameters

Centre field: 3515 G. Sweep width: 100 G. Resolution: 500 points in X (Instrumental details can be found in Appendix A.)

[‡] This is the same concentration of dithiadiazolyl and ZnTPP as at the end of the EPR titration. At the concentration used, the dithiadiazolyl radical is still clearly monomeric, so any changes observed to the EPR or UV spectra must be as a result of ligand-metalloporphyrin interactions.

Titration experiment

All glassware, except microsyringes, was dried in a 120 °C oven overnight. All solvents were dried over 3 Å molecular sieves. Microsyringes were flushed three times with clean, dry solvent and three times with the solution of interest before being used.

A 2 mM solution of the metalloporphyrin was made up in DCM in a screw-cap glass vial. A 2 mM solution of **R1** or **R2** was made up in 95:5 DCM : DMSO in an oven-dried 5 ml volumetric flask flushed with nitrogen. The flask was sealed with a septum and laboratory film. A portion (0.5 mL) of this dithiadiazolyl solution was transferred to an oven-dried quartz EPR tube using a disposable plastic syringe, the tube was capped and the EPR spectrum was collected. An aliquot of the metalloporphyrin solution (50 μL) was added to the tube using a glass Hamilton microsyringe, the sample inverted once to mix and the spectrum recollected. A total of four metalloporphyrin additions were performed. From start to finish, the experiments took between 21 and 23 minutes.

Control experiment

The control experiment was carried out in the same manner as for the titration experiment. Aliquots of dry DCM (50 μL) were added to the tube using a glass Hamilton microsyringe instead of the metalloporphyrin solution. A total of four solvent additions were performed. From start to finish, the experiment took 22 minutes.

For **R1**, the final EPR signal had an intensity 45 % of that of the original dithiadiazolyl signal. For **R2**, the final EPR signal was 40 % of the original dithiadiazolyl signal intensity.

4.6 References

(1) Adler, A. D.; Longo, F. R.; Kampas, F.; Kim, J. *J. Inorg. Nucl. Chem.* **1970**, *32* (7), 2443.

(2) Kadish, K. M.; Bottomley, L. A.; Beroiz, D. *Inorg. Chem.* **1978**, *17* (5), 1124.

(3) Yamamoto, K. *Inorg. Chim. Acta* **1986**, *113* (2), 181.

(4) Nappa, M.; Valentine, J. S. *J. Am. Chem. Soc.* **1978**, *100* (16), 5075.

(5) Kirksey, C. H.; Hambright, P.; Storm, C. B. *Inorg. Chem.* **1969**, *8* (10), 2141.

(6) Hard, A. P.; Jayasooriya, U. A.; Cammidge, A. N. *Analyst* **2003**, *128* (1), 70.

(7) Mills, M. B.; Hollingshead, A. G.; Maahs, A. C.; Soldatov, D. V.; Preuss, K. E. *CrystEngComm* **2015**, *17* (41), 7816.

(8) Shiedt, W. R.; Mondal, J. U.; Eigenbrot, C. W.; Adler, A.; Radonovich, L. J.; Hoard, J. L. *Inorg. Chem.* **1986**, *25*, 795.

Chapter 5

Investigating the interaction between dithiadiazolyl radicals and haematin

---

5.1 Introduction

In Chapter 3, the UV-Vis spectroscopic study of the coordination of eight dithiadiazolyl radicals to three cobalt porphyrins was described, with all eight of the radical ligands showing association to the cobalt (II) centre of the respective porphyrins. In Chapter 4, the study was extended to investigate the coordination of dithiadiazolyl radicals to a series of metalated tetraphenylporphyrins. UV-Vis and EPR spectroscopy confirmed that the two dithiadiazolyl radicals investigated could coordinate to copper (II), zinc (II) and iron (III) tetraphenylporphyrins. Having shown that dithiadiazolyl radicals could successfully coordinate to porphyrins with different metals and different peripheral substituents, attention turned to investigating if these radical ligands would interact with a porphyrin of biological origin, namely haematin (aqua/hydroxo-ferriprotoporphyrin IX), in order to illustrate a potential application of these dithiadiazolyl complexes to the understanding of haem chemistry and the treatment of malaria. These dithiadiazolyl ligands also represent a new class of heterocyclic sulfur-based ligands, which are uncommon in the literature for iron porphyrins.

Haemoglobin, the metalloprotein responsible for oxygen transfer in the red blood cells of vertebrates, consists of four protein subunits, each with an associated haem molecule.[1] The structure of haem B, the most common form of biologically occurring haem, is shown in Figure 5.1 and consists of a protoporphyrin IX macrocycle complex with an iron (II) centre. This Fe^{2+} ion is capable of coordinating diatomic oxygen, forming an Fe^{3+} complex. If haem is oxidised to haematin (Figure 5.1), an iron (III) complex, it is unable to coordinate diatomic oxygen and cannot perform its biological function. This oxidation of haem can occur as a by-product of haemoglobin digestion by parasites.[2]

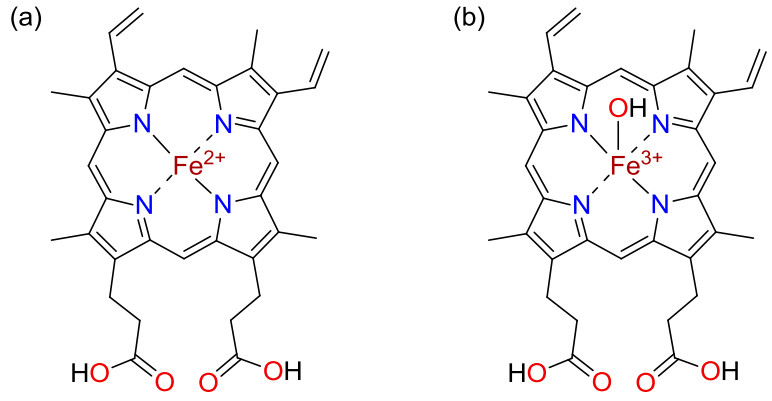

Figure 5.1: The molecular structure of (a) haem B and (b) haematin. The protoporphyrin IX macrocycle has four methyl, two vinyl and two propionic side chains attached to the pyrrole units. Haematin is an iron (III) protoporphyrin IX with a hydroxide axial ligand.

Malaria is a parasitic disease caused by *Plasmodium* protozoa, the most widespread of which is *Plasmodium falciparum*.[3] Approximately 3.2 billion people, almost half the global population, are at risk of contracting malaria, the largest proportion residing in Africa.[3] Preventative measures combined with chemotherapeutic treatments have made great strides in decreasing mortality rates: for example, the African region has seen mortality from malaria fall 66 % across all age groups since 2000.[3] However, lack of access to treatment and preventative measures still presents a significant challenge. Additionally, widespread resistance to previously-successful drug therapies is increasing.[3] Efforts to overcome this problem focus on better understanding the mechanisms of drug activity and resistance, as well as developing new drug derivatives that potentially bypass resistance pathways.

The malaria parasite *P. falciparum* has a complex lifecycle which takes place both in female *Anopheles* mosquitos, as the primary host, and in humans, as the secondary host. Within an infected human host, the parasite has a life cycle phase in the liver and a phase in the blood, particularly in the red blood cells, which is the phase responsible for the symptoms of malaria.[4–6] Parasites inside red blood cells digest haemoglobin, utilising the subunit proteins as a source of peptides and amino acids. The unwanted iron (II) protoporphyrin IX (also known as haem, see structure in Figure 5.1) is readily oxidised in the acidic environment of the digestive vacuole to form iron (III) protoporphyrin IX (Fe(III)PPIX, also known as haematin, see structure in Figure 5.1), with either a hydroxide or aqua axial ligand (depending on the pH). This free haematin is toxic as a result of the redox-active iron (III) centre, capable of generating reactive oxygen species and causing membrane damage.[7] Subsequently, the parasite has evolved to minimise the threat through the biocrystallisation of haematin into inert crystals, known as haemozoin or malaria pigment.[2,8] Disrupting this process leads to haem toxicity and parasite death; consequently many successful antimalarial drugs work by inhibiting the formation

of haemozoin.[7] While the exact mechanism of action for many antimalarial drugs is still unknown, hypotheses include the formation of complexes between haematin and the drug.[9–13] For some of these drugs, for example quinine and quinidine, drug-haem complexes have been synthesised and the crystal structures have been determined, confirming coordination between the drugs and iron protoporphyrin IX (Figure 5.2).[14] The formation of these complexes is thought to inhibit the incorporation of Fe(III)PPIX into crystalline haemozoin.

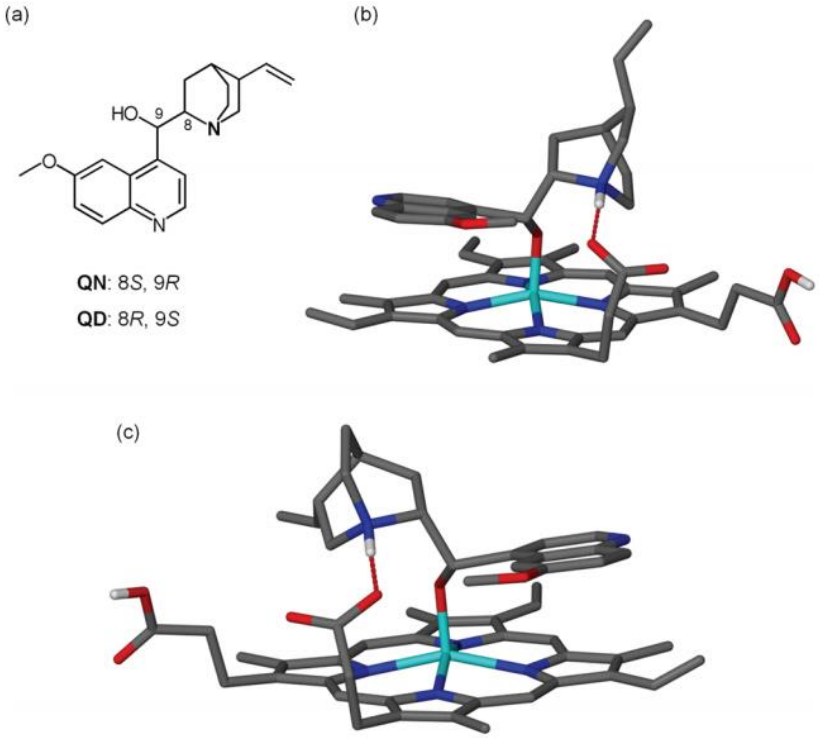

Figure 5.2: (a) Structures of the Cinchona alkaloid antimalarial compounds quinine (QN) and quinidine (QD). (b) The asymmetric unit of QN-Fe(III)PPIX and (c) the asymmetric unit of QD-Fe(III)PPIX. Hydrogen bonds shown as dashed red lines. Non-relevant hydrogen atoms are removed for clarity. Atom color: C, gray; H, white; N, blue; O, red; and Fe, cyan. (Figure from reference 14.)

In addition to the *Plasmodium* species parasites, other parasites that feed off of haemoglobin have also been observed to detoxify haem through crystallisation into haemozoin, including parasitic flatworms such as *Schistosoma mansoni*[15] and the blood-feeding insect *Rhodnius prolixus*.[16]

Biological studies of dithiadiazolyl metal complexes are currently very limited. Platinum dithiadiazolyl complexes, with similar square-planar coordination geometry to cisplatin, have been tested as anticancer agents against ovarian tumour cell lines. A PhDTDA-platinum complex was active against the tested cell lines, but further investigation showed poor selectivity, meaning the complex was toxic to all cells.[17] There are currently no examples in the literature of dithiadiazolyl radicals interacting directly with a biologically-occurring metal source.

Haematin appeared to be an attractive target for a preliminary investigation into the interaction between dithiadiazolyl radicals and biologically-occurring porphyrins, particularly considering the success with iron (III) tetraphenylporphyrin chloride in Chapter 4. The study of ligand coordination to metalloporphyrins is important to better understand the processes involved biologically with haem. To study the interaction between dithiadiazolyl radicals and haematin, two of the previously studied dithiadiazolyl radicals were used, *p*-PyrDTDA (**R1**) and PhDTDA (**R2**) (Figure 5.3).

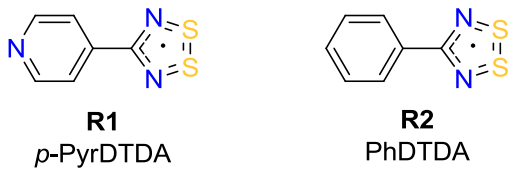

Figure 5.3: Structures of the two dithiadiazolyl radicals used in this study

5.2 Dithiadiazolyl radicals and haematin

5.2.1 Spectrophotometric titrations

The UV-vis spectrum of haematin in dichloromethane (DCM) is dominated by a broad, domed Soret band at 395 nm, with Q bands at 508, 545 and 639 nm.

Spectrophotometric titrations of haematin with *p*-PyrDTDA (**R1**) and PhDTDA (**R2**) were performed as described in previous chapters. The spectra for the titration of haematin with **R1** or **R2** in DCM are shown in Figure 5.4.

Addition of **R1** to haematin results in the Soret band at 395 nm decreasing in intensity for the initial ligand additions. Thereafter, the absorption intensity at 402 nm steadily increases until a narrow peak develops. Changes in the Q-band region are not well defined. Similarly, addition of **R2** to haematin initially decreases the broad Soret at 395 nm before a narrow band at 402 nm evolves. Neither

experiment displays distinct isosbestic points throughout the titration, suggesting a multi-step process is most likely occurring.

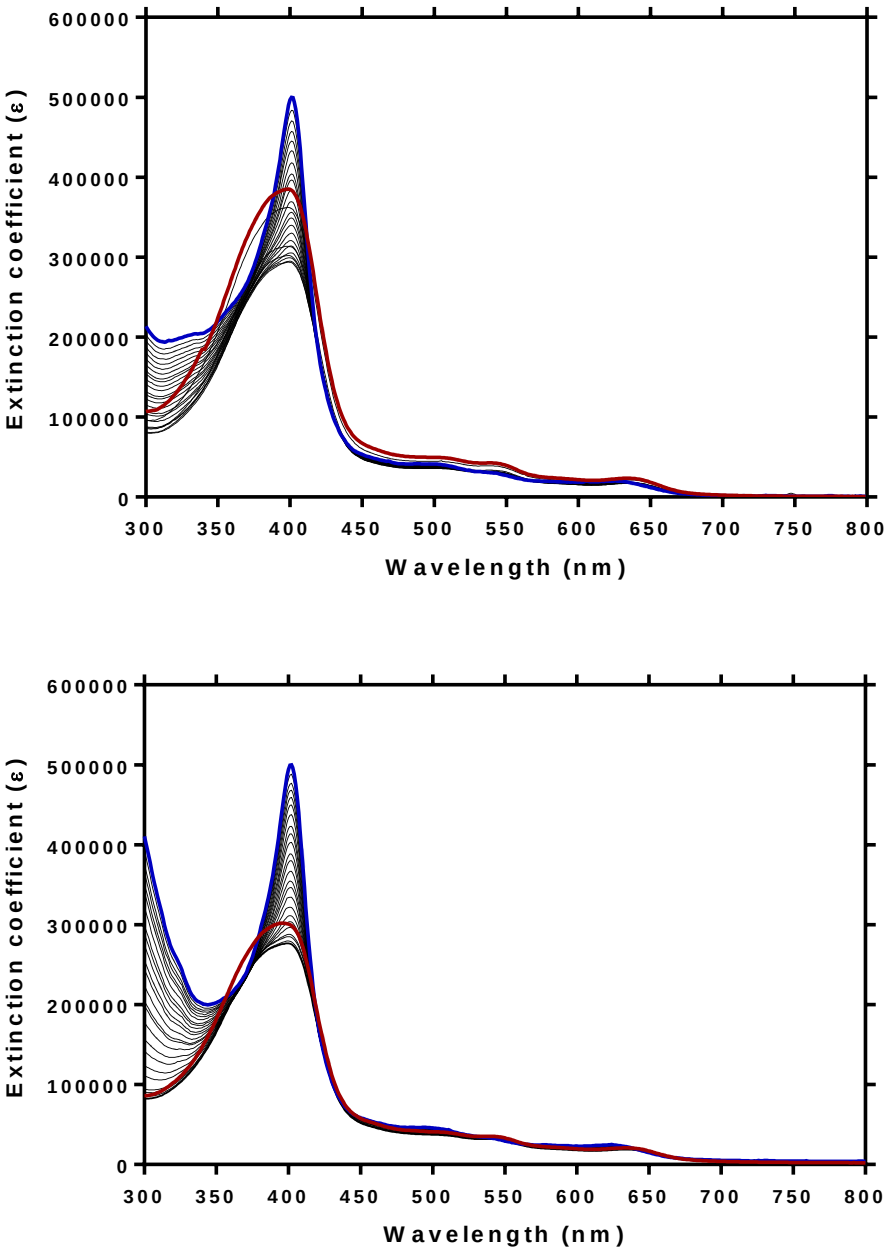

*Figure 5.4: UV-Vis spectrophotometric titration for haematin (**P8**) in DCM with increasing* p-*PyrDTDA (**R1**, top) and PhDTDA (**R2**, bottom) concentration, forming **R1•P8** and **R2•P8** respectively. The original haematin spectrum is shown in red. The final addition of dithiadiazolyl is shown in blue with intermediate additions shown in black. Titration spectra have been corrected for dilution.*

5.2.2 Association constants

The spectroscopic data from the spectrophotometric titrations were analysed and a binding model was fitted using HypSpec.[18] Both dithiadiazolyl radicals investigated showed 1:1 ligand-to-metal association to haematin. Spectrophotometric titrations were performed in triplicate and the association constant, logβ, was calculated for each titration. The average of these results was determined (Table 5.1).

Table 5.1: Association constants for dithiadiazolyl radicals coordinating to haematin (DCM, 25 °C)

	Dithiadiazolyl Ligand	Average logβ with Haematin
R1	*p*-PyrDTDA	3.07 ± 0.15
R2	PhDTDA	2.88 ± 0.07

For the association of *p*-PyrDTDA to haematin, the process has a logβ value of 3.07 ± 0.15. For PhDTDA, an association constant of 2.88 ± 0.07 could be determined, comparable to that of *p*-PyrDTDA (within 3 standard deviations).

To place these values in context, a spectrophotometric titration was performed with haematin and chloroquine (structure of chloroquine shown in Figure 5.5, spectra shown in Figure 5.6). Chloroquine is a widely-used antimalarial drug that is known to associate to haematin through π-stacking.[19,20] Under the same conditions as for those with the dithiadiazolyl radicals, the logβ value for chloroquine binding to haematin was determined as 5.31 ± 0.04.

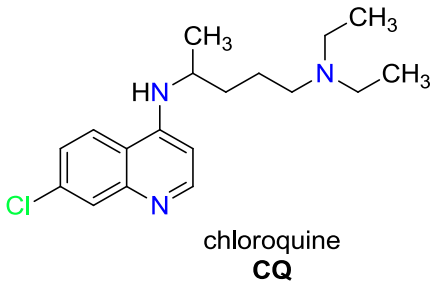

*Figure 5.5: Structure of chloroquine (**CQ**).*

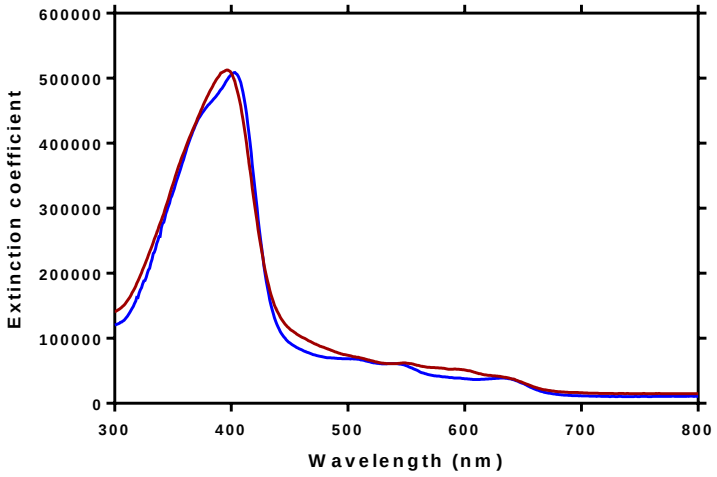

*Figure 5.6: UV-Vis spectrophotometric titration for haematin (**P8**) in DCM with increasing chloroquine (**CQ**) concentration, forming **CQ•P8**. The original haematin spectrum is shown in red. The final addition of chloroquine is shown in blue. Titration spectra have been corrected for dilution.*

5.3 Summary and Conclusions

The interaction between two dithiadiazolyl radicals and the biologically-relevant metalloporphyrin haematin was studied in solution through the use of UV-Vis spectroscopy. UV-Vis spectrophotometric titrations were carried out to assess if the relevant dithiadiazolyl radical – haematin complexes would form in solution. From this data, the association constant was determined. A summary of the association constants found is shown in Table 5.2.

For the association of *p*-PyrDTDA to haematin, the reaction has a logβ value of 3.07 ± 0.15. For PhDTDA, an association constant of 2.88 ± 0.07 could be determined, comparable to that of *p*-PyrDTDA (within 3 standard deviations). For both dithiadiazolyl radicals, a 1:1 ligand to haematin model was the best fit. These values are within an order of magnitude of those obtained with the synthetic model compound, iron (III) tetraphenylporphyrin chloride (3.73 ± 0.09 for **R1** and 2.39 ± 0.12 for **R2**) (see Chapter 4), indicating that the FeTPPCl was a good model for haem, as it was successful in predicting possible coordination to the more complex biological porphyrin.

*Table 5.2: Association constants for ligands **R1**, **R2** and **CQ** coordinating to porphyrin **P8***

Ligand		logβ values with Haematin (P8)
R1	*p*-PyrDTDA	3.07 ± 0.15
R2	PhDTDA	2.88 ± 0.07
CQ	Chloroquine	5.31 ± 0.04

In an analogous manner, the reaction of chloroquine and haematin in dichloromethane was investigated and a logβ value of 5.31 ± 0.04 was determined, again with a 1:1 ligand to haematin model. Chloroquine is a known inhibitor of haematin crystallisation and interacts strongly with the metalloporphyrin, as evident from the relatively high association constant. The association constants for the dithiadiazolyl radicals are two orders of magnitude lower than for that of chloroquine, indicating they interact more weakly with haematin. Nevertheless, there is evidence that both *p*-PyrDTDA and PhDTDA associate with haematin to form **R1•P8** and **R2•P8** respectively. The exact structure of these complexes is currently unknown. The spectroscopic changes observed when haematin is titrated with either dithiadiazolyl ligand differ visually from those observed with chloroquine, which is known to π -stack to haematin but not directly coordinate. In order to provide a direct comparison to the results seen for the synthetic porphyrins, the titrations were performed in dichloromethane. However, improved results may be obtained in acetonitrile, which is more commonly used for haematin systems.[14]

Based on what can be observed for **R1•P1**, it is possible that **R1•P8** and **R2•P8** form the same sulfur – metal bond between the radical and the metalloporphyrin, however structural studies would need to be carried out to confirm this. It is work noting that haematin contains acidic carboxylic acid and metal hydroxide groups, and that previous work in the literature has shown that Fe(II) dithiadiazolyl complexes form solution decomposition products where hydroxide groups add across the sulfur-nitrogen dithiadiazolyl bond.[21] Further work is needed to study the stability of these complexes as well as any potential magnetic behaviour or biological activity. Dithiadiazolyl radicals are moisture sensitive, which limits their potential as effective drug molecules, however the metal complexes appear to be far more stable than the uncoordinated radicals (see Chapter 2). The interaction of these sulfur-nitrogen heterocycles with haematin is interesting, as heterocyclic sulfur atoms have previously been computationally linked to poor antimalarial activity.[22] These dithiadiazolyl complexes show potential for the development of related sulfur-based ligands for haematin in the future.

5.4 Experimental details

5.4.1 Synthesis of dithiadiazolyl radicals **R1** and **R2**

The synthesis of 4-(4′-pyridyl)-1,2,3,5-dithiadiazolyl (**R1**) and 4-phenyl-1,2,3,5-dithiadiazolyl (**R2**) was previously described in Chapter 2 and Chapter 3 respectively.

5.4.2 Haematin (Fe(III)PPIX, **P8**)

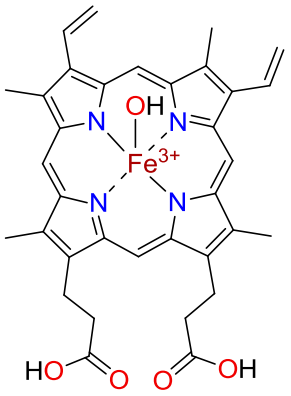

hematin
P8

Porcine haematin (**P8**) was purchased from Sigma-Aldrich and used without further purification or processing.

Haematin is known to adsorb onto glass surfaces.[23] All glassware exposed to haematin was soaked in 0.1 M sodium hydroxide, washed extensively with water, soaked in 0.1 M HCl to neutralise the glass and rinsed with water again to ensure complete removal of haem. Haematin stock solutions were prepared in previously unused glassware.

5.4.3 Free base chloroquine (**CQ**)

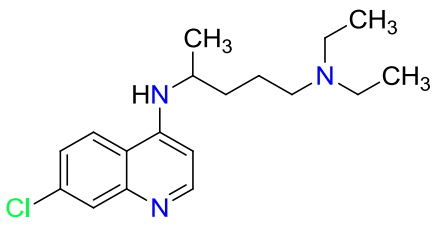

chloroquine
CQ

Chloroquine was purchased from Sigma-Aldrich as a diphosphate salt. Free-base chloroquine was obtained by treating with dilute sodium hydroxide and extracting the free base with dichloromethane.

5.4.4 UV-Vis spectrophotometric titrations

All glassware, except microsyringes, was dried in a 120 °C oven overnight. All solvents were dried over 3 Å molecular sieves. Microsyringes were flushed three times with clean, dry solvent and three times with the solution of interest before being used.

A fresh 2 mM stock solution of the dithiadiazolyl radical was made up in a 5 mL volumetric flask prior to each experiment using a 9:1 dichloromethane : dimethylsulfoxide solvent system. The flask was flushed with nitrogen for 1 minute before being sealed with a septum and paraffin laboratory film. A 1 mM stock solution of haematin was made up in a screw-cap glass vial using dimethylsulfoxide. A 2 mM stock solution of free base chloroquine was made up in a screw-cap glass vial using dichlormethane.

A 2mM working solution of the porphyrin was made up in a quartz cuvette with 1996 µL dichloromethane (measured by micropipette) and 4 µL of the porphyrin stock solution (measured by glass Hamilton microsyringe). A 2000 µL portion of dichloromethane was placed in the reference cuvette (measured by micropipette).

Both cuvettes, with their lids, were placed in the UV-vis spectrophotometer and allowed to equilibrate to 25 °C before the spectrum was collected between 300 and 800 nm.

Aliquots of the dithiadiazolyl stock solution were added to both the working solution cuvette and the reference solution cuvette using a glass Hamilton microsyringe. The solutions were stirred with a wire microsyringe plunger and the lids replaced. The spectrum was collected after each addition. This was continued until a total of 420 µL of the dithiadiazolyl solution was added.

In the time frame necessary to collect the wider spectral range (300 – 800 nm) for the titrations in triplicate, the concentration of the dithiadiazolyl stock solution could not be considered consistent; consequently a fresh dithiadiazolyl stock solution was prepared for each titration experiment.

Spectrophotometric titrations of haematin were performed by the addition of 4 × 5 µL followed by 20 × 20 µL aliquots of ligand stock solution (total volume 420 µL) to both sample and reference. The spectrophotometric titration performed in triplicate for each radical – porphyrin pair.

Titrations using chloroquine as the ligand were performed in the same manner as those with the dithiadiazolyl radicals.

For the visual representation of the spectra, data were normalised and a dilution correction was performed for each data set as previously described. Association constants (logβ values) were calculated in HypSpec using a 2-reagent model with a 1:1 molar ratio. The average logβ of each three identical spectrophotometric titrations was reported. All logβ values are given Table 5.3 (for **P8**).

*Table 5.3: All log values for Haematin (**P8**) and dithiadiazolyls **R1** and **R2***

Ligand		logβ values with Haematin (P8)			
		1	**2**	**3**	**Average**
R1	*p*-PyrDTDA	3.22	2.92	3.08	3.07 ± 0.15
R2	PhDTDA	2.93	2.80	2.90	2.88 ± 0.07
CQ	Chloroquine	5.31	5.34	5.27	5.31 ± 0.04

5.5 References

(1) Perutz, M. F.; Rossmann, M. G.; Cullis, A. N. N. F.; Muirhead, H.; Will, G.; North, A. C. T. *Nature* **1960**, *185* (4711), 416.

(2) Egan, T. J. *Mol. Biochem. Parasitol.* **2008**, *157* (2), 127.

(3) World Health Organisation. *World Malaria Report*; 2015.

(4) Wirth, D. F. *Nature* **2002**, *419* (6906), 495.

(5) Frederich, M.; Dogne, J.-M.; Angenot, L.; De Mol, P. *Curr. Med. Chem.* **2002**, *9* (15), 1435.

(6) Ashley, E.; McGready, R.; Proux, S.; Nosten, F. *Travel Med. Infect. Dis.* **2006**, *4* (3), 159.

(7) Ursos, L. M. B.; Roepe, P. D. *Med. Res. Rev.* **2002**, *22* (5), 465.

(8) Egan, T. J.; Combrink, J. M.; Egan, J.; Hearne, G. R.; Marques, H. M.; Ntenteni, S.; Sewell, B. T.; Smith, P. J.; Taylor, D.; van Schalkwyk, D. A.; Walden, J. C. *Biochem. J.* **2002**, *365* (2), 343.

(9) Warhurst, D. C. *Biochem. Pharmacol.* **1981**, *30* (24), 3323.

(10) Blauer, G. *Biochem. Int.* **1988**, *17* (4), 729.

(11) Sugioka, Y.; Suzuki, M. *Biochim. Biophys. Acta* **1991**, *1074* (1), 19.

(12) Adams, P. A.; Berman, P. A.; Egan, T. J.; Marsh, P. J.; Silver, J. *J. Inorg. Biochem.* **1996**, *63* (1), 69.

(13) Egan, T. J.; Mavuso, W. W.; Ross, D. C.; Marques, H. M. *J. Inorg. Biochem.* **1997**, *68* (2),

137.

(14) de Villiers, K. A.; Gildenhuys, J.; le Roex, T. *ACS Chem. Biol.* **2012**, *7* (4), 666.

(15) Chen, M. M.; Shi, L.; Sullivan, D. J. J. *Mol. Biochem. Parasitol.* **2001**, *113* (1), 1.

(16) Oliveira, M. F.; Silva, J. R.; Dansa-Petretski, M.; de Souza, W.; Lins, U.; Braga, C. M. S.; Masuda, H.; Oliveira, P. L. *Nature* **1999**, *400* (6744), 517.

(17) Banister, A. J.; Gorrell, I. B.; Howard, J. A. K.; Lawrence, S. E.; Lehman, C. W.; May, I.; Rawson, J. M.; Tanner, B. K.; Gregory, C. I.; Blake, A. J.; Fricker, S. P. *J. Chem. Soc. Dalt. Trans. Inorg. Chem.* **1997**, No. 3, 377.

(18) Hyp Spec, Protonic Software, Leeds, England.

(19) Buller, R.; Peterson, M. L.; Almarsson, Ö.; Leiserowitz, L. *Cryst. Growth Des.* **2002**, *2* (6), 553.

(20) de Dios, A. C.; Tycko, R.; Ursos, L. M. B.; Roepe, P. D. *J. Phys. Chem. A* **2003**, *107* (30), 5821.

(21) Hearns, N. G. R.; Fatila, E. M.; Clérac, R.; Jennings, M. C.; Preuss, K. E. *Inorg. Chem.* **2008**, *47* (22), 10330.

(22) Wicht, K. J.; Combrinck, J. M.; Smith, P. J.; Egan, T. J. *Bioorganic Med. Chem.* **2015**, *23* (16), 5210.

(23) de Villiers, K. A.; Kaschula, C. H.; Egan, T. J.; Marques, H. M. *J. Biol. Inorg. Chem.* **2007**, *12* (1), 101.

Chapter 6

Summary and proposals for future work

The aim of this study was to synthesize and investigate dithiadiazolyl radical – metalloporphyrin complexes in terms of their structural properties and coordination behaviour. Thiazyl radicals have been investigated as potential building blocks for the design of magnetic and conductive molecular materials.[1–3] An example of this class of organic radicals, the 1,2,3,5-dithiadiazolyl radicals are being investigated for their unusual properties.[3,4] A selection of dithiadiazolyl radicals have been shown to display magnetic behaviour in the solid state, however, the vast majority unfortunately dimerise in the solid state through π-π stacking which leads to loss of paramagnetism.[4] Consequently, the focus of most current research attempts to disrupt this dimerization, to direct the arrangement of the molecules in the solid state through crystal engineering or to investigate dithiadiazolyl metal complexes.[4,5] The work presented in this thesis describes the use of metalloporphyrins in forming novel dithiadiazolyl metal complexes with interesting coordination and redox behaviour.

6.1 Summary

Chapter 1 introduced the chemistry of dithiadiazolyl radicals, starting with an outline of the history of dithiadiazolyls, the structure of dithiadiazolyl radicals and the potential different dithiadiazolyl isomers. The general methods of synthesis of dithiadiazolyl radicals were described. The conductive and magnetic properties of dithiadiazolyl radicals, as well as the oxidation (to dithiadiazolylium cations) and reduction (to dithiadiazolyl anions) of dithiadiazolyl radicals was discussed. A brief overview of the dithiadiazolyl metal complexes currently found in the literature was given. Dithiadiazolyls have previously been observed coordinating to metals in several binding modes. The most common example in recent literature is coordination through one of the dithiadiazolyl nitrogens, usually through bidentate coordination with an adjacent *ortho*-pyridyl nitrogen with electron-withdrawing hexafluroacetylacetanoato-ligands to ensure coordination to the hard nitrogen atom rather than the softer sulfur atoms. Alternatively, both dithiadiazolyl sulfur atoms can coordinate to a metal centre, typically with simultaneous breaking of the sulfur-sulfur bond, although in some cases there is retention of the sulfur-sulfur bond. While some metal complexes are paramagnetic as a result of spin-pairing with the metal centre or through intermolecular dimerization, some are diamagnetic. A

brief introduction to the history, structure and synthesis of porphyrins and metalloporphyrins was outlined. The origin and complexities of UV-Vis spectra of porphyrins and metalloporphyrins was discussed. Literature precedent for the use of metalloporphyrins as supramolecular scaffolds was presented.

Chapter 2 presented the first example of a dithiadiazolyl-metalloporphyrin complex formed from *p*-PyrDTDA (**R1**) and CoTPP (**P1**). The complex crystallizes as a coordination polymer, **R1•P1(THF)**, with each dithiadiazolyl radical bridging two cobalt porphyrins. The dithiadiazolyl coordinates to one cobalt porphyrin through the pyridyl nitrogen, and coordinates to the next metalloporphyrin with a cobalt-sulfur bond. This is of particular interest as it is the first example of a dithiadiazolyl molecule coordinating to a metal through a single sulfur atom with an intact heterocyclic ring. The sulfur-sulfur bond, while intact, is unusually long at 2.121 Å, 0.032 Å longer than the average S – S bond length for dithiadiazolyl radicals and 0.019 Å than the longest bond length previously reported. It is proposed that this unusually long bond is as a result of delocalisation of the unpaired electron from the $3dz^2$ orbital of the Co(II) ion to the singly occupied molecular orbital (SOMO) of the dithiadiazolyl radical, as this orbital is antibonding with respect to the S – S bond. The result of this electron transfer is oxidation of the Co(II) centre to a Co(III) centre with associated reduction of the dithiadiazolyl radical to a dithiadiazolide anion. This is noteworthy as examples of dithiadiazolide anions are highly limited as a result of the poor stability of these anions. Only two examples of dithiadiazolyl anions that have been successfully isolated are reported in the literature: one in the form of an unstable salt and one stabilised by macrocyclic encapsulation. From the crystal structure data, it appears that this electron transfer is partial, with the coordination polymer representing a resonance hybrid of the Co(II)-dithiadiazolyl and Co(III)-dithiadiazolide moieties. The solution speciation of **R1•P1** was discussed in detail in Chapter 2. Upon dissolution of **R1•P1(THF)**, it appears that the sulfur-cobalt bond is the most labile, with the nitrogen-bound species **N- R1•P1** being the predominant species in solution. This species has the oxidised Co(III) centre and is diamagnetic, confirming reduction to the dithiadiazolide anion. In dimethylsulfoxide, a known coordinating solvent, **N-R1•P1(DMSO)** forms. However, when **R1** and **P1** are combined in solution, the thermodynamically-favoured sulfur-bound species **S-R1•P1** forms instead. Oligomerisation of this complex leads to formation of the coordination polymer. The formation of this complex was studied through UV-Vis spectrophotometry and a logβ of 4.19 ± 0.05 at 25 °C was determined. A thermodynamic study of the formation of **S-R1•P1** was also performed.

In **Chapter 3**, the formation of a range of complexes with dithiadiazolyl radicals and cobalt porphyrins was discussed, and the influence of different substituents on either the dithiadiazolyl or the

cobalt porphyrin was probed. A total of eight dithiadiazolyl radicals were investigated. The association of the eight dithiadiazolyls to **P1** was studied by means of UV-Vis spectrophotometry, with 1:1 ligand-to-metalloporphyrin coordination being observed for ligands **R2** to **R8** as for **R1**. Based on the similarity in association constants found for the eight ligands, and with the knowledge that **R1** forms the sulfur-bound complex in solution, it is proposed that all the ligands investigated form the sulfur-bound complexes in solution. The highest association constant was found for **R6**, with the lowest found for **R5**. Following the success of forming dithiadiazolyl radical complexes with CoTPP, the coordination of all eight dithiadiazolyls to the perfluorinated CoTFP (**P2**) was discussed. Association constants for the eight dithiadiazolyl radicals are significantly higher with CoTFP than with CoTPP. To establish if the presence of electron-donating methyl substituents on the porphyrin periphery would reverse the trend seen for **P2**, the same series of experiments was performed with cobalt tetratolylporphyrin (CoTTP, **P3**). As hypothesised, the association constants determined with **P3** are lower than those found for **P1** and **P2**. Again, there was relatively little difference in the association constants between the different dithiadiazolyl radicals. To confirm that the substituents on the dithiadiazolyl radical have a relatively minor influence on the electron density at the coordinating sulfur, electrostatic potential maps were generated for the eight dithiadiazolyl ligands and the electrostatic potential and partial charge at the sulfur atoms was determined. Differences in the association constants may result from electrostatic interactions between the dithiadiazolyl radical and the porphyrin molecule itself. Attempts to obtain pure solid-state material of these coordination compounds, beyond **R1•P1(THF)**, were unsuccessful.

Chapter 4 expanded the study of the interaction between dithiadiazolyl radicals and metalloporphyrins in solution to include a range of alternative metal ions. In addition to the d^7 Co(II)TPP, d^9 Cu(II)TPP (**P4**) and d^{10} Zn(II)TPP (**P5**) were investigated. As a simple model for chlorophyll, Mg(II)TPP (**P6**) was used, with Fe(III)TPPCl used as a model for haematin. Two of the previously used dithiadiazolyl radicals, **R1** and **R2**, were added to each of these porphyrins and the interaction was studied through the use of UV-Vis spectroscopy and EPR spectroscopy. From the UV-Vis spectrophotometric titrations, association constants could be determined. **P4** and **P7** displayed association constants one order of magnitude lower than that of **P1,** and **P5** showed association constants two orders of magnitude higher than that of **P1** for both **R1** and **R2**. No appreciable association was observed for **P6**. EPR spectroscopic titrations showed that the complexes formed between **R1** and **R2** with **P1**, **P4** and **P7** were diamagnetic, possibly as a result of spin pairing between the paramagnetic metal centre and the dithiadiazolyl radical. It appears that the complexes formed with **P5** are paramagnetic at low concentration, but that these complexes dimerise at higher concentrations, most likely through dithiadiazolyl pancake bonding. Rationalisation of the trends in association constants is difficult, however it does appear that coordination through the soft sulfur

ligand is favoured with larger, softer metal centres. Future work should focus on attempting to obtain crystalline material of these different complexes to study their magnetic behaviour in the solid state.

Finally, **Chapter 5** discussed the association of dithiadiazolyl radicals **R1** and **R2** to haematin (**P8**). Haematin is the metalloporphyrin responsible for oxygen transfer in red blood cells in vertebrates, as part of the metalloprotein haemoglobin. A brief outline of the role of haematin and haemoglobin in diseases caused by blood-feeding parasites such as *Plasmodium falciparum*, the malaria parasite, was given. Both **R1** and **R2** were shown though UV-Vis spectroscopy to associate to **P8**, with association constants in the same order of magnitude as for the model compound **P7.** However the interaction was significantly weaker than for chloroquine, a common antimalarial drug that is known to π-stack to haematin.

6.2 Future work

This work presented in this thesis represents the first known examples of dithiadiazolyl-metalloporphyrin complexes and opens up a vast array of potential avenues for future work. The coordination of the dithiadiazolyl radicals through a single sulfur atom to the metal centre is a novel binding mode for dithiadiazolyl radicals. This new type of bond opens up a new field of dithiadiazolyl coordination chemistry with the potential for new complexes with interesting properties. Additionally, the dithiadiazolide anion present in **R1•P1(THF)** and **N- R1•P1** is only the third example of a dithiadiazolyl anion that has been isolated. The dithiadiazolide appears to be remarkably stable, which is highly unusual. When the dithiadiazolyl first coordinates to the porphyrin, as in **S-R1•P1**, there is a clear interaction between the dithiadiazolyl unpaired electron and an unpaired electron on the metal. The two different coordination species found in solution could show different behaviours.

One thing that remains to be determined is if the electron transfer, which oxidises Co(II) to Co(III) while reducing the dithiadiazolyl, occurs after coordination or only after oligomerisation occurs. One way to establish this would be through the use of ^{59}Co NMR spectroscopy to follow the progress of the reaction between CoTPP and *p*-PyrDTDA. This would give insight into when the electron transfer takes place: on complex formation, or on oligomerisation.

It is clear that there is some interesting redox behaviour at work for the **R1•P1** system. Measurements of the redox behaviour of the system need to be carried out. Cyclic voltammetry will be an invaluable

tool for studying the redox potentials of these complexes. If the electron transfer is only happening following polymerisation, the result is a cobalt-dithiadiazolyl-cobalt chain with the potential for electron transfer along the chain. The resulting material is potentially directionally conductive. Studying this conductivity would present some practical challenges, particularly in terms of obtaining large enough crystals to study any potential conductivity. Introducing changes to the periphery of the porphyrin to increase intermolecular interactions between polymer chains may increase the rigidity of the material to template a more robust crystalline material.

The sulfur-bound coordination of the dithiadiazolyls to the cobalt porphyrins is noteworthy because coordination of heterocyclic sulfur-based ligands to metallo-tetraphenylporphyrins is rare. A search in the Cambridge Structural Database[6] for metallo-tetraphenylporphyrins with sulfur-donor ligands gave mainly thioether ligands coordinated to MTPPs (including CoTPP), with the few examples of neutral heterocyclic sulfur ligands being coordinated to FeTPP. Examples of sulfur ligands coordinating to the biological cobalt porphyrin, Vitamin B12, are also typically thiol ligands. With regards to N-S ligands, such as thiocyanate (NCS), coordination appears to always happen through the nitrogen atom to the metalloporphyrin. Somehow, the sulfur atom in dithiadiazolyl radicals is behaving differently to other sulfur atoms, which warrants further investigation.

The zinc complexes studied in this work show association at high concentration, presumably through pancake bonding between the paramagnetic dithiadiazolyl ligands. Altering the porphyrin periphery, to encourage intermolecular interactions, for example with carboxylate groups capable of hydrogen-bonding to each other, may encourage crystallization of the material, which would allow for the acquisition of solid-state evidence of this dimerization. Beer's Law studies should be performed for the remaining complexes to establish if similar dimerization occurs at high concentrations.

Additionally, in this study, dithiadiazolyl radicals have also been shown to associate to haematin, a biological porphyrin. While dithiadiazolyl radicals are moisture sensitive and consequently unlikely to make effective drug molecules, these metal complexes show potential for the development of related S-N based ligands for haematin in the future. The interaction of these sulfur-nitrogen heterocycles with haematin is interesting, as heterocyclic sulfur atoms have previously been computationally linked to poor antimalarial activity.[7] This work suggests that there is more to learn about these ligands. Dithiadiazolyl radicals could potentially be used as magnetic haematin sensors.

For the development of new dithiadiazolyl-metalloporphyrin complexes in the future, it is important to note that changing the substituents on the dithiadiazolyl radical has a limited effect on the strength of coordination, while changing the substituents on the porphyrin has a far greater effect. Weaker dithiadiazolyl coordination should be observed for porphyrins with electron-donating groups in comparison to porphyrins with electron-withdrawing groups. The choice of metal centre will affect the redox and magnetic behaviour of the system. The introduction of hydrogen-bonding functional groups, such as carboxylic acids, to the porphyrin may result in interesting intermolecular interactions. Expanding the study to include porphyrin-like macrocycles, such as phthalocyanines, is an alternative. Soft ionisation mass spectrometry may also be helpful to provide further evidence of these complexes, should solid-state material remain elusive. The use of cobalt together with a *para*-pyridyl dithiadiazolyl radical presents the greatest potential for coordination materials with interesting redox behaviour.

6.3 References

(1) Cordes, A. W.; Haddon, R. C.; Oakley, R. T. *Adv. Mater*. **1994**, *6*, 798.

(2) Rawson, J. M.; Palacio, F.; Veciana, J.; Editor. *Magnetic properties of thiazyl radicals, in: π-Electron Magnetism: From Molecules to Magnetic Materials*; Springer-Verlag, Berlin, 2001.

(3) Rawson, J. M.; Banister, A. J.; Lavender, I. *Adv. Heterocycl. Chem.* **1995**, *62*, 137.

(4) Haynes, D. A. *CrystEngComm* **2011**, *13* (15), 4793.

(5) Preuss, K. E. *Dalt. Trans.* **2007**, No. 23, 2357.

(6) Allen, F. H. *Acta Crystallogr*. **2002**, *B58*, 380.

(7) Wicht, K. J.; Combrinck, J. M.; Smith, P. J.; Egan, T. J. *Bioorganic Med. Chem.* **2015**, *23* (16), 5210.

Appendix A

Instruments and experimental procedures

7.1 Chemicals, solvents and synthetic procedures

All chemicals used in this investigation were purchased from Sigma-Aldrich. Chemicals were used without further purification, with the exception of pyrrole, which was freshly distilled prior to use. All glassware was oven-dried at 120 °C for 2 hours unless otherwise specified. Diethyl ether, tetrahydrofuran, dichloromethane and dimethylsulfoxide were dried over activated 3 Å molecular sieves in oven-dried glassware for 24 hours prior to use. Standard Schlenk techniques were employed where necessary. Low temperature reactions were performed in a Dewar using dry ice in acetone (–78 °C) or ice in water (0 °C).

7.2 Single crystal X-ray diffraction (SCD)

Suitable crystals for X-ray analysis were chosen for their morphology and ability to uniformly extinguish plane polarised light. The crystal was placed on a MiTeGen MicroMount in paratone oil. Intensity data were collected on a Bruker APEX DUO diffractometer equipped with Incoatec IμS Mo and Cu microfocus X-ray sources and an APEXII detector. The crystal was cooled to 1000 K under N_2 flow from an Oxford Cryosystems Cryostat (700 Series Cryostream Plum). APEX II software was used for data reduction. The crystal structure was solved using SHELXS-97[1] by direct methods and non-hydrogen atoms were refined anisotropically by means of full-matric least-squares calculations of F^2 by SHELXL-97. X-Seed[2,3] was used as a graphical interface for SHELX. Where possible, hydrogen atoms were placed in calculated positions through the use of riding models. Crystal structure images were generated using Mercury[4–6] and POV-Ray.[7]

7.3 Fourier transform infrared (FT-IR) spectroscopy

Infrared spectra were obtained using a Nexus Thermo-Nicolet Avatar 330 FT-IR instrument using a Smart Performer Zn/Se ATR attachment.

7.4 Electron paramagnetic resonance (EPR) spectroscopy

EPR spectra were recorded under ambient conditions using a Bruker EMXplus X-band EPR spectrometer (8 inch ER 072 magnet, 2.7 kW power supply, EMX-m40X microwave bridge, operating between 9.3 and 9.9 GHz) and a high sensitivity continuous-wave resonator.

7.5 ^{1}H and ^{59}Co nuclear magnetic resonance (NMR) spectroscopy

All ^{1}H and ^{59}Co nuclear magnetic resonance spectra were obtained using either a Varian Unity Inova 300 MHz spectrometer or a Varian Unity Inova 600 MHz spectrometer. Samples were run in deuterated chloroform ($CDCl_3$) or deuterated dimethylsulfoxide (DMSO-d_6). Chemical shifts (δ) are reported in ppm and are referenced relative to the residual solvent peak. Spectra were obtained at 25 °C.

7.6 Ultraviolet-visible (UV-Vis) spectroscopy

UV-Vis spectra were collected on a Shimadzu UV-1800 UV spectrophotometer fitted with a Shimadzu TCC-100 temperature controlled cell holder.

7.7 Powder X-ray diffraction

Powder X-ray diffraction was run on a Bruker D2 PHASER with Lynxeye 1-D detector and Ni-filtered Cu-Kα radiation (30 kV, 10 mA generator parameters; restricted by a 1.0 mm divergence slit and a 2.5° Soller collimator), with a 0.016° step width. Scans were between 5° and 35° 2θ. Samples were run on a zero-background holder and spun during data collection.

7.8 Graphing and data analysis

Graphing and data analysis was performed using GraphPad Prism 6.[8]

Appendix B

Determination of binding constant model

Spectrophotometric data were analysed in HypSpec.[9] To determine the association constant for the dithiadiazolyl-metalloporphyrin complex, a 1:1 ligand-to-metal binding model was employed. For comparison, the output data for a 1:1, 2:1 and 1:2 binding model applied to the reaction between *p*-PyrDTDA (**R1**) and CoTPP (**P1**) are shown below.

1:1 ligand-to-metal model

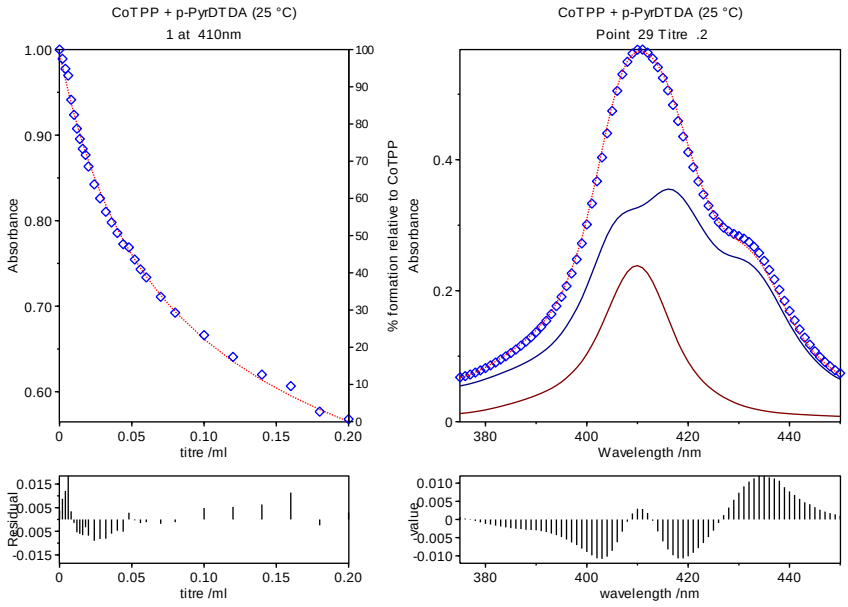

HypSpec refinement output. Version number 2.0.2

Project title CoTPP + p-PyrDTDA (25 °C)
Converged in 1 iterations with sigma = 3.4117E-03

CoTPPp-Pyr

Log beta value	standard deviation
4.1907	0.0036

2:1 ligand-to-metal model

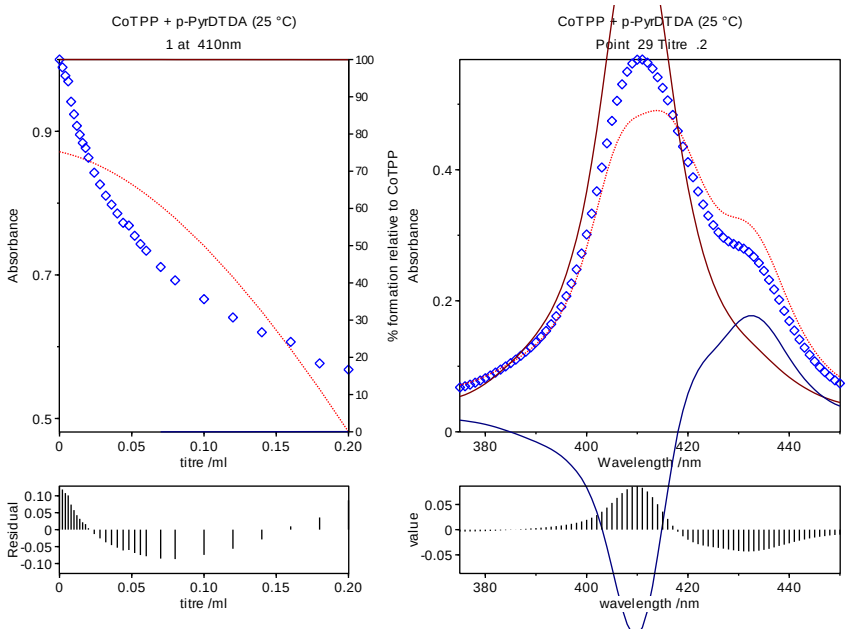

HypSpec refinement output. Version number 2.0.2

Project title CoTPP + p-PyrDTDA (25 °C)

Converged in 12 iterations with sigma = 0.025734

Negative molar absorbance found

Refinement results may erroroneous

CoTPPp-Pyr2

Log beta value	standard deviation
Not available	not available

1:2 ligand-to-metal model

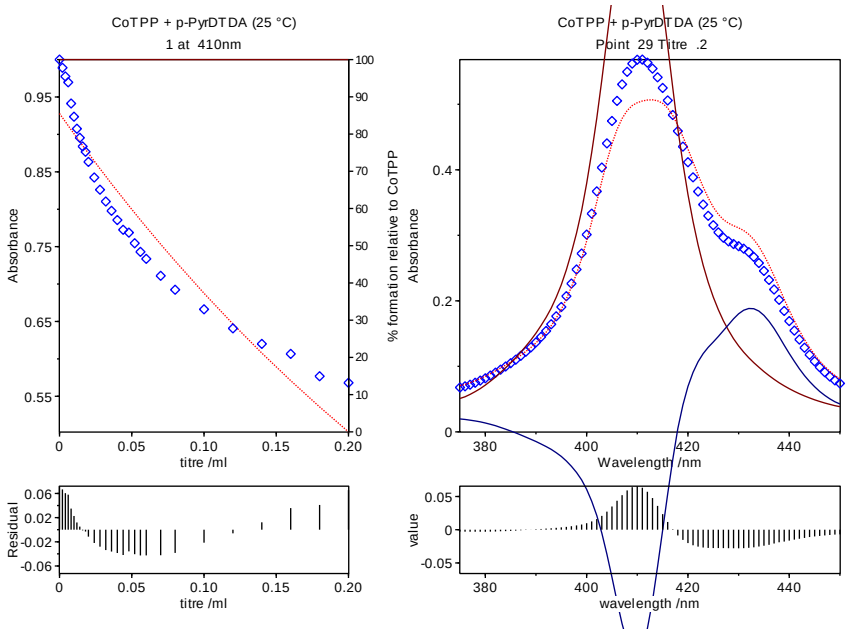

HypSpec refinement output. Version number 2.0.2

Project title CoTPP + p-PyrDTDA (25 °C)
Converged in 12 iterations with sigma = 0.025734

Negative molar absorbance found
Refinement results may erroroneous

CoTPP2p-Pyr	
Log beta value	standard deviation
4.58	not available

Thus, for this spectrophotometric titration of CoTPP + *p*-PyrDTDA, a logβ value of 4.19 was determined. The binding model was confirmed by curve-fitting with a 1:1 ligand-to-metal binding isotherm at 410 nm with CurveFit.[10]

Appendix C

Propagation of error

For logβ binding constants

$y = \log(a)$ where a = actual association value $(a \pm da)$

$$\frac{dy}{da} = 0.434 \times \frac{1}{a}$$

Get average $a \pm da$ value and determine y(avg) from a(avg), and get dy from:

$$dy = 0.434 \times \frac{da}{a}$$

Example: FeTPPCl + pPyrDTDA

$\log(a) = 3.66$ $a = 4570.88$

$\log(a) = 3.83$ $a = 6760.83$

$\log(a) = 3.71$ $a = 5128.61$

So $a(avg) = 5486.77 \pm 1138$

And $y(avg) = \log(a(avg)) = 3.74$ with $dy = 0.434 \times \frac{1138}{5486.77} = 0.09$

So for FeTPPCl + pPyrDTDA $\log\beta = 3.74 \pm 0.09$

For thermodynamic parameters

$$\Delta H = -\text{slope} \times R$$

$$\frac{\delta \Delta H}{\Delta H} = \sqrt{\left(\frac{\delta \text{slope}}{\text{slope}}\right)^2}$$

$$\delta \Delta H = \Delta H \times \left(\frac{\delta \text{slope}}{\text{slope}}\right)$$

where δslope is the uncertainity in the slope and δΔH is the uncertaintiy in ΔH.

And

$$\Delta S = \text{intercept} \times R$$

$$\frac{\delta \Delta S}{\Delta S} = \sqrt{\left(\frac{\delta \text{intercept}}{\text{intercept}}\right)^2}$$

$$\delta \Delta S = \Delta S \times \left(\frac{\delta \text{intercept}}{\text{intercept}}\right)$$

where δintercept is the uncertainity in the intercept and δΔS is the uncertaintiy in ΔS.

Appendix References

(1) Sheldrick. *Acta Crystallogr. Sect. A* **2008**, *64*, 112–122.

(2) Barbour, L. J. *J. Supramol. Chem.* **2003**, *1*, 189–191.

(3) Atwood, J. L.; Barbour, L. J. *Cryst. Growth Des.* **20003**, *3*, 3.

(4) Bruno, I. J.; Cole, J. C.; Edgington, P. R.; Kessler, M.; Macrae, C. F.; McCabe, P.; Pearson, J.; Taylor, R. *Acta Crystallogr. Sect. B* **2002**, *58* (3 Part 1), 389–397.

(5) Macrae, C. F.; Edgington, P. R.; McCabe, P.; Pidcock, E.; Shields, G. P.; Taylor, R.; Towler, M.; van de Streek, J. *J. Appl. Crystallogr.* **2006**, *39* (3), 453–457.

(6) Macrae, C. F.; Bruno, I. J.; Chisholm, J. A.; Edgington, P. R.; McCabe, P.; Pidcock, E.; Rodriguez-Monge, L.; Taylor, R.; van de Streek, J.; Wood, P. A. *J. Appl. Crystallogr.* **2008**, *41* (2), 466–470.

(7) POV-Ray(TM) for Windows, version 3.6; Peristence of Vision Raytracer Pty. Ltd.: Williamstown, Australia 2004.

(8) GraphPad Prism 6, GraphPad Software: La Jolla California USA.

(9) Hyp Spec, Protonic Software, Leeds, England.

(10) Perry, C. Curve Fit, v 1.0: Johannesburg, South Africa.